STUDIES IN HYDROFORMYLATION REACTIONS USING HOMOGENEOUS AND NOVEL HETEROGENIZED TRANSITION METAL CATALYSTS

NITIN SUDAM PAGAR

FOR THE DEGREE OF

DOCTOR OF PHILOSOPHY

IN

CHEMISTRY

RESEARCH GUIDE

Dr. R. M. DESHPANDE

HOMOGENEOUS CATALYSIS DIVISION

NATIONAL CHEMICAL LABORATORY

PUNE-411 008, INDIA

MAY 2007

STUDIES IN HYDROFORMYLATION REACTIONS USING HOMOGENEOUS AND NOVEL HETEROGENIZED TRANSITION METAL CATALYSTS

A THESIS

SUBMITTED TO

THE UNIVERSITY OF PUNE

FOR THE DEGREE OF

DOCTOR OF PHILOSOPHY

IN

CHEMISTRY

BY

NITIN SUDAM PAGAR

UNDER THE GUIDANCE OF

Dr. R. M. DESHPANDE

AT

HOMOGENEOUS CATALYSIS DIVISION

NATIONAL CHEMICAL LABORATORY

PUNE-411 008

INDIA

MAY 2007

राष्ट्रीय रासायनिक प्रयोगशाला
(वैज्ञानिक तथा औद्योगिक अनुसंधान परिषद)
डॉ. होमी भाभा मार्ग पुणे – 411 008. भारत
NATIONAL CHEMICAL LABORATORY
(Council of Scientific & Industrial Research)
Dr. Homi Bhabha Road, Pune - 411 008. India.

CERTIFICATE

This is to certify that the work incorporated in the thesis, **"Studies in hydroformylation reactions using homogeneous and novel heterogenized transition metal catalysts."** submitted by **Mr. Nitin S. Pagar,** for the Degree of **Doctor of Philosophy,** was carried out by the candidate under my supervision in the Homogeneous Catalysis Division, National Chemical Laboratory, Pune – 411 008, India. Such material as has been obtained from other sources has been duly acknowledged in the thesis.

Dr. R. M. Deshpande

(Research Supervisor)

DECLARATION BY THE CANDIDATE

I hereby declare that the thesis entitled **"Studies in hydroformylation reactions using homogeneous and novel heterogenized transition metal catalysts."** submitted by me for the degree of Doctor of Philosophy to the University of Pune is the record of work carried out by me during the period from February 2002 to November 2006 under the guidance of Dr. R. M. Deshpande and has not formed the basis for the award of any degree, diploma, associateship, fellowship, titles in this or any other University or other institution of Higher learning.

I further declare that the material obtained from other sources has been duly acknowledged in the thesis.

May, 2007 **Nitin S. Pagar**

Pune **(Candidate)**

Dedicated to

My Parents

…For the beautiful life they have bestowed on me

ACKNOWLEDGEMENT

There are many people who have been actively helped me during the tenure of my Ph.D. and I would like to thank all of them for their time, support, efforts, smiles and friendship. There are, however, several peoples that I would like to acknowledge in particular.

I wish to express my sincere gratitude to my research guide, Dr. R. M. Deshpande for his constant support and encouragement during the course of this work. It has been an intellectually stimulating and rewarding experience to work with him. His innovative ideas and scientific knowledge have inspired me profoundly. We experienced together all the ups and downs of routine work, shared the happiness of success and the depression of failure. I would also like to acknowledge his linguistic abilities, which were extremely useful, particularly in the beginning of my work and life in NCL.

My special thanks to Dr. R.V. Chaudhari, former Head, Homogeneous Catalysis Division, National Chemical Laboratory (NCL) for his constant support, valuable help, suggestions and guidance during my research work. His enthusiastic attitude and great understanding of the subject have inspired me profoundly. I truly feel privileged to have joined his research group.

I would like to express my sincere gratitude and respect to Dr. B. D. Kulkarni, Deputy Director and Head, CEPD & Homogeneous Catalysis Division, NCL. I am thankful to former Director Dr. Paul Ratnasamy and present Director Dr. S. Sivaram, NCL for allowing me to carry out research work and extending me all the possible infrastructural facilities.

I would like to gratefully acknowledge Dr. A. A. Kelkar, Dr. V. H. Rane, Mr. P .S. Ozarde, Dr. S. P. Gupte, Dr. R. Jaganathan, Dr. V. V. Ranade, Dr. C. V. Rode, Mr. P. B. Jadkar, Mr. S. S. Joshi, Dr. S. H. Vaidya, Dr. S. Sengupta, Dr. V. M. Bhandari, Dr. A. A. Kulkarni, Mrs. Savita Singote, and Mr. H. M. Raheja for their valuable help and co-operation during my research stay in NCL. I would like to thank supporting staff of Homogeneous Catalysis Division, Mr. Patne, Mr. Kedari, Mr. Kamble and Mr. Durai for their help.

I take this opportunity to express my sincere gratitude to Dr. Mrs. A. J. Chandwadkar, Mr. A. B. Gaikwad, Dr. Shubhangi Umbarkar, Dr. B.M. Bhanage, Dr. A. K. Nikumbh, Dr. A.S. Kumbhar, Dr. P.K. Chaudhary, and Dr. Milind Nikalje for their valuable help and guidance during my research work.

My sincere acknowledgement to Kalpendra for his help in kinetic modeling and Pippalad for solving software/computer related problems.

I also wish to thank my senior and moreover my friend Dr. Vivek Buwa, Dr. Yogesh B., Dr. Sunil T., Dr. Prashant G., Dr. Avinash K., Dr. Shrikant, Dr. Kausik M., Dr Manisha V., Dr. Manisha T., Dr. Charubala, Avinash M., Rajesh V., Dr. Rashmi, who have gone out of their way to help in various capacities and have been my extended family throughout the tenure of my work in NCL. I would like to express my deepfelt gratitude to my colleagues and friends Makarand, Sunil Shinde, Abhishek, Nandu, Deepak N., Kausik Ghosh, Sangeeta, Pradeep, Anamika, Lalita, Samadhan, Rajamani, Mandar, Nilesh, Rajesh H., Vivek Mate, Nilkanth, Siddharam, Dr. Prakash, Bibhas, Dr.

Debdut, Anand, Shashi, Mahesh, Ranjeet, Jaypraksh, Vikas, Ajit, Mahesh B., Amit Chaudhari, Amit Deshmukh, Narendra, Umesh, Ruta, Himadri, Ankush B., Neeta, Abhijit and Sulata, for their friendship and , for keeping a healthy working atmosphere.

Staying at Golden Jubilee Hostel (GJH) was a wonderful experience during this tenure. It provided me relaxation after the hectic work schedule. The involvement in cultural and sports activities of the hostel also made my social life enjoyable. I am lucky enough to have the support of many good friends. Life would not have been the same without them thanks to my roommate Thiru and my other friends from GJH/NCL, Kishor (Bhiya), Dr. Eshwar, Dr. Bennur, Dr. Subbamaniyam, Dr. Shivanand, Dr. Sanjay, Dr. Selevekennan (mama), Dr. Joly, Dr. Sasanka, Dr. Shivsnakar, Bhalchandra, M. Baag, Arif, Bapu, Sachin, Pandurang, Sriram, Ankush Mane, Nilesh, Amit Patwa, Mahesh Thakkar, Sambhaji (raje), Sattyanarayana R., M. Sanksr, Mallikarjun, Elengovan, Ganesh, Deepak J., Kedar, Prasad, Manmath, Abasaheb, Prashant Karandikar, Sivram P., Nilkanth Aher, and many in NCL who are not named in person, for their valuable suggestions and help.

I wish to thank CMC and Central NMR facility NCL, for characterization. I would like to acknowledge Dr. Sonawane from, CMET, Pune, for GFAAS and ICP analysis. I also acknowledge SIF, IISc, Bangalore for solid state NMR characterization.

I am grateful to Council of Scientific and Industrial Research (CSIR), India for the research fellowship. I would like to acknowledge a CSIR sponsored Project, Task–Force for catalysts and catalysis (CMM-0005), for funding.

I would like to gratefully acknowledge Subbu, Radha, Ravi, Shekhar, Dure, Narawde, Wanjale, Shinde and Murkute for their help in reactor maintainance. Additionally I would like to acknowledge store–purchase, work shop, civil, electrical, administration sections and other supporting staff of NCL for their co-operation.

This page will be incomplete without acknowledging my college friends and classmates Nitin Chandan (sir), Tushar, Gorakh, Sushant, Milind, Ajit Doke, Gajendra, Mahadev, Vivek, Archika, Deppak Hinge, Rohit, Pallavi, Prashant Manohar,Kaluram, Harsh, Praveen Jadhav, Shaktising, Sarang, Shyam, Mahesh bagul, Sunil Shewale (doctor), Digambar, Yogesh Ahire, Sunil Bachhav, Prasad Pawar, Amol Mankar, Arun, Vilas, Prashant Kapadnis, Prshant Pagar(dada).

I also wish to thank my school and forever friends, Chandrakant, Rajendra, Purushottam, Kailas, Sachin, Prakash, Ranjeet, Praveen S., Machindra, Raosaheb Praveen P., Deepak Pagar, Suresh, Pratik and Vivek Pagar for the support and encouragement during this research work.

Last but not least, I have to thank my parents, my brother Pankaj, sister Vidya, brother in law Satish and nephew Om (Dadu) for their continuous support, encouragement and love. Needless to say it was because of the efforts of my family, friends and relatives today I stand where I am.

May, 2007 ***Nitin S. Pagar***

List of Contents

CHAPTER 2: Hydroformylation of Terpenes using Homogeneous Rhodium-Phosphite Complex Catalyst.

CHAPTER 3: Hydroformylation of 1-Decene in Aqueous Biphasic Medium using Water Soluble Rhodium- sulfoxantphos Catalyst.

List of Schemes

List of Tables

List of Figures

List of Abbreviations

[BMIM][PF_6]	*n*-butyl-3- methylimidazolium hexafluorophosphate
μ-OAc	Bridged Acetate
μ-PC	Bridging ortho-metalated arylphosphane ligand
μ-S-t-Bu	μ-thiotertirybutyl
1,5-COD	1,5-Cyclooctadiene
2-EH	2-ethyl 1-hexanol
acac	Acetylacetone
ae	Axial-equitorial
aq.	Aqueous
Ar	Aryl
ARPGPPs	Arylpolyglycol-phenylene-phosphite
BDPP	(2S, 4S)-bis (diphenylphosphinopentane
BET	Brunauer- Emmett-Teller
BINAS	Sulphonated 2, 2'-bis (diphenylphosphinomethyl) - l, l'-binaphthalene
BISBI	2, 2'-bis (diphenylphosphinomethyl)-1, 1'-biphenyl
BISBIS	Sulfonated (2, 2'-bis (diphenylphosphinomethyl)-1, 1'-biphenyl
BMIM [BF_4]	*n*-butyl-3- methylimidazolium tetreafluoroborate
Bu	Butyl
CBL	Catalyst binding ligand
CD	Cyclodextrin
Conc.	Concentration
C-T	Concentration-time
CTAB	Cetyltrimethylammonium bromide
$CTAHSO_4$	Cetyltrimethylammonium bisulphate
DCE	Dichloro ethane
DCM	Dichloro methane
DDAPs	Dodecyldimethylammoniopropanesulfonate

DIPAMP	Dimer of phenylanisylmethylphosphine or ethane-1,2-diylbis[(2-methoxyphenyl)phenylphosphane
DMCD or DMβ-CD	Per(2,6-di-o-methyl)-β-cyclodextrins
DMF	N,N-Dimethyl foramide
DPBS	Dulbecco's Phosphate Buffered Saline
dppb	Dipheneyl phosphinobutane
DPPBTS	Tetrasulfonated 1,4-bis(diphenylphosphino)butane
dppe	diphenylphosphinoethane
DPPETS	Tetrasulfonated 1,2-bis(diphenylphosphino)ethane
DPPETS	Tetrasulfonated 1,3- bis(diphenylphosphino)ethane
dppf	1,1'-bis(diphenylphosphanyl)ferrocene
dppp or DPPP	Diphenylphosphinopropane
DPPPTS	Tetrasulfonated 1,3- bis(diphenylphosphino)propane
e.g.	For example
EDX	Energy dispersive X-ray
ee	Equitorial-equitorial
equiv	Equivalent (s)
EtOH	Ethanol
Et	Ethyl
FBS	Fluorous biphasic system
FID	Flame ionization detector
FTIR	Fourier transform infrared
GC	Gas chromatography
GC-MS	Gas chromatography-Mass spectrometry
GFAAS	Graphite furnace atomic absorption spectrophotometer
h	Hour (s)
HDPE:	High density polyethylene
HTMAP	2-hydroxy-3-trimethylammoniopropyl
i. e.	That is
ICP-AES	Inductive copuplled Plasma- atomic emission spectrophotometry
LDPE	Low density polyethylene

LPO	Low Pressure Oxo Process
LTAB	Lauryltrimethylammonium bromide
CP-MAS	Cross polarization magic angle spinning
MCM-41	Mobile crystalline materials –41
MEK	Methy Ethyl Ketone
MeOH	Methanol
ml	Milliliter
Mol	Mole
MPa	Megapascal
MTMAP	2-methoxy-3-trimethylammoniopropyl
MTPA	Metric tons per year
BINAP	2, 2'-bis (diphenylphosphinomethyl) - l, l'- binaphthalene
NBD	Norbornadiene
NMP	N-methyl 2-pyrolidone
NMR	Nuclear magnetic resonance
NORBOS	Sulphonated phosphanorbomadiene
OMe	Methoxy
OPGPP	Octylpolyglycol-phenylene-phosphite
org.	Organic
OTf	Triflate
OTPPTS	Triphenyl phosphine trisulfonate oxide
$P(OBu)_3$	Tri butylphosphite
$P(OEt)_3$	Tri ethylphosphite
$P(OMe)_3$	Tri methylphosphite
$P(OPh)_3$	Tri phenylphosphite
P_{CO}	Partial pressure of carbon monoxide
PEO-DPPSA	N, N-dipolyoxyethylene-substituted-4- (diphenylphosphino benzene sulfonamide
PEO-TPPs	Poly(ethylene oxide)-substituted triphenylphosphines
PETAPO	Polyether triphenyl phosphine oxide
Ph	Phenyl

P_{H2}	Partial pressure of Hydrogen
PHENEP	2, 2'-bis (diphenylphosphinomethyl)-1, 1'-phenylnapthalene
PMT	Photomultiplier tube
ppb	Parts per billion
ppm	Parts per million
PTA	Phosphotungstic acid
RAME-α or β-CD	Randomly methylated α and β-Cyclodextrin
RT	Room temperature
SAPC	Supported aqueous phase catalysts
$scCO_2$	Supercritical CO_2
SDS	Sodium dioctyl sulfosuccinate
Sec.	Second
SEM	Scanning electron microscopy
SILC	Supported ionic liquid catalyst
SLPC	Supported liquid phase catalysts
STAC	Stearyltrimethylammonium chloride
Sulfo-XANTPHOS	2, 7-bis (SO_3Na**)** 4,5–bis(diphenylphosphino) 9,9 dimethylxanthene
T	Temperature
t	Time
TEM	Transmission electron microscopy
THF	Tetrahydrofuran
TLC	Thin layer chromatography
TMGL	1,1,3,3-tetramethylguanidinium lactate
TOF	Turnover frequency
TON	Turnover number
TPA	Tons per annum
TPP or $P(Ph)_3$	Triphenyl phosphine
TPPDS	Triphenylphsosphine disulphonate disodium
TPPMS	Triphenyl phosphine monosulfonate monosodium
TPPO	Triphenyl phosphine oxide

TPPTC	Tris(m-carboxyphenyl)phosphane trilithium salt
Tppti	Tri(m-sulphonyl) triphenyl phosphine tris(1-butyl-3-methyl-imidazolium)salt
TPPTS	Triphenyl phosphine trisulfonate trisodium
TRPTC	Thermo regulated phase-transfer catalysis
VAM	Vinyl acetate monomer
viz.	Namely
Xantphos	4,5–Bis(diphenylphosphino) 9,9 dimethyl xanthene
XPS	X-ray photoelectron spectroscopy
XRD	X-ray diffraction
yr.	Years

Abstract of the Thesis

Conventional manufacturing processes using stoichiometric synthetic routes often involve toxic and corrosive reagents and formation of byproducts and waste products consisting of inorganic salts. Catalysis has played a vital role in developing new, environmentally benign technologies for replacing stoichiometric reactions. Catalytic processes play a very fundamental role in chemical industry, allowing the conversion of a wide variety of feedstock to high value products at lower cost, with minimum generation of byproducts[1]. Today, catalyst technology accounts for the large-scale industrial processes like the refining of oil to gasoline in petroleum industry, to small-scale synthesis of drugs in the pharmaceutical industries. The worldwide economy is based on the catalytic production of chemicals and fuels. Thus, the importance of catalysis to modern society is obviously based on its great economic impact in the production of a broad range of commodity products that improve our standard of living and quality of life. In this context, both homogeneous and heterogeneous catalysis have played an important role in the development of new chemistry and technology towards clean synthesis.

The hydroformylation reaction is one of the important and largest scale applications of homogeneous catalysis. It is used in the industry for the manufacture of aldehydes and alcohols[2]. About 5.9 million TPA aldehydes [C_4 to C_{20+} range] are produced by this process all over the world. These are further hydrogenated to alcohols for different applications. The aldehydes act as intermediates for a variety of bulk and fine chemicals whereas alcohols find applications in solvents, surfactants, detergents and plasticizers. Hydroformylation involves the reaction of alkenes with carbon monoxide and hydrogen in the presence of a catalyst to form linear and branched aldehydes. Selectivity to the n-isomer is an important consideration in the catalyst development, since; the normal products are more useful commercially.

Industrial hydroformylation is mainly dominated by rhodium and cobalt catalyst in the ratio of 80:20. The commercial hydroformylation plants use modified and unmodified homogeneous cobalt or rhodium catalysts namely $HCo(CO)_4$, $HCo(CO)_3(PBu_3)$ and $HRh(CO)(PR_3)_3$. Rhodium catalysts are very selective and applicable for the hydroformylation of lower olefins, functionalized olefins and other

complex olefins while cobalt catalysts are mainly used for the hydroformylation of higher olefins.

Even though majority of the hydroformylation applications utilize linear hydrocarbon olefins (especially α -linear olefins), there are few reports available on hydroformylation of complex olefins like cyclic olefins, diolefins, terpenes, functionalized olefins. In spite of the importance of the products in fine chemicals and pharmaceuticals the hydroformylation of complex olefins is somewhat ignored mainly because of the lower reaction rates than those found for linear hydrocarbon olefins, and selectivity issues.

One of the major limitations for the widespread application of homogeneous catalysts is the highly complex catalyst product separation. To overcome the problem of catalyst-product separation different attempts were made to heterogenise the homogeneous catalysts mainly via biphasic[3] and solid supported catalysis[4]. However, except aqueous biphasic catalysis none of the concepts has found any commercial application, due to issues like catalyst leaching, catalyst deactivation and poor activities.

The application of aqueous biphasic catalysis on commercial scale is also limited to lower olefins like C_3 and C_4 olefins, since higher olefins have very little solubility in water, resulting in poor reaction rates[3]. In addition, compared to lower olefins, the hydroformylation of higher olefins is more complicated due to the isomerization and hydrogenation side reactions, which results in a reduced n/i ratio and formation of side products like alkanes.

Considering the above facts, the present study was focused on the hydroformylation of two classes of olefinic substrates viz. terpenes and higher olefins. The hydroformylation products of terpenes are useful in perfume and pharmaceutical applications[5] and those of higher olefins are useful as intermediates in surfactant and detergent manufacture. The main objective of this work was thus to develop a highly active and selective catalytic system for the homogeneous hydroformylation of terpenes. Further to this, development of immobilized catalyst systems for the hydroformylation of higher olefins to achieve high activity, selectivity, and stability was also investigated. It was also important to study the kinetic behavior and mechanism of these reactions to

develop a deeper understanding. Therefore, following problems were chosen for the present work.

- Hydroformylation of terpenes using homogeneous transition metal complex catalysts. Screening of catalysts, ligands to achieve high activity, selectivity followed by kinetic studies on hydroformylation of terpenes using the catalyst system of choice.
- Hydroformylation of higher olefins using highly selective water-soluble Rhodium-sulfoxantphos catalyst in biphasic medium with and without cosolvent: Activity, selectivity and kinetic studies.
- Synthesis, characterization and catalytic activity of novel heterogenized catalyst for hydroformylation of higher olefins and detailed investigations on the activity selectivity and kinetic behavior of the catalyst for hydroformylation of 1-decene.

The **THESIS** will be presented in **Four** chapters, a brief summary of which is given below.

Chapter 1 presents, a detailed survey of the literature on the hydroformylation reaction. From the literature, it is realized that extensive work has been done on the hydroformylation reaction[2], the role of different catalysts, promoters, product distribution and selectivity towards desired product and the kinetics and reaction mechanism has been studied in detail for a variety of olefinic substrates. The hydroformylation of terpenes using various transition metal catalyst systems is also reviewed in the chapter. The various methods of immobilization of homogeneous catalysts as well literature on hydroformylation of higher olefins with respect to 1-decene as a model substrate using biphasic media and heterogenized homogeneous complexes, has been presented. The detailed survey on the kinetics and mechanism of hydroformylation is also presented.

Chapter 2 presents the experimental results and discussion on the hydroformylation of terpenes. Various complexes of rhodium, cobalt and platinum were synthesized and characterized. Initially, the well known Wilkinson catalyst[6], $HRh(CO)(PPh)_3$ was tested for the hydroformylation of terpenes such as camphene, limonene, α and-β-pinene, Δ-3-carene, γ-terpinene, citral and citronellol. The products were analyzed using GC, isolated by column chromatography and

identified/characterized using GCMS and IR. The results show that this catalyst hydroformylates only those terpenes having terminal double bonds with a very low TOF. To obtain a better catalyst for terpene hydroformylation, various transition metal catalysts were screened. For this purpose, camphene was chosen as a model substrate.

The results show that the rhodium complex $Rh(CO)_2(acac)$ modified with triphenyl phosphite ligand is the best catalyst system for hydroformylation of camphene. No isomerisation or hydrogenation products were observed. Homogenous complexes of cobalt and platinum show no reaction for hydroformylation of camphene under similar reaction conditions. The solvent screening studies with $Rh(CO)_2(acac)/P(OPh)_3$ catalyst show that the hydroformylation rates are higher in polar protic solvents and lower in nonpolar solvents[4a]. The highest activity (TOF=417 h^{-1}) was observed in MEK solvent with an exo/endo aldehyde ratio of 47:53. The ligand screening shows that the activity of various phosphite ligand in the order of $P(OPh)_3 > P(OBu)_3 > P(OEt)_3$. No reaction was observed in the presence of bidentate ligand such as dppe, dppp and dppb. The $Rh(CO)_2(acac)/P(OPh)_3$ catalyst system was found to be equally good for the hydroformylation of limonene, β-pinene and R-carvone.

Kinetics of hydroformylation of camphene was investigated using $Rh(CO)_2(acac)/P(OPh)_3$ catalyst system in the temperature range of 363–383K. The influence of the reaction parameters such as agitation speed, camphene concentration, catalyst concentration, ligand concentration and partial pressures of H_2 and CO on the activity and selectivity of the catalyst has been studied. The rate was found to be first order with respect to catalyst and substrate concentration. The effect of partial pressure of hydrogen shows partial order dependence. The plot of rate vs. $P(OPh)_3$ concentration and CO partial pressure passes through maxima and shows a typical case of inhibition at higher concentrations. An empirical rate equation has been proposed which was found to be in good agreement with the observed rate data within the limit of experimental error. The kinetic parameters and activation energy (84.7 kJ/mol) were also evaluated.

Chapter 3 presents the experimental results and discussion on the hydroformylation of higher olefins in aqueous biphasic medium using sulfoxantphos ligand. The sulphonated Xantphos (sulfoxantphos) ligand was synthesized and characterized[7]. The hydroformylation of higher olefins such as hexene, octene, decene

and dodecene was studied in aqueous biphasic medium using water-soluble Rh-sulfoxantphos catalyst. The reaction rates were very poor but the n/i ratios obtained were in the range of 26-32, which is very high. 1-decene was chosen as a model substrate for detailed study. The effect of aqueous phase hold up and presence of various cosolvents on the reaction rate and chemo and regioselectivity was also investigated. N-methyl pyrrolidone (NMP) was found to be the best cosolvent, which enhances the rate dramatically compared to the reaction in pure biphasic medium (i.e. in the absence of cosolvents). Interestingly the n/i ratio improves in the presence of the cosolvent. The aqueous catalytic phase was recycled for four times without a drop in activity and selectivity. An interesting observation was the improvement in the activity for the first recycle over the virgin reaction. This activity then remains constant for subsequent recycles.

The kinetics of hydroformylation of 1-decene has been investigated in a temperature range of 383-403 K using the water-soluble Rh-sulfoxantphos catalyst in biphasic medium in presence of NMP cosolvent. The influence of the reaction parameters such as agitation speed, 1-decene concentration, catalyst concentration, ligand concentration and partial pressures of H_2 and CO on the activity and selectivity, of the catalyst has been studied. The rate was found to be first order with respect to catalyst and substrate concentration, and was independent of ligand concentration. The effect of partial pressure of hydrogen shows partial order dependence. The plot of rate vs. CO partial pressure passes through a maximum and shows a typical case of inhibition at higher concentrations. The rate had a linear dependence on P_{CO} at lower partial pressure of 0.34 MPa. An empirical rate equation has been proposed which was found to be in good agreement with the observed rate data within the limit of experimental error. The kinetic parameters and activation energy (64.76 kJ/mol) were also evaluated.

Chapter 4 presents the synthesis, characterization and catalytic activity of novel hetrogenized catalyst for the hydroformylation of olefins. The concept involves the precipitation of the water soluble catalyst $HRh(CO)(TPPTS)_3$ into its insoluble analog as a Gr.2 metals (Ca, Sr or Ba) salts. This new concept of heterogenization is termed as ‘ossification’. The precipitation of the complex is also possible on the porous support, and such catalysts are termed as ‘supported ossified catalyst’. This technique yields a

highly dispersed catalyst with a much larger surface area. Both the ossified catalysts (Supported and unsupported), were characterized by FTIR, solid state ^{31}P NMR, powder XRD, SEM, TEM, EDX and XPS. The BET surface area, pore size and pore volume were also determined using N_2 desorption method. Both the catalysts were tested for the hydroformylation of linear and functionalized olefins. The carbon supported ossified catalyst shows a significantly higher activity (TOF) for hydroformylation of olefins as compared to other known heterogenized catalyst including unsupported ossified catalyst. The important feature of this catalyst was the high activity observed for higher olefins like 1-decene and 1-dodecene where the availability of true heterogeneous catalysts has been a challenge.

The catalyst was found to be stable and the activity and selectivity of the catalyst was maintained during several recycles. The ICP analysis shows negligible leaching in the organic phase (<0.6 % of rhodium metal taken) after five recycles. The ossified catalysts supported on SiO_2, Al_2O_3, ZrO_2, TiO_2, La_2O_3 and MgO also show good hydroformylation activity. The mesoporous supported carbon shows around 20% improvement in activity than the microporous carbon.

The kinetics of hydroformylation of 1-decene using the carbon supported ossified catalyst $HRHCO(TPPTS)_3$ was studied in the temperature range of 343–363K. The effect of agitation speed, concentration of 1-decene, catalyst loading, and partial pressure of H_2 and CO, on the rate of reaction has been studied. The rate was found to be first order with respect to catalyst and partial pressure of hydrogen. The plot of rate vs. 1-decene passes through maximum and shows a typical case of inhibition at higher concentrations. The rate had a linear dependence on P_{CO} upto CO partial pressure of 5-6 MPa and decreases thereafter. This is an unusual observation for this catalyst as for most rhodium-catalyzed systems severe inhibition is observed at much lower pressures of CO (0.2-0.3 MPa).

A rate equation of the type as shown in equation **1** has been proposed which was found to be in good agreement with the observed rate data within the limit of experimental error. The kinetic parameters and activation energy was evaluated.

$$r = \frac{k_1 \, ABCD}{(1+ k_2 D)^2 \, (1+ k_3 B)^2} \qquad \mathbf{1}$$

Where,

r =Rate of hydroformylation, kmol/m^3/s, k= Reaction rate constant, $kmol^3/m^9$/s

A= Concentration of hydrogen, kmol/m^3, B= Concentration of CO kmol/m^3,

C= Concentration of catalyst, kmol/m^3, D= Concentration of 1-decene, kmol/m^3

References:

1 R. J. Farranto, C.H. Bartholomew (Eds) *Fundamentals of Industrial Catalytic Processes*, Blackie Academic and Professional, London, **1997**.

2 (a) B.Cornils in *New synthesis with carbon monoxide* (Eds J. Falbe) Springler-Verlag, Berlin, Heidelberg, New York, **1980**. (b) P.W. N.M. van Leeuwen, C. Claver (Eds.) *Rhodium Catalyzed Hydroformylation* Kluwer Academic Publishers **2000**.

3 B. Cornils, W. A. Herrmann (Eds.), *Aqueous Phase Organometallic Catalysis,* VCH, Weinheim, **1998**.

4 (a) F.R. Hartley, *Supported Metal Complexes*, Reidel, Dordrechiet, **1985** (b) D. J. Cole-Hamilton, *Science*, **2003**, *299*, 1702

5 (a) Karl A.D. Swift *Topics in Catalysis,* **2004**, *27 (1–4)*, 143. (b) N.Ravasioa, F. Zaccheriab, M. Guidottia, R. Psaroa, *Topics in Catalysis,* **2004**, *27 (1–4)*, 159. (c) J. L. F. Monteiro, C. O. Veloso, *Topics in Catalysis,* **2004**, *27 (1–4)*, 169.

6 D. Evans, J. A. Osborn, G. Wilkinson, J. Chem. Soc. A, **1968**, 3133.

7 M. S. Goedheijt, Paul C. J. Kamer, P.W. N. M. van Leeuwen *J. Mol. Catal. A: Chemical* **1998**, *134*, 243.

CHAPTER 1

Introduction and Literature Survey

1.1 Introduction

"Chemistry without catalysis would be a sword without a handle, a light without brilliance, a bell without sound." ……A. Mittasch

Catalysis is fundamental to life! In fact, without catalysis no form of life could exist. Most of the life supporting reactions in our body are catalyzed by enzymes, which are nature's catalysts. The global economy is based on catalytic production of chemicals and fuels worth over 10 trillion dollars per year[1]. Catalysis has played a vital role in developing new, environmentally benign technologies to replace stoichiometric synthetic routes often involving toxic and corrosive reagents and associated with generation of waste products. Catalysis plays a very fundamental role in the oil and chemical industry, allowing the conversion of a wide variety of feedstocks to high value products at lower cost, with minimum generation of byproducts. Catalyst technology not only accounts for the large-scale conversion of oil to gasoline in petroleum industry but also to small-scale synthesis of drugs in the pharmaceutical industries. Almost all chemicals, fuels, polymers and fibers are manufactured by catalytic processes. Thus, the importance of catalysis to society is obviously based on its great economic impact in the production of a broad range of commodity products that improve our standard of living and quality of life.

The word 'catalysis' was coined by Berzelius in 1836 which is a Greek word, the prefix, 'cata' meaning down, and the verb 'lysein' meaning to split or break. A catalyst breaks down the forces that inhibit the reactions of the molecules by lowering the activation energy. The widely accepted definition of a catalyst is 'a substance that changes the rate at which reaction equilibrium is attained, without itself being consumed in the reaction processes'. Catalysis is broadly classified into three categories depending on the physical nature of the catalyst employed[2]:

1. Homogeneous catalysis: The reactants, products and catalyst are present in the same phase.
2. Heterogeneous catalysis: Reactants/products and catalyst are present in separate phases; the catalyst is generally solid and the reactants are either liquid or gas.
3. Biocatalysis or enzymatic catalysis: It mainly involves all biological and related reactions

Some general features *of homogeneous catalysis* are mild reaction conditions, high activity and selectivity, difficult and expensive catalyst-product separation, better mechanistic understanding *etc*. The catalyst is usually, a dissolved metal complex, which makes all the catalytic sites accessible to the reactants. Most of the processes involving homogeneous catalysis [***e.g.*** carbonylation, hydrogenation, hydroformylation, oxidation, Heck and Suzuki coupling, telomerization, co-polymerization, metathesis *etc*.] produce important bulk and fine chemicals for the polymer, pharmaceutical, paint, and fertilizer industries[3a]. The main drawback of homogeneous catalysis is the expensive catalyst-product separation, and the recycle/recovery of the catalyst. *Heterogeneous catalysts,* on the other hand, generally employ relatively severe temperature and pressure conditions and mostly operate in a continuous mode. Heterogeneous catalysts generally have a higher catalyst life, are stable to temperature and offer an easy catalyst-product separation [***e.g.*** catalytic reforming, catalytic cracking, hydrogenation, hydro-desulfurization and other bulk chemical processes such as ammonia synthesis, sulfuric acid synthesis *etc*.]. The importance of the catalyst product separation is evident from the fact that in commercial practice, about 25% of the industrial catalytic reactions involve homogeneous catalysis, and 75% employ heterogeneous catalysis[3b]. *Enzyme catalysis* is also homogeneous in nature and provides regioselective and stereoselective transformations at ambient reaction conditions with almost no byproduct formation. The enzymes are the most efficient catalysts known to human being, as they are substrate specific, regio/stereo and chemoselective with nearly 100% atom efficiency[3c].

Homogeneous catalysis has advanced considerably in the last few decades. Generally, transition metal complexes are used as catalysts because of their stability in the varying oxidation states during the course of reaction cycle. The performance of homogeneous catalysts depends not only on the reaction conditions but also on type of the metal, ligands, promoters and co-catalysts used. The systematic progress in the field of co-ordination chemistry has led to the discovery of new complex catalysts. Their applications have helped many homogeneous catalytic processes to achieve higher selectivities at milder reaction conditions[4]. The improved techniques of catalyst characterization enable us to understand the reaction mechanism at the molecular level. Mechanistic studies on homogeneous catalytic reactions provide better understanding of

the overall reaction and thus help to modify the environment around the metal and tune the chemo, regio and/or enantio selectivity. The progress of homogeneous catalysis is also significant in the area of fine chemicals. A list of important industrial applications of homogeneous catalysis is given in Table 1.1.

Table 1.1: Important industrial applications of homogeneous catalysis

No.	Process	Catalyst	Company
1	Oxidation of ethylene to acetaldehyde	$PdCl_2/CuCl_2$	Wacker-Werke[5]
2	Oxidation of p-xylene to terephthalic acid/ester	Co/Mn-salts	Du Pont[6]
3	Polymerization of ethylene to HDPE/LDPE	Ni-complex	Shell[7]
4	Hydrocyanation of butadiene to adipic acid	Ni-complex	Du Pont[8]
5	Asymmetric hydrogenation of acetamido cinnamic acid (3-methoxy-4-acetoxy derivative) (l-dopa process)	$[Rh(diene)(solvent)]^+$ /DIPAMP	Monsanto[9]
6	Hydroformylation of propene to butyraldehyde	$NaCo(CO)_4$	BASF[10]
		$HCo(CO)_3PBu_3$	Shell[11]
		$HRh(CO)(PPh_3)_3$	Union Carbide[12]
		$[Rh(COD)Cl]_2$/ TPPTS	Ruhrchemie-Rhone-Poulenc[13]
7	Hydroformylation of higher olefins to oxo alcohols	$HCo(CO)_3PBu_3$	Shell[14]
8	Hydroformylation of diacetoxy butene to 1-methyl-4-acetoxy butanal (Vitamin A intermediate)	$HRh(CO)(PPh_3)_3$	Hoffmann-La Roche [15]
		Rh catalyst	BASF[16]
9	Carbonylation of methanol to acetic acid	Rh/ iodide	Monsanto [17]
		$Co_2(CO)_8$	BASF [18]
		Ir/iodide	BP chemicals[19]
10	Carbonylation of methyl acetate to acetic anhydride	Rh/MeI	Halcon [20]
		Rh/MeI	Eastman Chemical[21]
11	Carbonylation of ethylene to propionic acid	$Ni(OCOC_2H_5)_2$	BASF[22]
12	Carbonylation of acetylene to acrylic acid	Ni-salts or carbonyls	BASF[23]
13	Carbonylation of benzyl chloride to phenyl acetic acid	$Co_2(CO)_8$	Montedison[24]
14	Carbonylation of 1-(4-isobutylphenyl) ethanol to ibuprofen	$PdCl_2(PPh_3)_2$/HCl	Hoechst-Celanese[25]
15	Oxidative carbonylation of methanol to dimethyl carbonate	$PdCl_2$-$CuCl_2$	Assoreni[26]
16	Hydroformylation of ethylene oxide to 2-hydroxy propanal	$Co_2(CO)_8$	Shell[27]

Though homogeneous catalysis has played an extremely important role in providing highly efficient processes, they suffer serious drawbacks, mainly in terms of catalyst-product separation and re-usability of the catalyst. These shortcomings have led researchers to investigate new, stable and easily separable catalyst systems[28].

The hydroformylation reaction is a typical reaction where homogeneous catalysts are exclusively used in industrial practice. Inspite of decades of research, there is no heterogeneous (solid phase) alternative for application to hydroformylation. Many variants of the industrial hydroformylation process are operating in practice. They mainly differ in the catalyst, ligand and the reaction medium used. There is a need to further improve the catalysts and processes to achieve high activity and selectivity as well as the separation of catalyst from products.

The aim of this thesis is to study in detail the catalysis, chemistry, kinetics, mechanism and reaction engineering aspects of the hydroformylation of complex substrates like terpenes and higher olefins. Hence the focus of this chapter is a detailed survey of the relevant literature on catalysis, kinetics and chemistry of both homogeneous and heterogenized (biphasic and solid supported) catalysts for hydroformylation reaction.

1.2 The hydroformylation reaction

Hydroformylation is one of the important and largest scale applications of homogeneous catalysis. It is used in the industry for the manufacture of aldehydes and alcohols from olefins. About 5.9 million TPA aldehydes [C_4 to C_{20+} range] are produced by this process all over the world[3a]. These are further hydrogenated to alcohols for different applications. The aldehydes act as intermediates for a variety of bulk and fine chemicals, whereas alcohols find applications as solvents, surfactants, detergents and plasticizers. Hydroformylation involves the reaction of alkenes with carbon monoxide and hydrogen in the presence of a catalyst to form linear and branched aldehydes. The stoichiometric reaction is as shown in scheme 1.1.

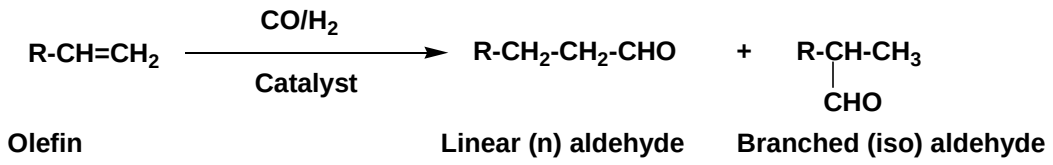

Scheme 1.1: General hydroformylation reaction

The reaction was discovered by Otto Roelen in 1938[29]. He named this reaction as "Oxo" reaction, with oxo being a short form of oxonation, i.e. addition of oxygen to double bond. Later on, the reaction was renamed as "Hydroformylation" since there is addition of hydrogen and formyl group across the double bond. Linear and branched aldehydes are the major products in the hydroformylation reaction alongwith some side products like alcohols and saturated hydrocarbons by hydrogenation of olefins and aldol derivatives by condensation of aldehydes. Selectivity to the n-isomer is an important consideration in the catalyst development, since the normal products are generally more useful in commercial practice.

Extensive work has been done on the hydroformylation reaction, which is very well documented in the literature[30]. The role of different catalysts and promoters on product distribution and selectivity towards desired product and the kinetics and reaction mechanism has been studied in detail using cobalt and rhodium catalysts. These are incidentally the two metals around which the hydroformylation processes are built. Table 1.2 shows the comparison of various industrial oxo processes.

Table 1.2: Comparison of various industrial oxo processes

Particulars	Cobalt		Rhodium		
Variant	Classical[a]	Modified[b]	Classical[c]	Modified [d] (LPO)	Water-soluble[e]
Catalyst	$HCo(CO)_4$	$[HCo(CO)_3PBu_3]$	$HRh(CO)_4$	$[HRh(CO)(PPh_3)_3]$	$[HRh(CO)(TPPTS)_3]$
T (ºC)	110-180	160-200	100-140	60-120	110-130
P (bar)	200-350	50-100	200-300	1-50	40-60
Product	aldehyde	alcohol	aldehyde	aldehyde	aldehyde
n:iso ratio	80:20	88:12	50:50	92:8	97:3
By-product	alcohols, acetals and heavy ends.	paraffins	isomeric aldehydes	condensation products	n-butanol isobutanol

a = BASF, Ruhrchemie; b= Shell; c= Ruhrchemie; d= Union Carbide; (LPO); e= Ruhrchemie/Rhone-Poulenc, Hoechst.

The *first generation* hydroformylation processes were exclusively based on cobalt catalyst[31]. The reaction conditions needed for this catalyst were relatively harsh (200-350 bar pressure and 150-180°C temperature). Later on, researchers[32] at Shell discovered that phosphines (or arsines) were able to replace carbon monoxide as electron donating ligand

to produce a modified cobalt catalyst, which shows improved regioselectivity towards the n-isomer, due to the electronic and steric properties of the phosphine ligand. The Shell process using cobalt-phosphine catalyst also gave alcohol as the major product, and reduced the operating pressure of syngas markedly (50-100 bar). The temperature required was in the range of 80^0C to 200^0C. The major drawback of this process was the side reaction of hydrogenation of olefins to paraffins.

The *second generation processes* combined the advantages of ligand modification with a change over from cobalt to rhodium as the catalyst. The rhodium-phosphine catalysts achieved very high chemoselectivity and regioselectivity towards n-aldehydes, at milder reaction conditions (60-120^0C and 1-50 bars) and hence this process is termed as the Low Pressure Oxo Process (LPO process)[33]. Owing to this advantage of LPO, most of the cobalt-based hydroformylation processes were shifted to LPO, especially for hydroformylation of propylene. The catalyst employed in LPO process is $HRh(CO)(PPh_3)_3$, also popularly known as Wilkinson's catalyst. These ligand modified rhodium complex catalysts made considerable advances over the cobalt catalysts. The rhodium catalysts were very active and could be employed in lower concentrations. They are however, highly susceptible to poisons such as free sulfur, iron compounds and oxygen, thus demanding a feed of very high purity. Other rhodium-based processes are also being practiced and these are described in later sections. Considerable advances have been made in second generation processes especially with respect to material and energy utilization.

The *third generation process* using aqueous biphasic catalysis was developed by Kuntz[34] of Rhone–Poulenc in 1984, which addressed the catalyst product separation issue to some extent. The basic idea was to immobilize the catalyst in to an immiscible *liquid*. The necessity of this variation was to convert the organic soluble ligand to its water-soluble counterpart. Aqueous biphasic catalysis particularly gained importance because of the many advantages of water as the reaction solvent. The best example of the aqueous-biphasic catalysis is the hydroformylation of propylene using $[Rh(COD)Cl]_2$-TPPTS (triphenyl phosphine trisulfonate trisodium), which has been commercialized by Ruhrchemie-Rhone Poluenc at a 300 MTPA scale. The success of aqueous biphasic

catalysis on large industrial scale has triggered off extensive research and developments in designing novel biphasic systems.

The hydroformylation reaction is mainly explored with rhodium or cobalt catalysts. Other transition metal complexes of Ni, Pd, Se, Cu, Fe, Ru, Ir, Pt, Ag or Mn are also reported to be active for the oxo reaction but they are mainly of academic interest[30a]. Tin (II) chloride modified platinum catalysts have significantly gained importance in the field of asymmetric hydroformylation. The order of hydroformylation activity with regard to the central metal atom follows the trend Rh>Co>Ir,Ru>Os>Pt>Pd>Fe>Ni. The Rh catalyzed hydroformylation has been applied for a variety of olefins from linear α-olefins to higher olefins as well as functionalized olefins, with numerous applications of the aldehyde products. A list of the rhodium catalyzed commercial hydroformylation processes is given in Table 1.3.

Table1.3: Survey of commercial application of Rh catalyzed hydroformylation[30b]

Alkene	Products	Developed by	Year	Ligand	Capacity kTPA
C_6-C_{14} 1-alkenes	higher alcohols	Mitsubishi	1970	None	23
ethene	propanal	Celanese, Union Carbide	1974	TPP	400
propene	butanol , isobutanol 2-EH, neopentyl glycol	BASF, Celanese, Union Carbide, Mitsubishi	1974	TPP	4000
		RCH-RP	1984	TPPTS	600
1,2-diacetoxy 3-butene	vitamin-A	BASF	70's	None	3
1,4-diacetoxy 2-butene	vitamin-A	Hoffmann-LaRoche	70's	TPP	3
1-hexene, 1-octene	carboxylic acids	Celanese	1980	TPP	18
branched internal octenes	isononanol	Mitsubishi	1987	TPPO	30
3-methyl 3-butene1-ol	3-methyl-1,5-petanediol	Kuraray	1988	bulky mono-phosphite	3
allyl alcohol	1,4-butanediol	Kuraray	1990	TPP + dppb	180
7-octenal	1,9-nonanediol	Kuraray	1993	TPPMS	2-3
				bulky mono-phosphite	

1-butene	2-propyl-1-heptanol	Hoechst	1995	TPPTS	40
1-butene/ 2-butenes	2-propyl-1-heptanol	Union Carbide	1995	Diphosphites	80
higher 1-alkenes	detergent alcohols	Kvaerner, Union Carbide	2001	DPBS	120

Similarly, a large variety of ligands has been screened for the cobalt and rhodium catalyst systems to improve activity/selectivity of hydroformylation. Phosphines are the most widely studied ligands in hydroformylation chemistry. Nitrogen containing ligands like amines, amides or isonitriles[35] though active, show lower reaction rates in the oxo reaction due to their stronger coordination to the metal center. The order of reactivity of ligands according to the donor atom: $Ph_3P > Ph_3N > Ph_3As$, $Ph_3Sb > Ph_3Bi$ proves the superiority of phosphine ligands[36]. Polydentate phosphines have also been used for hydroformylation reaction but their uses are limited, as they show much lower activities than their monodentate counterparts. In addition, the regioselectivities are not as high as expected for these bulky ligands[37]. Due to the extensive use of phosphines in catalysis, their coordination chemistry has been studied in more detail[38]. Carbene ligands obtained from imidazolium salts also show good activity and selectivity for hydroformylation of 1-hexene[39].

The phosphites having the general formula $(RO)_3P$ have also been used as ligands in rhodium-catalyzed hydroformylation and they give very high activity even for internal olefins. Bulky mono and biphosphites (Figure 1.1) have enabled the hydroformylation of long-chain olefins with considerably high activities (TOF=10000-40000 h^{-1})[40].

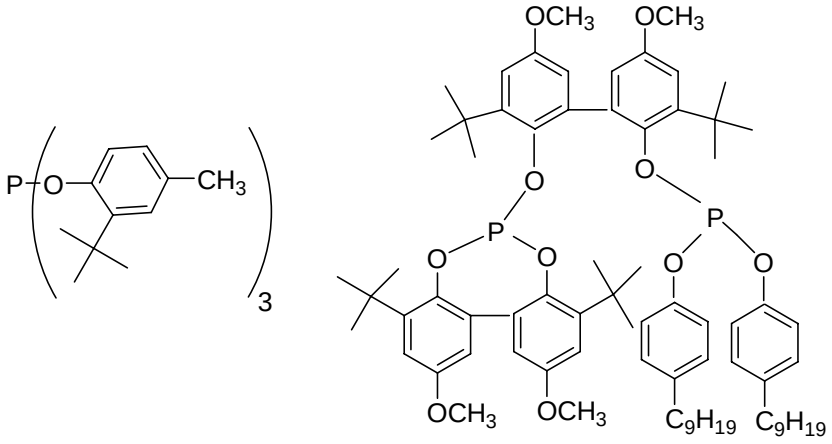

Figure 1.1: Bulky mono and biphosphites

Hughes and Unruh[41] of Celanese used diphosphine ligands of the type dppe, dppp, which led to higher n/i ratios (83:17) for hydroformylation of 1-hexene. Ferrocene based diphosphine ligands (dppf) also give n/i ratio in the range of 5-12 for hydroformylation of linear olefins[42]**.** A major breakthrough in regioselective hydroformylation of linear olefins was achieved by development of Rh-diphosphine complex catalyst with BINAP[43], BISBI and PHENAP [44] by Eastman Kodak **(**Figure 1.2**)**. Normal to branched ratios of 96/4 was observed at very low phosphine/Rh ratios. van Leeuwen and coworkers developed the series of xanthene based diphosphine (XANTPHOS) ligands having wide range of bite angles,[45] which give the highest n/i ratio (35-70) reported so far for hydroformylation of higher olefins[46].

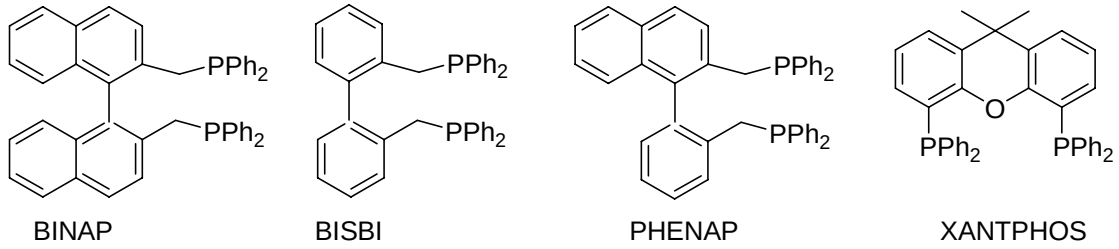

Figure 1.2: Structures of some diphosphine ligands

The promising results obtained by using the above bulky diphosphines as ligands in the homogeneous hydroformylation reaction, prompted the development of their sulphonated water-soluble analogs, BISBIS, NORBOS[47a], BINAS[47b] and sulfo-XANTPHOS[47c]. Their water-soluble rhodium complex catalysts also gave good activity with very high n/i ratio (in the range of 24-40) in aqueous biphasic medium.

Casey[48a] developed the concept of 'natural bite angle' as an additional characteristic of diphosphine ligands, based on molecular mechanics calculations, similar to the concept of cone angle proposed by Tolman[48b] for monophosphines, to determine the steric properties of ligands. Catalytic results and selectivities for linear versus branched products can now be estimated from the ligand's structure in some cases and from their electronic parameters. Researchers now have an almost rational understanding of the regioselectivities to be expected, since classifications of ligands in terms of their steric demands are available.

Besides the influence of the electronic and steric properties of organometallic catalyst of suitable central atom or ligands, the variation of application phase has been

another subject of intensive research in homogeneous catalysis[49].In this context aqueous –biphasic reaction has been studied after its commercial success in catalyst product separation for lower olefins. Other biphasic systems such as fluorous biphasic system (FBS)[50], ionic liquid –organic, ionic liquid –aqueous[51] biphasic systems, and use of supercritical fluids[52] as reaction media are also reported. One of the major limitations of the aqueous biphasic catalysis is their lower reaction rate for the hydroformylation of higher olefins due to their poor solubility in the aqueous catalyst phase. Different attempts to increase the solubility of higher olefins in water (catalyst phase) based on introduction of various additives such as co solvents[53], surfactants[54], phase transfer agents[55] and promoter ligands[56] to the reaction mixture were reported, with reasonable successes.

Intensive research is also in progress on the immobilization of metal complexes on to a variety of organic and inorganic solid supports to achieve efficient catalyst product separation. Anchored catalysts[57] in which well-defined metal complexes are bound to a solid support either by covalent/ionic bonding or by chemi or physisorption; polymer bound catalysts[58] in which organic polymers have been used to graft metal complexes on an insoluble support; encapsulated catalysts[59] where the metal complexes are entrapped in the pores of the zeolites matrix; Supported Liquid Phase Catalysts (SLPC) [60] where the catalyst is immobilized in a thin film of a high boiling solvent adsorbed on a solid support and Supported Aqueous Phase Catalysts (SAPC)[61] where the catalyst is immobilized in a film of water adsorbed on a solid support, are some of the approaches for heterogenization. The heterogenization of homogeneous complexes using either biphasic catalysis or solid supported catalysts is discussed in detail in later sections.

Among various substrates, simple linear olefins are the most important for commercial applications of hydroformylation, and are hence some of the most studied substrates. Generally, olefins with 2 to 5 carbon atoms (C_2 to C_5) are considered as lower olefins and olefins with six or more carbon atoms (C_6 onwards) are considered higher olefins[62]. In lower olefin hydroformylation, propene hydroformylation accounts for nearly 73% production, thus the economic importance of hydroformylation is mainly based on the hydroformylation of propene. The key issues in lower olefin

hydroformylation are (i) Regioselective synthesis of *n*-aldehydes, (ii) Chemoselectivity to the oxo-aldehydes (iii) Catalyst-product-separation, and (iv) Mechanistic understanding.

Higher olefins (C_6 and onwards) account for more than 20% of the commercial hydroformylation capacity and cobalt dominates rhodium by nine times[63]. Almost all the products of higher olefins hydroformylation are converted to either plasticizer or detergent grade oxo alcohols. Higher olefins hydroformylation is more complicated and has additional issues to that observed in lower olefin hydroformylation. (i) Isomerization of higher olefins is a prominent side reaction under hydroformylation conditions, which ultimately affects the TON and n/i ratio. (ii) Heavy ends formation at higher reaction temperatures (via condensation, trimerization, aldolization, acetalization side reactions). (iii) Catalyst-product separation is more cumbersome as the aldehydes of higher olefins are high boiling and their distillative separation from reaction mixture is difficult and (iv) Aqueous biphasic hydroformylation as an alternative is extremely slow as higher olefins have very poor solubility in water.

Functionalized olefins are important substrates for hydroformylation as they produce dual functional organic compounds, which are very useful fine chemicals for organic synthesis. The commercial utility of hydroformylation of functionalized olefins is very well demonstrated by various processes[64] like, Ajinomoto process for acrylonitrile hydroformylation to L-glutamic acid (Na-salt), Vit. A synthesis from diacetoxy butenes, Shell process for 1,3-propanediol from ethylene oxide etc. In spite of their importance, the research on functionalized olefins is lagging mainly because (i) Due to two functional groups, chemoselectivities and regioselectivities are often low. (ii) Substrates sometimes are unstable under hydroformylation conditions (iii) Products formed, sometimes act as catalyst poisons (iv) In general, reaction rates are lower than those found for linear olefins.

1.3 Kinetics and mechanism of the hydroformylation reaction

Compared to the large volume of literature on catalysis of hydroformylation, there are not many reports on the kinetics of this important reaction using either homogeneous, biphasic or heterogeneous catalysts[65-85]. The study of the kinetics of any reaction is essential in understanding the active catalyst and catalytic mechanism. Brown and Wilkinson[65] studied the kinetics of hydroformylation of 1-hexene using $HRh(CO)(PPh_3)_3$

complex catalyst at 298K. The rate of hydroformylation was first order with respect to catalyst and hexene concentration and hydrogen partial pressure. The rate was negative order with respect to partial pressure of carbon monoxide and PPh_3 concentration. The observed trends have been explained based on the mechanism shown in Scheme 1.2. The negative order dependence of the reaction rate at higher carbon monoxide pressures is mainly due to the formation of di- and tri-carbonyl rhodium complexes $(RCO)Rh(CO)_2(PPh_3)_2$ and $(RCO)Rh(CO)_3(PPh_3)$, which are unreactive towards oxidative addition of hydrogen. At lower carbon monoxide partial pressure, the formation of these species is expected to be negligible. A positive order dependence of the rate is observed for CO at low pressure as the mono carbonyl species $(RCO)Rh(CO)(PPh_3)_2$ is stabilized.

Chaudhari and co-workers have extensively studied kinetics and reaction engineering aspects of hydroformylation of a variety of olefinic substrates such as 1-hexene[66a], vinyl acetate[66b], allyl alcohol[66c], 1-decene[66d], 1-dodecene[66e], styrene[66f] and 1,4 diacetoxy butene[66g]. The trends observed are generally first order with respect to catalyst, substrate (upto a certain concentration) and hydrogen, whereas inhibition was observed with partial pressure of CO. Kalck and co-workers[67] have studied the hydroformylation of terminal olefins using a dimeric $[Rh(\mu\text{-}S^tBu)(CO)(PPh_3)]_2$ catalyst. Preliminary kinetic studies show that CO has an inhibiting effect but surprisingly the reaction is also inhibited by high pressure of hydrogen.

Kinetics of biphasic hydroformylation of ethylene[68a], 1-octene[68] and styrene[68c] using water-soluble Rh-TPPTS catalyst has also been studied and the rate equations were proposed by Chaudhari and co-workers. In contrast to the earlier reports using homogeneous catalysts, the substrate inhibition with CO was not observed due to the lower concentrations of dissolved CO in the aqueous catalyst phase. Purwanto and Delmas[69] have reported the effect of co-solvents on the kinetics of biphasic hydroformylation of 1-octene using $[Rh(COD)Cl]_2$ / TPPTS catalyst. Due to enhancement of CO solubility in the presence of the ethanol co-solvent, a substrate inhibition with CO was observed. The kinetics of hydroformylation of various olefins in aqueous biphasic medium has also been reviewed in detail[70].

The kinetics of hydroformylation of propylene[71a], allyl alcohol[71b] and 1-butene[71c] using supported liquid phase catalyst (SLPC), $HRh(CO)(PPh_3)_3$ was reported by Scholten and coworkers. The reaction order for propylene was found to be one, while for hydrogen the order was close to zero. The reaction order in CO pressure was found to 0.23 at lower CO pressure to 0.08 at higher CO pressure. The kinetics of hydroformylation of 1-octene[72], styrene[67c] and linalool[73] was studied using Rh/TPPTS supported aqueous phase catalyst (SAPC). The trends were similar to those observed in the homogeneous medium except for the substrate inhibition observed at higher concentration. Similar observations were reported for the kinetics of hydroformylation of 1-hexene using Rh/TPPTS complex exchanged on anion exchange resin[74].

In general, the trends observed for kinetics of hydroformylation using phosphine-modified rhodium catalysts for different parameters can be summarized as follows.

1. First order in catalyst concentration
2. First order in hydrogen partial pressure
3. First order in olefin concentration and in some cases substrate inhibition at higher concentration.
4. At lower CO partial pressure (P_{CO} < 1 MPa), positive order and at high CO partial pressure, negative order

The detailed literature on kinetics of hydroformylation of olefins is shown in Table 1.4.

Table 1.4: Literature on kinetics of hydroformylation of olefins using rhodium catalysts

Sr. no.	Catalyst	Olefin	Range of conditions		Remarks	Rate model	Ref.
			T, K	P_{syngas}, MPa.			
1	$Rh_4(CO)_{12}$	Heptene Cyclohexene	348	15.2	R independent of D R ∝ A, C, D	$R = \frac{kAC}{B}$ $R = KA^{1/2}C^{1/4}D$	75
2	$Rh_4(CO)_{12}$	Hexene	423	B<90 B>90	R ∝ A, B, $C^{1/4}$, D R ∝ A, B, $C^{1/4}$, D	-	76, 77
3	$Rh(CO)Cl(PPh_3)_2$	Olefins	343-323	3.5-777	R ∝ D, (A+B)		78
4	$HRh(CO)(PPh_3)_3$	Hexene	298	0.65	R ∝ A, B, D R ∝ 1/B	$R = \frac{kACD}{B}$	65
5	$HRh(CO)(PPh_3)_3$	Hexene	363		R ∝ A, B, D R ∝ 1/B	$R = \frac{kACD}{B}$	79
6	$HRh(CO)(PPh_3)_3$	Hexene	303-323	2.2	Critical conc. of catalyst is needed	$R = \frac{kAC(C_0 - C_c)D}{(1+K_BB)^{2.5}(1+K_DD)^2}$	66a
7	$HRh(CO)(PPh_3)_3$	Allyl alcohol	363-383	5.4	R ∝ $A^{1.5}$, B, D R ∝ 1/B	$R = \frac{kA^{1.5}BCD}{(1+K_BB)^3(1+K_DD)^2}$	66c
8	$[Rh(CO)_2Cl]$	Vinyl acetate	353	-	-	$R = \frac{kABCD}{(1+K_CC+K_DD^2}$	66b
9	$HRh(CO)(PPh_3)_3$	Poly-butadiene	350-390	2.17	-	$R = \frac{kAC^{\alpha}D^{\beta}}{B}$	80

Sr. no.	Catalyst	Olefin	Range of conditions		Remarks	Rate model	Ref.
			T, K	P_{syngas}, MPa.			
10	$Rh(CO)_{2(}acac)$/ tris(2-ter-butyl-4-methyl phenyl phosphine	Octene Cyclo-hexene	323-363	-	-	$R = \frac{kAC}{(K_B B)}$ $R = \frac{K_1 kCD}{(K_1 + B)}$	81
11	$HRh(CO)(PPh_3)_3$	1-Decene	323-363	2.72	$R \propto A^{1.2}$, C, D $R \propto 1/B$	Mechanistic model	66d
12	$HRh(CO)(PPh_3)_3$	1-dodecene	323-363	4.08	R ∝ A,1/B, C, 1/D	$R = \frac{kA^* B^* CE}{(1 + K_B B^*)^2 (1 + K_E E)}$	66e
13	$HRh(CO)(PPh_3)_3$	styrene	333-353	-	R ∝ A, 1/B, C, independent on D	$R = \frac{kK_1K_2ABCD}{1 + K_1B + K_1K_2BD + K_1K_2K_3B^2D + K_1K_2K_3K_4B^3D}$	66f
14	$RhCl(CO)(TPPTS)_2$/ TPPTS	Propylene-	373	3.1	R ∝ A, 1/B, C, D Kinetics was investigated in aqueous phase.	$r_0 = \frac{A_0 \exp(-E/(R_G T)) p_{H_2} p_{CO} p_P C_{Rh}}{(1 + k_1 p_{H_2})(1 + k_2 p_{CO})^2 (1 + k_3 p_P)^2 (1 + k_5 C_L)^3}$	82
15	$HRh(CO)(PPh_3)$ and $RhCl(1,5\text{-}COD)]_2$ /TPPTS	Ethylene	333-373	5.5	Organic ($R \propto A^{1.5}$, 1/B, C, 1/D) and Aqueous phase (R ∝ A,1/B, C, 1/D) rates were compared	$R = \frac{KA^{*1.5} B^* E^*}{(1 + K_B B^*)^2 (1 + K_E E^*)^2}$ $R = \frac{34550 A^* B^* E^*}{(1 + 278 B^*)^2 (1 + 3829 E^*)^2}$	66h
16	$HRh(CO)(PPh_3)_3$	1,4-diacetoxy-butene	338-358	6.8	R ∝ A, ,C, 1/D independent on B	$r_1 = \frac{kK_1K_2C_0C_1[CO][H_2]}{(1 + K_1[CO] + K_1K_2[CO]C_1 + K_1K_2K_3[CO]^2C_1 + K_1K_2K_3K_4[CO]^3C_1}$	66g

Sr. no.	Catalyst	Olefin	Range of conditions		Remarks	Rate model	Ref.
			T, K	P_{syngas}, MPa.			
17	$RhCl(AsPh_3)_3$	1-hexene	353	6.0	R ∝ A,1/B, 1/C, 1/D	$R=\frac{k_0 e^{-E/RT}[1-hexene][H_2[CO][C]}{(1+K_1[CO][1-hexene]+K_2[CO]^2[1-hexene]}$ $K_4[CO]^3[1-hexene])$	83
18	$[RhCl(1,5\text{-}COD)]_2$ /TPPTS	Octene	333-343	2.0	Biphasic Catalysis	$R=\frac{kABCD}{(1+K_B B)^2(1+K_A A)}$	69
19	$[RhCl(1,5\text{-}COD)]_2$ /TPPTS	1-octene	323-343	5-15	R ∝ $A^{0.4}$,1/B, C, D Kinetics in presence of ethanol cosolvent	$R=\frac{k'_2 ABCD}{1.0+K_a A+K_b AB+K_c B^2}$	68b
20	$[RhCl(1,5\text{-}COD)]_2$ /TPPTS-	1-octene	343	5-15	R ∝ $A^{0.4}$,1/B, C, D pH Effect in presence of ethanol	-	68d
21	Polymer immobilized Rh-complex	Ethylene	373	-	-	$R=\frac{kACD}{B^{0.5}}$	84
22	SLPC-$HRh(CO)(PPh_3)_3$	propylene	363	1.57	R ∝ A^0, $B^{0.23\text{-}0.08}$, D	$R=k_0[Rh]P_{C3}{}^a=P_{H2}{}^b P_{CO}{}^c \exp(-Ea/RT)$	71a
23	SLPC-$HRh(CO)(PPh_3)_3$	1-butene	333-373	1.2	R ∝ $A^{0.22}$, $B^{0.08}$, $D^{1.41}$	$R=k_0 P_{butene}{}^a P_{H2}{}^b P_{CO}{}^c \exp(-Ea/RT)$	71c
24	SAPC-$HRh(CO)(TPPTS_3)_3$	linalool	363	1	R ∝ A+B, C, D	$R=kmD_2C_{lin}P$	73
25	SAPC-$HRh(CO)(TPPTS_3)_3$	1-octene	373	1	R ∝ A *1*/B, C,1/D	$R=\frac{kC_{H2}C_{CO}C_{cat}C_{oct}}{(1+K_A C_{H2})^l(1+K_B C_{CO})^m(1+K_D C_{oct})^n}$	72a

Sr. no.	Catalyst	Olefin	Range of conditions		Remarks	Rate model	Ref.
			T, K	P_{syngas}, MPa.			
26	Rh/TPPTS complex on to an anion exchange resin Amberlite IRA-93	1-hexene	353-373	4.14	R ∝ A,1/B, C, 1/D	$R = \frac{k P_A P_B [D]}{1.0 + K_b P_B^2}$	74
27	Tethered Rh cat supercritical	1-hexene	348	2.4	R ∝A, 1/B, C, D (P_{CO2} 18.64)	$(r_{HF})_0 = \frac{K_A[\text{1-hexene}]_0[H_2]_0[CO]_0}{1 + K_C[\text{1-hexene}]_0 + (1 + K_B[CO]_0)^2}$	85

Where, R = Rate of reaction A = P_{H2}; B = P_{CO}; C = Concentration of the catalyst; D = Concentration of olefin; P = PPh_3; R = Rate of reaction; k = Rate Constant

Wilkinson and co-workers[86] reported the first mechanistic study on the hydroformylation of olefins over 35 years ago. The catalytic cycle (Scheme 1.2) proposed by them is well accepted, however new insights largely concerning the structure, relative stability, exchange processes of either active intermediates or resting states continue to be discovered as new spectroscopic or computational techniques have become available. This has enabled researchers to explain in detail the mechanism of the hydroformylation reaction with rhodium and cobalt catalyst involving monodentate as well as bidentate ligands. The newly accepted mechanism may have similarities with the Wilkinson mechanism; however particularly for the newer ligands, variation in the mechanism of hydroformylation have been reported[30]. The hydroformylation reaction using phosphine modified rhodium complex proceeds either via 'Associative' or 'Dissociative' pathways. $HRhCO(PPh)_3$ after several equilibria generates the key active species $HRh(CO)_2(PPh_3)_2$ (Species C) as shown in scheme 1.2.

The associative mechanism is initiated by the coordination of an olefin to $HRh(CO)_2(PPh_3)_2$ to give a alkyl rhodium complex $RRh(CO)_{2(}PPh_3)_2$ (E). On the other hand the dissociative pathway is initiated by dissociation of either PPh_3 or carbon monoxide ligand from $HRh(CO)_2(PPh_3)_2$ to give $HRh(CO)_2(PPh_3)$ or $HRh(CO)(\ PPh_3)_2$. Olefin coordination, formation of the alkyl complex and coordination of a PPh_3 or carbon monoxide ligand generates the alkyl rhodium complex $RRh(CO)_2(PPh_3)_2$ (E).

For both the mechanisms, subsequent steps are the same, which involve: Alkyl migration (CO insertion) leading to the formation of the acyl complex (F), Oxidative addition of hydrogen (considered to be the RDS) to give the species (G), Reductive elimination of product from the species (G) to regenerate the active species (B) and followed by (C).

Today the dissociative mechanism is generally considered the major pathway especially under industrial operating conditions. The associative mechanism is preferred at very high concentration of catalyst and phosphine

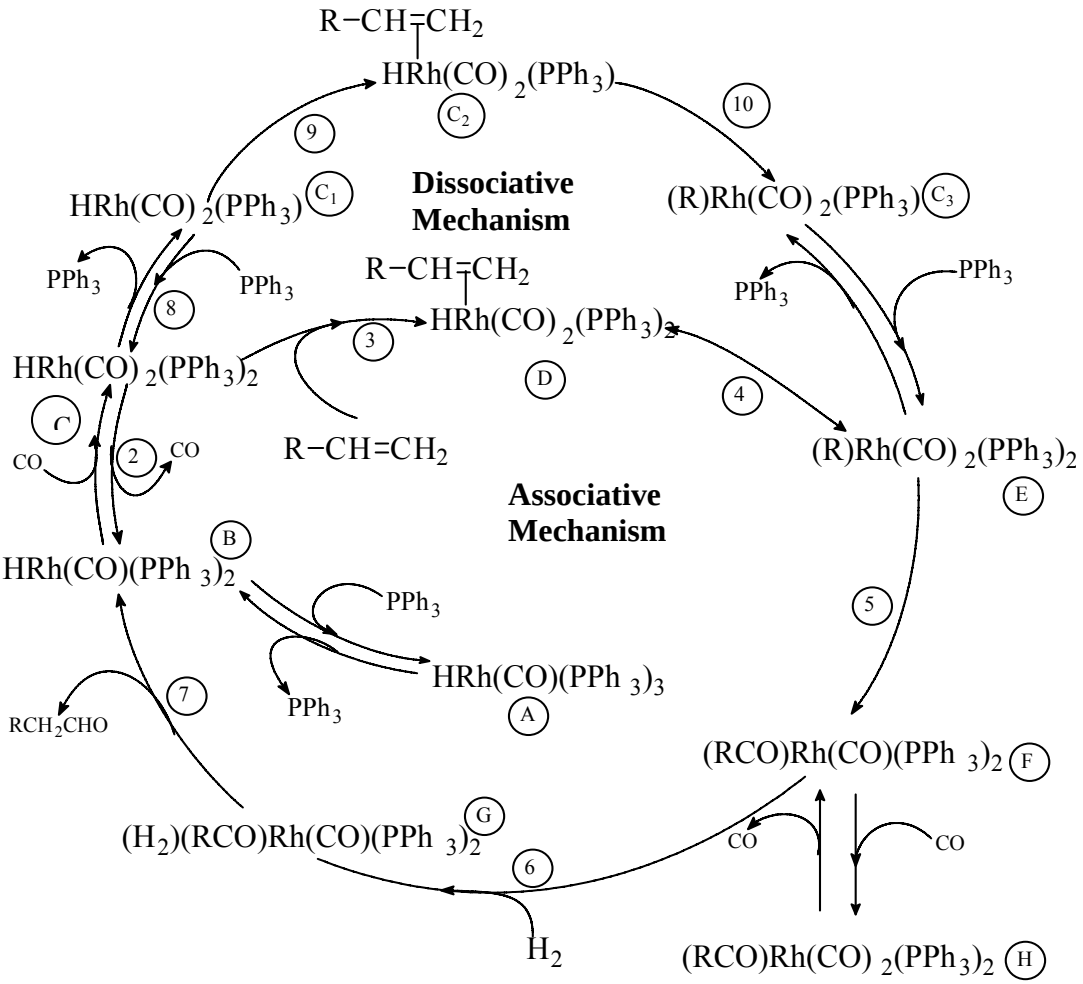

Scheme 1.2: Mechanism for hydroformylation of olefins proposed by Wilkinson and coworkers

Since the major objective of this work was to study hydroformylation of complex substrates like terpenes, and to address the catalyst-product separation issues with special reference to higher olefins hydroformylation, a detailed literature search was conducted keeping these objectives in mind. An overview of the important investigations on (i) hydroformylation of terpenes using rhodium complex catalyst and (ii) hydroformylation of 1-decene using biphasic catalysis and heterogenized homogeneous catalysts is presented in the following sections. Initially the literature on terpene hydroformylation has been presented in section 1.4 and thereafter literature on 1-decene hydroformylation has been presented alongwith a detailed account on heterogenization of homogeneous complexes for the hydroformylation of higher olefins (section 1.5).

1.4 Literature review on hydroformylation of terpenes:

Terpenes are widespread in nature, mainly in plants as constituents of essential oils. The building block of the terpenes is the isoprene unit (C_5H_8). Terpene feedstocks are a natural, renewable and sustainable supply of building blocks for the fine chemical industry. Within this industry, they are an important source of intermediates and ingredients for flavors and fragrances. Major catalytic transformations of the monoterpene feedstocks involve isomerization, hydration, condensation, hydroformylation, hydrogenation, cyclization, oxidation and rearrangement reactions[87]. From the plethora of terpenes available, camphene, limonene, myrcene, carene, carvone, citral, α- and β-pinene, are the most studied.

Naturally occurring monoterpenes are a useful source of inexpensive olefins. Their hydroformylated products are useful in the perfume, flavor and pharmaceutical industries[87]. There is very little information in the literature concerning the hydroformylation of terpenes and diastereoisomeric excess (d.e.) achieved in this reaction. Examples of some naturally occurring monoterpenes are shown in Figure1.3.

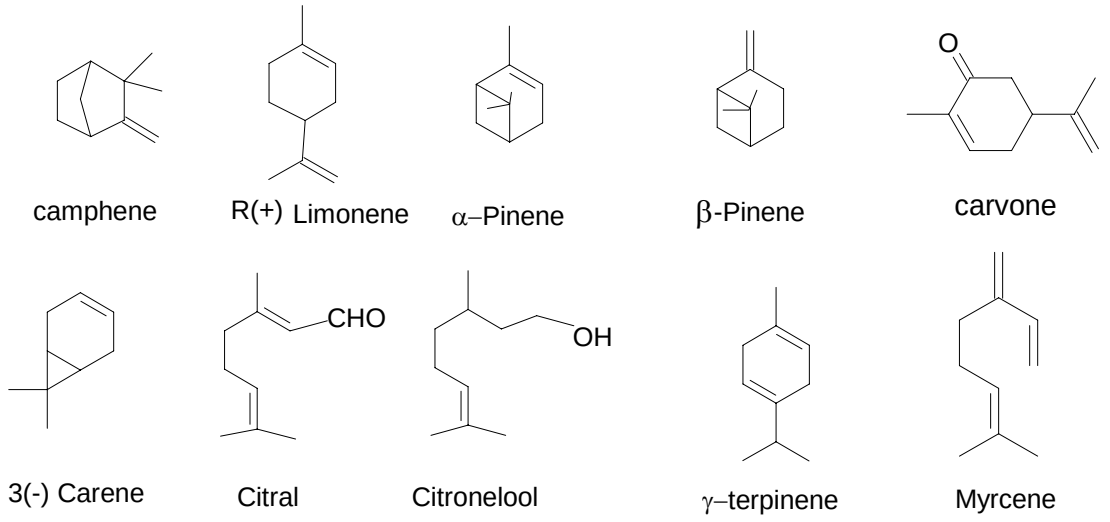

Figure 1.3: Some naturally occurring terpenes

A majority of studies on hydroformylation of terpenes have employed rhodium complex catalysts and very few reports are available on hydroformylation of terpenes using cobalt catalyst. Recently, platinum complexes alongwith tin are reported as catalysts for the hydroformylation of terpenes with desired distereoselectivity. The

detailed literature on hydroformylation of terpenes using homogeneous, biphasic and heterogenized catalysts has been discussed in the following sections.

1.4.1 Cobalt catalyzed hydroformylation of terpenes

The first report on hydroformylation of camphene was in the late 60's by Johnson and coworkers[88] using $Co_2(CO)_8$ catalyst. It was observed that camphene undergoes oxo reaction without any Wagner Rearrangement (under the acidic conditions of $HCo(CO)_4$, which is believed to be the catalyst), giving camphene-2-aldehyde as a product. The reaction conditions used were T=125-150^{0}C and syngas pressure of 3000 psi.

Four representative terpenes such as α-pinene, dipentene, α-terpinene, and myrcene were hydroformylated in presence of $Co_2(CO)_8$, each in three solvent systems-*viz*- hexane, methanol, and 6% aqueous-acetone at 150^{0}C under identical conditions. Dipentene and α -pinene showed similar reactivities, products and yields in methanol and aqueous acetone. Myrcene and α-terpinene reacted at much slower rates. All reactions led to complex, highly saturated mixtures of monofunctional aldehyde products, with little or no bifunctional products. Surprisingly, α-pinene and dipentene yield identical, unsaturated ether in methanol. The possible reaction schemes and the rate behavior observed have been described[89].

1.4.2 Rhodium catalyzed hydroformylation of terpenes

Various monomeric as well as dimeric rhodium complexes were used as catalyst precursors for terpene hydroformylation. Wilkinson and coworkers reported the hydroformylation of *dl*-limonene using the $HRhCO(PPh_3)_3$ catalyst at room temperature and atmospheric pressure of syngas. The rate of the reaction was poor compared to that observed for linear olefins[90]. Similarly, hydroformylation of terpinolene, *S*-(-)-limonene, α-and β-cedrenes, α- and β-caryophyllenes and caryophyllene oxide in the presence of $HRhCO(PPh_3)_3$ catalyst showed hydroformylation of the endocyclic bond except for the terpinolene[91]. These new compounds could be used in perfumery.

Hydroformylation of α-pinene, using rhodium catalyst led to the diastereoselective synthesis of (+)-3-pinanecarbaldehyde. Depending on the reaction conditions, the aldehyde selectivities obtained were about 85%[92]. β-pinene was formed as a by-product, by isomerization of the double bond. In the analogous hydroformylation of (+)-3-carene, the reaction proceeded with a selectivity of only 60-65% to the (+)-2-

caranecarbaldehyde owing to comparably little steric hindrance by the isopropylidene bridge[93]. (Scheme 1.3)

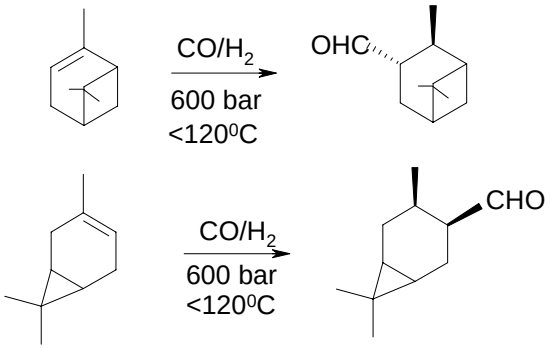

Scheme 1.3: Hydroformylation of α –pinene and (+)-3-carene

Hydroformylation of monocyclic and bicyclic monoterpenes (e.g. camphene, limonene, β-pinene, α-terpinene) was carried out at 70-160^{0}C under a pressure of 100-400 bar using $Rh(CO)Cl(PPh_3)_2/PPh_3$ catalyst system. The hydroformylation of camphene gives 3, 3 dimethyl-2-norbornaneacetaldehyde with about 77% yield[94]. Hydroformylation of limonene and β-pinene gave aldehyde yields of 83% and 67% respectively[95]. The hydroformylation of α-terpinene using the similar catalyst gave aldehyde yield of 68%, which have application in perfumes.

Hydroformylation of carvone in presence of rhodium 2-ethylhexanoate catalyst with triphenyl phosphine as a ligand yielded 80% of 3-(4-methyl -3-3-cyclohex-4-enyl) butyraldehyde. This aldehyde finds application as a cross linking agent in the preparation of polyurethanes[96]. Similarly, phosphine modified rhodium catalyst was used to produce various aroma chemicals by hydroformylation of terpenes and substituted olefins under mild reaction condition[97].

The effect of phosphorus ligands on the rhodium catalyzed hydroformylation of β-pinene and camphene has been reported. In unmodified $[Rh(COD)(OAc)]_2$ systems, β-pinene undergoes a fast isomerization to α-pinene. At longer reaction times and higher temperatures 80% chemoselectivity for β-pinene hydroformylation products (97% trans 10-formylpinane) was obtained[98]. The addition of various diphosphines, phosphines or phosphites improves the chemoselectivity and shifts the hydroformylation towards cis aldehyde. Camphene gave linear aldehyde, with virtually 100% regio- and

chemoselectivity in both modified and unmodified rhodium catalyst systems (Figure 1.4). The addition of phosphorus ligands favors the formation of *endo* isomer (exo/endo=1/1.5), whereas the exo/endo ratio is 1/1 in unmodified systems. Neither steric nor electronic parameters of the ligands have been found to significantly influence the diastereoselectivity of the camphene hydroformylation.

Figure 1:4: Hydroformylation products of β-pinene and camphene

Selective hydroformylation of limonene, α-pinene, β-pinene and camphene was carried out using rhodium catalyst[99] such as $[Rh(COD)(OAc)]_2$, $[Rh(COD)_2]OTs$, $[Rh(COD)_2]PF_6$. For β-pinene, higher temperature favours the formation of the thermodynamically more stable trans isomer. The addition of PPh_3 or dppe, dppp and DIOP ligands decreases the isomerisation of β-pinene into less reactive α-pinene and also switches the hydroformylation selectivity from trans to cis isomer. Limonene and camphene gives the diastereomeric mixtures of aldehydes (d.e. 10 and 15% respectively).

The hydroformylation of myrcene catalyzed by Rh and Pt/Sn catalysts containing different P-donor ligands leads to the formation of a nine mono- and dialdehydes[100]. The, 4-methylene-8-methyl-7-nonenal is the major aldehyde formed with Rh/Xantphos and Pt/Sn catalysts.

Hydroformylation of α-pinene using rhodium catalyst of the type $[Rh(COD)Cl]_2$ and $Rh(CO)Cl(PPh_3)_2$ yields 3-formylpinane with good conversion (46-91%) and moderate selectivity (52-71%)[101]. Hydroformylation of limonene using **[**$Rh(COD)Cl]_2$ alongwith various phosphite ligands e.g. tris(2-t-butylphenyl) phosphite, tris(2-phenylphenyl) phosphite, tris(2-t-butyl 4-methyl phenyl) phosphite gives very high rates (TOF = 1500-4000 h^{-1}) at reaction conditions of 90^0C and syngas pressure of 15 bar. At comparable reaction conditions, Rh-TPP system gives activity in the range of only 100 h^{-1}. These high rates observed were explained in terms of electronic and steric properties of the phosphite ligands[102].

Hydroformylation of camphene in the presence of $[Rh(COD)Cl]_2$ and various phosphine ligands under 10 MPa syngas was investigated at 100°C[103]. The selectivity to

exo- or endo-products (aldehyde and/or alc.) was found to be decided by the cone angle of the ligand carried by the rhodium carbonyl. The ligand with large cone angles such as P(*o*-tolyl)$_3$ tend to give more exo-alcohols because the attack of the hydrogen occurs from the position cis to the complex. The bidentate phosphine ligands which have relatively smaller bite angles, give more endo-product. The possible mechanism for the formation of exo- and endo-products has also been discussed.

The dinuclear rhodium complexes [$Rh_2(\mu\text{-}SR)_2(CO)_2L_2$], where L= PPh_3, $P(OPh)_3$ or $P(OMe)_3$ were found to be efficient and selective precursors for the hydroformylation of limonene, isopulegol, isopulegyl acetate, α- and β–pinene, (-)-camphene and other terpenes[104a]. At higher pressures (13-20 bar), (-)-α-pinene and (-)-camphene were selectively hydroformylated and d.e. values in a range of 26 to 85% were obtained with phosphite ($P(OPh)_3$) or diphosphine (dppb, dpph or DIOP) ligands[104b]. The aldehyde selectivity was found to depend on the type of ligand, solvent, the nature of the monoterpene and syngas pressure used. Other dinuclear complexes of the type [$Rh_2(\mu$-penicillamine$)_2(CO)_4$][$OTf]_2$ and [$Rh_2(\mu$-cysteine$)_2(CO)_4$][$OTf]_2$ were also efficient catalyst for the hydroformylation of β-pinene and trans-isolimonene (Scheme 1.4**)** in the presence of four equivalents of $P(OPh)_3$ in triethyl orthoformate as solvent/reactant to yield corresponding aldehyde and acetals[105].

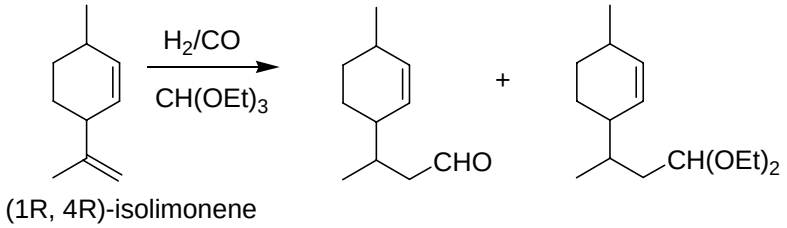

Scheme 1.4: Hydroformylation of trans-isolimonene in triethyl orthoformate.

Rhodium clusters like $Rh_6(CO)_{16}$, $Rh_4(CO)_{12}$ and mixed clusters of the type $Co_2(CO)_8$/ $Rh_6(CO)_{16}$, $Co_2(CO)_8/Ru_3(CO)_{12}$, $Rh_6(CO)_{16}/Ru_3(CO)_{12}$ and $Co_2(CO)_8/Rh_6(CO)_{16}$ both unmodified and modified with PPh_3, $P(OPh)_3$ have been reported for hydroformylation of α- and β–pinene[106]. No synergistic rate enhancement in the hydroformylation of α–pinene was observed. Similarly bimetallic catalyst $CoRh(CO)_7$ as such or modified with $[N(PPh_3)_2]Cl$ and bis(diphenylphosphino)ethane (dppe) ligands are reported for diastereoselective hydroformylation of((1S,5S)-(-)- and (1R,5R)-(+)- β –pinene[107].

Hydroformylation of myrcene and limonene in a toluene/water biphasic system has been reported to give high activity in presence of cationic surfactant cetyltrimethylammonium chloride (CTAC) using Rh/TPPTS (tris(3-sulfonatophenyl)phosphine) catalyst[108]. There was no reaction for myrcene in biphasic medium while in presence of high concentration of CTAC about 95% conversion could be obtained in 24 hours (TOF=33 h^{-1}). Surprisingly, such enhancement in rate was not observed for camphene hydroformylation**.** Hydroformylation of limonene in aqueous biphasic media using $[Rh_2(\mu\text{-}S_tBu)_2(CO)_2(TPPTS)_2]$/TPPTS catalyst showed poor rates and conversion due to very low solubility of the substrate in water. The addition of small amounts of PPh_3 as a catalyst binding ligand (CBL) or β-cyclodextrin as a phase transfer agent enhanced the rate of the reaction[109].

Haza et al[110] have studied the hydroformylation of monoterpenes such as limonene, linalool and geraniol by SAPC catalyst using $[Rh_2(\mu\text{-S-t-Bu})_2(CO)_2(TPPTS)_2]$ as the catalyst precursor. The structure of the monoterpene, as well as the size of the pores and the amounts of water in the support were the determining factors contributing to activity in the SAPC hydroformylation of monoterpenes. Tethered rhodium complexes derived from $Rh(CO)_2(acac)$ and the commercially available 3-(mercapto)propyl- and 3-(1-thioureido)propyl-functionalized silica gel, respectively, have been used as catalysts in the hydroformylation of limonene[111]. Good conversion (75–88%) was obtained with 100% aldehyde selectivity after 6 h of reaction at 80^0C. The activity of this catalytic system decreased after three recycles**.** $Rh(PPh_3)_3Cl$ anchored on montmorillonite clay showed reasonably good activity for hydroformylation of limonene at 70^0C and 60 atm syngas pressure[112].

1.4.3: Platinum catalyzed hydroformylation of terpenes

(+)-R-Limonene and (-)-R-carvone underwent hydroformylation in the presence of Pt-bisphosphine-$SnCl_2$ catalyst systems to yield exclusively the linear products. The diastereomeric composition of the aldehydes is dependent on of the type and nature of chelating phosphine[113]. The hydroformylation of (+)-(R)-limonene**,** (+)-(1R)-isolimonene**,** camphene**,** and (+)-β-cedrene resulted in the regiospecific formation of the corresponding linear aldehyde in the presence of homogeneous platinum and, in some

cases, rhodium catalysts[114]. The epimeric composition of products could be influenced slightly by optically active catalyst formed with chiral bidentate phosphines.

Hydroformylation of limonene using $PtCl_2(PPh_3)_2/PPh_3/SnCl_2$ and $PtCl_2$(diphosphine)/$PPh_3/SnCl_2$ leads to two diastereoisomers of 4,8-dimethyl-bicyclo[3.3.1]non-7-en-2-ol, useful as perfumes, in one step[115] (Scheme 1.5). The diphosphines used were dppp and dppb. The $PtCl_2$(dppb)/$PPh_3/SnCl_2$ system, gives 82% selectivity at 95% conversion of limonene**.** This catalyst acts as a bifunctional catalyst that promotes both the hydroformylation of limonene and then intramolecular cyclization of the aldehyde formed in a convenient one-pot synthesis.

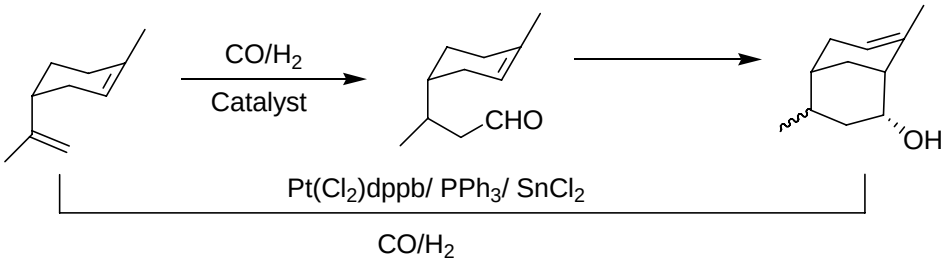

Scheme 1.5: One-step hydroformylation of limonene using bifunctional catalyst.

(-)-β-Pinene, R-(+)-limonene, and (-)-camphene have been hydroformylated regiospecifically to give exclusively the linear aldehydes using $PtCl_2(PPh_3)_2/SnCl_2/PPh_3$, and $PtCl_2$(diphosphine)/$SnCl_2/PPh_3$[116]. The diphosphines used were dppe, dppp and dppb. The hydroformylation of β-pinene results in trans-10-formylpinane with a 98% diastereoisomeric excess (d.e.), while limonene and camphene gave the diastereoisomers of the corresponding aldehydes in approximately equal amounts (d.e. of ca. 10 and 15%, respectively). Under optimized conditions, chemoselectivities for aldehyde formation of ~ 90% have been attained for all monoterpenes studied. Platinum/tin/(*R*)- or (*S*)-BINAP (2,2'-bis(diphenylphosphino)-1,1'-binaphthyl) system gave the highest d.e. of 60% with ca. 90% chemoselectivity for hydroformylation products at 90% camphene conversion[117]. The detailed literature on hydroformylation of terpenes is presented in Table1.4.

In summary, terpenes are an important class of olefins for producing the aldehydes having perfumery value. Although hydroformylation of various terpenes with different transition metals complex catalyst has been studied, their rates of hydroformylation were very poor. The most studied terpenes were limonene and β-

pinene. The highest rates were observed for monocyclic terpene such as limonene but for bicyclic terpenes like β-pinene and camphene poor rates were observed due to their steric properties. There are very few reports available on the hydroformylation of camphene. The maximum TOF and d.e. obtained for hydroformylation of camphene is 80 h^{-1} and 60% respectively using Pt/BINAP catalysts.

Table 1.5: Literature on hydroformylation of terpenes

Sr. no.	Substrate	Catalyst System	Reaction conditions.			Result				Remark	Ref.
			T ºC	P_{syngas}, psi	t, (h.)	Conv. (%)	Sel/ Yield (%)	d.e.	TOF h^{-1}		
1	Camphene	$Co_2(CO)_8$	125-150	3000	1.5	75	7.1	-	20	First report on synthesis of aldehydes and their derivatives by terpene hydroformyaltion.	88
2	α-Pinene, Dipentene, α-Terpinene, Myrcene	$Co_2(CO)_8$	150	3000	-	-	-	-	2-5	Dipentene and α-pinene react faster than α-terpinene and myrcene.	89
3	dl-Limonene	$HRhCO(PPh_3)_3$/ PPh_3	25	15	-	-	-	-	7	Wilkinson catalyst hydroformylate limonene with poor rates at mild reaction conditions.	90
4	(-)-α-Pinene	$Rh_4(CO)_{12}$	100	4500-10000	-	-	85	1.3:1		Isomeric aldehydes obtained from β-pinene formed during the reaction.	92
5	(+)-3-Carene	$Rh_4(CO)_{12}$	100	4500-10000	-	-	60-65	-	-	Lesser aldehyde selectivity is explained on the basis of steric hindrance of substrate.	93
6	α-Pinene	$[Rh(COD)Cl]_2$/ $RhCOCl(PPh_3)_2$	80-110	9555	6-12	46-91	52-71	-	-	Preparation of various derivatives of α-pinene by hydroformylation.	101

Sr. no.	Substrate	Catalyst System	Reaction conditions.			Result				Remark	Ref.
			T ºC	P_{syngas}, psi	t, (h.)	Conv. (%)	Sel/ Yield (%)	d.e.	TOF h^{-1}		
7	Limonene, Camphene, α-Terpinene, β-Pinene	$RhCOCl(PPh_3)_2$/ PPh_3	120-130	3000	4	-	77	-	19	Process having industrial importance for the production of the perfumery chemicals.	94
8	α-Terpinene	$RhCOCl(PPh_3)_2$/ PPh_3	130-140	3000	5	-	68	-		Products constitute new perfume with salicylate and cumin perilla note and extraordinary retentivity.	95
9	Limonene	$[Rh(COD)(\mu\text{-}OAc)]_2$/various phosphite ligands	90	205 $CO:H_2$ =2:1	0.5-2	90%	-	-	3500 - 4000	High rates observed explained in terms of electronic and steric properties of the phosphite ligands.	102
10	Carvone	Rhodium 2-etthylhexanoate/ PPh_3 $RhCl(PPh_3)_3$/ PPh_3	150	4100	1-4	-	80	-	-	The keto-butyraldehydes produced used as crosslinking agents in the preparation of polyurethanes.	96
11	Various terpenes	Phosphines modified Rhodium catalyst	Details not found								97
12	Camphene	$[RhCODCl]_2$/ various phosphine ligand	100	1470	-	-	-	-	-	Influence of ligand cone angles on the selectivity of exo or endo (ald./alc.) products. Possible mechanism for exo and endo product formation discussed.	103

Sr. no.	Substrate	Catalyst System	Reaction conditions.			Result				Remark	Ref.
			T ºC	P_{syngas}, psi	t, (h.)	Conv. (%)	Sel/ Yield (%)	d.e.	TOF h^{-1}		
13	α-and β – Pinene, Limonene, Isopulegol, Isopulegyl-acetate	$Rh_2(\mu\text{-S-t-Bu})_2CO_2L_2$(L= PPh_3, $P(OPh)_3$, $P(OMe)_3$	85	75	16	43-94	87.5-100	1 (cis/ trans)	-	The effects of P- containing ligands, solvents, and the nature of monoterpene on the reaction and regioselectivity were investigated.	104[a]
14	(+)-R-Limonene, (-)-R-Carvone	$PtCl(SnCl_3)^-$ /(bis phosphines) i.e. BDPP, DPPP	100-120	600	7-35	20-60	25	24- 26		The diasteriomeric composition of aldehyde varies with the chelating phosphines in the catalyst system.	113
15	Terpinolene, S- (-)-Limonene, α and β-cedrenes	$HRhCO(PPh_3)_3$	Details not found								91
16	α-and β – Pinene,	$Rh_6(CO)_{16}$ and $Co_2(CO)_8$	60-130	600	0.5-46	3-78	45-100	44 (cis)	0.8-9.0	$Rh_6(CO)_{16}$ gives 10-formylpinane as a major product in contract with mononuclear Rh-complex with phosphine ligands.	106
17	Limonene	$Rh(PPh_3)_3Cl$ anchored on montmorillonite clay	70	900	24	25	50	-	10	The reaction proceeds with simultaneous double bond hydroformylation and hydrogenation to give respective oxo products.	112

Sr. no.	Substrate	Catalyst System	Reaction conditions.			Result				Remark	Ref.
			T ºC	P_{syngas}, psi	t, (h.)	Conv. (%)	Sel/ Yield (%)	d.e.	TOF h^{-1}		
18	(+)-(R)-Limonene, (+)- (R)-Isolimonene, Camphene, (+)-β–Cedrene	[Rh (NBD)Cl]$_2$ and $PtCl_2$ catalyst with mono and bisphosphine ligands	100	1175	8-38	9-98	100	60 (endo) 38 (exo)	-	Good diastereoselectivities were obtained.	114
19	(-)-β–Pinene, 1R,4R-Isolimonene	[Rh_2 (μ-penicillamine)$_2$ $(CO)_4$][OTf]$_2$ and [Rh_2 (μ-cysteine)$_2$ $(CO)_4$] [OTf]$_2$ /$P(OPh)_3$	84	175-305	18	56-97	44-76	-	-	Direct synthesis of acetals of the terpenes was possible by using this new catalyst precursor and triethyl orthoformate as solvent and reactant.	105
20	(1S,5S)-(-) and (1R,5R)-(+)-β–Pinene	$CoRh(CO)_7$ and [$Rh_4(CO)_{12}$] with mono and bisphos-phine ligands	70-150	0.5-8	-	17-96	100	90 (trans)	-	The possible factors favoring the distereoselective hydroformylation of β–Pinene has been discussed.	107
21	Limonene	$PtCl_2(PPh_3)_2$ or bisphosphines /PPh_3/ $SnCl_2$	130	1300	50	83-100	29-100	-	-	$PtCl_2$(dppb)/PPh_3/ $SnCl_2$ shows excellent selectivity at higher conversions too.	115
22	Limonene Camphene α--Pinene	Rh_2(μ-S-t-Bu)$_2$ CO_2 L_2/ phosphite and diphosphite ligands	78	300	-	57	26-85	26	16-57	These reactions gives lower yields of aldehyde with 22% d.e.	104[b]

Sr. no.	Substrate	Catalyst System	Reaction conditions.			Result				Remark	Ref.
			T ºC	P_{syngas}, psi	t, (h.)	Conv. (%)	Sel/ Yield (%)	d.e.	TOF h^{-1}		
23	Limonene	$Rh_2(\mu\text{-S-t-Bu})_2CO_2(TPPTS)_2$ and β-cyclodextrin	80	220	20	-	14	-	6	No reaction was observed in aqueous biphasic medium but addition of catalyst binding ligand (PPh_3)or β-cyclodextrin as PTC led to the modest yield.	109
24	Limonene Camphene β -Pinene	$PtCl_2(PPh_3)_2/SnCl_2/PPh_3$ $PtCl_2$ (diphosphine) $/SnCl_2/PPh_3$	100	1350	45	40-53	100	16 (exo)	2	Selectivity at Sn/Pt =1 is good but it decreases at higher ratios (Sn/Pt =5).	116
25	β -Pinene Camphene Limonene	$[Rh(COD)(OAc)]_2$, $[Rh(COD)_2]OTs$, $[Rh(COD)_2]PF_6$ alongwith mono and bisphosphines	100	1350	4	10-95	52-74	60 (exo) 94 (trans)	-	Unpromoted catalyst shows selectivity to trans product while promoted catalyst system shows selectivity to cis product.	99
26	Camphene	$PtCl_2(PPh_3)_2/SnCl_2/$ $PtCl_2$ (diphosphine) $/SnCl_2/$ With chiral and achiral ligands like BINAP	100	1350	45	92	92	60 (exo)	2.2	(S)-BINAP catalytic system gives 90% chemoselectivity at maximum 90% conversion.	117
27	Camphene β -Pinene	unmodified $[Rh(COD)(OAc)]_2$ and Modified with ligands	60-120	1350	20	98	96	4-20 (endo)	5-66	This report deals with the study of temperature and ligand variation effect on distereoselectivity.	98

Sr. no.	Substrate	Catalyst System	Reaction conditions.			Result				Remark	Ref.
			T ºC	P_{syngas}, psi	t, (h.)	Conv. (%)	Sel/ Yield (%)	d.e.	TOF h^{-1}		
28	Myrcene	Rh and Pt/Sn catalyst with various p-donor ligands	70	660	48	16-94	100	-	-	Good control of chemo- and regioselectivity was achieved by appropriate combination of metals and the ligands for hydroformylation of myrcene.	100
29	Myrcene Camphene limonene	Rh(COD)(μ-OAc)$_2$/TPPTS	80	1160	48	35-71	100	14 (endo)	11	Biphasic hydroformylation of camphene shows no effect of surfactant addition on rate of reaction	108
30	Limonene Linalool	SAPC-[Rh_2(μ-S-t-Bu)$_2$(CO)$_2$(TPPTS)$_2$]	80-100	75-145	-	100	-	-	-	Hydroformylation of terpenes using SAPC [Rh_2(μ-S-tert-Bu)$_2$(CO)$_2$ (TPPTS)$_2$] as the catalyst.	110
31	Limonene	$Rh(CO)_2$acac tethered on two different commercially available silica.	80	600	6	84-88	84.7-88	-	83	The activity of both the catalytic systems decrease after three recycles	111

1.5 Heterogenization of homogeneous complex catalysts for the hydroformylation of olefins:

To overcome the problem of catalyst-product separation, different methodologies have been investigated to heterogenize the homogeneous catalysts. These catalysts could then combine the advantages of homogeneous catalyst i.e. high activity and selectivity with those of heterogeneous catalysts viz-long lifetime and ease of separation. Different methodologies proposed to overcome the problem of separation, have been broadly categorized as biphasic catalysis and solid supported catalysis, which are described below.

1.5.1 Biphasic catalysis

This is one of the more successful methods of heterogenization of homogeneous catalysts, which involves the use of two immiscible liquid phases, one containing the catalyst and the other containing substrates and products. The two phases can be separated by conventional phase separation techniques. In effect, one can say that here the homogeneous catalysts are immobilized on a mobile support (liquid). The biphasic catalysis is more advantageous than conventional homogeneous catalysis in the following respect.

1. It provides an easier way of separation of product and catalyst. This has direct impact on the recycle/recovery of the catalysts and the economy of the process.
2. Contamination of product with the catalyst is minimized and helps in preventing deactivation of the catalyst.
3. For substrate-inhibited kinetics, higher activity is achievable in such systems as the concentration of reactants in the catalyst phase can be controlled by taking advantage of solubility limitations.

The two-phase catalysis further involves aqueous biphasic and non- aqueous biphasic systems.

1.5.1.1 Aqueous biphasic catalysis

Kuntz of Rhone–Poulenc, first realized the fundamental concept of aqueous biphasic catalysis[34]. The general principle of two-phase aqueous catalysis is the use of a water-soluble catalyst, which is insoluble in the organic phase containing reactants and

products. The catalyst brings about the particular catalytic reaction in the aqueous phase and is removed from the desired product at the end of reaction by simple phase separation and decantation. Aqueous biphasic catalysis particularly gained importance because of the many advantages of water as the support/solvent. The subject is reviewed in depth in the literature[49]. Aqueous homogeneous catalysis depends on the development of polar water-soluble ligands and their incorporation into organometallic complexes. The solubility in water is usually achieved by introduction of highly hydrophilic substituents such as $–SO_3H$, -COOH, NR_3^+, PR_3^+ and -OH (or their salts) into the phosphine ligands[49]. Water-soluble ligands containing phosphorous and nitrogen as donor atoms are some of the most utilized ligands. The water-soluble analog of PPh_3 ligand, TPPTS is the most studied ligand in aqueous biphasic hydroformylation. Figure 1.5 shows some of the important sulphonated water-soluble ligands used in aqueous biphasic hydroformylation.

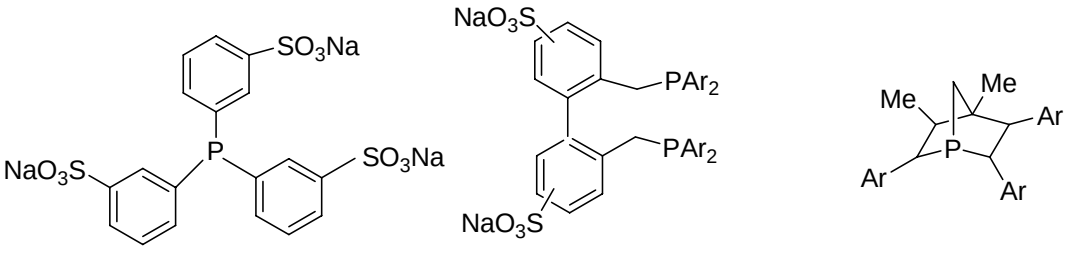

TPPTS **BISBIS** **NORBOS**

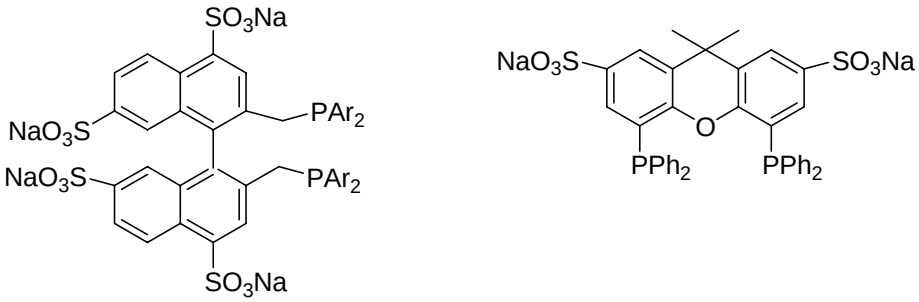

BINAS **SULFO-XANTPHOS**

Ar= C_6H_4-m-SO_3Na

Figure1.5: Structures of some water soluble ligands

The biphasic system proved to be commercially viable and found industrial application for the reactions like hydroformylation, hydrogenation, hydrodimerisation, and telomerisation[118] (Table 1.6**)**: The production of more than two million tons of n-

butanal in ten years from the hydroformylation of propylene using water soluble $HRh(CO)(TPPTS)_3$ demonstrates the strength of aqueous biphasic oxo process.

Table 1.6: Industrial aqueous biphasic catalysts and commercial processes[118]

Process/product	Catalyst	Capacity tons/yr.	Operated by
Hydroformylation (n-butanal and pentanal)	Rh/TPPTS	300000	Ruhrchemie/ (Hoschet AG)
n-butanal	Rh/TPPMS	No data	Union carbide
Selective hydrogenation (unsaturated alcohols)	Ru-TPPTS	No data	Rhone –Poulenc
Hydrodimerisation (octadienol, octanol/ nonanediol)	Ru/TPPMS	5000	Kuraray
C-C bond formation (geranyl acetone)	Rh/TPPTS	>1000	Rhone –Poulenc

Aqueous biphasic catalysts offer facile separation for many homogeneous reactions. However, aqueous biphasic system cannot be used where the component of reaction undergoes undesired chemical reactions with water. Furthermore, low solubility of many organic compounds in water could limit the application of aqueous catalysts. The two most preferentially used non-aqueous systems are fluorous biphasic system and ionic liquids as a solvent.

1.5.1.2 Fluorous Biphasic System (FBS)

In this system, aqueous phase is replaced by fluorohydrocarbons, which contains the dissolved catalyst and second phase, which may be an organic solvent with limited solubility in fluorous phase. Organometallic complexes can be solublised in fluorous phase by the attachment of fluorocarbon moieties to ligands such as phosphines, phosphites and porphyrin. The fluorohydrocarbons are miscible with organic phase at temperatures typical for reaction but immiscible at lower temperature. This property facilitates easy catalyst and product separation. The fluorous biphasic reaction could be either in the fluorous phase or at the interface of the two phases, depending upon the solubilities of the reactants in the fluorous phase. The concept has been tested for hydroformylation and oligomerisation reactions[50]. The major drawback of this system is

the residual fluorocarbons produced cause environmental damage. In addition, it involves use of costly fluorinated phosphines, the availability of which is a problem.

1.5.1.3 Other solvent systems

Non-aqueous ionic liquids (NAILS), have been investigated as a new class of alternative solvents for transition metal catalysis from the past two decades. Ionic liquids comprising alkylimidazolium, alkylpyridinium cations with tetrafluoroborate and hexafluorophosphate anions (Figure 1.6) are found to be excellent solvents for numerous homogeneous catalytic reactions. The catalyst is usually a charged complex dissolved in ionic liquid. The use of ionic liquids as solvents give results comparable to that of homogeneous reaction in hydroformylation of olefins[51]. The use of ionic liquids as solvents for transition metal catalysis opens up a wide field for future investigations, although they are expensive.

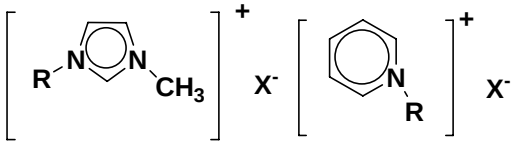

X= BF_4, PF_6

Figure 1.6: Alkylimmidazolium and alkylpyridinium ionic liquids

Supercritical CO_2 has also been used as a medium for hydroformylation of olefins in homogeneous or biphasic mode[52,119]. The rates of reactions are improved under supercritical conditions. The only disadvantage is the requirement of high pressure and temperature.

Since the different approaches for biphasic, catalysis did not provide any major advantage over aqueous phase hydroformylation of higher olefins, other means of enhancing the reactivity of aqueous biphasic system were investigated.

1.5.1.4 Approaches to improve reaction rates in aqueous biphasic medium

One of the major limitations of the aqueous biphasic catalysis is the lower activity for the hydroformylation of higher olefins due to their poor solubility in the aqueous catalyst phase. Different attempts were made to increase the solubility of higher olefins in water (catalyst phase). These involve addition of various components such as co-solvents, surfactants, phase transfer agents and promoter ligands to the reaction mixture.

Addition of co-solvent to the catalyst (aqueous) phase improves the solubility of higher olefins (substrate) in the aqueous phase within a wide range of operating conditions[53]. The ideal co-solvent should have following properties.

- Sufficient solubility in water
- Inertness towards reactant and products.
- Negligible solubility in organic phase.
- Should not enhance solubility of water in the organic phase

The most common co-solvents used are lower alcohols. Studies with ethanol as a co-solvent shows that it is very effective in improving reaction rates in two-phase hydroformylation of 1-octene[53b]. It is estimated that the solubility of 1-octene in a 50:50 mixture of ethanol and water is 10^4 times greater than in water alone. Effect of co-solvents for 1-octene hydroformylation using dimeric rhodium complex catalyst [$Rh_2(\mu\text{-}S^tBu)_2(CO)_2(TPPTS)_2$] was studied[53e] and rate enhancement by several orders has been reported. One major disadvantage of the use of a reactive co-solvent like alcohol is its interaction with the product formed in the reaction, affecting the overall selectivity of the product.

Amphiphilic ligands can act as a surfactant (surface-active agent)[54a] and can aggregate in aqueous nonpolar media forming micelles, which increase liquid-liquid interfacial area and thereby reaction rates. Typical micelle forming surfactants are SDS, CTAB, STAC and DDAPs. Chen et. al.[54d] reported the considerable improvement in the activity for hydroformylation of higher olefins using Rh/TPPTS catalyst in the presence of surfactants. The major drawback of the use of surfactant is the separation of product from the micellar system.

It is also possible to achieve better activity and selectivity to aldehyde in biphasic hydroformylation reaction using phase transfer catalysis. Russell and Murrer[55] have carried out considerable work by modifying the microstructure of the liquid assembly. When one carries out the reaction with a phase transfer agent, there is a reasonable increase in conversion and it is possible to carry out the reaction at lower temperatures and pressures. The important advantage of phase transfer catalyst is the easy separation of catalyst from product.

Chaudhari and coworkers[56] have shown that the rate of biphasic hydroformylation reaction can be enhanced several folds by addition of promoter ligand having strong binding affinity to the catalyst metal. For example triphenyl phosphine acts as a promoter ligand, in the aqueous biphasic hydroformylation of 1-octene using water-soluble $HRhCO(TPPTS)_3$ catalyst. The ligand PPh_3 facilitates the reaction at the phase boundary of the two phases. This phenomenon is named as interfacial catalysis using catalyst-binding ligand.

1.5.1.5 Literature on hydroformylation of 1-decene in biphasic medium

The hydroformylation of higher olefins has been extensively studied in homogeneous medium. Since the main objective of this literature survey is to address the catalyst-product separation issue in context with hydroformylation of 1-decene, only the relevant literature in biphasic medium has been presented. Most of the literature for higher olefins hydroformylation in biphasic medium deals with 1-hexene and 1-octene as substrates with Rh-TPPTS catalyst system. Of these, there are very few reports, which deal with the hydroformylation of 1-decene. A detailed literature survey on the studies in hydroformylation of 1-decene in aqueous biphasic medium is given below.

Since the major issue regarding the biphasic hydroformylation of 1-decene is the poor solubility of decene in the aqueous phase, a number of attempts to improve the activities by enhancing the solubility have been made.

The use of surfactants (LTAB, CTAB and SDS) alongwith the water-soluble Rh/TPPTS catalyst has improved the activity and selectivity in hydroformylation of 1-decene[120]. A high n/i ratio of 38 was obtained[121]. Rhodium complexes $[Rh(\mu\text{-}OMe)(cod)]_2$ of water soluble sulfonated diphosphines gave efficient hydroformylation of linear alkenes (1-octene and 1-decene) in presence of ionic surfactants SDS and $CTAHSO_4$, in methanol[122]. For 1-decene hydroformylation, a conversion of 63% and aldehyde selectivity of 97% was obtained. Moreover, the system could be recycled maintaining the same activity and selectivity to aldehydes. Chen and coworkers[123] reported the synergistic effect of TPPTS and TPPDS in improving the regioselectivity of long-chain olefin hydroformylation (from 6.5 to 20.9) in presence of various cationic surfactants with good activity (TOF=324 h^{-1}).

Cyclodextrins due to their capacity to function as PTC and to solubilize organic substrates in water, have also been studied as a means of enhancing the activity of the biphasic Rh/TPPTS catalytic system, particularly for higher olefins. The hydroformylation of 1-decene using Rh/alkyl-sulfonated diphosphines ligands (DPPETS, DPPPTS and DPPBTS) in the presence of methylated α- or β–cyclodextrin leads to increased conversion and the chemoselectivity[124]. A 100% conversion of 1-decene was achieved with 95% aldehyde selectivity using chemically modified β-cyclodextrins. The activity is strikingly dependent on the degree of substitution of the β-cyclodextrin[125]. Ten times rate enhancement was obtained in the solvent free biphasic hydroformylation of 1-decene using Rh/TPPTS in presence of per(2,6-di-o-methyl)-β-cyclodextrin (DMCD)[126]. A similar application of modified cyclodextrin has been illustrated for rate enhancement in 1-decene hydroformylation using Rh-TPPTS catalyst in biphasic medium[127,128,129].

The dinuclear rhodium complex $[Rh_2(\mu\text{-}S^tBu)_2(CO)_2(TPPTS)_2]$ has been used for hydroformylation of 1-octene and 1-decene alongwith heptakis(2,6-di-O-methyl)-β-cyclodextrin (DM-β-CD)[130]. The yields and linearity (5-65%, 81-87%) for hydroformylation of 1-decene are better as compared with octene (9-41%, 68-76%), as, the double bond of the alkene is outside the DM-β-CD in decene and is thus more accessible to the coordination of the rhodium centre.

A Rh phosphine complex encapsulated within the surface alkylated poly (propylene imine) dendrimers, results in dendrimer complexes which function as nanoreactors for hydroformylation of olefins (Figure 1.7)[131].

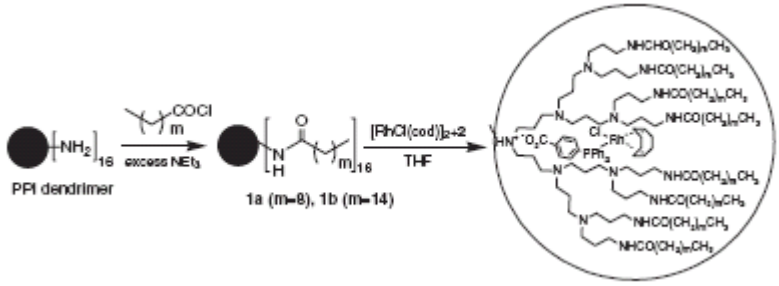

Figure 1.7: Dendrimer complexes as nanoreactors for hydroformylation of olefins.

The congested surface of dendrimers with long alkyl chains favored hydroformylation of higher olefins (1-decene and 1-octadecene) with higher catalytic

activity. One-pot three reactions composed of hydroformylation, the Knoevenagel reaction, and hydrogenation has also been studied within the dendritic nanoreactor.

A new class of cationic α-cyclodextrins, mono, di and tetra HTMAP α-CD and MTMAP α-CD bearing 2-hydroxy-3-trimethylammoniopropyl groups have shown their efficiency as mass-transfer promoters in a Rh-TPPTS catalyzed biphasic hydroformylation[132]. The methylated cyclodextrin (Rame-α-CD or Rame-β-CD)/m-TPPTC [tris(m-carboxyphenyl)phosphane trilithium salt] couples have also proved to be more efficient in terms of activities and selectivities for the Rh-catalyzed hydroformylation of higher olefins (1-octene, 1-decene and 1-dodecene) in an aqueous-organic system. The conversions obtained with m-TPPTC were notably higher (by a factor of 47, 21 and 16 for 1-octene, 1-decene and 1- dodecene, respectively) as compared to the biphasic reaction[133].

The potential of sulfonated Xantphos ligand for a cyclodextrin-based hydroformylation process has been investigated by van Leeuwen and coworkers[134]. In addition to an activity enhancement, an increase in aldehyde selectivity (>99%) and linear to branched aldehydes ratio (n/i=26 and 32) was observed when randomly methylated α- or β-cyclodextrins were used as inverse phase-transfer catalysts for the hydroformylation of 1-decene.

A new concept of thermo regulated phase-transfer catalysis (TRPTC) in aqueous/organic two-phase catalysis has been described using novel poly(ethylene oxide)-substituted triphenylphosphines, (PEO-TPPs) i.e. $Ph_{3-m}P[C_6H_4\text{-}p\text{-}(OCH_2CH_2)_nOH]_m$ ligands based on the temperature-dependent solubility in water and clouding property, for extremely water-immiscible substrates. The concept involves the catalyst transfer into the organic phase to catalyze a reaction at a higher temperature, and returns to the aqueous phase to be separated from the products at a lower temperature. Application of this novel strategy to the rhodium-catalyzed two-phase hydroformylation of higher olefins gave desirable results with an average turnover frequency of 180 h^{-1} for 1-decene[135,136]. Similar activity (TOF=195 h^{-1}) has been reported with Rh complex of the water-soluble phosphine, PEO-DPPSA, which possesses the characteristics of TRPTC for hydroformylation of 1-decene[137]. The conversion of 1-decene and the yield of aldehydes

as high as 99.5% and 99.0%, respectively was achieved, under optimized conditions. The catalyst was recycled with ease[138].

A water-soluble Rhodium complex modified by octyl polyethylene glycol phenylenephosphite[139] and polyether triarylphosphine oxide, (PETAPO)[140] has proved to be an efficient ligand for the rhodium-catalyzed hydroformylation of 1-decene. A conversion of 99.3% and aldehyde yield of 97.3% with high activity (TOF=202 h^{-1}) was obtained when 1-decene was employed as substrate. The catalyst was recoverable and recycled for several successive reactions without any loss in activity.

Utilizing water-soluble octylpolyglycol-phenylene-phosphite (OPGPP)/Rh complex, over 90% conversion of 1-decene was obtained, avoiding the limitation of insolubility of substrates in water[141]. Preliminary results indicated that micellar catalysis and TRPTC coexist in the reaction system. Considerable loss in activity was observed after three successive recycles, which is attributed to hydrolysis of OPGPP during the reaction. A rhodium catalyst system for non-aqueous (organic-organic) hydroformylation of 1-decene is reported using a polyether phosphite, OPGPPs (polyether chain of over 19 ethylene glycol units) [142]. The ruthenium complex OPGPP/$Ru_3(CO)_3$ formed in situ has also proved to be a moderate catalyst for the non-aqueous hydroformylation of 1-decene.

Horvath and coworkers[143] have demonstrated the concept of Fluorous Biphasic System (FBS) for the hydroformylation of octene and decene. The catalyst was prepared in situ from $Rh(CO)_2(acac)$ and $P[CH_2CH_2(CF_2)_5CF_3]_3$ (P/Rh = 40) under 5 bar syngas pressure [CO/H_2(1:1)] . The hydroformylation of decene was studied at 100°C and 1.1 MPa of CO/H_2) in a 50/50 (v/v), in toluene/$C_6F_{11}CF_3$ solvent mixture. The results obtained were comparable to the aqueous biphasic system. Kinetic studies in FBS for the hydroformylation of ethylene and decene show that the reaction was first order in both rhodium and olefin[144]. While the hydroformylation of decene was inhibited by ligand $P[CH_2CH_2(CF_2)_5CF_3]_3$, the n/i ratio of the undecanals increases with increasing phosphine concentration.

The rhodium complexes of fluorous soluble polymer ligands such as poly(fluoroacrylate-co-tryldiphenylphosphine) were found to be active and selective catalysts for the fluorous biphasic hydroformylation of various olefins. The average turnover frequency (TOF) for the hydroformylation of decene was 136 h^{-1} with an

aldehyde selectivity of 99% at more than 90% conversion[145]. Hydroformylation of 1-decene using $Rh(CO)_2(acac)$/fluorous triphenylphosphites (i.e. perfluoro deceyl phenyl phosphite, perfluorododeceyl phenyl phosphite) in fluorous-toluene biphasic system gives high activity (TOF=3500 h^{-1}) with good conversion and selectivity (98%)[146]. The activity and selectivity were found to vary markedly with the position of the perfluoroalkyl group on the aromatic ring. A slight decrease in aldehyde selectivity and n/i ratio was observed on recycle.

A rhodium-catalyzed hydroformylation of higher olefins in supercritical CO_2 ($scCO_2$), has been studied with the perfluoroalkylated ligands [$P(C_6H_4R\text{-}m)_3$ (m = 4, R = n-C_6F_{13} , n-$CH_2CH_2C_6F_{13}$, n-C_6H_{13} , n-$C_{10}H_{21}$ or n-$C_{16}H_{33}$; m = 3, R = n-C_6F_{13})] [147]. High activity for the hydroformylation of 1-decene (TOF=2794 h^{-1}) was obtained as compared to the alkylated ligand (TOF=195 h^{-1}). The high rates derived probably originate from the strong electron withdrawing effect of fluoro-ponytails, while the slow rates observed with arylated ligands are mainly due to the low solubility of these ligands in $scCO_2$.

$Rh(CO)_2(acac)$/sulfonated-Xantphos dissolved in [BMIM][PF_6] (*n*-butyl-3-methylimidazolium hexafluorophosphate) ionic liquid catalyzes the hydroformylation of heavy olefins (C_8–C_{12}) [148]. The system gives TOF of 245 h^{-1} and aldehyde selectivities upto 99% for 1-octene and TOF of 33 h^{-1} and aldehyde selectivites upto 94% for 1-decene hydroformylation. The selectivity is strongly influenced by the nature of the ionic phase and co-solvent water. A detailed review on the hydroformylation of 1-decene using rhodium complex catalysts in aqueous biphasic medium is shown Table 1.7.

In summary, the various attempts made for the hydroformylation of 1-decene in two phase systems basically focus on the use of surfactant, cyclodextrins and polyether substituted phosphine or phosphite ligands which posses the property of solubility in both organic as well as aqueous phases. The use of this additive in some cases makes the catalyst –product separation even more difficult.

Table 1.7: Literature on hydroformylation of 1-decene in biphasic medium.

Sr. no.	Catalyst system	solvent system,	Additive / modifier	Reaction conditions		Results				Remark	Ref.
				T (^{0}C)	P_{syngas} (Psi)	Conv. (%)	Sel. (%)	n/i	TOF (h^{-1})		
1	$Rh(CO)_2(acac)$ $RhCl_3$ $3H_2O$/ (TPPTS)	Aqueous -organic biphasic	LTAB, CTAB	40-150	300-10000	33	89	38	0.3	A catalytic process for the hydroformylation of C_3-C_{20} olefins with high n/i ratio of aldehyde product for wide reaction conditions is claimed.	121
2	$Rh(CO)_2$ (acac), $HRhCO\{P[CH_2CH_2(CF_2)_5CF_3]_3\}$/$\{P[CH_2CH_2(CF_2)_5CF_3]_3\}$	Fluorous - organic biphasic	$C_6F_{11}CF_3$	100	150	100	80	2.9	-	The concept of FBS has been demonstrated for the hydroformylation of octene and decene	143
3	$Rh(CO)_2(acac)$/ TPPTS	Aqueous -organic biphasic	Various modified β-cyclodextrins	80	735	7-100	57-95	1.9-2.8	0.5-1.2	Chemically modified β-CD act as PTC and effective for the hydroformylation of water insoluble olefins	125
4	$Rh(CO)_2$ (acac)/ TPPTS	Aqueous -organic biphasic	Per(2,6-di-o-methyl)-β-cyclodextrins (DM-β-CD)	80	735	100	95	1.9	-	Solvent free biphasic hydroformylation of various water insoluble olefins has been achieved in high yields and selectivities	126
5	$Rh(CO)_2(acac)$ /(PEO-TPPs)	Aqueous -organic biphasic	PEO-TPPs	100	725	100	93	-	-	A new concept of TRPTC has been successfully demonstrated for higher and functionalized olefins	135
6	$[Rh_2(\mu\text{-}S^tBu)_2(CO)_2(TPPTS)_2]$	Aqueous -organic biphasic	β-cyclodextrin	80	220	-	81-87	4.3-6.7	-	The linearity for aldehydes is higher for decene compared to octene	130

Sr. no.	Catalyst system	solvent system,	Additive / modifier	Reaction conditions		Results				Remark	Ref.
				T (^{0}C)	P_{syngas} (Psi)	Conv. (%)	Sel. (%)	n/i	TOF (h^{-1})		
7	$Rh(CO)_2(acac)$ /TPPTS	Aqueous -organic biphasic	Modified β-cyclodextrin	80	750	32-100	73-95	2-2.5	-	Nature of CD, P/Rh and CD/Rh ratios influences the conversion and selectivity.	127
8	$Rh(CO)_2(acac)$ /$P[CH_2CH_2(CF_2)_5CF_3]_3$	Fluorous - biphasic	$C_6C_{11}CF_3$ /toluene (50:50)	100	160	80	91.5	3.25	1494	High pressure NMR and kinetics for hydroformylation of decene in batch and semicontinuous flow reactor is studied	144
9	$Rh(CO)_2(acac)$ /TPPTS	Aqueous -organic biphasic	Surfactant (polyglycols and ethers)	125	440	95	95	3.76	-	The effect of reaction parameters on the behavior of reaction in micellar and nonmicellar systems were compared.	120
10	$Rh(CO)_2(acac)$ /OPGPP	Aqueous -organic biphasic	OPGPP	80	725	98.3	97.3	0.91	-	The catalyst can be recycled only for successive two runs, the decrease in activity was attributed to the partial hydrolysis of ligand.	139
11	$Rh(CO)_2(acac)$/L [$L=P(C_6H_4R\text{-}m)_3$ m=4 R=n-C_6F_{13},]	Fluorous -$scCO_2$	fluorinated aryl phosphines	80	300	3-49	96-99	3.8	195-2871	More electron withdrawing fluoro-ponytails affording faster rates in comparison with the more electron donating one	147
12	$Rh(CO)_2(acac)$/L L=poly(fluoroacrylate-co-styrldiphenylphosphine)	Fluorous - biphasic	Two Rh-fluoropolymer catalyst in FBS	100	150	90-97	99	4.8-5.9	141	Rh/fluorous soluble polymer ligand shows good activity and selectivity in hydroformylation of higher olefins	145
13	$Rh(CO)_2(acac)$ /TPPTS	Aqueous -organic biphasic	Modified β-cyclodextrins	80	735	7-100	69-95	1.8-2.8	-	The effects of reaction parameters on the rate and aldehyde selectivity was studied	128

Sr. no.	Catalyst system	solvent system,	Additive / modifier	Reaction conditions		Results				Remark	Ref.
				T (^{0}C)	P_{syngas} (Psi)	Conv. (%)	Sel. (%)	n/i	TOF (h^{-1})		
14	$RhCl_3.3H_2O$/ PEO-DPPSA	Aqueous -organic biphasic	PEO-DPPSA	100	725	97.8	95.6	0.64	191	This novel non-ionic water soluble ligand shows inverse temperature dependent water solubility.	137
15	$Rh(CO)_2(acac)$ /sulfoxantphos	Aqueous -ionic liquid	Catalyst immobilized in BMIM-PF_6 ionic liquid	100	225	79	94	61.0	33	BMIM-PF_6 immobilized Rh / Sulfoxantphos catalyst is an efficient catalyst system in biphasic hydroformylation of higher olefins.	148
16	$Rh(CO)_2(acac)$ /OPGPP	organic-organic biphasic	Polyether phosphite i.e. OPGPP	90	725	99.4	97.6	0.94	228	OPGPP is used for hydro-formylation in nonaqueous system. Effect of reaction parameter was also investigated.	142
17	$Rh(CO)_2(acac)$ /PETAPO	Aqueous , non-aqueous - organic	PETAPO	100	1015	92	90	0.47	225	Rh-PETAPO can be used efficiently in aqueous-organic and nonaqueous–organic biphasic system.	140
18	$RhCl(CO)(TPPTS)_2$	Aqueous -organic biphasic	CTAB and TPPDS	100	217	62	95.4	20.9	324	Synergistic effect of TPPTS and TPPDS into the biphasic catalyst system increases ragioselectivity.	123
19	$Rh(CO)_2(acac)$ /PEO-TPP	Aqueous -organic biphasic	P-[p-C_6H_4 $(OCH_2CH_2)_n$ OH]$_3$ and Ph_2P-[p-C_6H_4 $(OCH_2 CH_2)_n$ OH]	100	725	93	90	-	180	The strategy of TRPTC can be applied to water soluble or insoluble substrates and provide a novel approach for separation and recycle of the catalyst.	136

Sr. no.	Catalyst system	solvent system,	Additive / modifier	Reaction conditions		Results				Remark	Ref.
				T (^{0}C)	P_{syngas} (Psi)	Conv. (%)	Sel. (%)	n/i	TOF (h^{-1})		
20	$Rh(CO)_2(acac)$ /fluorous triarylphophites	Fluorous - biphasic system	perfluoro deceyl ands dodeceyl phenyl phosphite	80	600	100	85-98	2-3.6	1300-11000	Rhodium complexes of these phosphites efficiently catalyse the hydroformylation of higher olefins but they are not stable.	146
21	$RhCl_3$. $3H_2O$/(PEO-DPPSA)	Aqueous -organic biphasic	PEO-DPPSA	70-120	725	54.5-94.6	54.2-94	2.1-0.64	271-470	The catalytic system is recyclable for hydroformylation of higher olefins. Effect of reaction parameters on rate and regioselectivity was investigated.	138
22	$Rh_2(\mu\text{-}OMe)(cod)]_2$ /dppbts, dppts	Aqueous -organic biphasic	Cationic surfactant SDS and $CTAHSO_4$	80	205	3-88	20-96	1.1-3.5	.0.3-6	For 1-decene hydroformylation, the results were best using $CTAHSO_4$ compared to SDS as a surfactant.	122
23	Rh-ARPGPPs	Aqueous -organic biphasic	Polyether phosphite	100		90				Results indicate presence of miscellar catalyst and TRPTC coexist in the reaction system	141
24	$[Rh(COD)Cl]_2$ / surface alkylated poly (propylene imine)dendrimers	Aqueous -organic biphasic	Encapsulation of rhodium complex inside dendrimer	60	75	49-98	100	3.0	50	Encapsulation of rhodium complex inside dendrimer functioned as nanoreactors for hydroformylation of olefins.	131
25	$Rh(CO)_2(acac)$ /TPPTS,	Aqueous -organic biphasic	Modified α-cyclodextrin (α-CD)	80	735	24-89	88-94	3.0-5.4	21	Modified α-CDs are efficient mass transfer promoters for the hydroformylation of higher olefins.	132

Sr. no.	Catalyst system	solvent system,	Additive / modifier	Reaction conditions		Results				Remark	Ref.
				T (^{0}C)	P_{syngas} (Psi)	Conv. (%)	Sel. (%)	n/i	TOF (h^{-1})		
26	$Rh(CO)_2$ (acac)/ Sulfoxantphos	Aqueous -organic biphasic	RAME- α- or β-CD	120	750	63-71	99	26-32	15	The conjugated effects of the sulfoxantphos and CD/substrate complex led to remarkable performance in terms of chemoselectivity and regioselectivity.	134
27	$Rh(CO)_2$(acac)/ TPPTS	Aqueous -organic biphasic	HP- α –CD and RAME- α - or β-CD	80	750	15-97	74-98	1.8-3.0	13-83	Contrary to the β-CD, the use of α –CD as a mass transfer promoter in the biphasic hydroformylation preserves the intrinsic properties of Rh/TPPTS catalyst system,	129
28	$Rh(CO)_2$ (acac)/ m-TPPTC	Aqueous -organic biphasic	m-TPPTC and RAME- α- or β-CD	80	600	43-100	86-96	1.8-2.4	72-167	The methylated CDs/m-TPPTC systems proved to be more efficient in terms of activities and selectivities for hydroformylation of higher olefins.	133
29	$Rh(CO)_2$ (acac)/ DPPETS, DPPPTS, DPPBTS	Aqueous -organic biphasic	RAME-α-CD and RAME-β-CD	80	300	15-75	60-94	1.2-2.3	10-20	Use of RAME-α-CD or RAME-β-CD results in increase in activity and chemoselectivity but decrease in n/i ratio.	124

1.5.2 Solid supported catalysts: Over a period of more than 20 years research has been devoted to the development of supported (anchored or immobilized) metal complex catalysts[63]. The investigations on these types of catalysts have been driven by the vision of combining the positive aspects of homogeneous catalyst i.e. high activity, selectivity, good reproducibility, with those of heterogeneous catalysts i.e. long lifetime and ease of separation.

A variety of organic and inorganic polymers have been used for immobilization of metal complex catalysts. Different functionalized organic polymers can bind to the catalytic complex by covalent bonding to produce a heterogenized catalyst. Most frequently used organic supports are polystyrene and styrene divinylbenzene copolymer beads with diphenylphosphine, tertiary amino[149], cyanomethyl[150], thiol[151] and cyclopentadienyl[152] functional groups. Other polymers used for this purpose are polyvinyls, polyacrylates, and cellulose. A more accepted route for the preparation of such type of catalysts is the displacement of ligand already coordinated to a metal complex by a polymer-bonded ligand[153] or the weakly bridged dimeric metal complexes,[154] **(**Scheme 1.6**)**.

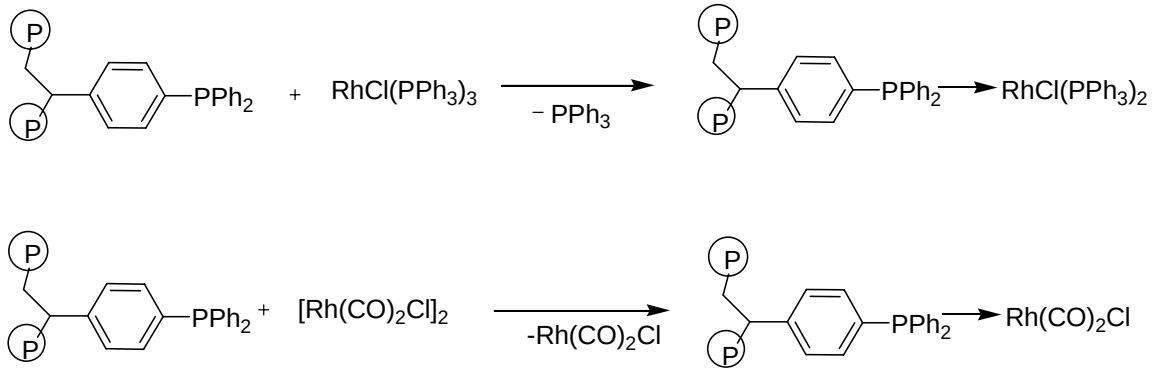

Scheme1.6: Organic polymer anchored catalysts

A number of investigations using polymer bound metal complexes show lower activities with respect to their homogeneous counterparts, but regio and stereoselectivities are significantly different. This is because of shape discrimination effect due to steric and electronic interaction within the matrix of the support[155].

The polymer supported rhodium phosphines[156] and cobalt carbonyl[157] catalysts were evaluated for hydroformylation of olefins. For the hydroformylation of 1-pentene

Pittmann et al[158] found that selectivities toward linear product are higher (n/i = 6-12) using polymer bonded $HRh(CO)(PPh_3)_3$ than with the homogeneous analog (n/i = 2-4) depending on the temperature. One step synthesis of 2-ethylhexanol including sequential hydroformylation, aldol condensation and hydrogenation was achieved using polyfunctional carbonyl phosphine rhodium complex catalyst immobilized on to polystyrene carrying amino groups close to metal center[159].

Inorganic supports like silica, clay, alumina, magnesia, glass and ceramics are also used for the immobilization of catalytic complexes. Advantages of these oxide supports are their rigid and defined pore structure and resistance to higher temperature, solvent and aging[160]. Silica is the most preferred inorganic support in terms of availability of number and nature of surface groups, surface area, pore size and volume. Anchoring of homogeneous catalyst to silica can be achieved by different methods. In the first route, the surface silanol groups can directly interact with appropriate metal complex or with intermediate ligand group. Direct surface bonding has often been practiced for the anchoring of metal carbonyl complex[63a]. **(**Scheme 1.7**)**.

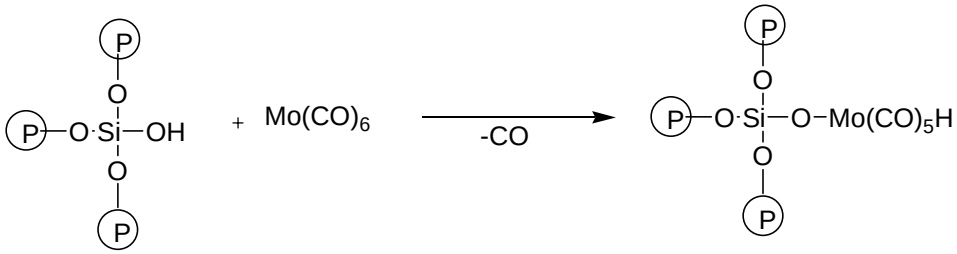

Scheme 1.7: Anchoring of homogeneous catalyst by direct surface bonding

Second, the most frequent method is the fixation of catalyst via donor ligand attached to a support by covalent bonding. In order to achieve chemical linkage between a soluble metal complex catalyst and support, a suitable functionality forming covalent or ionic bonding has to be introduced onto the original support, or through the reaction of preformed complex bearing silicon substituted ligands as shown in Scheme 1.8[136]. Application of phosphinated silica supported metal complexes in hydroformylation do not reveal any surprising results[161].

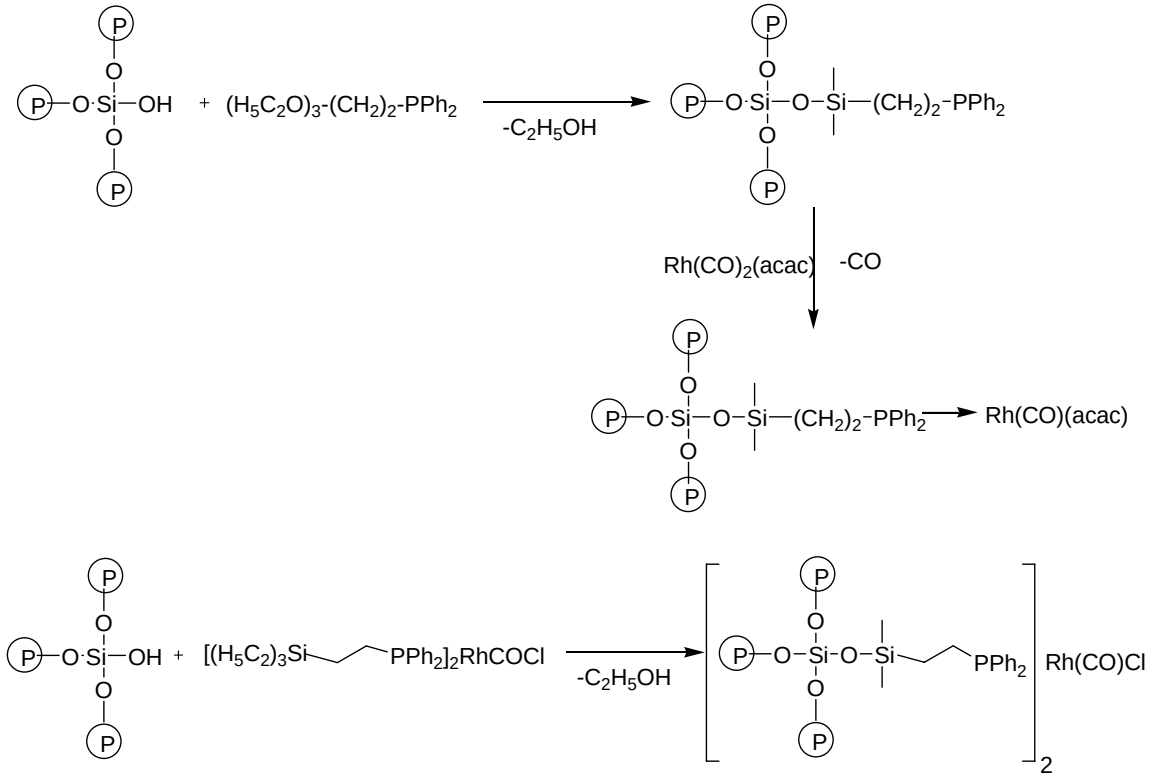

Scheme 1.8: Fixation of catalyst via donor ligand

Anchoring of the homogeneous catalyst to a support can be achieved by covalent or ionic bonding. Tethering or anchoring of the complex catalyst is also possible by introducing suitable tethering agent such as phosphotungstic acid (PTA) or other polyoxoanions[162] . Silica is widely used as a support since transition metal complexes can be easily tethered to its surface through a ligand in the complex, which has alkoxyl- or chlorosilane functional groups.

Various supports with ion exchange capabilities can also be used for binding of the catalytic complex. These include standard organic and inorganic ion exchange resins, inorganic material with polarized groups and zeolites. Various cationic rhodium and palladium complexes immobilized by this way were reported for hydroformylation[74] and carbonylation[163a] reactions. The method of ionic fixation is especially used when dealing with the chiral metal complexes to perform enantioselective transformation in pharmaceutical applications[163b]. The applications of such catalysts are limited by the ion exchange equilibrium, as ionic bonding of the metal complexes is generally not as efficient as fixation via covalent bonding.

Fixation of metal complex to support via chemi—or physisorption and entrapping in porous material is also possible. This type of binding is a bridge between homogeneous catalyst and conventional heterogeneous catalysts. Entrapment of the catalyst is achieved in the porous network of zeolites where the reactants are small enough to enter the large cavities, but the catalyst clusters are too large to escape. This technique of immobilization is commonly known as '*Ship in the bottle'* synthesis. The catalysts are termed as encapsulated catalysts. The substrate diffuses through the pores to come in contact with catalyst where the reaction takes place. The method is proven to give good catalyst for hydroformylation of olefins[59]. The products formed diffuse outside after reaction. Other methods of encapsulating metal complexes utilize polymerization or polycondensation reactions such as the sol-gel method. In this method, the metal complex is dissolved in the medium to be polymerized and is therefore trapped in the matrix formed[164]. The major drawback of these methods is that catalyst leaching can occur along with the product from the wide pores of the matrix.

Immobilization of metal complex is also possible by impregnation of liquid medium containing homogeneous catalyst to a solid support. This medium can be either organic medium or aqueous medium. The example includes SLPC, SILC and SAPC.

In Supported Liquid Phase Catalysts (SLPC), the homogeneous catalyst is dissolved in a nonvolatile solvent. This catalyst solution is adsorbed and distributed in the pores of porous support by capillary forces. The reaction takes place in the supported liquid or at the interface of the supported liquid film and the gas phase. On practical application of the catalyst, one has to take care that the catalyst concentration in the solution is not altered by evaporation of solvent. Most of the literature describes the use of SLPC in the hydroformylation of ethylene, propylene and butene using Rh-triphenylphosphine complexes and excess PPh_3[60]. This method is effectively applicable only for the gaseous reactants and inapplicable with the reactants or products miscible with the nonvolatile organic solvent being used for immobilization.

Mehnert et al[165] developed a new concept of supported ionic liquid catalyst (SILC). It involves the surface of a support material that is modified with a monolayer of covalently attached ionic liquid fragments (Figure1.8). Treatment of this surface with additional ionic liquid results in the formation of a multiple layer of free ionic liquid on

the support. These layers serve as the reaction phase in which the homogeneous catalyst is dissolved. Although the resulting material is a solid, the active species is dissolved in the ionic liquid phase and performs as a homogeneous catalyst. The concept is applied for the variety of reactions including hydroformylation and hydrogenation[165]. This supported system containing the ligand tri(m-sulphonyl) triphenyl phosphine tris(1-butyl-3-methyl-imidazolium)salt, (tppti) in [BMIM] [BF_4] ionic liquid is tested for hydroformylation of 1-hexene. The results obtained (TOF = 65 min^{-1}, n/i = 2.4) were superior to the biphasic reaction (TOF = 23 min^{-1}, n/i = 2.2). The improved activity is attributed to the higher concentration of the active rhodium species at the interface and the generally larger interface area of the solid support in comparison to the biphasic system.

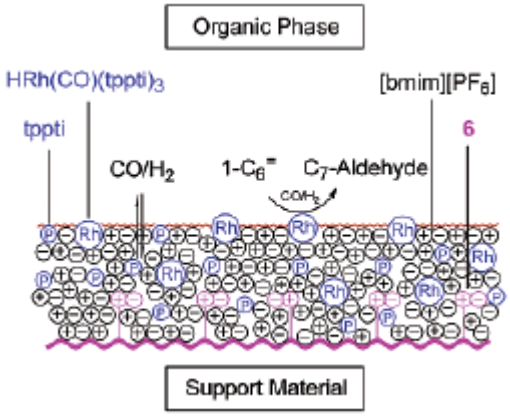

Figure1.8: A schematic of Supported Ionic Liquid Catalyst (SILC) used in the hydroformylation of 1-hexene

Supported Aqueous Phase Catalyst (SAPC) consists of a thin film of an aqueous solution of organometallic complexes, immobilized in the pores of a high surface area solid support[61]. The catalytic reaction takes place at the water organic interface where the organic phase contains the reactant and products. Several reactions have been reported using $HRhCO(TPPTS)_3$ immobilized as an SAPC[61]. Such catalysts showed significantly higher activities for hydroformylation reaction without any leaching (<1 ppb) of rhodium into the organic phase. The water content in the SAPC strongly influences the performance of the catalyst. Deactivation of the catalyst was observed when polar solvents or products are involved in the reaction.

Heterogenization of the homogeneous catalysts onto solids has shown promise. However, due to inherent problem of the system regarding leaching of the catalyst, diffusion and deactivation none of these has been applied in commercial practice.

1.5.2.1 Literature on hydroformylation of 1-decene using solid supported catalyst

There are very few reports on hydroformylation of 1-decene using heterogeneous catalyst and most of the reports are mainly on hexene and octene as a substrate.

Silica supported $Ru_3(CO)_{12}$ catalyst with 2,2' bipyridine and other heterocyclic bases has been reported for the hydroformylation of 1-decene[166]. This catalyst had a significant tendency towards isomerization of terminal olefins to internal olefins giving poor n/i ratio**.**

The rhodium carbonyl thiolate complex, $Rh_2[\mu\text{-}S(CH_2)_3Si(OCH_3)_3]_2(CO)_4$, (Rh–S) and $Rh_2[\mu\text{-}S(CH_2)_3Si(OCH_3)_3]_2\ Ph_2P(CH_2)_3Si(OC_2H_5)_3\ ]_2(CO)_2$, (Rh–S-P) was tethered to phosphine-modified Pd–SiO_2(P–(Pd–SiO_2)) to give the tethered catalyst. These tethered catalysts, were used for the hydroformylation of higher olefins under mild reaction conditions of 60ºC and 1 atm of syngas pressure[167]. For the hydroformylation of decene, 78-84% aldehyde selectivity was obtained at 99% conversion with TOF of 28-35 h^{-1}. The catalyst was recycled for three times with 1% rhodium leaching in the organic phase.

Lindner and coworkers[168] have demonstrated that rhodium (I) complex $Rh(CO)[Ph_2P(CH_2)_xSi(OMe)_3]_3$, incorporated into a polysiloxane matrix, $(MeO)_3Si(CH_2)_6Si(OMe)_3$ by the sol–gel method results in flexible, but highly cross-linked inorganic–organic hybrid polymers. The hydroformylation of the higher olefins (1-decene and 1-tetradecene) was most efficiently and selectively catalyzed when a polymer containing phosphine ligand with hexyl instead of propyl spacers was employed. The highest activity (TOF = 120 h^{-1}) was obtained in polar solvents, while selectivities were best in solvents of medium polarity. Rhodium complexes $[RhCl(CO)_2]_2$ or $[Rh(OMe)(COD)]_2$ with dppe ligand entrapped inside the porous systems of inorganic or hybrid matrices via the sol–gel method were tested as catalysts for hydroformylation of higher olefins such as 1-hexene, 1-decene and styrene[169]. High turnover numbers were obtained in the hydroformylation of either 1-hexene or 1-decene (TOF=150 h^{-1}) at moderate conversion. The microporous materials could be recycled without any rhodium leaching, being active even in the absence of a solvent.

Dinuclear rhodium (II) complexes $[Rh_2(\mu\text{-}PC)_2(\mu\text{-}O_2CR)_2]$ (μ-PC=bridging ortho-metalated arylphosphine ligand) immobilized on amorphous silica supports as well as on MCM-41 by surface-tethered phosphine ligands have been employed in the hydroformylation of 1-decene[170]. The hydrogenated side-product, n-decane, increases steadily at the expense of hydrocarbonylated products in subsequent catalytic runs and some catalyst leaching took place as exhibited by a low degree of hydroformylation activity for filtrates.

Heterogenization of $HRh(CO)(PPh_3)_3$ by tethering through phosphotungstic acid to zeolite Y support **(**Figure1.9**),** also gives a hydroformylation catalyst with excellent stability, reusability and improved activity. The hydroformylation of decene with this catalyst shows 98.6% conversion with the highest TOF of 328 h^{-1}. The catalyst was recycled for five times without loss of any activity and 0.01% overall rhodium loss in the organic phase[171]**.**

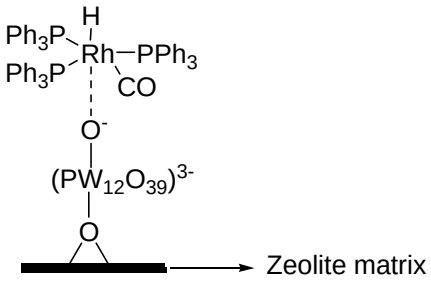

Figure1.9: Tethering of $HRh(CO)(PPh_3)_3$ complex to zeolite Y by PTA

Disser and coworkers[172] show the immobilization of carbonylhydrido-tris-(m-sulfo-triphenylphosphine)-rhodium on activated carbon treated at high temperature. This type of immobilized catalyst has been applied for the hydroformylation of long-chain alkenes such as 1-hexene, 1-decene, 1-tetradecene, 2-hexene and 2,3-dimethyl-2-butene. For all linear α-olefins the same n/iso (2:1) ratio was obtained in the product. For the hydroformylation of 1-decene initial TOF obtained was 90 h^{-1}. Catalyst leaching turned out to be a function of solvent polarity. Using n-heptane as solvent the immobilized catalyst remained stable on the carrier.

Chaudhari and coworkers[173] reported a heterogeneous catalyst for hydroformylation of higher olefins by encapsulation and anchoring $HRh(CO)(PPh_3)_3$ in zeolite Na-Y, MCM-41 and MCM-48 mesoporous materials. The encapsulation of the catalyst inside the pores of mesoporous material was proven by CP-MAS NMR, FT-IR,

TEM, XPS, and powder XRD characterization. The catalyst is air stable and showed high activity for the hydroformylation of higher olefins. The hydroformylation of decene showed 99% conversion with the TOF of 109 h^{-1}.The catalyst was recycled for six times with 0.05% overall rhodium loss.

Immobilization of water-soluble Rh-TPPTS complex in the ionic liquids such as [BMIM][BF_4], [BMIM][PF_6] and TMGL (1,1,3,3-tetramethylguanidinium lactate) on mesoporous MCM-41 silica's gave supported ionic liquid-phase catalysts (SILC) [174]. This SILC catalyst gave TOF of 74 h^{-1} for hydroformylation of 1-decene at 18% conversion at mild reaction conditions and could be reused several times without significant loss of activity or selectivity.

The hydroformylation of higher linear olefins can be performed in solventless conditions using ligand-modified or unmodified Rh(0) nanoparticles prepared in imidazolium ionic liquids as catalyst precursors. There is a strong influence of the nanoparticle size on the hydroformylation reaction[175]. Aldehydes are generated when 5.0 nm Rh(0) nanoparticles are used in the hydroformylation of 1-alkenes and n/i selectivities up to 25 can be achieved by addition of Xantphos. For the hydroformylation of 1-decene 99% aldehyde selectivity was obtained at 100% conversion. TEM, XRD, IR and NMR experiments indicated that these Rh(0) nanoparticles are probably degraded under the reaction conditions into soluble catalytically active mononuclear Rh-carbonyl species. The numerous heterogenized catalysts used for the hydroformylation of 1-decene are presented in Table 1.7

In summary, techniques like anchoring, tethering, encapsulation, SILC and even modified and unmodified Rh-nanoparticle have been used for the hydroformylation of 1-decene. Each technique has its own merits and demerits. The highest activity was reported using the tethered catalyst, which is also far less compared to the activity for homogeneous catalyst.

Table 1.7: Literature on hydroformylation of 1-decene using heterogenized homogeneous catalysts.

Sr. no.	Heterogenized Catalyst	Support	Reaction cond.			Results				Remark	Ref.
			T (^{0}C)	P_{syngas} (Psi)	t (h.)	Conv. (%)	Sel. (%)	n/i	TOF (h^{-1})		
1	$Ru_3(CO)_{12}$ with 2,2' bipyridine and heterocylic bases	Silica	100-150	750	17		5	0.7	-	Directly C_{11} alcohols were obtained as a major product	166
2	Rhodium carbonyl thiolate tethered complex on silica Rh-S/P-(Pd-SiO_2), Rh-S-P/(Pd-SiO_2)	Silica	60	15	20.5-23.5	99.0	77.6-83.4	3.8	28-35	Rh-S/P-(Pd-SiO_2), and Rh-S-P/(Pd-SiO_2)are more active catalyst than simple tethered catalyst. Isomeisation of olefin was observed.	167
3	Blend of carbonyl tris[diphenyl(polysinoxanylhexyl)phosphine] hydridorhodium(I)	polysiloxane	100	300	2.5	29	92	5.25	116	In ethanol solvent the catalyst shows excellent selectivity for hydroformylation of decene	168
4	Immobilized dinulclear rhodium (II) complex $[Rh_2(\mu\text{-}PC)_2(\mu\text{-}O_2CR)_2]$	MCM-41	80	450	4	97	81	1.52	81	The aldehyde selectivity drops while n/i ratio increases on recycle. hydrogenated and isomerised product increases on recycle	170
5	Rhodium complex $[RhCl(CO)_2]_2$+dppe entrapped inside the pores of inorganic or hybrid matrix	silica	80	750	48	72	100	1.4	150	The entrapped catalyst is less active than its homogeneous counterpart owing to the diffusion problem	169

Sr. no.	Heterogenized Catalyst	Support	Reaction cond.			Results				Remark	Ref.
			T (^{0}C)	P_{syngas} (Psi)	t (h.)	Conv. (%)	Sel. (%)	n/i	TOF (h^{-1})		
6	Encapsulated and anchored $HRh(CO)(PPh_3)_3$	Na-Y, Zeolite MCM-41, MCM-48	100	600	3.5	99	99.2	1.5	109	The catalyst is highly stable and recyclable without any metal leaching	173
7	Tethered $HRh(CO)(PPh_3)_3$ on Na-Y zeolites using phosphotungstic acid	Na-Y zeolite	100	600	3.25	98.6	99.3	1.5	328	Highest TOF (328 h^{-1}) was obtained using this catalyst. The catalyst was highly stable and recyclable.	171
8	MCM-41 supported Rh-TPPTS ionic liquid catalyst (SILCs)	MCM-41	100	300	4	18	100	1.3	74	The catalytic activity was not satisfactory and depended on the type of IL phase and the organic phase	174
9	$[Rh(\mu\text{-}Cl)(CO)_2]_2$ /TPPTS SAPC catalyst	Activated carbon pellet	110	600	4	-	-	2.0	90	The reaction rates decreased with increasing chain length of olefin.	172
10	ligand modified or unmodified Rh(0) nanoparticle		100	750	18	100	99	1.5	12	Induction period of 2.5 hours, and isomerization of olefin was observed. Actual active species still to be identified.	175

1.6 Scope and Objective of the thesis

It is evident from the literature review presented here that hydroformylation of terpenes and higher olefins is an industrially important reactions. The activities obtained in hydroformylation of terpenes are generally very poor and not many literature reports are available. It is thus important to develop catalysts that can give better activity and chemo and diastereoselectivity for terpene hydroformylation. Also, the various aspects of phosphite-catalyzed hydroformylation, like the kinetics and mechanism, stability of catalyst, etc. need detailed investigations. Similarly, in hydroformylation of higher olefins, the catalyst product separation issue is the major challenge. Although various immobilization techniques have been proposed, not a single one has been commercially viable, except biphasic catalysis, which also cannot be applied to hydroformylation of higher olefins.

Still, the area of immobilization is open for the development of new heterogeneous catalysts, which can satisfy the commercial requirement. Based on the literature reports the main objective of this work was to develop new heterogenized homogeneous catalyst systems, like biphasic catalysis and heterogenized catalysts immobilized on solid supports, for the hydroformylation reaction. This is directly relevant to the catalyst-product separation issues for such an industrially important reaction. With these objectives the following problems were chosen for this work:

- Hydroformylation of terpenes using homogeneous Rhodium-phosphite complex catalysts: Activity, selectivity and kinetic study.
- Hydroformylation of higher olefins using water-soluble Rhodium-sulfoxantphos catalyst in biphasic medium: Activity, selectivity and kinetic study.
- Synthesis, characterization and catalytic activity of ossified catalyst for hydroformylation of higher olefins. Activity, selectivity and kinetic studies.

References

1 R. J. Farranto, C.H. Bartholomew (Eds.) *Fundamentals of Industrial Catalytic Processes*, Blackie Academic and Professional, London, **1997**.

2 (a) G. W. Parshall, *Homogeneous Catalysis*, Wiley-Interscience, New York, **1980**. (b) C. Masters, *Homogeneous Transition-Metal Catalysis*, Chap-man and Hall, London, **1981**.

3 (a) B. Cornils, W. A. Herrmann (Eds.), *Applied Homogeneous Catalysis with Organometallic Compounds*, VCH, Weinheim, *Vol-1, 2, ,* **2002**. (b) G. C. Bond (Eds.) *Heterogeneous Catalysis: Principles and Application*, second edition Oxford Clarendon Press **1987**. (c) J. Wetley, H. O. Halvorson, H. L. Roman, E. Bell *Enzymic Catalysis* Harper and Row Publishers Inc. New York, **1969**.

4 M. Beller, C. Bolm (Eds.), *Transition Metals for Organic Synthesis: Building Blocks and Fine chemicals*, Wiley-VCH, Weinheim, *Vol-1, 2,* **2004.**

5 R. Jira in *Ethylene and its industrial derivatives*, (Ed. S.A. Miller), Ernest Benn Ltd. **1969**, p.650

6 W. Partenheimer, *Catal. Today,* **1995**, *23*, 69.

7 E. F. Lutz, *J. Chem. Educ.*, **1986**, *63*, 202.

8 V. D. Ludecke, J. J. Mcketta, W. A. Cunningham (Eds.), *Encyclopedia of chemical processing and design*, Maedetl and Decker, **1976**, p. 146

9 W.A. Knowles, *Acc. Chem. Res.,* **1983**, *16*, 106.

10 (a) BASF AG, *Hydrocarbon Process,* 1977, *11*, 135 (b) BASF AG, *Hydrocarbon Process,* **1977**, *11*, 172.

11 T.H. Johnson, (Shell Oil Co.), *US 4584411,* **1985**.

12 Anon, *Chem.Eng.,* **1977**, *84*, 110.

13 B.Cornils, E. Kuntz, *J. Organomet. Chem.,* **1995**, *502*,177.

14 C. R.Greene, R. E Meeker, *Shell Oil Co. DE-AS 1212953,* **1967**.

15 P. Fitton and H. Moffet, *US 4124619*, **1978**.

16 H. Pommer and A. Nuerrenbach *Pure. Appl. Chem*., **1975**,43 527.

17 J. F. Roth, J. H. Craddock, A. Hershmann, F. E .Paulik, *CHEMTCH*, **1971**, *1*, 600.

18 H. Hohenshutz, N. von Kutepow, W. Himmele, *Hydrocarbon Process*, **1966**, 45, 141.

19 D.J. Watson in *Catalysis of Organic reactions*, (Eds. F. E. Herkes, H. Heinemann), Marcell Decker Inc. **1998**, 369

20 H.W. Coover, R. C. Hart, *Chem. Eng. Prog*., **1982**, 72.

21 V. H. Agreda, D. M. Pond, J. R. Zoeller, *CHEMTCH,***1992**, 172.

22 H. Hohenschutz, D. Franz, H. Bulow and G.Dinkhauser (BASF AG), *DE 2133349,* **1973**.

23 B. Blumenberg, *Nahr. Chem. Tech. Lab.,***1984**, 480.

24 (a) L. Casssar, *Chem. Ind.,* 1985, 67, 256. (b) G. W. Parshall, W.A. Nugent, *CHEMTCH,* **1988**, 314.

25 V. Elango, M. A Murphy, G. N. Mott, E. G Zey, B. L. Smith, G. L. Moss, *EP 400 892*, **1990**.

26 R. Ugo, T.Renato, M.M.Marcello, R.Plerluigi, *Ind. Eng. Chem. Prod. Res. Dev*., **1980**, *19* 396.

27 J. B. Powell, L. H. Slaugh, S. B. Mullin, T. B. Thomason, P. R. Weider, *US 5981808*, **1999**.

28 (a) D. J. Cole-Hamilton *Science*, **2003**, *299*, 1702. (b) S. Vancheesan, D. Jesudurai in *Catalysis, Principles and applications* (Eds. B. Vishwanathan, S. Shivshankar, A. V. Ramaswamy), Narora Publication New Delhi, **2002** pp311-337. (c) M. Beller, B. Cornils, C. D. Frohning, C. W. Kohlpaintner *J. Mol. Catal.,* **1995**, *104*, 17.

29 O. Rolen (Ruhrchemie A.G.) *DE 849.548*, **1938.**

30 (a) B. Cornils, *New Synthesis with Carbon Monoxide* (Eds. J. Falbe) Springler-Verlag, Berlin, Heidelberg, New York, **1980**. (b) P. W. N. M. van Leeuwen, C. Claver (Eds.) *Rhodium catalyzed Hydroformylation,* Kluwer Academic Publishers **2000**.

31 (a) H. Moell, *BASF AG DE 1272911,* **1966**.(b) F. M. Hibbs, *ICI Ltd. GB 1458375* **1976**. (c) R. Papp, F. Mongenet, *DE-OS 2927979,***1980**. (d) Ruhrchemie AG., *Hydrocarbon Proc.,* **1977**, *11*, 134.

32 C. R. Greene, R. E. Meeker, *Shell Oil Co., US 3274263,* **1966**.

33 R. L. Pruett, J. A. Smith, *Union Carbide Corp*. *US 3917661,* **1975**.

34 E.G. Kuntz ,*CHEMTECH*, **1987**, 570.

35 M. Beller, *J. Mol. Catal A: Chemical,* **1995**, *104*, 17.

36 J.T. Carlock, *Tetrahedron*, **1984**, *40*, 185.

37 (a) F.A. Cotton, B. Hong, *Progress Inorg. Chem.*, **1992**, *40*, 179. (b) H.A. Mayer, W. C. Kaska, *Chem. Rev.*, **1994**, *94*, 1239.

38 L. H. Pignolet (Ed.) *Homogeneous Catalysis with Metal Phosphine Complexes*, Plenum Press, London **1983**.

39 (a) A. J. Arduengo, R.L. Harlow, M. Kline, *J. Am. Chem. Soc*., **1991**,*113*, 361. (b) D. A. Dixon, A. J. Arduengo, *J. Phys. Chem.*, **1991**, *95*, 4180. (c) A. J. Arduengo, H. V. Rasika-Diaz, R. L. Harlow, M. Kline, *J. Am. Chem. Soc.*, **1992**,*114*, 5530.

40 (a) P. W. N. M. van Leeuwen, C. F. Roobcek, *J. Organomet. Chem.*, **1983**, *258*, 343. (b) A. Polo, J. Real, C. Claver, S. Castillon, J. C. Bayon, *J. Chem. Soc. Chem. Commun.*, **1990**, 600. (c) A. van Rooy, E.N. Orij, P. C. J. Kamer, F. van denardweg, P.W.N.M. van Leeuwen, *J. Chem. Soc. Chem. Commun.,* **1991**, 1096. (d) T. Jongsma, G. Challa, P. W. N. M. van Leeuwen, *J. Organomet. Chem.*, **1991**, *421*, 121. (a) D. R. Bryant. E. Billig, 4th *Int. Conf. Chem. Plat. Group Met.,* **1990**. (b) Union Carbide Corp. (E. Billig, A.G. Abatjoglou. D.R. Bryant), Eur.Pat. Appl. *EP 0.213639* **1987**; Chem. Abstr., **1987,** 107, 7392. (c) UCC (E. Billig, A.G. Abatjoglou, D.R. Bryant), EP Appl. EP 0.214.622, **1987**; Chem. Abstr., **1987**,107 25126. (d) UCC (E. Billig, A.G. Abatjoglou, D.R. Bryant), *US 4.769.498* **1988**; Chem. Abstr., **1989**, 111, *117*, 287. (e) UCC (J. M. Maher, J. E. Babin, E. Billig, D. R. Bryant, T.W. Leung), US 5.288.918, **1994**; Chem. Abstr., **1994**, *121*, 56996.

41 O. R. Hughes, J. D. Unruh, *J. Mol. Catal.,* **1981**, *12*, 71

42 J. R. Christenson, J. D. Unruh *J. Mol. Catal.,* **1982**, *14*, 19 (b) J. D. Unruh, W. J. Wells, *Belgian Patent 840906*, **1976**.

43 K. Tamao, H. Yamamoto, H. Matsumoto, N. Miyake, T. Hayashi, M. Kumada, *Tetrahedron Lett.*, **1977**, *16*, 1389.

44 (a) All patents from Eastman Kodak (T.J. Devon, G.W. Phillips, T. A. Puckette, J. L. Stavinoha, J. J. Vanderbilt), PCT Int. Appl. *WG 87/ 07 600*, **1987**; Chem. Abstr., **1988,** *109* 8397. (b) T. J. Devon, G. W. Phillips, T. A. Puckette, J.L. Stavinoha, J. J. Vanderbilt, *US 4.694.109*, **1987**; Chem. Abstr., **1988**, *108*, 7890. (c) T. A. Puckette, T. J. Devon, G. W. Phillips, J. L. Stavinoha, *US 4.879.416* , **1989**; Chem. Abstr., **1990**, *112*, 217.269. (d) J.L. Stavinoha, G.W. Phillips, T.A. Puckette, T.J. Devon, *EP 0.326.286*, **1989**; Chem. Abstr., **1990**, *112*, 98.823.

45 P. Dierkes, P. W. N. M. van Leeuwen *J. Chem. Soc. Dalton Trans.,* **1999**, 1519.

46 L. A. Vanderveen, P. H. Keeven, Schoemeker, J. N. H. Reek, P. C. J. Kamer, P. W. N. M. van Leeuwen, M. Lutz, A. Speak,*Organometallics*, **2000**, *19*, 872.

47 (a)W. A. Hermann, C. W. Kohlpainter, H. Bharmann, W. Konkol *J. Mol. Catal. A: Chemical, **1992**, 73,* 191. (b) W. A. Hermann, C. W. Kohlpaintner, R. B. Mantesberger, H. Bharmann, *J. Mol. Catal. A: Chemical*, **1995**, *97*, 65. (C) M. S. Goedheijt, P. C. J. Kamer, P. W. N. M. van Leeuwen *J. Mol. Catal. A: Chemical,* **1998**, *134,* 243.

48 (a) C. P. Casey, G. T. Whiteker, M. G. Melville, L. M. Petrovich, J. Gamey, D. R. Powell, *J. Am. Chem. Soc.,* **1992**, *114*, 5535. (b) C. A. Tolman, W. C. Seidel, L. W. Gosser, *J. Am. Chem. Soc.*, **1974**, *96*, 53.; C. A. Tolman, *Chem. Rev.*, **1977**, *77*, 313.

49 B. Cornils, W. A. Herrmann (Eds.) *Aqueous Phase Organometallic Catalysis: Concept and Application,* Viley-VCH, Weinheim (Germany) **1998.**

50 (a) I. T. Horvath, J. Rabai, *Science* **1994**, 266.(b)*Exxon Research and Engineering Co*. (I. T. Horvath and J. Rabai) *EP 633.062* Al **1995**, *US5.463.082* **1995**.(c) D. P. Curran, S. Hadida *J. Am. Chem.Soc.*, **1996**, *118*, 2531. (d) S. G. Dimgno, S. G. Dussault *J. Am. Chem. Soc.,* **1996**, *118*, 5312.

51 (a) R. Reichardt, *Solvents and Solvent Effects in Organic Chemistry*, VCH, Weinheim **1990**. (b) Y. Chauvin, H. Olivier *CHEMTECH*, **1995**, *25*, 26. (b) K. R. Seddon, *Kinet. Catal*., **1996**, *37*, 693.(c) K. R. Seddon, *J. Chem. Tech. Biotechnology*, **1997**, *68*, 351. (d) P. Wasserscheid, T. Welton (Eds.) *Ionic Liquids in Synthesis*, Wiley-VCH: Weinheim, **2003.**

52 D. Koch, W. Leitner, *J. Am. Chem. Soc.,* **1998**, *120,* 13398.

53 (a) F. Monteil, R. V. Kastrup, A. A. Ostwald, *Catal. Lett.,* **1985**, *2*, 85. (b) Purwanto, H. Delmas, *Catal. Today* **1995**, *24*, 134. (c) R.M. Deshpande, Purwanto, H. Delmas, R. V. Chaudhari, *Ind. Eng. Chem. Res.,* **1996**, 35, 3927. (d) Y. Zhang, Z. Mao, J. Chen, *Catal. Today,* **2002**, *74*, 23. (e) R. M. Deshpande, Purwanto, H. Delmas, R.V. Chaudhari, *J. Mol. Catal A: Chemical,* **1997**, *126*,133. (f) F. Monteil, R. Dueau, P. Kalck *J. Organomet. Chem.,* **1994**, *480*, 177.

54 (a) F. M. Menger, *Angew. Chem.,* **1994**, *103*, 1104. (b) E. Kissa, *Fluorinated Surfactants: Synthesis, Properties, Application,* Marcel Dekker, New York, **1994**. (c) J. M. Brown, S. K. Baker, A. Colems in Enzymic and Non-enzymic Catalysis (Eds. P. Dunill, A. Wiseman) Horword, Chichester, **1980**, P111. (d) H. Chen, Y. Li, J. Chen, P. Cheng, Y. He, X. Li, *J. Mol. Catal. A: Chemical,* **1999**, *149*, 1

55 M. J. H. Russel, B. A. Murrer, *US. Patent 4399312* to Johnson Matthey Public Ltd. Co, **1981** b) M. J. H. Russel, *Platinum Metal Review,* **1998**, *32*, 179.

56 R. V. Chaudhari, B. M. Bhanage, R. M. Deshpande, H. Delmas, *NATURE,* **1995**, *373*, 501.

57 (a) D. C. Bailey, S. H. Langer, *Chem. Rev.*, **1981**, *81*, 109. (b) D. D. Whitehurst, *CHEMTECH*, **1980**, *10*, 44. (c) Y. I. Yermakov, B. N. Kuznetsov, V. A. Zakharov, *Stud. Surf. Sci. Catal.*, 1981, *8*, 1. (d) F. R. Hartley, *Supported Metal Complexes*, Reidel, Dordrechiet, **1985**.

58 E. Bayer, V. Schurig *CHMTECH*, **1976**, 212.

59 D. C. Bailey, J. H. Langer *Chem. Rev.,* **1981**, 81, 109. (b) U. Schubert, C. Egger, K. Rose C. Alt. *J. Mol. Catal.,* **1989**, *55*, 220. (c) A. Rosenfeld, D. Avnir, J. Bulm, *J. Chem. Soc. Chem. Commun*., **1993**, 583.

60 (a) P.R. Roney, J. F. Roth, *U.S. 3.855.307*, **1974**. (b) J. Hjortkjaer, M. S. Scurrell, P. Simonsen, *J. Mol. Catal.,* **1979**, *6*, 405. (c) J. Hjortkjaer, M.S. Scurrell, P. Simonsen, H. Svendsen, *J. Mol. Catal.*, **1981**, *12* , 179

61 (a) J. P. Arhancet, M. E. Davis, J. S. Merola, B. E. Hanson *NATURE,* **1989**, *339*, 454. (b) J. P. Arhancet, M. E. Davis, J. S. Merola, B. E. Hanson *J. Catal.*, **1990**, *121*, 327.(c) M. E. Davis *CHEMTECH*, **1992**,198.(d) K. T. Wan, M. E. Davis *J. Catal.*, **1994**, *148*, 1.

62 Ullmann's *Encyclopedia of Industrial Chemistry* (5th Ed.) Vol. A13, VCH, Weinheim, page 240.

63 H. Bohnen, B. Cornils, *Advances in Catalysis,* **2002**, *47*, 1.

64 A. Yamamoto, (Eds.) in *Kirk-Othmer, Encyclopedia of Chemical Tehnology*, 3rd edition, *vol. 2*, Wiley, New York, **1978**, 410 and refs. therein.

65 C. K. Brown, G. Wilkingson *J. Chem. Soc. A,* **1970**, 2753
(a) R. M. Deshpande, R. V.Chaudhari, *J. Catal.,* **1989**, *115*, 326. (b) R. M. Deshpande, R. V. Chaudhari, *Ind. Eng. Chem. Res.,* **1988,** *27*, 1996. (c) R. M. Deshpande, R. V.Chaudhari, *J. Mol. Catal.*, **1989**, *57*, 177 (d) S. S. Divekar, R. M. Deshpande, R. V. Chaudhari, *Catal. Lett.*, **1993**, *21*, 191.(e) B. M. Bhanage, S. S. Divekar, R. M. Deshpande, R. V. Chaudhari, *J. Mol. Catal. A: Chemical*, **1997**, *115*, 247. (f) V. S. Nair, S. P. Mathew, R. V. Chaudhari, *J. Mol. Catal. A: Chemical,* **1999**, *143*, 99. (g) R. Chansarkar, K. Mukhopadhyay, A. A. Kelkar, R. V. Chaudhari *Catal. Today,* **2003**, *79–80*, 51. (h) R. M. Deshpande, B. M. Bhanage, S. S. Divekar, S. Kanagasabapathy, R. V. Chaudhari *Ind. Eng. Chem. Res.,* **1998**, *37,* 2391

67 P. Kalck, F. Monteil, *Adv. in Organomet. Chem.,* **1992**, *34*, 219.

68 (a) R. M. Deshpande, B. M. Bhanage, S. S. Divekar, S. Kanagasabapathy, R. V. Chaudhari, *Ind. Eng. Chem. Res.,* **1998**, *37*, 2391. (b) B. M. Bhanage, Ph.D. Thesis, University of Pune, **1995**. (c) V. S. Nair, Ph.D. Thesis, University of Pune, **1999**. (d) R. M. Deshpande, Purwanto, H. Delmas, R. V. Chaudhari *J. Mol. Catal. A: Chemical,* **1997,** *126*, 133.

69 P. Purwanto, H. Delmas, *Catal. Today*, **1995**, *24*, 134.

70 R. V. Chaudhari, B .M. Bhanage in Aqueous Phase *Organometallic Catalysis: Concept and Application* (Eds. B. Cornils and W.A. Herrmann) Viley-VCH, Weinheim (Germany) **1998** pp 283-294.

71 (a) L. A. Girritsen, W. Klut, M. H. Vreugdenhil, J. J. F. Scholten *J. Mol. Catal.,* **1980**, *9*, 265.(b) N. A. Munck, J. P. A. Notenboom, J. E. Deleur, J. J. F.

Scholten *J. Mol. Catal.,* **1981**, *11*, 233. (c) H. E. Pelt, R. P. J. Verburg, J. J. F. Scholten *J. Mol. Catal.,* **1985**, *32*, 77.

72 (a) U. J. Jauregui-Haza, E. P. Fontdevila, P. Kalck, A. M. Wilhelm, H. Delmas *Catal. Today* **2003**, *79–80*, 409. (b) U. J. Jauregui-Haza, O. Dıaz-Abın, A. M. Wilhelm, H. Delmas, *Ind. Eng. Chem. Res.,* **2005**, *44,* 9636.

73 M. Benaissa , U. J. Jáuregui-Haza, I. Nikov, A. M. Wilhelm, H. Delmas *Catal. Today,* **2003**, *79–80*, 419.

74 M. M. Diwakar, R. M. Deshpande, R. V. Chaudhari *J. Mol. Catal. A: Chemical,* **2005**, *232*, 179

75 (a) B. Heil, L. Marko *Chem. Berr.* **1971**, *104*, 3418. (b) G. Csontos, B. Heil, L. Marko *Ann. N. Y. Acad. Sci.,* **1974**, *239*, 47

76 (a) Y. Gankin, D. M. Rudkowski *Kinet. Katal.,* **1967**, *8*, 908. (b) Y. Gankin, L. S. Genender, D. M. Rudkowski *Zh. Prikl. Khim.,* **1967**, *40*, 2029.

77 Y. Gankin, L. S. Genender, D. M. Rudkowski, *Zh. Prikl. Khim.* **1968**, *41*, 1577.

78 L. Marko *Aspects of Homogeneous Catalysis* (Ed.) R. Ugo Riedel Publishing Co. Dordrecht, Holland **1899**.

79 W. Strohmeier, M. Z. Michel *Phy-Chem.* Wiesbaden **1981**, *124*, 23.

80 P. L. Mills, S. J. Tremont, E. E. Remson *Ind. Eng. Chem. Res.* **1990**, *29*, 1443

81 A. van Rooy, E. N. Origi, P. C. J. Kamer, P. W. N. M van Leeuwen. *Organometallics*, **1995**, *14*, 3.

82 C. Yang, Z. Mao, Y. Wang, J. Chen, *Catal. Today,* **2002**, *74*, 111.

83 V. K. Srivastava, S.K. Sharma, R. S. Shukla, N. Subrahmanyam, R. V. Jasra *Ind. Eng. Chem. Res.,* **2005**, *44,* 1764.

84 H. Arai, T. Kaneko, T. Kunuji, *Chem. Lett.* **1975**, *3*, 265.

85 A.R. Tadd, A. Marteel, M. R. Mason, J. A. Davies, M.A. Abraham *Ind. Eng. Chem. Res.* **2002**, *41,* 4514.

86 D. Evans, J. A. Osborn, G. Wilkinson, *J. Chem. Soc. A*, **1968**, 3133.

87 (a) Karl A. D. Swift *Topics in Catalysis,* **2004**, *27(1–4)*, 143. (b) N. Ravasioa, F. Zaccheriab, M. Guidottia, R. Psaroa, *Topics in Catalysis,* **2004,** *27 (1–4)*, 159. (c) Jose L. F. Monteiro, C. O. Veloso *Topics in Catalysis,* **2004**, *27 (1–4)*, 169. (d) A. J. Chalk in *Catalysis of Organic Reactions*, (Eds. P. N. Rylander, H. Greenfield, R. L. Augustine) *Vol 22* Marcel Dekker, New York, *1988*, 43.

88 J. C. Locicero, R. T. Johnson, *J. Am. Chem. Soc.,* **1952**,*74*, 2094.

89 W. H. Clement, M. Orchin *J. Chem. Soc.,* **1965**, *4*, 283.

90 C. K. Brown, G. Wilkinson *Tetrahedron Lett.,* **1969**, *22*, 1725,

91 J. C. Chalchat, R. P. Garry, E. Lecomte, A. Michet, *Flavor Fragrance J.*, **1991**, *6(3)*, 179.

92 W. Himmele, H. Siegel, *Tetrahedron Lett.* **1976**, 907.

93 W. Himmele, H. Siegel, unpublished work

94 J. Hagen, K. Bruns *DE 2849742*, **1980**.

95 J. Hagen, K. Bruns *US4283561*, **1981**.

96 G. Klein, D. Arlt, R. Braden, *US 4505860*, **1985**

97 A. J. Chalk *Dev. Food Sci. 18 (flavours Fragrances)* **1988**, 867.

98 H. J. V. Barros, M. L Ospina, E. Arguello, W. R Rocha, E. V Gusevskaya, E. N. dos Santos, *J. Organomet. Chem.*, **2003,** *671(1-2)*, 150.

99 E. V. Gusevskaya, E. N.dos Santos, R Augusti, A. O. Dias, P. A. Robles-Dutenhefiner, C. M. Foca, H .J. V. Barros, *Stu. Surf. Sci. Catal.* **2000**, *130*, 563.

100 C. M. Foca, H. J. V. Barros, E. N. dos Santos, E.V. Gusevskaya, J. C. Bayon *New J. Chem.***, 2003,** *27*, 533.

101 Hoffmann et al. US4081477,**1978**

102 P. W. N. M. van Leeuwen, C.F. Roobeek *J. Organomet. Chem., **1983,** 258,* 343 and P. W. N. M. van Leeuwen, C.F. Roobeek, *US4467116*, **1984**.

103 Y. Kou,Y.Yin, *Fenzi Cuihua*, **1989**, *3(4)*, 262.

104 (a) I. Cipres, P. Kalck, D.C.Park and F. Serein-Spirau J. Mol. Catal. **1991**, *66*, 399.(b) S. Sirol, P. Kalck, *N. J. Chem.* **1997**, *21*, 1129

105 K. Soulantica, S. Sirol, S. Koinis, G. Pneumatikakis, P. Kalck, *J. Organomet. Chem.* **1995**, *498*, C10-13.

106 E. N. dos Santos C. U. Pittman, Jr., H. Toghiani, *J. Mol. Catal. A: Chemical*, **1993**, *83*, 51.

107 F. Azzaroni, P. Biscarini, S. Bordoni, G. Longoni, E. Venturini *J. Organomet. Chem.,* **1996**, *508*, 59.

108 H. J. V. Barros, B. E. Hanson, E. V. Gusevskaya, E.N. dos Santos, *Applied catalysis A: General*, **2004,** *278*, 57.

109 P. Kalck, L. Miquel, M. Dessoudeix, *Catal. Today,* **1998**, 42, 431.

110 U. J. Jauregui-Haza, R. Nikolova, A. M. Wilhelm, H. Delmas, I. Nikov, *Bulgarian Chem. Commun.*, **2002**, *34(1)*, 64.

111 M. Marchetti, S. Paganelli, E. Viel, *J. Mol. Catal. A: Chemical*, **2004**, *222*, 143.

112 S. B. Halligudi, K. N. Bhatt, K. Venkatasubramanian*, React. Kinet. Catal. Lett.*, **1993**, *51(2)*, 459.

113 L. Kollar, J. Bakos, B. Heil, P. Sandor, G. Szalontai, *J. Organomet. Chem.* **1990**, *385*, 147.

114 L. Kollar, G. Bodi, *Chirality*, **1995**, *7*, 121.

115 A. d. O. Dias, R. Augusti, E. N. dos Santos, E. V Gusevskaya,. *Tetrahedron Lett.*, **1997**, *38(1)*, 41.

116 E. V. Gusevskaya, E. N.dos Santos, R. Augusti, A. d. O. Dias, C. M. Foca, *J. Mol. Catal. A: Chemical*, **2000**, *152(1-2)*, 15.

117 C. M. Foca, E. N. dos Santos, E. V. Gusevskaya, *J. Mol. Catal. A: Chemical*, **2002,** 152, 15.

118 B. Cornils, W.A. Hermann, R. W. Rckl, *J. Mol. Catal. A: Chemical*, **1997,** *116*, 27.

119 (a) P. G. Jessop, T. Ikariya, R. Noyori, *Chem. Rev.*, **1999**, *99*, 475. (b) J. W. Rathke, R. J. Klingler, T. Krause *Organometallics* **1991**, *10*, 1350.

120 F.V. Vyve, A. Renken, *Catal. Today,* **1999,** *48*, 237.

121 Michel J.H. Russell *US4399312*, **1983**

122 M. Gimenez-Pedros, A. Aghmiz, C. Claver, A. M. Masdeu-Bulto, D. Sinou, *J. Mol. Catal. A: Chemical*, **2003,** *200*, 157.

123 H. Chen, Y. Li, J. Chen, P. Cheng, X. Li, *Catal. Today*, **2002,** *74*, 131.

124 S. Tilloy, G. Crowyn, E. Monflier, P. W. N. M. van Leeuwen, J. N. H. Reek, *New J. Chem.*, **2006,** *30*, 377.

125 E. Monflier, G. Fremy, Y. Castanet, A. Mortreux, *Angew. Chem. Int. Ed. Engl.* **1995**, *34*, 2269.

126 E. Monflier, S. Tilloy, G. Fremy, Y. Castanet, A. Mortreux *Tetrahedron Lett.* **1995**, *36*, 9481.

127 E. Monflier *US 5847228,* **1998.**

128 T. Mathivet, C. Meliet, Y. Castanet, A. Mortreux, L. Caron, S. Tilloy, E. Monflier, *J. Mol. Catal. A: Chemical,* **2001,** *176*, 105.

129 L. Leclercq, M. Sauthier, Y. Castanet, A. Mortreux, H. Bricout, E. Monflier, *Adv. Synth. Catal.,* **2005,** *347*, 55.

130 P. Kalck, L. Miquel, M. Dessoudeix, *Catal. Today* **1998,** *42*, 431.

131 T. Mizugaki, Y. Miyauchi, M. Murata, K. Ebitani, K. Kaneda, *Chemistry Lett.* **2005,** *34(3)*, 286.

132 B. Sueur, L. Leclercq, M. Sauthier, Y. Castanet, A. Mortreux, H. Bricout, S. Tilloy, E. Monflier, *Chem. Eur. J.,* **2005,** *11*, 6228.

133 S. Tilloy, E. Genin, F. Hapiot, D. Landy, S. Fourmentin, Jean-Pierre Genet, V. Michelet, E. Monflier *Adv. Synth. Catal.,* **2006,** *348*, 1547.

134 L. Leclercq, F. Hapiot, S. Tilloy, K. Ramkisoensing, J. N. H. Reek, P. W. N. M. van Leeuwen, E. Monflier, *Organometallics,* **2005,** *24*, 2070.

135 X. Zheng, J. Jiang, X. Liu, Z. Jin, *Catal. Today,* **1998**, *44*, 175.

136 Y. Wang, J. Jiang, Q. Miao, X. Wu, Z. Jin, *Catal. Today* **2002**, *74*, 85.

137 J. Jiang, Y. Wang, C. Liu, Q. Xiao, Z. Jin *J. Mol. Catal. A: Chemical,* **2001,** *171*, 85.

138 C. Liu, J. Jiang, Y. Wang, F. Cheng, Z. Jin, J. *Mol. Catal. A: Chemical* **2003,** *198*, 23.

139 L. Xiaozhong, W. Yanhua, J. Jingyang, J. Zilin, *Chemical Journal on Internet* **2000,** *2(2)*, 1.

140 L. Xiaozhong, L. Hongmei, K. Fanzhi, *J. Organomet. Chem.*, **2002,** *654*, 1.

141 X. Liu, Y. Wang, F. Kong, Z. Jin, *Chinese Journal of Chemistry*, **2003,** *21(5)*, 494,

142 X. Liu, H. Li, Y. Wang, Z. Jin, *J. Organomet. Chem.*, **2002,** *654*, 83.

143 (a) I T. Horvath, J. Rabai, *Science*, **1994,** 266. (b) I T. Horvath, J. Rabai *US 5463082*, **1995**

144 I. T. Horvath, G. Kiss, R. A. Cook, J. E. Bond, P. A. Stevens, J. Rabai, E. J. Mozeleski, *J. Am. Chem. Soc.* **1998**, *120,* 3133.

145 W. Chen, L. Xu, J. Xiao, *Chem. Commun.,* **2000**, 839

146 T. Mathivet, E. Monflier, Y. Castanet, A. Mortreux, J. Luc-Couturier, *Tetrahedron,* **2002,** *58*, 3877

147 A. M. B. Osuna, W. Chen, E. G. Hope, Ray D. W. Kemmitt, D. R. Paige, A. M. Stuart, J. Xiao, L. Xu, *J. Chem. Soc. Dalton Trans.*, **2000,** 4052.

148 J. Dupont, S. M. Silva, R.F. de Souza, *Catal. Lett.* **2001,** *77*, 1.

149 (a) M. Capka, P. Svoboda, M. Kraus, J. Hetflejs, *Chem. Ind. (London)* **1972**, 650. (b) I. Dietzmann, D. Tomanova, J. Hetflejs, *Collect. Czech Chem. Commun.,* **1974**, *39*, 123.

150 M. Kraus *Collect. Czech Chem. Commun.* **1974**, *39*, 1318.

151 L. D. Rollmann, *Inorg. Chim. Acta.* **1972**, *6*, 137.

152 R.H. Grubbs, C. Gibbons, L.C. Kroll, W. D. Bonds, C. H. Brubaker, *J. Am. Chem. Soc.,* **1973**, *95*, 2373.

153 R. H. Grubbs, L. C. Kroll, *J. Am. Chem. Soc.,* **1971**, *93*, 3062.

154 C. U. Pittman Jr., *CHEMTECH***, 1971**, 416.

155 F.R. Hartley, P.N. Vezeyin, *Adv. Organomet. Chem,.* **1977**, *15*, 189.

156 (a) M. Capka, P. Svoboda, M. Cerny, J. Hetflejs, *Tetrahedron Lett.***, 1971**, 4787. (b)W. O. Hagg, D. D. Whitehurst, *Proc. 5th Int. Cong. Catal.,* **1972**, 465.

157 (a) J. Haggin, *Chem. Eng. News*, **1982**, *60*, 11. (b) A. J. Moffat, *J. Catal.* **1970**, *19*, 322.

158 C.U. Pittmann Jr., A. Hirao, C. Jones, R. M. Hanes, Q. N. Ann, *N. Y. Acad. Sci.* **1977**, *12*, 295.

159 G. Braca, *Chim Oggi,* **1988**, *11*, 23.

160 B. C. Gates, *Chem. Rev.* **1995**, *95*, 511.

161 L. L. Murrell in *Advanced Materials in Catalysis* (Eds. J.L.Burton, R.L. Garten) Acedemic press, New York, **1977.**

162 (a)R. Augustine, S. Tanielyan, S. Anderson, H. Yang, *Chem. Commun.,* **2001**, 1257. (b) S. Tanielyan, R. Augustine *US Patent 6025245*, **1999**. (c) M. J. Bark, A. Gerlach, D. Semmerji, *J. Org. Chem.* **2000,** *65*, 8933.

163 (a)Degussa AG(P. Pantser, R. Gradl) *DE3643894*, **1986** (b) J. Hetflejs in *Catalytic hydrogenation* (Ed. L. Cerveny) Elsevier, Amsterdam, **1986**, p.497

164 (a)U.Schubert, C. Egger, K. Rose, C. Alt, *J. Mol. Catal.,* **1989**, *55*, 220 (b) R. Rosenfeld, D. Avnir, J. Blum, *J. Chem. Soc. Chem Commun.* **1993**, 583.

165 (a) C. P. Mehnert, R. A. Cook, N. C. Dispenziere, M. Afeworki, *J. Am. Chem. Soc.* **2002**, *124*, 12932. (b) C. P. Mehnert, E. J. Mozeleski, R. A. Cook *Chem. Commun*, **2002**, 3010.

166 L. Alvila, T. A. Pakkanen, *J. Mol. Catal. A: Chemical*, **1993,** *84*, 145.

167 H. Gao, R.J. Angelici, *J. Mol. Catal. A: Chemical,* **1999,** *145*, 83.

168 E. Lindner, F. Auer, A. Baumann, P. Wegner, H. A. Mayer, H. Bertagnolli, U. Reinohl, T. S. Ertel, A. Weber *J. Mol. Catal. A: Chemical,* **2000,** *157*, 97.

169 J. D. R. de Campos, R. Buffon, *New. J. Chem.* **2003,** *27*, 446.

170 M. Nowotny, T. Maschmeyer, Brian F. G. Johnson, P. Lahuerta, J. M. Thomas, J. E. Davies, *Angew Chem. Int. Ed. Engl.* **2001**, *40*, 955.

171 K. Mukhopadhyay, R. V. Chaudhari, *J. Catal.* **2003,** *213*, 73.

172 C. Disser, C. Muennich, G. Luft, *Applied Cat. A: General***, 2005,** *296*, 201.

173 K. Mukhopadhyay, A. B. Mandale, R. V. Chaudhari, *Chem. Mater.* **2003**, *15,* 1766.

174 Y. Yang, C. Deng, Y. Yuan, *J. Catal.* **2005,** *232*, 108.

175 A. J. Bruss, M. A. Gelesky, G. Machadoa, J. Dupont, *J. Mol. Catal. A: Chemical*, **2006,** *252*, 212.

CHAPTER 2
Hydroformylation of Terpenes using Homogeneous Rhodium-Phosphite Complex Catalyst

2.1 Introduction

Terpenes are a renewable and useful source of inexpensive olefins derived from citrus and pine oils. They are a natural and sustainable supply of building blocks for the fine chemical industry. Hydroformylation of these naturally occurring olefinic monoterpenes seems to be a promising synthetic procedure to obtain a wide variety of aldehydes with application in the perfume, flavor and pharmaceutical industries. The aldehydes can be further converted to alcohols, acetals etc. for similar applications. Optically pure terpenes containing prochiral centers are easily available and their stereoselective functionalization could be useful for the production of chiral synthetic intermediates (chiral synthones).

The hydroformylation of a number of terpenes has been investigated using rhodium, cobalt and platinum complex catalysts. This includes camphene (**1**), limonene (**2**), β pinene (**3**), 3-carene (**4**), γ-terpinene (**5**) and carvone (**6**). The detailed literature search on terpene hydroformylation is presented in chapter 1 (section 1.4). A majority of studies have centered on hydroformylation of limonene and α- and β pinene. There are very few reports available in the literature concerning the hydroformylation of camphene[1]. The possible products formed by the hydroformylation of camphene (**1**), limonene(**2**) and β- pinene (**3**) are shown in scheme 2.1. Hydroformylation of camphene is found to give only the terminal aldehyde 3, 3-dimethyl-2-norbornaneacetaldehyde, as a diastereomeric mixture of exo (**7a**) and endo (**7b**) isomers. A small quantity of byproducts namely tricyclene (**8**) and isocamphane (**9**) are formed by hydrogenation side reaction while fenchene (**10**) was obtained as byproduct by isomerization reaction. Similarly, hydroformylation of limonene and β-pinene gives 3-(4-methylcyclohex-3-enyl) butanal (**11**) and 10-formylpinane (cis (**13a**) and trans (**13b**) isomer) as aldehydes and isomerized limonene (**12**) and α-pinene (**14**) as isomerization byproducts respectively. One of the major problems of these terpene hydroformylation reactions is the prolonged reaction time and drastic reaction conditions which is reflected in the lower TOF obtained. In addition, the low reactivity of terpenes, their isomerization tendency and poor regio and stereoselectivity of hydroformylation products are the major challenges in hydroformylation of terpenes.

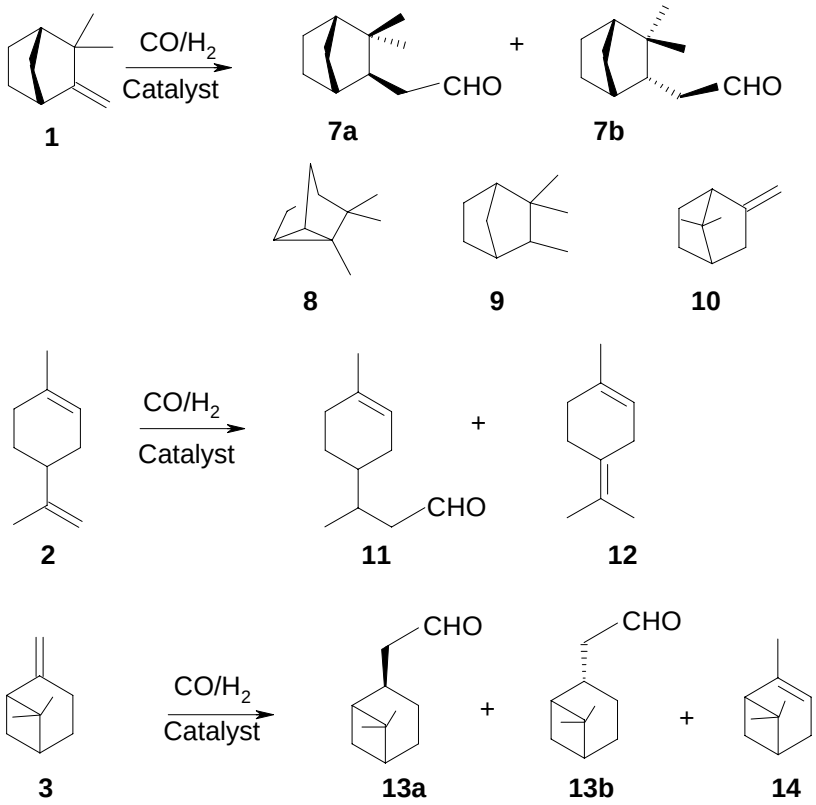

Scheme 2.1: Possible products for hydroformylation of camphene, limonene and β-pinene.

The diastereomeric excess (d.e.) achieved for the aldehyde product in hydroformylation of camphene with both rhodium and platinum complexes bearing either achiral or chiral ligands is relatively low. The molecular model analysis shows that both the diastereotopic faces of the camphene double bond are sterically hindered and there is very little steric difference between them[1e]. The best activity reported in literature using any catalyst (Rh and Pt complexes) for camphene hydroformylation is very low (TOF= 80 h^{-1})[1f]. The maximum reported selectivity to aldehyde was also around 90%. The use of phosphite ligands for the rhodium complex catalyzed hydroformylation of terpenes has also not been investigated in detail. Besides, as per our knowledge, there is also no report on a kinetic study of the hydroformylation of camphene.

In this work, we have developed a highly efficient $Rh(CO)_2(acac)/P(OPh)_3$ catalyst for the hydroformylation of camphene and other terpenes. This is a first detailed report on

phosphite ligand promoted hydroformylation of terpenes. The effect of different process parameters on the activity and selectivity in the hydroformylation of camphene using $Rh(CO)_2(acac)/P(OPh)_3$ catalyst was studied. Knowledge of the kinetics and development of rate equations is important in understanding the mechanistic features of such complex reactions. The detailed investigation on the kinetics of hydroformylation of camphene was carried out in the temperature range of 363-383 K. The effect of catalyst, substrate, and ligand concentration, partial pressure of CO and partial pressure of H_2 on the concentration-time profiles was studied. A detailed analysis of the rate data was done, since homogeneous hydroformylation of camphene is an example of a complex reaction system, which involves simultaneous dissolution of two or more gases, followed by a catalytic reaction. An empirical rate model was proposed to fit the data.

2.2 Experimental

2.2.1 Material

Rhodium chloride trihydrate ($RhCl_3.3H_2O$, 40% Rh), cobalt chloride hexahydrate ($CoCl_2.6H_2O$) and chloroplatinic acid ($H_2[PtCl_6]$) were obtained from Hindustan Platinum and used as received. (-)-Camphene, R-(+)-limonene, (-)-β-pinene, γ-terpinene, 3-(-)-carene, α-pinene, R-(-) carvone, myrcene, citral, (±)-β-citronellol, $P(OPh)_3$, $P(OBu)_3$, $P(OEt)_3$, dppe, dppp, and dppb, 1,5 cyclooctadiene and cobalt (II) acetate tetrahydrate, were procured from Sigma-Aldrich USA and used without further purification. PPh_3, acetyl acetone, potassium acetate, KOH, HCHO (40% w/w), $NaBH_4$, dimethylformamide (DMF), acetic acid were purchased from Loba Chemie India. The solvents ethanol, methanol, MEK, 1,2 dichloroethane (DCE), dichloromethane (DCM), xylene, toluene, hexane, cyclohexane, pet ether, ethylacetate obtained from Merck, India were freshly distilled and dried prior to use. Hydrogen and nitrogen gas supplied by Indian Oxygen, Mumbai and carbon monoxide (> 99.8 % pure, Matheson gas USA) were used directly from the cylinders. The syngas mixture (CO + H_2) 1:1 was prepared by mixing H_2 and CO in a reservoir vessel.

2.2.2 Synthesis of transition metal catalysts

(A) Synthesis of $HRhCO(PPh_3)_3$

$HRh(CO)(PPh_3)_3$, was prepared by a method described by Evans and coworkers[2]. In the first step, $Rh(CO)Cl(PPh_3)_2$ was synthesized and in the next step, it was used as a staring material for the preparation of $HRh(CO)(PPh_3)_3$.

(i) Synthesis of $Rh(CO)Cl(PPh_3)_2$: To a refluxing solution of PPh_3 (7.2 g, 2.75×10^{-2} mole) in ethanol (300 ml), $RhCl_3.3H_2O$ (2 g, 9.55×10^{-3} moles in 70 ml ethanol) was added under constant stirring. $RhCl(PPh_3)_3$ was formed after sometime (indicated by red-brown coloration of the solution). Formaldehyde (40% w/w, 10-20 ml) was added slowly to this red-brown solution, under constant stirring. After 30 minutes, $RhCl(PPh_3)_3$ was converted to $Rh(CO)Cl(PPh_3)_2$, as indicated by a color change from red-brown to yellow. This complex was obtained as a solid precipitate, which was filtered from the hot solution and repeatedly washed with hot, and then cold ethanol and dried. The product thus obtained was trans-$Rh(CO)Cl(PPh_3)_2$, a highly crystalline, bright yellow complex, Yield = 4.6 g (70 %). The IR spectrum of this complex showed a carbonyl stretch at 1965 cm^{-1}, which is typical for this complex (Figure 2.1(a)). The elemental analysis of $Rh(CO)Cl(PPh_3)_2$ Found: C=64.39%; H=2.43%; P= 9.0%. Calculated: C=64.30%; H=2.46%; P=8.98%.

(ii) Synthesis of $HRh(CO)(PPh_3)_3$: To prepare $HRh(CO)(PPh_3)_3$, $Rh(CO)Cl(PPh_3)_2$ (1.0 g, 1.44×10^{-3} moles) and PPh_3 (1.5 g, 5.72×10^{-3} moles) were added to ethanol (100 ml) and refluxed under constant stirring. To this solution, $NaBH_4$ (0.5 g, 1.56×10^{-2} moles) in ethanol (60 ml) was added very slowly. After complete addition, the mixture was refluxed, till a small sample of the suspended catalyst (washed and dried) showed no absorption at 1965 cm^{-1} corresponding to $Rh(CO)Cl(PPh_3)_2$. A weak absorption observed at 2020 cm^{-1} (ν_{Rh-H}) and a carbonyl stretch at 1924 cm^{-1} is typical of the $HRh(CO)(PPh_3)_3$ complex. The complex was filtered from the hot solution, washed several times with hot ethanol followed by cold ethanol, and dried, Yield=1.3 g (98%). The infrared spectrum of the complex (KBr pellet) showed the characteristic absorption at 1919 cm^{-1} and 2013 cm^{-1} (See Figure 2.1(b)). Elemental analysis of $HRh(CO)(PPh_3)_3$ Found: C=71.96%; H=5.3%; P=10.1%. Calculated: C=71.90%; H=5.12%; P=10.13%. ^{31}P NMR for $HRh(CO)(PPh_3)_3$ showed a singlet at 28.6 ppm

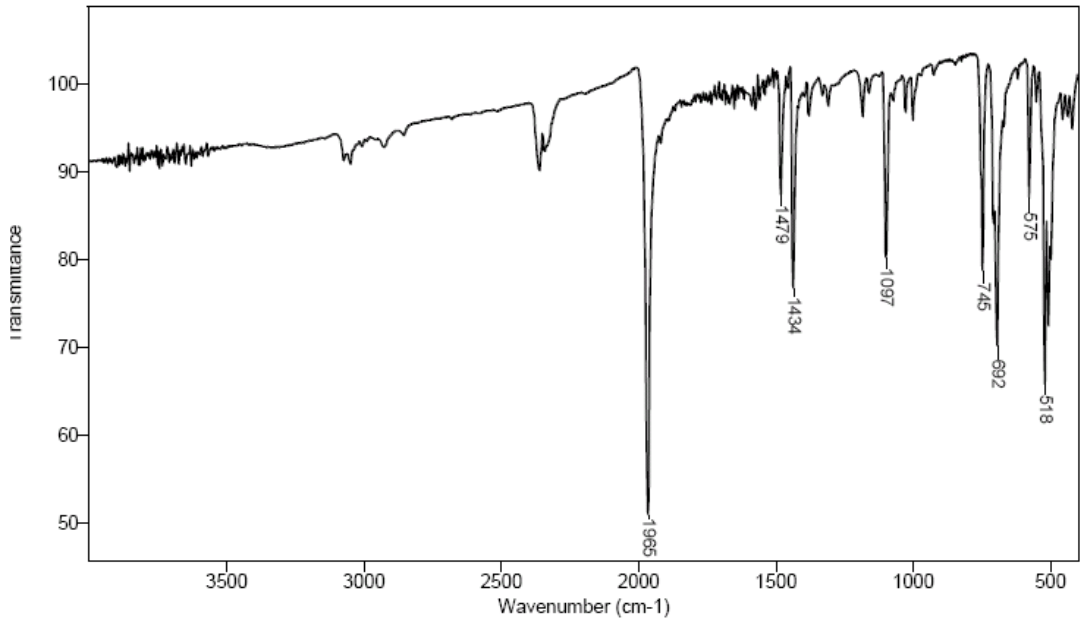

Figure 2.1(a): FTIR spectrum of $Rh(CO)Cl(PPh_3)_2$

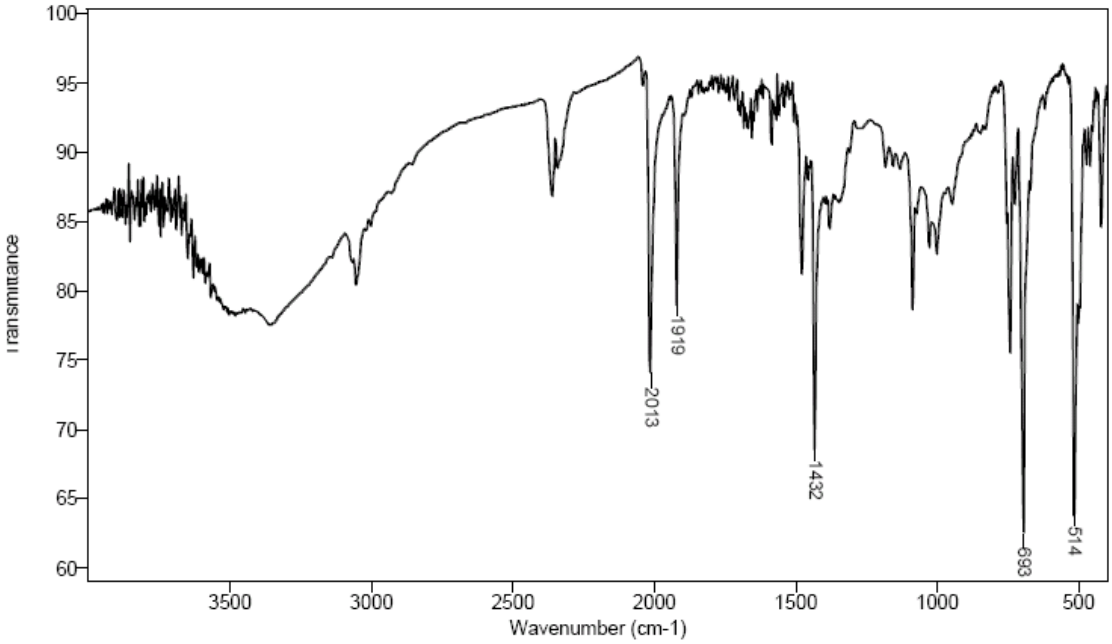

Figure 2.1(b): FTIR spectrum of $HRhCO(PPh_3)_3$

(B) Synthesis of $Rh(CO)_2(acac)$

$Rh(CO)_2(acac)$ was prepared by a method described by Varshavskii and Cherkasova[3]. Acetylacetone (12 ml) was added to a solution of $RhCl_3.3H_2O$ (3.0 g, 1.43 $\times 10^{-2}$ moles) in DMF (60 ml) with stirring. The solution was refluxed for 30 minutes and then cooled. It was diluted to twice the volume with distilled water. Addition of water resulted in a voluminous crimson precipitate. The precipitate was filtered and washed with alcohol and ether. The complex was recrystallized from hexane solution at room temperature. The needle shaped red green crystals were obtained by the slow cooling of the hexane solution. The yield (2.6 g) was about 70%. The elemental analysis of $Rh(CO)_2(acac)$ showed C=32.6%, H=2.9%. Calculated: C=32.4; H=3.08%. Characteristic IR shifts for this complex at 2065 cm^{-1}, 2006 cm^{-1} and 1525 cm^{-1} are shown in Figure-2.2.

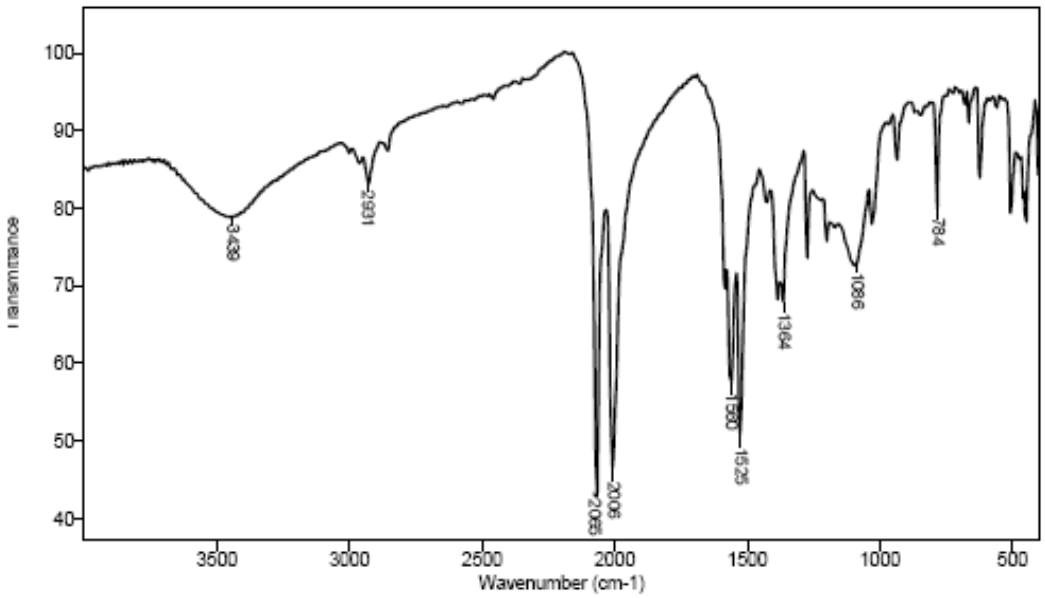

Figure 2.2: FTIR spectrum of $Rh(CO)_2acac$

(C) Synthesis of $[Rh(COD)Cl]_2$

[$Rh(COD)Cl]_2$ was prepared according to a procedure reported by Chatt and Venanzi[4]. Rhodium trichloride trihydrate (1 g, 4.77 $\times 10^{-3}$ moles) in ethanol (3 ml) was boiled under reflux with a solution of 1, 5 cyclo-octadiene (COD) (2 ml) for 3 hours. The solution was cooled and the orange solid filtered, washed with ethanol, dried and recrystallized from acetic acid. (Yield, 0.7 g, 60%). Characteristic IR shifts for this

complex at 2874 cm^{-1}, 1468 cm^{-1} and 960 cm^{-1} are shown in Figure 2.3. The elemental analysis of $[Rh(COD)Cl]_2$ Found: C=39.1%; H=4.85%; Cl=14.3%. Calculated: C=39.05%; H=5.0%; Cl=14.4%.

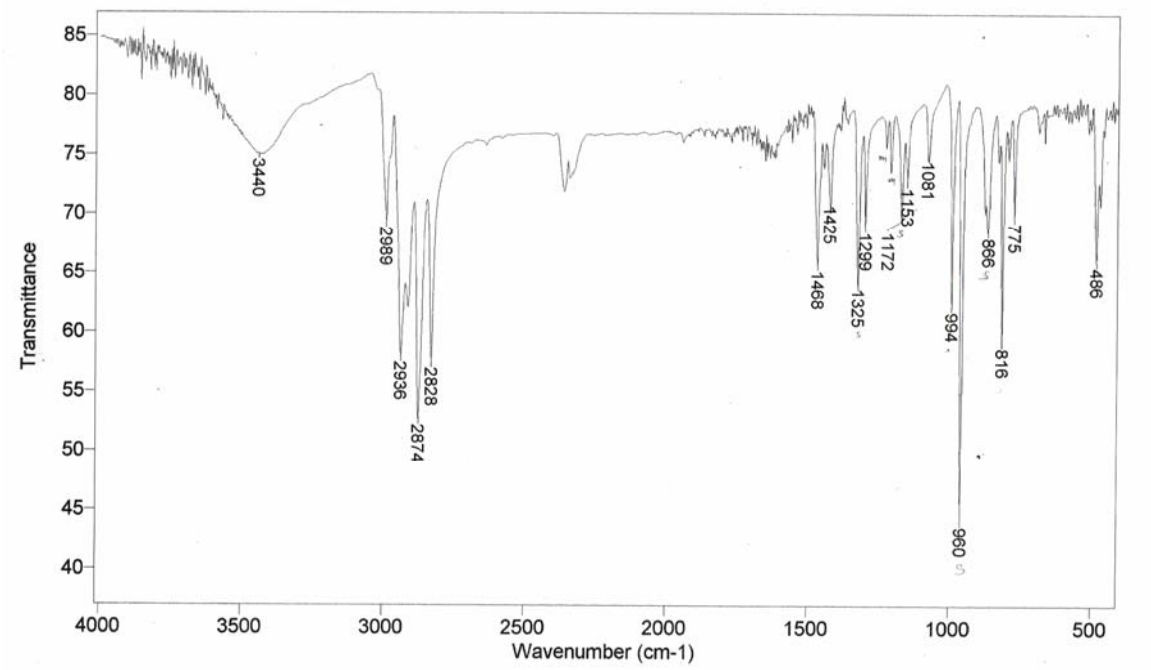

Figure 2.3: FTIR spectrum of $[Rh(COD)Cl]_2$

(D) Synthesis of $[Rh(\mu\text{-}OAc)COD]_2$

The complex was prepared using the method described by Chatt and Venanzi[5]. An acetone solution of the $[Rh(COD)Cl]_2$ (0.1 g, 2.03×10^{-4} moles) and potassium acetate (0.1 g) was boiled under reflux for two hours. The solution was then filtered and the filtrate was evaporated to dryness at 15 mm of Hg. The residue was recrystallized from ethyl acetate to give orange crystals of $[Rh(\mu\text{-}OAc)COD]_2$ pure product. (Yield, 0.09 g, 83%). Characteristic IR shifts for this complex at 2876 cm^{-1}, 1560 cm^{-1} and 959 cm^{-1} are shown in Figure 2.4. Elemental analysis of $[Rh(\mu\text{-}OAc)COD]_2$ Found C= 44.4%; H=5.7%. Calculated C= 44.5%; H=5.6%.

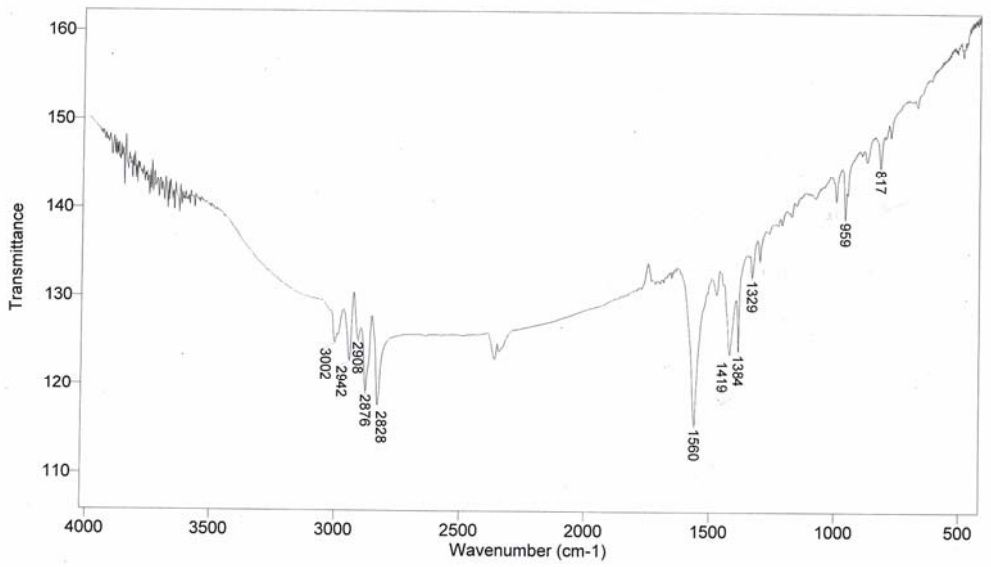

Figure 2.4: FTIR spectrum of $[Rh(\mu\text{-}OAc)COD]_2$

(E) Synthesis of $[Rh(\mu\text{-}OMe)COD]_2$

The complex was prepared using the method described by Usan and coworkers[6]. A 50 ml round bottom flask containing a magnetic stirrer bar was charged with a solution of $[Rh(COD)Cl]_2$ (0.175 g, 0.355 moles) in DCM (15 ml). The addition of KOH (0.04 g, 0.713 moles) solution in methanol (5ml) gives rise to an immediate precipitate of yellow solid.

After stirring for 30 minutes at RT, the solvent was completely removed in a rotary evaporator. Then 10 ml of methanol and subsequently 15 ml of water were added to the residue, after which, the solid was collected by filtration using fine sintered glass filter. The residue was washed with water (ten 5 ml portions) and then vacuum dried over phosphorous (II) oxide. (Yield: 0.1 g, 59%). The yellow crude product can be used without purification. An analytically pure sample is obtained by recrystallization from a mixture of DCM and hexane. The elemental analysis of the $[Rh(\mu\text{-}OMe)COD]_2$ Found C=44.80%; H=6.10%. Calculated C=44.65%; H=6.24%. Characteristic IR shifts for this complex at 3339 cm^{-1}, 2874 cm^{-1} 1074 cm^{-1} and 963$cm^{-1}$are shown in Figure 2.5**.**

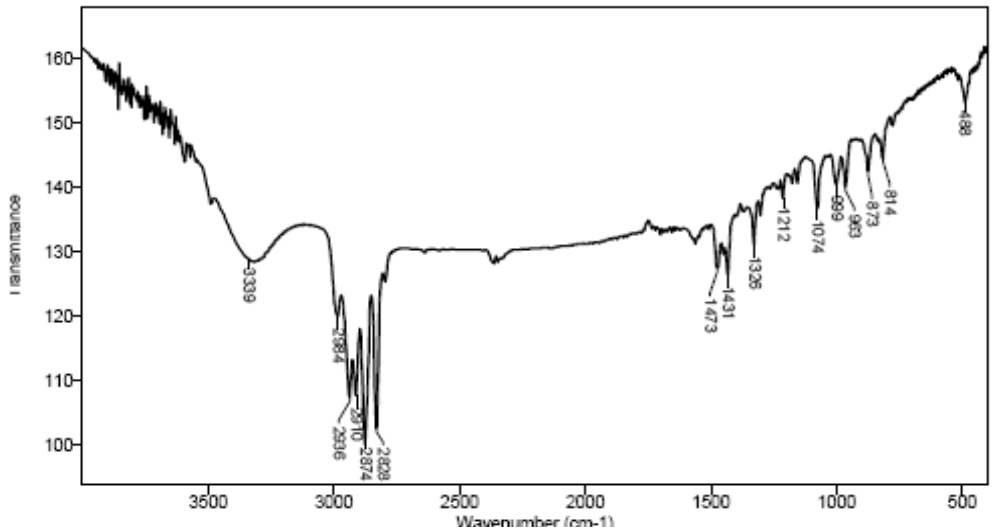

Figure 2.5: FTIR spectrum of $[Rh(OMe)COD]_2$

(F) Synthesis of $Rh(acac)(P(OPh)_3]_2$

The complex was prepared by using the method described by Trzeciak and Ziolkowski[7]**.** To $Rh(CO)_2(acac)$ (0.1 g, 3.85×10^{-4} moles), $P(OPh)_3$ (0.3 ml, 1.14×10^{-3} moles) was slowly added. CO was liberated and the yellow precipitate was allowed to settle down. The precipitate was filtered off, washed with ethanol and dried. The complex was purified on $A1_2O_3$ column, using $CHC1_3$ as an eluent. (Yield: 0.22 g 70%). Elemental analysis Found: C = 59.3%; H = 5.0%. Calculated: C = 59.9%; H = 4.5%. Characteristic IR shifts for this complex at 907 cm^{-1}, 1170 cm^{-1}, 1197 cm^{-1}, 1499 cm^{-1} and 1586 cm^{-1} are shown in Figure 2.6.

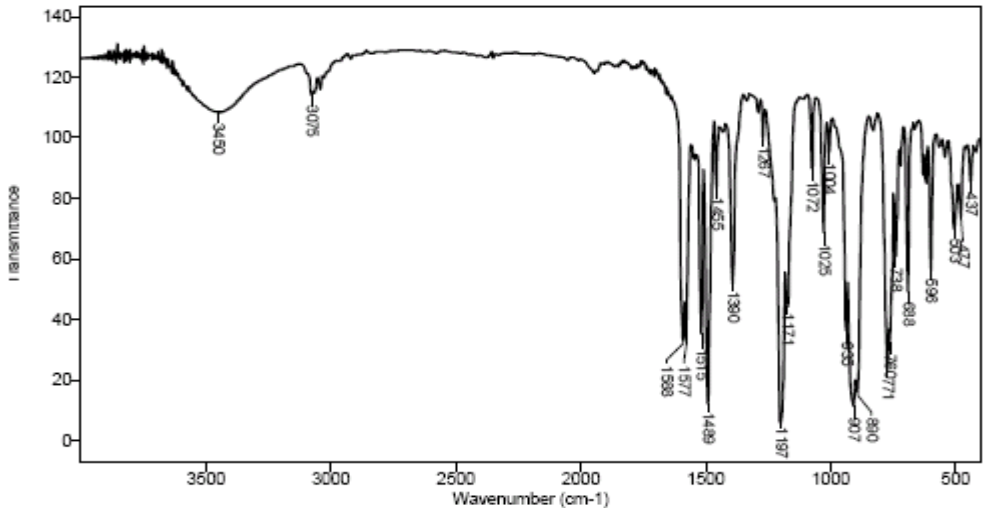

Figure 2.6: FTIR spectrum of $Rh(acac)(P(OPh)_3]_2$

(G) Synthesis of [Rh(acac)[P(OPh)$_3$]$_2$(CO)]

The complex was prepared using the method described by Trzeciak and Ziolkowski[7]. A solution of Rh(acac)[P(OPh)$_3$]$_2$ (0.2 g, 3.24 × 10^{-4} moles) in $CHCl_3$ was saturated with CO for 1-2 hours. following this, the solvent was evaporated under reduced pressure and the residue was washed with ether to give the final product. (Yield: 0.18 g, 88%). Elemental analysis Found: C = 59.4%; H = 4.7%. Calculated: C = 59.22%; H = 4.45%. Characteristic IR shifts for this complex at 2003 cm^{-1}, 1499 cm^{-1}, 1025 cm^{-1} and 907 cm^{-1} are shown in Figure 2.7.

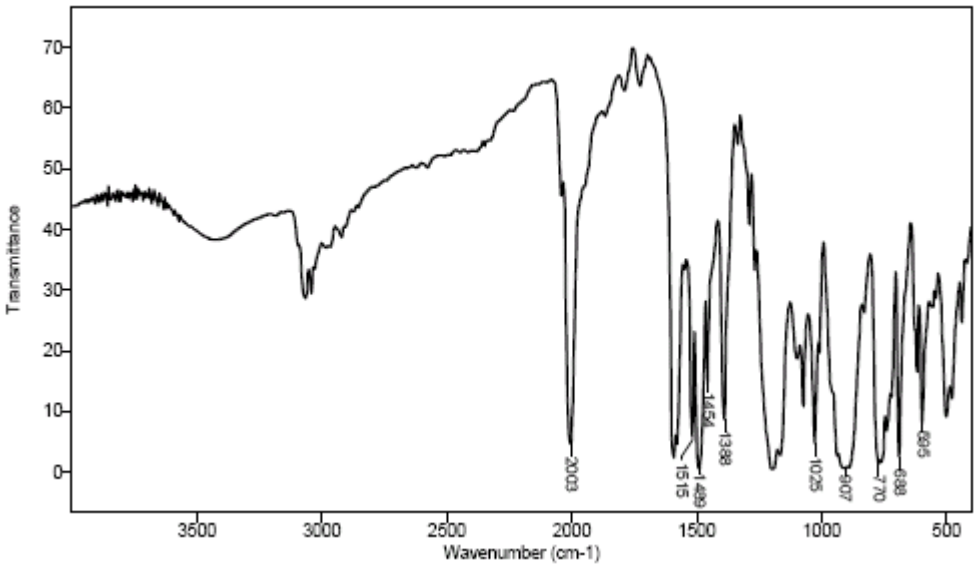

Figure 2.7: FTIR spectrum of Rh(acac)[P(OPh$_3$)]$_2$ CO]

(F) Synthesis of $Co_2(CO)_8$

The synthesis of $Co_2(CO)_8$ was carried out in a 50 ml Parr Autoclave made of Hastelloy C-276, (Rating -maximum pressure 20.7 MPa at 548 K) having facilities for gas inlet, outlet, intermediate sampling, temperature controlled heating (±1 K) and variable agitation speed (0–33.3 Hz). The typical reaction set-up is shown in Figure 2.10. As a safety precaution, a rupture disc (gold faced), with a capacity to withstand a maximum pressure of 20.7 MPa was fitted to the reactor.

Generally, the pressures required for $Co_2(CO)_8$ synthesis are in the range of 15.2–16.6 MPa at temperatures in the range of 190-200ºC. In view of the absence of gas-cylinders of such high pressures, we used a different technique to boost up the pressure. After charging the cobalt precursor ($CoCl_2.6H_2O$), and solvent to the reactor, the reactor

was chilled down to 0-3 ºC. At this low temperature, the reactor was pressurized to ~ 11.2 MPa with syngas (usually with high $CO:H_2$ ratio of 2:1) at a constant agitation of 20 Hz. The reactor was allowed to attain the room temperature and then heated to the desired temperature at constant stirring of 8 Hz. The reaction was started by increasing the stirring speed to 20 Hz. Due to large temperature gradient of ~ 190ºC, while attaining the temperature of 195 ºC, the pressure increased to ~ 16.5 MPa (depending upon the solvent and initial pressure). Even at this temperature and pressure, an induction period of ~ 20-40 minutes was observed. The induction period was found to vary with the $CO:H_2$ ratio of the syngas. All the reactions were conducted till the gas absorption stopped. After cooling the reactor to ~ 7-12ºC, it was depressurized slowly, flushed thrice with argon and the liquid contents were poured into a 100 ml beaker. The black particles obtained (if any) were weighed and discarded. The solvent was removed by bubbling argon through the reaction crude following which, shining dark-red crystals of $Co_2(CO)_8$ were obtained. These were immediately transferred into a high-pressure container under CO atmosphere. The Infra-red analysis (Figure 2.8) of the $Co_2(CO)_8$ prepared was found to be consistent with the reported spectra[8,9] with a characteristic absorption band at 1857 cm^{-1}(ν_{CO}).

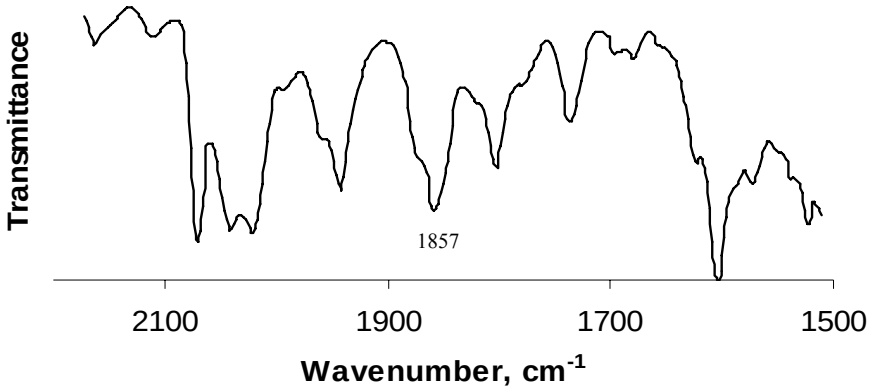

Figure 2.8: FTIR spectrum of $Co_2(CO)_8$

(G) Synthesis of cis-$PtCl_2(PPh_3)_2$

The complex was prepared using the method described by Toniolo and coworkers[10]. An ethanolic (10 ml) solution of chloroplatinic acid hexahydrate (38-40% Pt), $H_2[PtC1_6]$. $6H_2O$ (0.2 g, 3.86×10^{-4} moles) and PPh_3 (0.44 g, 1.68×10^{-3} moles) was stirred at room temperature. In a few minutes a white solid forms. The reaction mixture was heated under reflux for 1 hour. After cooling to room temperature, the suspension was filtered. The white precipitate was washed with EtOH and ether and dried under vacuum. (Yield: 0.262 g, 80.5%). The IR spectra of the complex shows characteristic bands at 1434 cm^{-1}, 1100 cm^{-1} and 697 cm^{-1} as shown in Figure 2.9

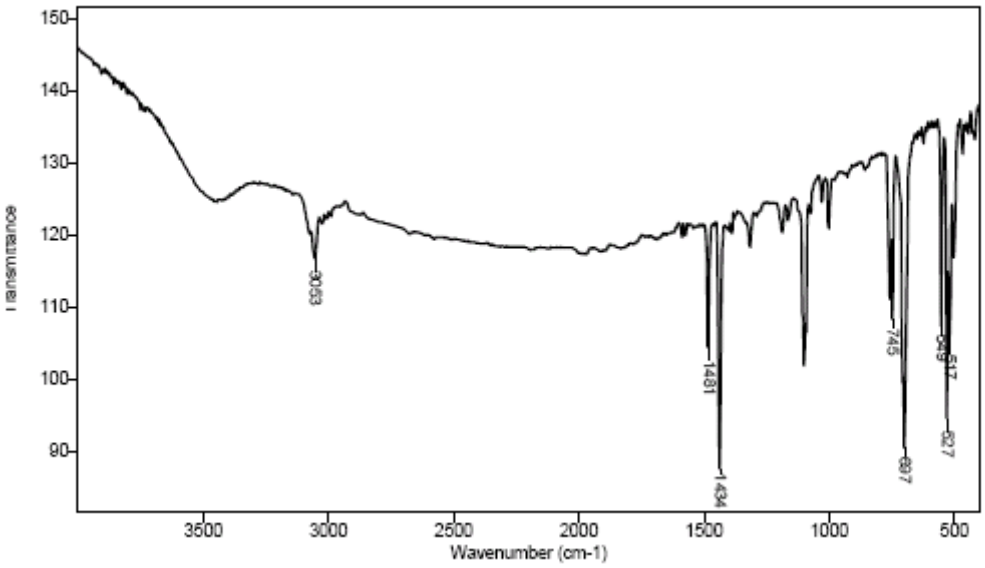

Figure 2.9: FTIR spectrum of cis-$PtCl_2(PPh_3)_2$

2.2.3 Experimental set up for hydroformylation

All the hydroformylation experiments were carried out either in a 50 ml autoclave, made of stainless steel, supplied by Amar Instruments India Pvt. Ltd. or a 300 ml Parr reactor (USA). The reactors were provided with arrangements for sampling of liquid and gaseous contents, automatic temperature control and variable agitation speed. The reactor was designed for a working pressure of 20.7 MPa and temperature up to 250^oC. As a safety precaution, a rupture disc (gold faced), was attached to the reactor. The consumption of CO and H_2 at a constant pressure was monitored by observation of the pressure drop in the gas reservoir, from which ($CO+H_2$) mixture was supplied

through a constant pressure regulator at a 1:1 ratio. The pressure in the reservoir was recorded using a pressure transducer to follow the consumption of $CO+H_2$ as a function of time. A schematic diagram of the experimental set up is shown in Figure-2.10.

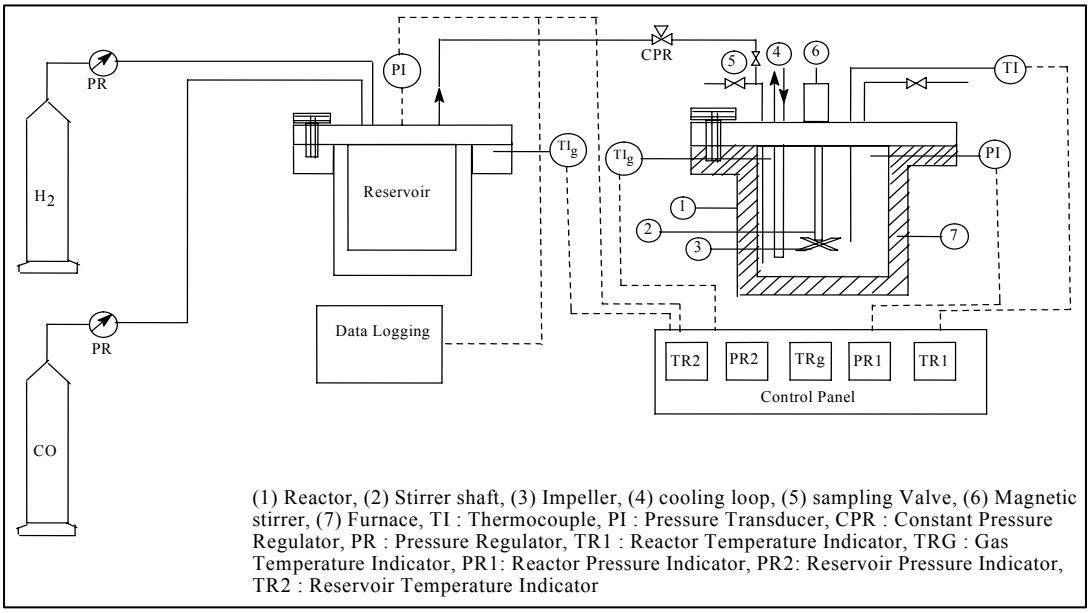

Figure 2.10: A schematic of the reactor setup used for hydroformylation reaction

2.2.4 Experimental procedure

In a typical experiment, known quantities of the catalyst, ligand, olefin (terpene), and the solvent were charged into the autoclave and the reactor was flushed with nitrogen. The contents were then flushed with a mixture of CO and H_2 and heated to a desired temperature. A mixture of CO and H_2, in the required ratio (1:1), was introduced into the autoclave, a sample of liquid withdrawn, and the reaction started by switching the stirrer on. The reaction was then continued at a constant pressure by supply of $CO+H_2$ (1:1) from the reservoir vessel. Since, the major products formed were aldehydes, supply of $CO+H_2$ at a ratio of 1:1 (as per stoichiometry) was adequate to maintain a constant composition of CO and H_2 in the autoclave, as introduced in the beginning. This was confirmed in a few cases by analysis of the CO content in the gas phase at the end of the reaction. In each run, samples were withdrawn at regular intervals of time and analysed for reactants and products in order to check the material balance. The reproducibility of the experiments was found to be in a range of 5-7%. Following the similar procedure, the experiments for the kinetic studies were carried out.

2.2.5 Analytical methods

^{31}P NMR spectra were obtained on a Bruker AC-200 or MSL-300 spectrometer in $CDCl_3$ at room temperature. The peak positions are reported with positive shifts in ppm downfield of external H_3PO_4 (^{31}P). FT-IR spectra were recorded on a Bio-Rad Spectrophotometer 175C. The reaction products were identified using GCMS, (Agilent GC 6890N with 5973 mass selective detector instrument).

The quantitative analysis of the reactant and hydroformylation products was carried out by an external standard method using a gas chromatographic technique. For this purpose, HP 6890 gas chromatograph controlled by the HP Chemstation software and equipped with an auto sampler unit, fitted with HP-5 capillary column (30M × 320μm × 0.25 μm film thickness with a stationary phase of phenyl methyl siloxane) and FID detector was used. Authentic standards were prepared in the range of concentrations studied, and a calibration-table was constructed for the quantification. The standard GC conditions for the analysis of products of different reactions are given in Table 2.1.

Table 2.1: Conditions for GC analysis

Injector (split) Temperature	250ºC		
Flame ionization detector Temp	250ºC		
Inlet flow–total (He)	20.2 ml/min		
Split ratio for Injector	50:1		
Column Temperature	Rate (ºC /min)	T (ºC)	Hold time (min)
		125	20
	40	300	1
Column Pressure	Rate (psi/min)	Pressure (Psi)	Hold time (min)
		5	20

A typical GC chart (Figure 2.11) shows the reactant camphene and exo and endo aldehyde product under the analysis condition given in Table 2.1.

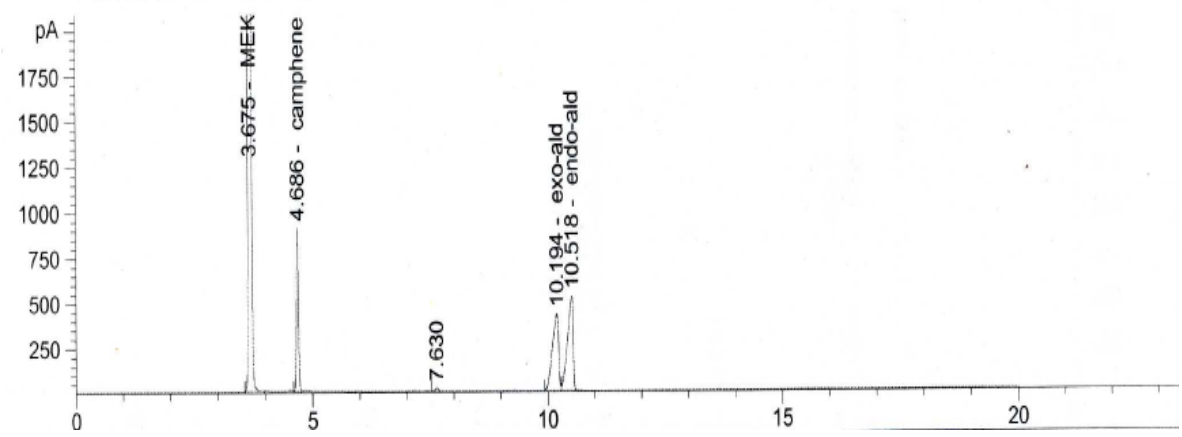

Figure 2.11: A typical GC chart showing the solvent MEK, reactant camphene, and product exo and endo aldehyde.

Complete mass balance of the liquid phase components was thus obtained from the quantitative GC analysis. The observed syngas absorption was found to match with the products formed within ~ 5 % error. Thus, the complete mass balance of liquid and gases was established. The percent conversion, percent selectivities, turnover number (TON) and frequency (TOF h^{-1}) were calculated using the formulae (Eq. 2.1-2.4) given below. The percent conversion was calculated based on the liquid substrate charged.

$$Conversion,(\%) = \left(\frac{Initial\ concentration\ of\ \ substrate - Final\ concentration\ of\ \ substrate}{Initial\ concentration\ of\ \ substrate} \right) \times 100 \qquad 2.1$$

$$Selectivity,(\%) = \frac{No.\ of\ \ moles\ of\ \ a\ \ product\ \ formed}{No.\ of\ \ moles\ of\ \ substrate\ converted} \times 100 \qquad 2.2$$

$$TON = \frac{No.of\ moles\, of\ hydroformylation\ products\ \ formed}{No.of\ moles\, of\ catalyst} \qquad 2.3$$

$$TOF, h^{-1} = \frac{No.of\ moles\, of\ hydroformylation\ products\ \ formed}{No.of\ moles\, of\ catalyst \times time\, in\, hours} \qquad 2.4$$

2.2.6 Separation and identification of the products

The terpene hydroformylation products were identified on GC-MS. The aldehyde products obtained after hydroformylation of camphene, limonene, β-pinene, 3-carene, γ-terpinene and carvone were isolated from the reaction mixture by distillation under reduced pressure. They were separated by column chromatography (silica) using a mixture of hexane, CH_2Cl_2 and methanol as eluents and characterized by IR and MS. The details of identification and characterization of the terpenes hydroformylation products are presented in Table 2.2 (Appendix I).

Table 2.2: Identification/ Characterization of terpenes hydroformylation products

Sr. No.	Terpene	Product	Identification/ Characterization
1	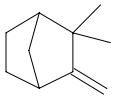 Camphene (**1**)	3,3 dimethyl-2-norbornaneacetaldehyde (exo (**7a)**, shorter GC retension time)	**IR (KBr):** 1726 cm^{-1}, 2713 cm^{-1}(CHO), 1366 cm^{-1}, 1385 cm^{-1} (mixed dimethyl)
			MS (*m*/*z*/rel. int.): 166/4 (M+); 133/15; 122/53; 109/31; 107/52; 97/100; 83/22; 81/32; 79/41; 69/47;67/51; 55/40; 41/44.
		3,3-dimethyl-2-norbornaneacetaldehyde (endo (**7b)**, longer GC retention time)	**IR (KBr):** 1726 cm^{-1},2713 cm^{-1}(CHO), 1366 cm^{-1} , 1385 cm^{-1} (mixed dimethyl)
			MS (*m*/*z*/rel. int.): 166/3; (M+); 133/11; 122/38; 109/22; 107/39; 97/100; 83/18; 81/24; 79/31; 69/37; 67/40; 55/30; 41/35.
2	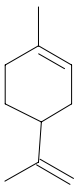 Limonene (**2**)	3-(4-Methylcyclohex-3-enyl) butanal (**11)**	**MS *(m/z/* rel. int.):** 166/7 (M+)*;* 148/47; 133/33; 121/25; 106/34; 91/59; 93/100; 67/57; 55/23; 41/26.
		1-methyl-4-(propan-2-ylidene)cyclohex-1-ene (**12)** (Isomerised limonene)	**MS (m/z/ rel. int.):** 136/86 (M+); 121/100; 105/22; 93/85; 91/43; 79/31; 77/25
3	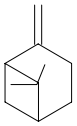 β-pinene (**3**)	10-Formylpinane (cis (**13a**), longer GC retention time)	**MS *(m/z/* rel. int.):** 166/2 (M+); 151/18; 133/17; 122/90; 107/52; 95/31; 93/30; 81/57; 79/100; 69/69; 67/71; 55/80; 41/82
		10-Formylpinane (trans (**13b)**, shorter GC retention time)	**MS *(m/z/* rel. int.):**166/3 (M+), 151/23; 133/21; 122/91; 107/54; 93/32; 81/62; 79/100; 69/68; 67/68; 55/86; 41/80.
		α-pinene (**14)**(Isomerised product of β-pinene)	**MS *(m/z/* rel. int.):**136/10 (M+); 121/13; 105/10; 93/100; 77/25; 41/9

Sr. No.	Terpene	Product	Identification/ Characterization
4	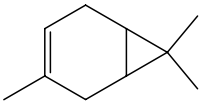 3-Carene (**4**)	2-caranecarbaldehyde (**15**) or (3,7,7-trimethylbicyclo [4.1.0]heptane-2-carbaldehyde)	**MS *(m/z/* rel. int.):** 166/6 (M+); 151/22; 137/94; 123/9; 109/34; 105/27; 95/81; 93/39; 81/100; 69/42; 67/42; 55/43; 41/40.
		3-caranecarbaldehyde (**16**) or (3,7,7-trimethylbicyclo [4.1.0] heptane-3-carbaldehyde)	**MS *(m/z/* rel. int.):** 166/19 (M+); 151/31; 135/77; 123/48; 109/33; 105/27; 93/100, 81/94; 67/69; 55/48; 41/63.
5	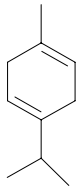 γ-terpinene (**5**)	3-isopropyl-6-methylcyclohex-3-enecarbaldehyde (**17**) (major)	**MS *(m/z/* rel. int.):** 166/43 (M+); 151/17; 137/61; 123/26; 109/24; 93/100; 81/63; 67/26; 55/26; 43/30.
		6-isopropyl-3-methylcyclohex-3-enecarbaldehyde (**18**) (minor)	**MS *(m/z/* rel. int.):** 166/43 (M+); 151/17; 137/61; 123/26; 109/24; 93/100; 81/63; 67/26; 55/26
		3-isopropyl-6-methylcyclohexa-1,4-diene (**21**) (Isomerized product)	**MS *(m/z/* rel.int):** 136/54 (M+);121/100; 105/17; 93/75; 91/36; 79/21; 77/25
		1-isopropyl-4-methylcyclohex-1-ene (**19**)	**MS *(m/z/* rel.int):** 138/32 (M+); 123/24; 95/100; 81/69; 6729; 55/14; 41/15.
		4-isopropyl-1-methylcyclohex-1-ene (**20**)	**MS *(m/z/* rel.int):** 138/34 (M+);179/34; 95/100; 81/27; 68/40; 67/44; 55/15; 41/16
6	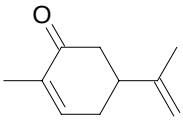 Carvone (**6**)	3-(4-Methylcyclohex-4-en-3-onyl) butanal (**22**)(major)	**MS (m/z /rel.int.):** 180/3(M+); 162/5: 136/65; 109/100; 82/40.
		5-(4-hydroxybutan-2-yl)-2-methylcyclohex-2-enone (**23**) (alcohols)	**MS(m/z /rel.int.):** 182/22(M+); 138/47; 122/33; 109/100; 94/30; 81/27; 69/39; 55/33; 41/42. and
		3-(4-methyl-3-oxocyclohexyl)butanal (**24**)	**MS (m/z/ rel. int.):** 182/1(M+*);* 164/6; 138/100; 111/67, 95/33, 81/24, 69/35; 55/70; 41/41.
		5-isopropyl-2-methylcyclohex-2-enone (**25**)	**MS (m/z /rel.int.):** 152/100(M+); 137/32; 109/60; 95/25; 81/65; 69/70; 41/41.

2.3 Results and discussion

2.3.1 Hydroformylation of terpenes using $HRhCO(PPh_3)_3$catalyst

As a preliminary investigation, hydroformylation of various terpenes was carried out in toluene at 373 K in the presence of the Wilkinson's catalyst, $HRhCO(PPh_3)_3$ (known to be a very active catalyst for olefin hydroformylation). The results are presented in Table 2.3. The main purpose of this study was to asses the activity of the Wilkinson's catalyst for the hydroformylation of less reactive substrates like terpenes, particularly since the majority of studies indicate that this catalyst is highly active for terminal olefins.

Table 2.3: Hydroformylation of terpenes using $HRhCO(PPh_3)_3$catalyst

Sr. no	Substrate (terpene)	Time (h.)	Conversion (%)	Aldehyde selectivity (%)	Iso/hd. terpene (%)	exo/ endo ratio	TOF h^{-1}
1	(-) Camphene	24.9	98.3	91.8	9.2	1.18	14
2	R(+) Limonene	18.5	94.4	87.9	11.1	-	16
3	β-Pinene	17.7	95.9	15.2	84.8	-	2
4	α-Pinene	7.2	No reaction				
5	3(-) Carene	8.0	No reaction				
6	γ-Terpinene	6.5	No reaction				
7	Citral	11.1	No reaction				
8	Citronellol	9.4	No reaction				

Reaction conditions: *substrate: 0.64 kmol/m^3, $HRhCO(PPh_3)_3$: 1.23 × 10^{-3} kmol/m^3, PPh_3: 7.4 ×10^{-3} kmol/m^3 (Rh:P=1:6), T: 373K, agitation speed : 16.6 Hz, P_{CO+H2}: 4.14 MPa, solvent: toluene, total charge: 8.1 ×10^{-5} m^3*

The results in Table 2.3 show that hydroformylation of camphene, limonene and β-Pinene using Wilkinson's catalyst takes prolonged reaction time, with poor activity. This is probably due to the bulkiness of the terpene substrates which prevents the metal olefin interaction with the ease observed in case of linear olefins. Along with the hydroformylation products, isomerisation and hydrogenated products of the terpenes

were also observed. In the case of hydroformylation of camphene, the distereoselectivity towards exo product was found to be more than endo product (de = 8.3%). A little amount of isomerized and hydrogenated camphene was observed. Hydroformylation of limonene yields **11** in good yield alongwith small amount of isomerized limonene. Isomerisation of terminal double bond to internal one is more prominent for β-pinene under the hydroformylation condition. In β- pinene hydroformylation trans-10-formylpinane (**13b**) was formed as a major product (83%). The β-pinene isomerizes to the α-pinene (**14**) and thereafter no reaction occurs. Other terpenes such as α-pinene, Δ-3(-) carene, γ-and terpinene do not undergo hydroformylation reaction. Terpenoids such as citral and citronellol also do not show any hydroformylation activity. For citral, only hydrogenation was observed under similar reaction conditions. The results indicate that terpenes having a terminal double bond undergo hydroformylation reaction using Wilkinson's catalyst. The internal olefins are inherently less reactive as compared to the terminal olefins and hence the internal double bond of the terpenes does not undergo reaction.

The hydroformylation of camphene was also carried out in aqueous biphasic medium using a water soluble $HRh(CO)(TPPTS)_3$ catalyst. The reaction shows very poor activity (TOF= 6 h^{-1}) and poor conversion (26.4%) was obtained with exo diastereoselectivity (exo/endo ratio = 1.26).

2.3.2 Screening of transition metal catalysts for hydroformylation of camphene

The various transition metal complex catalysts were screened by choosing camphene as a model substrate (since its hydroformylation products find application in fine/perfumery chemical industry) and the results are presented in Table 2.4. As discussed earlier, there is very little information available in the literature concerning the hydroformylation of camphene in homogeneous medium. The best activity (TOF) reported in literature for camphene hydroformylation using any catalyst is 80 h^{-1}, which is very low compared to the hydroformylation of other substrates. The maximum reported selectivity to aldehyde was also around 90%[1f].

Table 2.4: Screening of catalyst for hydroformylation of camphene

Run no	Catalyst	Time (h.)	Conversion (%)	Aldehyde selectivity (%)	Iso/hd. camphene (%)	exo/ endo	TOF (h^{-1})
1	$HRhCO(PPh_3)_3$	24.9	98.3	91.8	9.2	1.18	14
2	$Rh(CO)_2$ (acac)	18.1	97.6	92.7	7.3	1.24	16
3	$[Rh(COD)Cl)]_2$	16.0	96.7	97.9	2.1	1.22	23
4	$Rh(CO)_2$(acac)/ $P(OPh)_3$	1.8	94.3	98.8	1.2	0.84	186
5	$[Rh(COD)Cl)]_2$ /$P(OPh)_3$	5.0	99.1	98.7	1.3	0.89	57
6[a]	[Rh (μ-OAc)$COD]_2$)/ $P(OPh)_3$	4.0	81.6	99.4	0.6	0.64	72
7[a]	[Rh(μ-OMe)$COD]_2$)/ $P(OPh)_3$	4.0	96.2	99.5	0.5	0.65	85
8[b]	Co(acetate)$_2$ / PPh_3	8.3	No reaction				
9[b]	$Co_2(CO)_8$	9.1	No reaction				
10[b]	Co(acetate)$_2$/ $P(OPh)_3$		Catalyst formation not observed.				
11[b]	$PtCl_2(PPh_3)_2$	7.0	Platinum metal precipitates out as platinum black.				

Reaction conditions: *camphene: 0.64 kmol/m^3, catalyst: 1.23 ×10^{-3} kmol/m^3, ligand: 7.4 ×10^{-3} moles (Rh:P=1:6), T: 373K, agitation speed : 16.6 Hz, P_{CO+H2}: 4.14 MPa, solvent: toluene, total charge: 8.1 ×10^{-5} m^3 a=Solvent : MEK, b = P_{CO+H2} : 8.6 MPa*

As discussed in section 2.3.1 the Wilkinson's catalyst shows poor activity and gives aldehydes and hydrogenated and isomerized products in the hydroformylation of camphene (entry 1, Table 2.4). On the other hand the unmodified rhodium complex catalyst such as $Rh(CO)_2$(acac), $[Rh(COD)Cl)]_2$ shows improved activity over Wilkinson's catalyst (entry 2, Table 2.4). When phosphite ligand was added to this catalyst the activity and selectivity increased dramatically (entry 4, Table 2.4). $Rh(CO)_2$(acac)/$P(OPh)_3$ catalyst system gave the highest activity (TOF =186 h^{-1}) with 99% selectivity to aldehyde (d.e. = 9% to endo). No alcohol formation was observed. The possible reason for observed rate enhancement could be the facile dissociation of phosphite ligand which facilitates faster coordination of olefins to the metal center. This

results in better stabilization of the intermediate catalytic species. Similar observation of rate enhancement was reported for linear as well as internal olefin hydroformylation using Rh-phosphite complex catalysts[11]. The hydrogenation and isomerized camphene products also reduced substantially with phosphite containing catalyst. This suggests that the presence of phosphite ligand suppresses the side reactions like isomeristion and hydrogenation.

Dimeric rhodium complexes such as $[Rh(COD)Cl)]_2$, $[Rh(\mu\text{-}OMe)(COD)]_2$, $[Rh(\mu\text{-}OAc)(COD)]_2$ in the presence of phosphite ligand show lesser activity compared to the $Rh(CO)_2(acac)/P(OPh)_3$ complex catalyst system (entry 5,6 and 7, Table 2.4). The dissociation of the dimer to monomeric species is slow, and hence results in lower activity. No reaction was observed using complexes of cobalt and platinum under similar reaction conditions (entry 8, 9, 10 and 11, Table 2.4). This is probably due to the fact that these catalysts are effective at higher syngas pressure (>9 MPa) compared to the existing conditions.

2.3.3 Hydroformylation of camphene using $Rh(CO)_2(acac)/P(OPh_3)_3$ catalyst system

2.3.3.1 Effect of solvent

Solvents are known to play a major role in the activity as well as selectivity in hydroformylation reactions. To understand the role of solvents in hydroformylation of camphene, reactions were taken in a number of solvents using $Rh(CO)_2(acac)/P(OPh)_3$ catalyst and the results are presented in Table 2.5. It was observed that the solvents have a prominent influence on the selectivity and activity of the catalyst. The rates of hydroformylation are high in polar protic (ethanol, methanol, MEK) solvents and low in nonpolar solvents (cyclohexene, hexane). Methanol and ethanol give higher rates (TOF 488 and 486 h^{-1} respectively) but acetals were formed by condensation of the aldehyde with the alcohol solvent. The best activity with 100 % selectivity to aldehydes was observed in methyl ethyl ketone (MEK) wherein a TOF of 417 h^{-1} was observed. In general, solvents with a higher polarity gave better activity over those with a lower polarity in hydroformylation of olefins[12]. It was also observed that with decrease in polarity of solvent the distereoselectivity towards exo product increases.

Table 2.5: Effect of solvent on the activity and selectivity in hydroformylation of camphene using $Rh(CO)_2(acac)/P(OPh)_3$ catalyst.

Sr. No	Solvent	Relative Polarity	Time (h.)	Conver-sion (%)	Aldehyde selectivity (%)	Iso/hd. Camphene (%).	exo/ endo	TOF (h^{-1})
1	Ethanol[a]	5.2	1.16	98.5	64.3	-	0.76	488
2	Methanol [b]	5.1	1.18	99.1	2.4	1.0	0.77	486
3	MEK	4.7	1.23	99.3	99.5	0.5	0.87	417
4	1,2 DCE	3.5	2.16	97.9	97.5	2.5	0.88	241
5	Xylene	2.5	1.83	97.7	98.5	1.4	0.80	232
6	Toluene	2.4	1.85	94.3	98.8	1.2	0.84	186
7	Cyclohexane	0.2	2.70	98.1	95.9	4.1	0.89	182
8	Hexane	0.06	2.91	95.8	96.1	3.9	0.92	136

Reaction conditions: *camphene: 0.64 kmol/m^3, $Rh(CO)_2(acac)$: 1.23 × 10^{-3} kmol/m^3, $P(OPh)_3$: 7.4 ×10^{-3} kmol/m^3 (Rh:P=1:6), T: 373K, agitation speed : 16.6 Hz, P_{CO+H2}: 4.14 MPa, solvent: toluene, total charge: 8.1 ×10^{-5} m^3. % acetals selectivity: a=35.7, b= 96.6*

A comparison of the relative polarity of solvents with the activity and exo/endo ratio is presented in Figure 2.12 for the hydroformylation of camphene. In all the reactions only the terminal aldehyde was formed, and the exo/endo ratio was found to vary from 0.76 to 0.92 for the entire range of solvents with relative polarity ranging from 5.2(ethanol) to 0.06 (hexane).

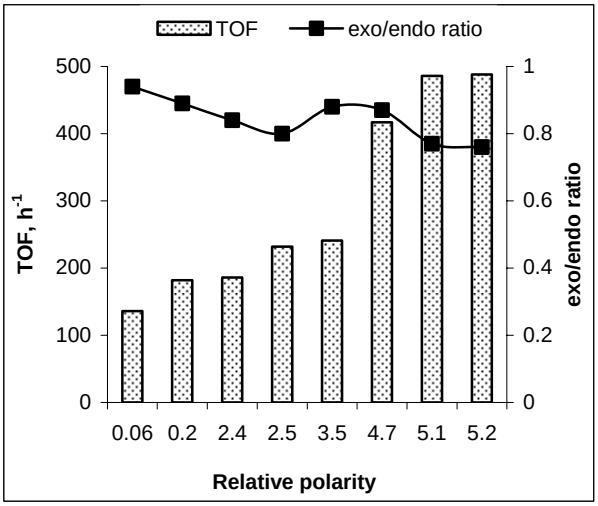

Figure 2.12: A plot of activity and exo/endo ratio vs. relative polarity

Reaction conditions: *As in Table 2.5.*

Hydroformylation of neat camphene (20 g) (i.e. without solvent) has also been carried out, using the $Rh(CO)_2(acac)$/ $P(OPh)_3$ catalyst system at 373 K. The reaction was extremely slow (TOF = 32 h^{-1}) and 95% camphene conversion was obtained after 45 hrs reaction time with >95% selectivity to aldehyde product. Five percent of isomerized camphene was formed due to the extended reaction period.

2.3.3.2 Screening of ligands

The type and nature of ligands can have a dramatic influence on the activity and selectivity of catalytic reactions[13]. It is well known that phosphites are poor σ-donor, and good π-acceptor ligands. The π acidity of phosphites is about half as that of CO which makes them good ligands for hydroformylation reaction. The influence of phosphite ligands on the activity and selectivity of the $Rh(CO)_2(acac)$ catalyst was investigated for the hydroformylation of camphene in MEK solvent at 373K. The results are presented in Table 2.6. Triphenyl phosphite ($P(OPh)_3$), triethyl phosphite ($P(OEt)_3$) and tri n-butyl phosphite($P(OBu)_3$) promoted systems were found to be active for the hydroformylation of camphene. However, the Rh/triphenyl phosphite catalyst was by far the most active for camphene hydroformylation. This observation can be explained on the basis of the electronic factor i.e. higher electronegativity (χ) value of the $P(OPh)_3$ with respect to $P(OBu)_3$ and $P(OEt)_3$. The high electronegativity of the ligand makes the rhodium centre electron deficient, and induces a fast replacement of CO ligand, which promotes

faster coordination of olefin to the rhodium centre[14]. The high exo/endo ratio observed is due to the large cone angle of $P(OPh)_3$ (128º) compared to $P(OBu)_3$ (109º) and $P(OEt)_3$, (123º). However, no reaction was observed when bidentate ligands such as diphenyl phosphinoethane (dppe), diphenyl phosphinopropane (dppp) and diphenyl phosphinobutane (dppb) were used under similar reaction conditions. These bidentate ligands are known to be less active even for the hydroformylation of linear olefins as compared to monodentate ligands[15].

Table 2.6: Ligand screening studies for Hydroformylation of camphene

Sr. No.	Ligand	Conversion (%)	Aldehyde selectivity (%)	Iso./hd. camphene (%)	Exo/ endo	TOF (h^{-1})	Time (h.)
1	$P(OPh)_3$[a]	99.3	98.8	1.2	0.87	417	1.2
2	$P(OEt)_3$[b]	20.7	99.2	0.8	0.71	20	9.0
3	$P(OBu)_3$[b]	74.9	99.5	0.5	0.69	29	9.0
4	dppe[b]	No reaction					7.0
5	dppp[b]	No reaction					7.0
6	dppb[b]	No reaction					7.0

Reaction conditions: *a: reaction conditions are as mentioned in table 2.5.*
b: $Rh(CO)_2(acac)$: 1 × 10^{-3} kmol/m^3, ligand: 6 ×10^{-3} kmol/m^3, camphene : 0.37 kmol/m^3 ,Rh:P= 1:6, MEK: 2.82 × 10^{-5} m^3, total charge : 3.0 × 10^{-5} m^3 , T: 373 K P_{CO+H2}: 4.14 MPa, agitation speed : 16.6Hz.

2.3.3.3 Effect of P/Rh ratio

The dependence of the activity and product distribution on the P/Rh ratio for camphene hydroformylation was studied using $Rh(CO)_2(acac)$ in presence of additional $P(OPh)_3$ ligand. The results are presented in Figure 2.13. The effect of Rh to phosphite ratio on activity was studied in the initial range of olefin conversion (~35%). A strong negative effect of the $P(OPh)_3$ concentration on activity of camphene hydroformylation was observed. It was observed that the activity increases with the concentration of ligand upto Rh:P of 1:3. Thereafter it decreases with the further phosphite addition from a Rh:L ratio of 1:3 (TOF = 397 h^{-1}) to 1:12 (TOF = 172 h^{-1}). The aldehyde selectivity however

remains unaffected (> 99%). The highest activity was observed at a P/Rh ratio of three as seen in Figure 2.13. At low P/Rh ratio, the phosphite ligand is partially replaced by a carbonyl ligand resulting in a higher rate. As per the hydroformylation mechanism, (which has been discussed in detail in section 2.3.5.5) phosphite dissociation must occur to form the coordinatively unsaturated intermediate. This dissociation is suppressed by increased $P(OPh)_3$ concentration, which serves to reduce the concentration of active Rh species in the catalytic cycle. This observation also supports the hydroformylation mechanism using phosphite ligand[16].

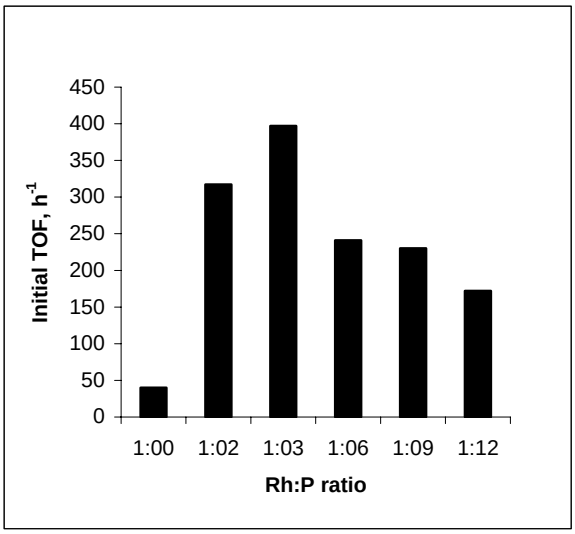

Figure 2.13: A plot of initial activity vs. Rh:P ratio

Reaction conditions: *$Rh(CO)_2(acac)$: 1 × 10^{-3} kmol/m^3, camphene: 0.37 kmol/m^3 , T: 373K, P_{CO+H2}: 4.14 MPa, MEK: 2.82 × 10^{-5} m^3, total charge : 3.0 × 10^{-5} m^3, agitation speed : 16.6Hz.*

2.3.3.4 Effect of temperature

The effect of temperature on hydroformylation of camphene has been investigated in a temperature range of 353-383 K under the following reaction conditions $Rh(CO)_2(acac)$: 1 × 10^{-3} kmol/m^3, $P(OPh)_3$: 6 × 10^{-3}kmol/m^3, camphene : 0.37 kmol/m^3 , P_{CO+H2} : 4.14 MPa. As expected, the rate increases with the temperature, however the exo/endo ratio decreases (Figure 2.14).

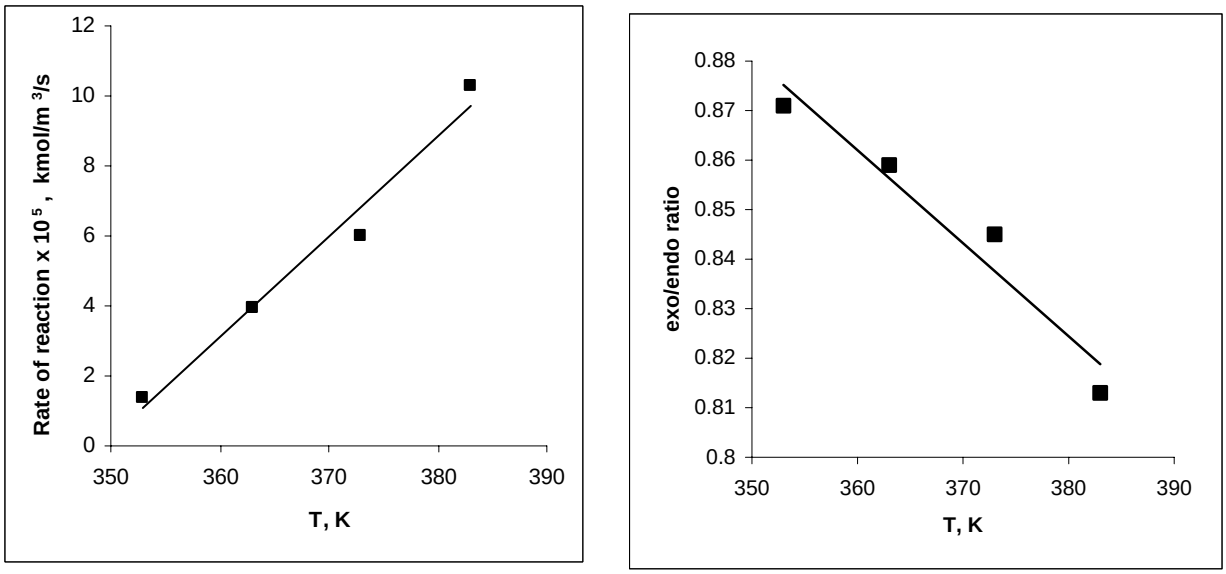

Figure 2.14: Effect of temperature on rate and exo/endo ratio in hydroformylation of camphene

Reaction conditions: *$Rh(CO)_2(acac)$: 1 × 10^{-3} kmol/m^3, $P(OPh)_3$: 6 × 10^{-3} kmol/m^3, Rh:P:1:6, camphene : 0.37 kmol/m^3 , P_{CO+H2}: 4.14 MPa, agitation speed: 16.6 Hz, MEK: 2.82 × 10^{-5} m^3, total charge = 3.0 × 10^{-5} m^3 .*

2.3.4 Hydroformylation of various terpenes using $Rh(CO)_2(acac)/P(OPh_3)_3$ catalyst

The highly active $Rh(CO)_2(acac)/P(OPh)_3$ catalyst was tested for the hydroformylation of other terpenes at a total pressure of 4.14 MPa (CO/H_2=1), $Rh(CO)_2(acac)$: 1 × 10^{-3} kmol/m^3, $P(OPh)_3$: 6 × 10^{-3} kmol/m^3, and terpene concentration of 0.37 kmol/m^3 at 373K. The results are presented in Table 2.7 and the reactions are shown in scheme 2.2. In addition to the hydroformylation of camphene the catalyst was found to be very active for the hydroformylation of R(+)limonene, β-pinene, and a terpenoid (R)- carvone. Very, little hydroformylation activity was observed for 3-carene and γ- terpinene. The hydroformylation of 3-carene (**4)** gives 2-caranecarbaldehyde (**15)** and 3-caranecarbaldehyde (**16)** in equal proportion. For γ- terpinene isomerization and hydrogenation activity was more as compared to hydroformylation activity. γ- terpinene (**5)** on hydroformylation gives 3-isopropyl-6-methylcyclohex-3-enecarbaldehyde (**17)** as a major and 6-isopropyl-3-methylcyclohex-3-enecarbaldehyde (**18)** as a minor aldehyde product. The other products formed are hydrogenated products such as (1-isopropyl-4-methylcyclohex-1-ene (**19)** and 4-isopropyl-1-methylcyclohex-1-ene (**20)**) and

isomerized product (3-isopropyl-6-methylcyclohexa-1,4-diene (**21)**) by hydrogenation and isomerization side reaction (scheme 2.2). No reaction was observed with α-pinene and myrcene. In case of myrcene only isomerization was observed.

Table 2.7: Screening of terpenes using $Rh(CO)_2(acac)/P(OPh)_3$ in MEK

Run no.	Terpene	Conversion (%)	Aldehyde selectivity (%)	Iso / hd. terpenes (%)	Exo/endo or cis/trans ratio	TOF h^{-1}	Time (h.)
1	(-)-camphene[a]	99.3	99.5	0.5	0.87	417	1.2
2	(R) -Limonene[b]	99.3	99.4	0.6	-	526	0.7
3	β-Pinene[b]	78.9	70.0	30.0	0.88	56.6	3.3
4	γ-Terpinene[b]	45.5	28.0	72.0	-	9.2	5.0
5	3-carene[b]	10.7	98.3	1.7	-	9.5	4.0
6	R-(-) Carvone[b]*	94.4	92.7	1.0	-	688	0.5
7	α-Pinene[b]	No reaction					4.0
8	Myrcene[b]	No reaction, only isomerisation is observed					7.3

Reaction conditions: *a: reaction conditions are as mentioned in table 2.5.*
*b: $Rh(CO)_2(acac)$: 1×10^{-3} kmol/m^3, $P(OPh)_3$: 6×10^{-3} kmol/m^3, Rh:P=1:6, terpene : 0.37 kmol/m^3, T: 373K, P_{CO+H2}: 4.14 MPa, agitation speed : 16.6 Hz, MEK: 2.82×10^{-5} m^3, total charge : 3.0×10^{-5} m^3, * Reaction in toluene as substrate is insoluble in MEK and alcohol selectivity of 6.3%.*

The catalyst was found to be more active for the hydroformylation of carvone (**6)** as compared to camphene and limonene and a TOF of 688 h^{-1} was obtained. The major product for carvone hydroformylation is 3-(4-meth1cyclohex-4-en-3-onyl) butanal (**22).** The other minor products include 3-(4-methyl-3-oxocyclohexyl) butanal (**23)** and alcohol namely 5-(4-hydroxybutan-2-yl)-2-methylcyclohex-2-enone (**24)** by aldehyde hydrogenation. A small extent of isomerized and hydrogenated carvone (**25)** products were also observed (Scheme 2.2). The products of these all reactions were identified by GCMS (see Table 2.2 or Appendix I).

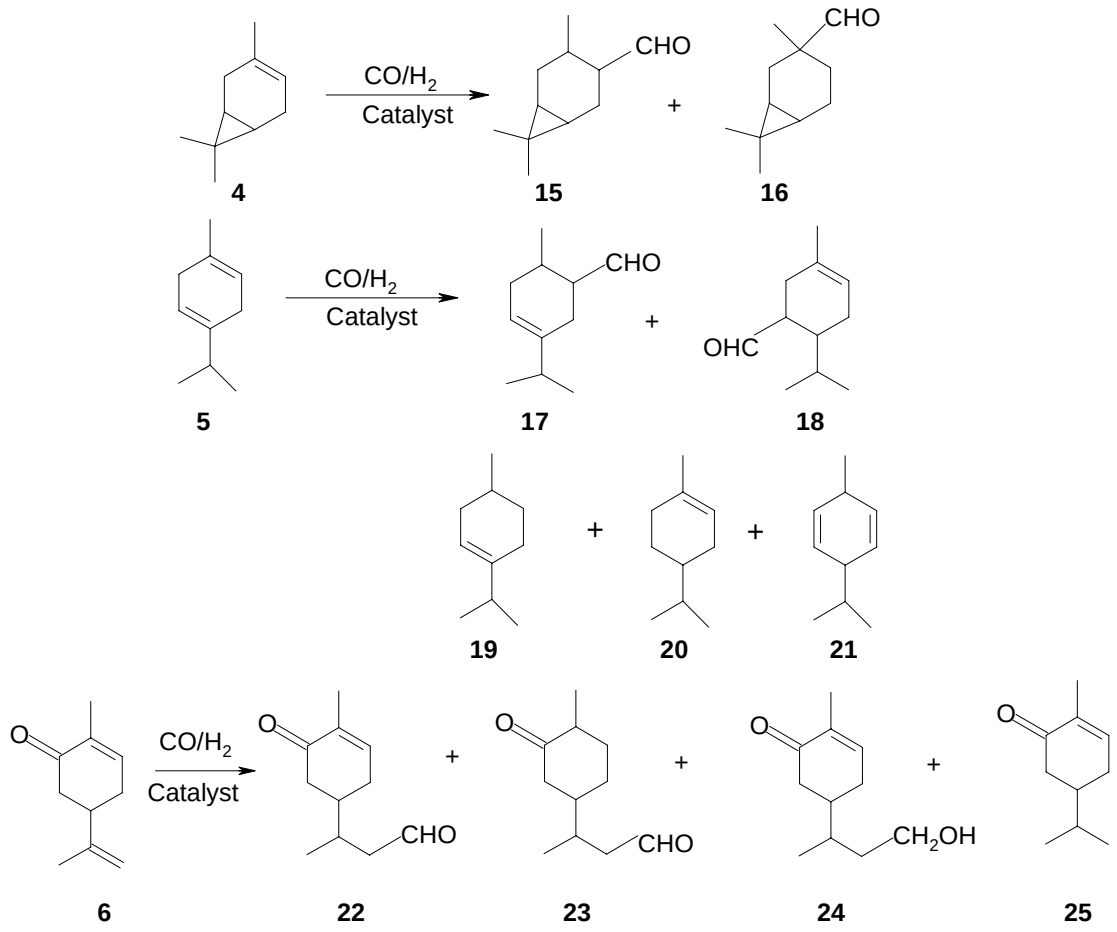

Scheme 2.2: Product obtained in hydroformylation of 3-carene, γ-terpinene and (R)-carvone

2.3.5 Kinetics of hydroformylation of camphene using $Rh(CO)_2(acac)/P(OPh_3)_3$ catalyst system

Kinetics of hydroformylation of linear olefins has been extensively studied[17]. However, to our knowledge there are no reports on kinetics of hydroformylation of terpenes and in particular for camphene. Knowledge of the kinetics is important in understanding the mechanistic features of such complex catalytic reactions. Considering the industrial importance of this reaction in synthesis of perfumery chemicals, the study would also provide useful data for the purpose of reactor designing. The main aim of the present study was to carry out the kinetic study of hydroformylation of camphene using the highly active catalytic system $Rh(CO)_2(acac)/P(OPh)_3$ in the temperature range of 363-383 K. For this purpose, the effect of catalyst precursor, ligand and camphene concentration and partial pressures of CO and H_2 on the rate of hydroformylation was

studied. An empirical rate equation has been proposed and the activation energy evaluated.

2.3.5.1 Preliminary experiments

Before studying the kinetics of the reaction, it is necessary to first check the material balance and reproducibility of the experiments. For this purpose, a few experiments were carried out till > 90% conversion of camphene in which the amount of camphene consumed, products formed, and $CO+H_2$ consumed were compared. A typical concentration time profile for hydroformylation of camphene is shown in is Figure 2.15.

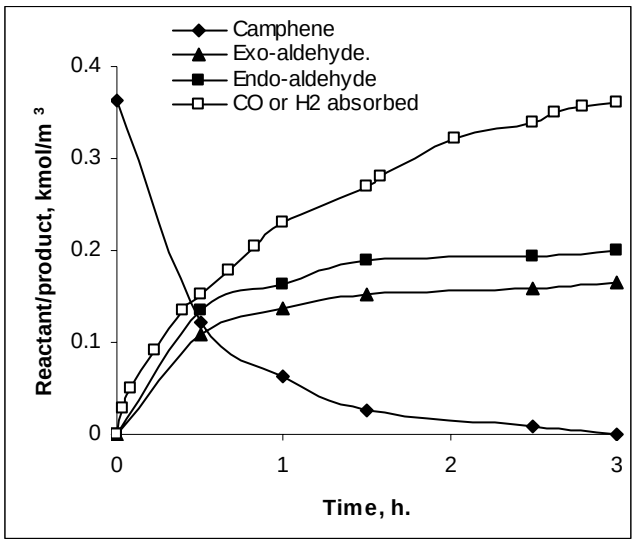

Figure 2.15: Concentration -Time profile for hydroformylation of camphene.

Reaction conditions: *camphene : 0.37 kmol/m^3, $Rh(CO)_2(acac)$: 1 × 10^{-3} kmol/m^3, $P(OPh)_3$: 6 × 10^{-3} kmol/m^3, Rh:P=1:6, T: 373K, P_{CO+H2}: 4.14 MPa, agitation speed : 16.6 Hz, MEK: 28.2 × 10^{-5} m^3, total charge : 3.0 × 10^{-5} m^3.*

In general, it was observed that the material balance of CO, H_2 and camphene consumed was consistent with the amount of total aldehyde products formed. In addition, in the range of conditions covered in this work, besides the exo and endo aldehydes no hydrogenation or isomerization products were observed. In order to study the kinetics of the hydroformylation of camphene using $Rh(CO)_2(acac)/P(OPh)_3$ complex catalyst in MEK, several experiments were carried out in the range of conditions as shown in Table 2.8.

Table 2.8: Range of conditions used for the kinetic studies

Parameter	Range
Concentration of catalyst (kmol/m^3)	$5 \times 10^{-4} – 2.0 \times 10^{-3}$
Concentration of Camphene (kmol/m^3)	0.19-1.96
Ligand concentration (kmol/m^3)	$3.2 \times 10^{-3} – 1.24 \times 10^{-2}$
Partial pressure of hydrogen (MPa)	0.34-3.82
Partial pressure of carbon monoxide (MPa)	0.34-3.82
Temperature (K)	363 - 383
Solvent	MEK
Agitation speed (Hz)	13.3-24.1
Reaction volume (m^3)	3.0×10^{-5}

The initial rates of hydroformylation were calculated from the plot of aldehyde formation as a function of time. A typical plot showing rate of aldehyde formation is shown in Fig. 2.16. Under the conditions chosen for the kinetic study, no side reactions were found to occur and hence, these data would be representative of the overall hydroformylation of camphene to the corresponding aldehydes. The rate of hydroformylation was calculated as follows (Eq. 2.5):

$$R = \frac{\text{Slope of product formation vs. time plot}}{\text{Volume of liquid}} \qquad 2.5$$

These were essentially initial rates of reaction, observed under differential conditions. The results showing the dependence of the rates on different parameters and a kinetic model based on these data are discussed in the following sections.

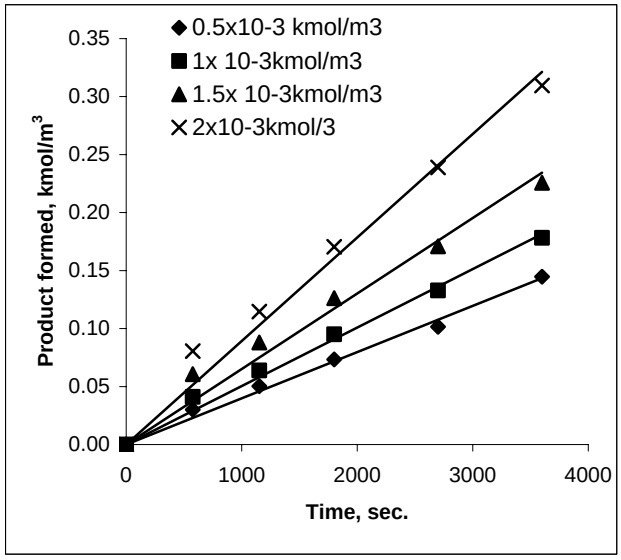

Figure 2.16: A plot of product formation vs. time for different catalyst concentration

Reaction conditions: *camphene: 0.37 kmol/m^3, P(OPh)$_3$: 0.31-1.23 × 10^{-3} kmol/m^3 Rh:P=1:6, T: 363-383K P_{CO+H2}: 4.14 MPa, agitation speed : 16.6 Hz, MEK: 2.82 × 10^{-5} m^3, total charge : 3.0 × 10^{-5} m^3, time 1h .*

2.3.5.2 Solubility of H_2 and CO in camphene, MEK and mixtures

For interpretation of kinetic data, knowledge of the concentration of the gaseous reactants in the reaction medium is essential. The solubility of CO and H_2 in MEK, camphene and camphene/MEK mixtures was determined experimentally in the temperature range of 353-383 K, using a method described by Chaudhari and coworkers[18]. The solubility of H_2 and CO was measured in a 5×10^{-5} m^3 capacity stirred autoclave designed for 13.5 MPa pressure (see Figure 2.10). The equipment was provided with automatic temperature control and a pressure recording system. The temperature of the liquid in the reactor was controlled within ±1 K. A pressure transducer having a precision of ±1 kPa was used to measure the autoclave pressure.

In a typical experiment for the measurement of solubility of H_2 and CO, a known volume (3×10^{-5} m^3) of solvent was introduced into the autoclave and the contents were heated to a desired temperature. After the thermal equilibrium was attained, the void space in the reactor was carefully flushed with a solute gas (CO or H_2) and pressurised to the required level (P_i). The contents were then stirred for about ten minutes to equilibriate the liquid phase with the solute gas. In general, it required, about 5 minutes to saturate the liquid phase. The drop in the pressure in the autoclave was recorded as a

function of time, till it remained constant, indicating the saturation of the liquid phase at the final pressure (P_f). From the initial and final pressure readings, the solubility was calculated as (Eq. 2.6):

$$X_a = \left(P_i - P_f\right) V_g \Big/ RTV_L \qquad 2.6$$

Where X_a represents the solubility (kmol/m^3) of the solute gas prevailing at P_f, P_i and P_f are the initial and final pressure readings in the autoclave, MPa, V_g and V_L (m^3) are the volumes of the gas and liquid phases, respectively, R is the gas constant and T is the temperature (K). Following this procedure, the solubility data were obtained for hydrogen and CO in toluene and MEK-camphene mixtures in the temperature range of 353-383 K, and the solubility of H_2 and CO in the different solvent composition was measured in the pressure range from 2-6 MPa.

Calculation of Henry's constant: The solubility of the gas was calculated in kmol/m^3 for the individual gas at particular pressure in MPa. The plot of solubility of gas (X_a) vs the pressure of gas (P_f) in MPa at different temperatures gave straight line, from the slopes of which the Henry's constant was calculated as per Eq-2.7

$$H = P_f \Big/ X_a \qquad 2.7$$

Where H is Henry's constant in kmol.m^3/MPa. Figure 2.17 shows the Henry's constant obtained for H_2 and CO at the MEK-camphene composition of 100:0, 80:20 and 60:40 v/v. The graph of Henrys constant vs MEK composition after extrapolation gives the values of Henry's constant at any intermediate solvent–substrate composition as shown in Table 2.9

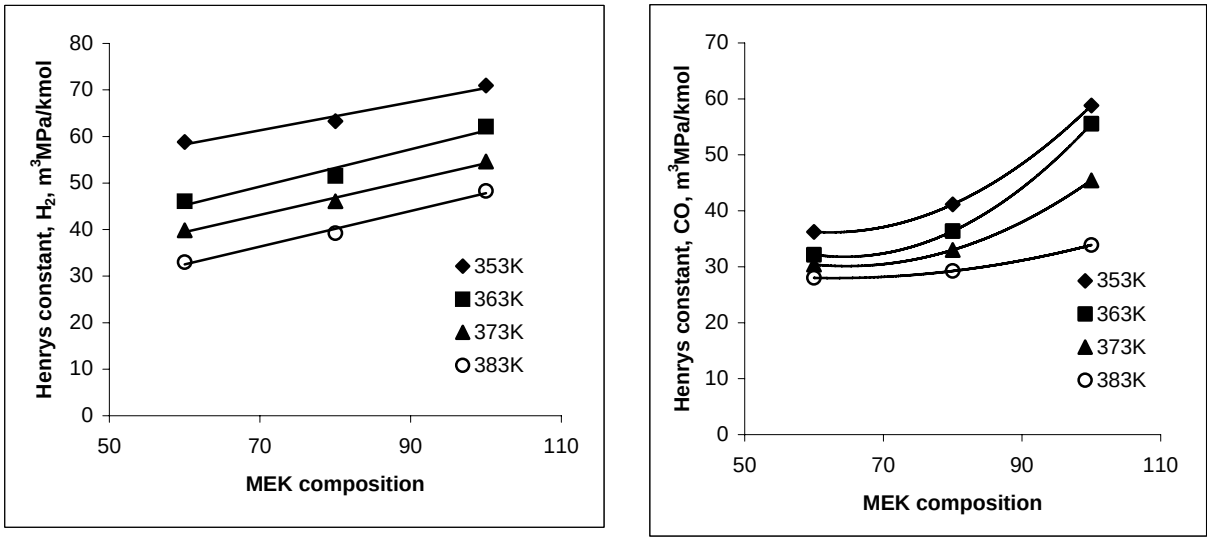

Figure 2.17: A plot of Henry's constant for H_2 and CO vs. MEK composition at various temperatures

Table2.9: Henry's constant (m^3MPa/kmol) of H_2 and CO in various MEK-camphene composition at 353, 363, 373 and 383 K.

MEK composition % (v/v)	353K		363K		373K		383K	
	H_2	CO	H_2	CO	H_2	CO	H_2	CO
100	70.92	58.82	62.11	55.55	54.64	45.45	48.31	33.89
96.81	68.39	51.97	59.82	50.20	53.93	41.76	46.58	31.62
93.82	67.24	48.68	58.07	45.67	52.07	38.94	44.77	30.98
87.2	65.40	44.50	55.37	40.38	49.24	35.51	42.06	30.08
80.8	65.53	41.30	52.75	36.72	46.54	33.06	39.51	29.31
80	63.29	41.15	51.54	36.36	16.08	33.00	39.21	29.23
74.5	61.80	39.06	50.41	34.39	44.16	31.52	37.28	28.73
64.0	59.59	37.06	47.55	32.63	41.30	30.46	34.65	28.18
60	58.82	36.23	46.08	32.15	39.84	30.39	33.00	28.01

2.3.5.3 Effect of agitation speed

The effect of agitation speed on the rate of hydroformylation of camphene was studied at $Rh(CO)_2(acac) = 2 \times 10^{-3}$ kmol/m^3, $P(OPh)_3 = 1.2 \times 10^{-2}$ kmol/m^3 (Rh:P=1:6), camphene = 0.37 kmol/m^3 , P_{CO+H2}= 4.14 MPa at 383K and the results are shown in Figure 2.18. The rate as well as exo/endo ratio was found to be independent of the agitation speed beyond 800 rpm, and therefore all the reactions were carried out at an agitation speed of 1000 rpm to ensure that the reaction occurred in the kinetic regime.

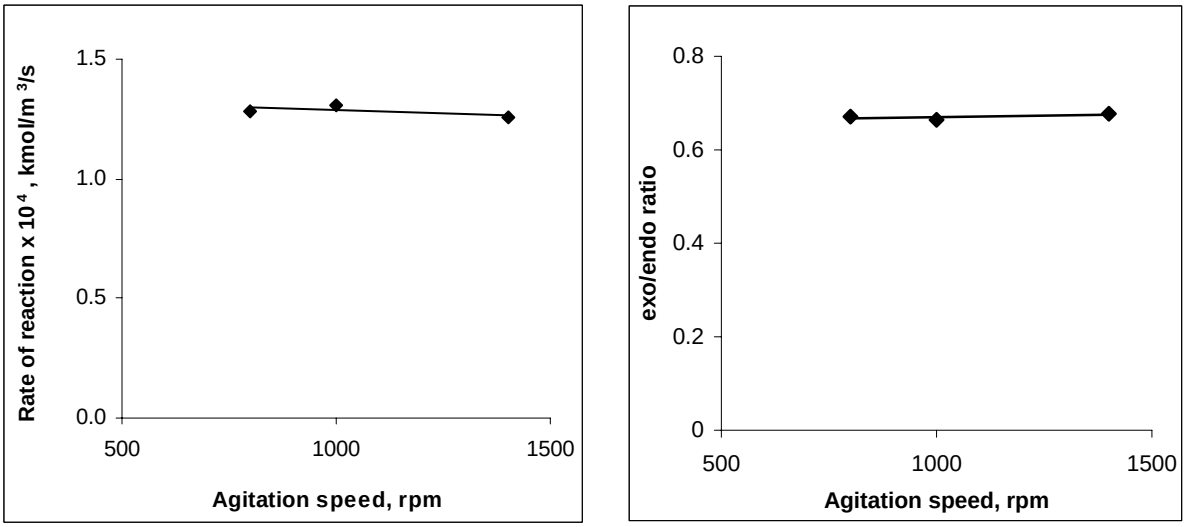

Figure 2.18: Effect of agitation speed on the rate and exo/endo ratio in hydroformylation of camphene.
Reaction conditions: *$Rh(CO)_2(acac)$: 2×10^{-3} kmol/m^3, $P(OPh)_3$:1.2×10^{-2} kmol/m^3, Rh:P=1:6, camphene : 0.37 kmol/m^3, T: 383K, P_{CO+H2}: 4.14 MPa, MEK: 2.82×10^{-5} m^3, total charge : 3.0×10^{-5} m^3 .*

2.3.5.4 Effect of catalyst concentration

The effect of $Rh(CO)_2$acac concentration on the rate of hydroformylation of camphene was studied in the temperature range of 363-383 K, camphene concentration of 0.37 kmol/m^3 and a total pressure of CO + H_2= 4.14 MPa (CO/H_2 = 1) and Rh:L ratio of 1:6. The results are shown in Figure 2.19. The rate was found to be linearly dependent on the catalyst concentration, indicating a first order kinetics. A first order dependence is expected from the mechanism shown in Figure 2.20. An increase in concentration of $Rh(CO)_2(acac)$ will cause an increase in active catalyst concentration and thereby increase the rate of reaction. The exo/endo ratio decreases with increasing catalyst

concentration. At higher catalyst concentration both the faces of camphene can have easy accessibility of the catalyst and this could probably lead to a drop in the exo/endo ratio.

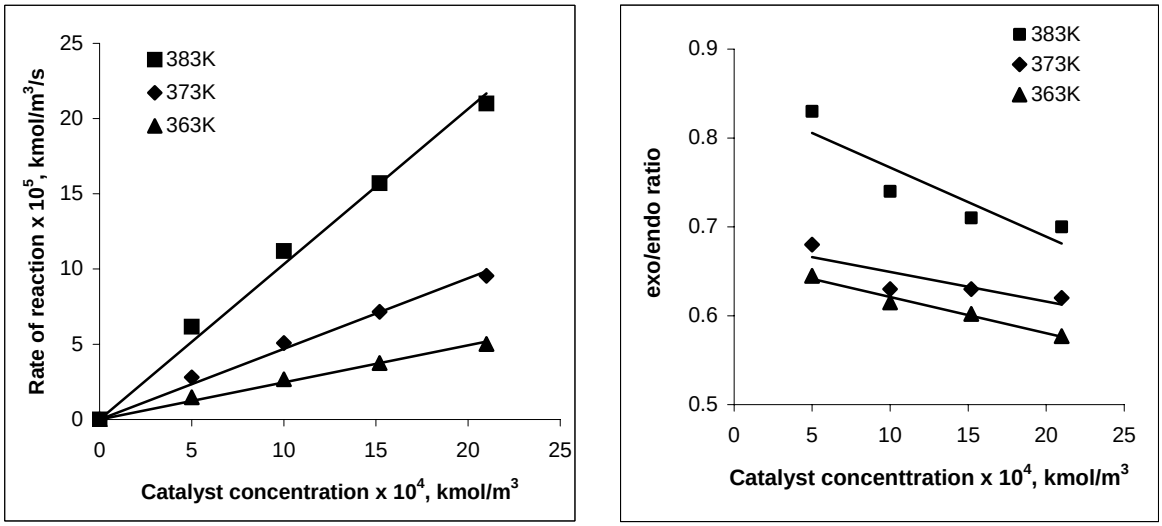

Figure 2.19: Effect of catalyst concentration on the rate and exo/endo ratio in hydroformylation of camphene

Reaction conditions: *camphene: 0.37 kmol/m^3, P(OPh)$_3$: 0.31-1.23×10^{-2} kmol/m^3, Rh:P=1:6, T: 363-383K P_{CO+H2}: 4.14 MPa, agitation speed : 16.6 Hz, MEK: 2.82 × 10^{-5} m^3, total charge = 3.0 ×10^{-5} m^3.*

2.3.5.5 Mechanism

Ziolkowski and coworkers[16,19] have extensively studied the hydroformylation of olefins using Rh-triphenyl phosphite catalyst. Initially they proposed the full catalytic cycle (Figure 2.20) for hydroformylation of olefins using $HRh(CO)[P(OPh)_3]_2$ catalyst by means of insitu IR spectra. In this study, they observed the formation of the alkyl complex, aldehyde, and regeneration of the active catalyst. The stoichiometric reactions show that the addition of $P(OPh)_3$ to the $Rh(CO)_2(acac)$ gives a 16 electron square planer complex $Rh(acac)[P(OPh)_3]_2$ by the facile displacement of the CO ligand. (This has also been visually observed in our experiments. As soon as the phosphite ligand was added to the $Rh(CO)_2(acac)$ solution the CO is liberated in the form of bubbles.) $Rh(acac)[P(OPh)_3]_2$ is a Rh (I) species suitable for use as a model homogeneous catalyst for the activation of diatomic molecule such as H_2 and CO as well as olefins. In presence of syngas atmosphere and excess ligand concentration it leads to the highly stable

hexacoordinated species $HRh(acac)(CO)[P(OPh)_3]_2$, which is also one of the species active for hydroformylation reaction.

In their later work Ziolkowski et al[19c] proposed that the presence of syngas and excess of free $P(OPh)_3$ causes the stepwise substitution of acetylacetonate ligand in the $Rh(acac)[P(OPh)_3]_2$. This leads to the formation of 18 electron pentacoordinated $HRh(CO)[P(OPh)_3]_3$ species in the trigonal planer geometry and Rh-H bond perpendicular to the plane. $HRh(CO)[P(OPh)_3]_3$ is an active species for hydroformylation of olefins and gives aldehyde by the dissociative pathway similar to the mechanism proposed by Wilkinson and coworkers[20], for the $HRhCO(PPh_3)_3$ catalyzed hydroformylation.

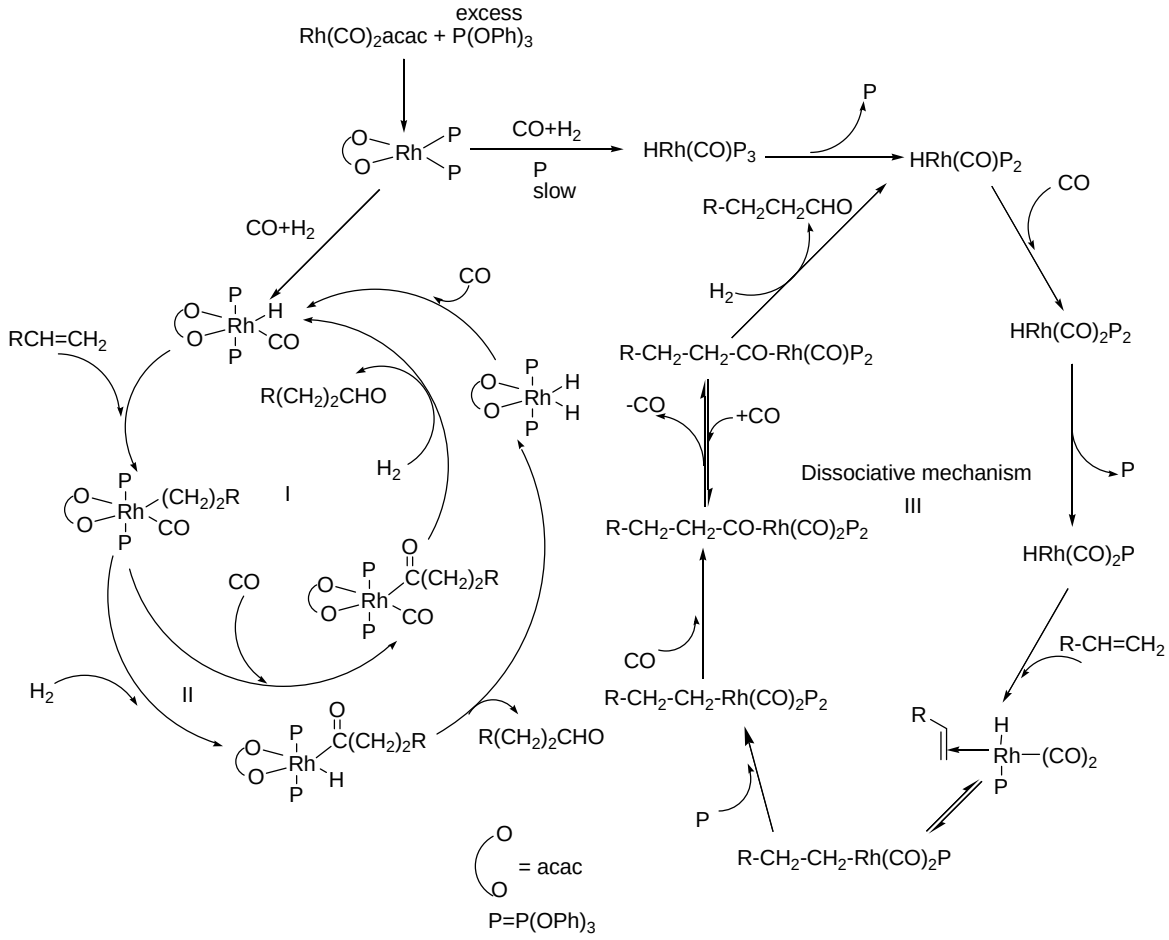

Figure 2.20: Mechanism of hydroformylation using $HRh(acac)(CO)\ [P(OPh)_3]_2$ and $HRh(CO)[P(OPh)_3]_3$ catalyst[19].

2.3.5.5 Effect of camphene concentration

The effect of camphene concentration on the rate of hydroformylation has been studied in the temperature range of 363-383K, catalyst concentration of 1×10^{-3} kmol/m^3, and Rh:L of 1:6 and total pressure of CO + H_2= 4.14 MPa (CO/H_2 = 1) and the results are presented in Figure 2.21. The rate was found to be first order with camphene concentration, which is in agreement with the mechanism shown in Figure 2.20. The exo/endo ratio also increases with increasing substrate concentration. This observation is explained on the basis of substrate to catalyst ratio. Under condition of high substrate loading the substrate:catalyst ratio increases. As is seen in the effect of catalyst concentration (see Figure: 2.19) with a reduction in substrate catalyst ratio the exo /endo ratio decreases.

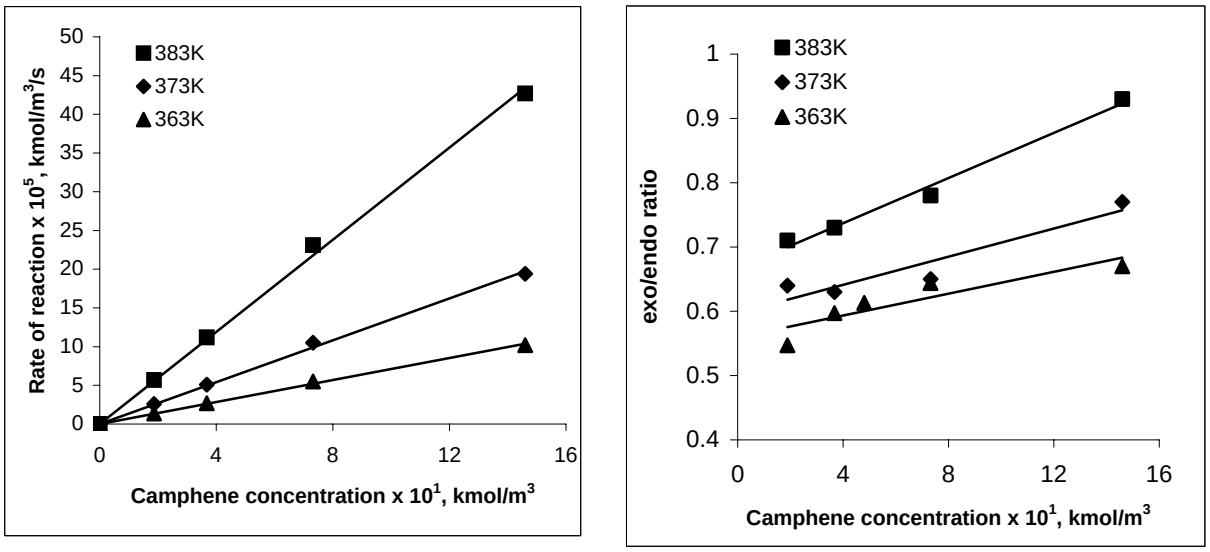

Figure 2.21: Effect of camphene concentration on the rate and exo/endo ratio in hydroformylation of camphene

Reaction conditions: *$Rh(CO)_2(acac)$: 1×10^{-3} kmol/m^3, $P(OPh)_3$: 6×10^{-3} kmol/m^3, Rh:P=1:6, T: 363-383K, P_{CO+H2}: 4.14 MPa, agitation speed : 16.6 Hz, MEK: 2.82×10^{-5} m^3, total charge : 3.0×10^{-5} m^3.*

2.3.5.6 Effect of ligand concentration

The effect of excess $P(OPh)_3$ on the rate of hydroformylation has been studied at $Rh(CO)_2(acac)$= 1×10^{-3} kmol/m^3, camphene = 0.37 kmol/m^3, P_{CO+H2}=4.14 MPa in the

temperature range of 363-383K and the results are shown in Figure 2.22. The plots of rate vs ligand concentration pass through maxima. In the lower concentration range, the rate was found to be first order with respect to ligand but at higher concentration negative order dependence was observed. The highest rates were observed at P/Rh ratio of three. Similar observations were reported by Ziolkowski and coworkers[19] who observed a rate depletion at $P(OPh)_3$: Rh ratios >2:1 for hexene hydroformylation. In case of triphenyl phosphite ligand the active species is either $HRh(acac)CO[P(OPh)_3]_2$ or $HRhCO[P(OPh)_3]_3$ depending on the reaction condition, concentrations and gas composition[15,19ab]. At higher ligand concentration the transition state becomes more crowded which makes coordination of olefin to the rhodium center difficult and and hence rate decreases. This fact is also supported by the observation of a drop in exo/endo ratio of the aldehydes, with increasing $P(OPh)_3$: Rh ratios.

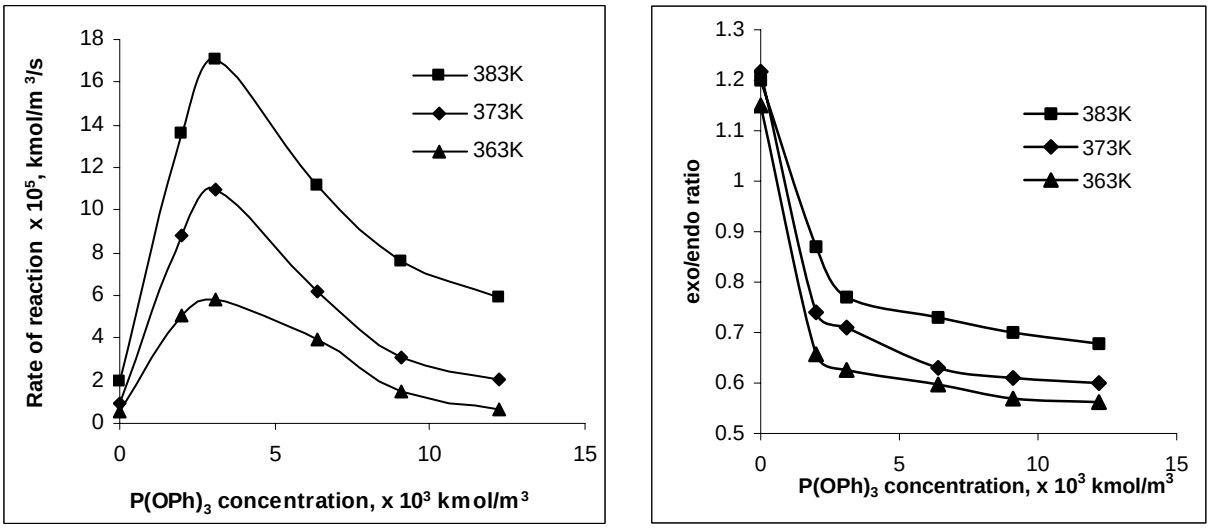

Figure 2.22: Effect of ligand concentration on the rate and exo/endo ratio in hydroformylation of camphene

Reaction conditions: *$Rh(CO)_2(acac)$: 1 × 10^{-3} kmol/m^3, camphene : 0.37 kmol/m^3, T: 363-383K, P_{CO+H2}: 4.14 MPa, agitation speed: 16.6 Hz, MEK: 2.82 × 10^{-5} m^3, total charge : 3.0 × 10^{-5} m^3.*

2.3.5.7 Effect of partial pressure of H_2 (P_{H2})

The effect of partial pressure of H_2 on the rate of hydroformylation of camphene was investigated at a constant partial pressure of CO = 2.07 MPa, $Rh(CO)_2(acac)$ = 1 × 10^{-3} kmol/m^3, $P(OPh)_3$ = 6 × 10^{-3} kmol/m^3, camphene = 0.37 kmol/m^3 in the temperature

range of 363-383K and the results are shown in Figure 2.23**.** The rate of reaction was found to be partial order with P_{H2}. The fractional order dependence shows that the oxidative addition of hydrogen is not the rate determining step in this mechanism. The partial order P_{H2} dependence and first order olefin dependence suggest that for the less reactive substrates like camphene, the olefin coordination or hydride migration ($\pi \rightarrow \sigma$ transfer) is rate-determining step as demonstrated by van Leeuwen and coworkers[21]. The exo/endo ratio is found to decrease with increasing H_2 partial pressure.

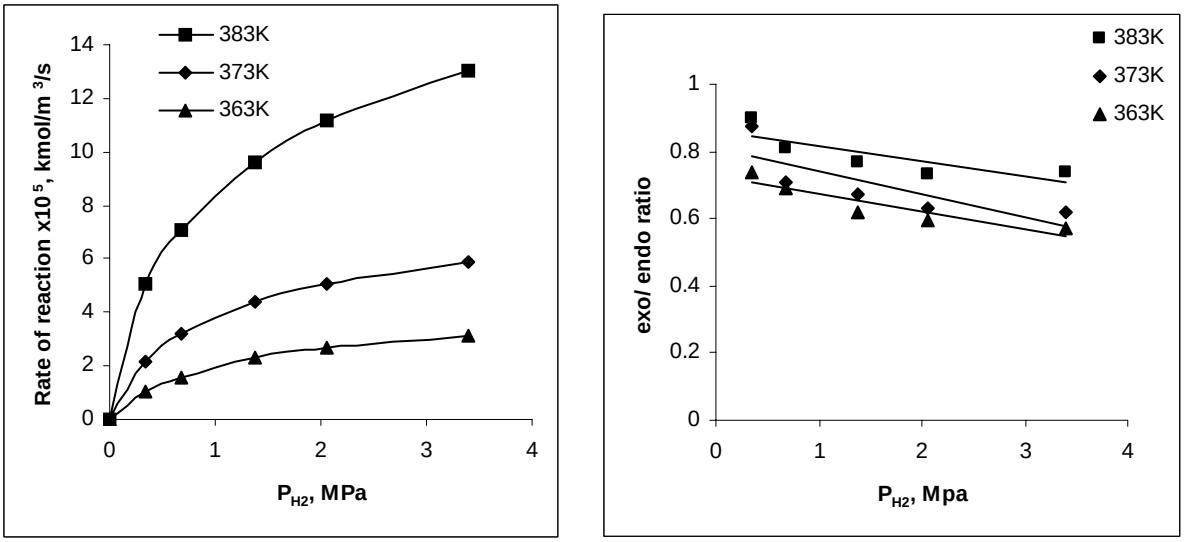

Figure 2.23: Effect of partial pressure of hydrogen on the rate and exo/endo ratio in hydroformylation of camphene

Reaction conditions: *$Rh(CO)_2(acac)$: 1 × 10^{-3} kmol/m^3, $P(OPh)_3$: 6 × 10^{-3} kmol/m^3, Rh:P=1:6, camphene : 0.37 kmol/m^3 , T: 363-383K P_{CO} :2.07 MPa, agitation speed: 16.6 Hz, MEK=2.82 × 10^{-5} m^3, total charge : 3.0 × 10^{-5} m^3 .*

2.3.5.8 Effect of partial pressure of CO (P_{CO})

The effect of P_{CO} on the rate of hydroformylation of camphene was studied at constant H_2 partial pressure of 2.07 MPa, $Rh(CO)_2(acac)$ = 1 × 10^{-3} kmol/m^3, $P(OPh)_3$: 6 × 10^{-3} kmol/m^3, camphene = 0.37 kmol/m^3 in a temperature range of 363-383K and the results are shown in Figure 2.24. The rate was found to have a very complex dependence on P_{CO}. After an initial range of P_{CO} wherein a linear dependence was observed, the rate was almost independent of P_{CO} upto ~ 2 MPa. Thereafter the rate showed a positive order

dependence followed by inhibition at high P_{CO} after attaining a maximum. The complex trend was stronger at the higher temperature. This observation is different from the phosphine catalyzed reactions, where inhibition is observed at lower CO pressure. This observation may be due to the combination of the various steps as shown in Figure 2.20. (i) The initial enhancement in activity with P_{CO} is observed, as sufficient amount of CO is present to form a catalytically active species $HRhCO[P(OPh)_3]_2$. (ii) At lower CO pressures the gas composition is mainly dominated by the hydrogen and the cycle II is favored giving a marginal increase in rates (see Figure 2.21) with P_{CO}. (iii) As the gas composition changes to a CO rich composition i.e. at high CO pressure the cycle I and III dominate leading to improved rates. (iv) At still higher CO pressures the rate is reduced due to the formation of inactive di and tricarbonyl species such as $Rh(CO)_2(acac)[P(OPh)_3]_2$ or $HRh(CO)_3[P(OPh)_3]$ by the displacement of the weak phosphite ligand. These species reduce the effective concentration of the active catalytic species and hence, the reaction is inhibited.

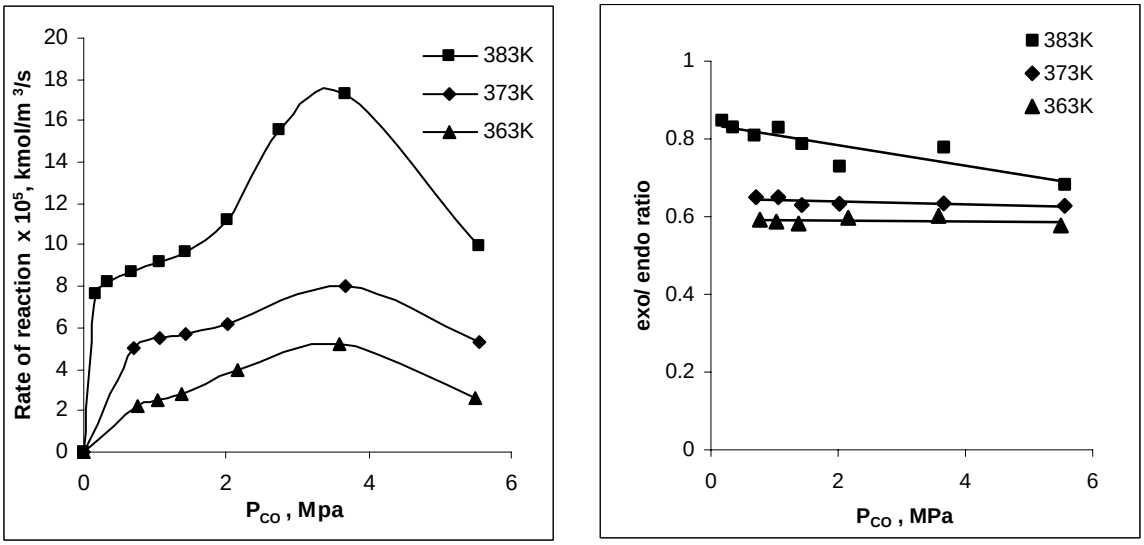

Figure 2.24: Effect of partial pressure of carbon monoxide on the rate and exo/endo ratio in hydroformylation of camphene

Reaction conditions: *$Rh(CO)_2(acac)$: 1×10^{-3} kmol/m^3, $P(OPh)_3$: 6×10^{-3} kmol/m^3, Rh:P=1:6, T: 363-383K, camphene : 0.37 kmol/m^3, P_{H2} : 2.07 MPa, agitation speed: 16.6 Hz, MEK: 2.82×10^{-5} m^3, total charge : 3.0×10^{-5} m^3.*

2.3.5.10 Kinetic model: For the purpose of development of rate models, an empirical approach was followed. Prior to discrimination of rate equations, the rate data were analyzed for the importance of mass transfer resistances. The homogeneous hydroformylation of camphene is a typical gas–liquid (G-L) reaction. The effect of agitation speed on the rate was investigated at the highest catalyst concentration and at highest temperature. The rate was found to be independent of the agitation speed which indicates that the data were representative of the true kinetics of the reaction (Figure 2.18, section 2.3.5.3). Also, the analysis of the initial rate data according to the criteria laid down by Ramachandran and Chaudhari[22] confirmed that the gas–liquid mass transfer resistances (α_{gl}) were negligible. The initial rate data were hence used to evaluate the intrinsic kinetic parameters.

In order to fit the observed rate data, several rate equations were examined using a nonlinear regression analysis. The results on the kinetic parameters estimated for the different models are presented in Table 2.10. For this purpose, an optimization program based on Marquardt's method[23] was used. The objective function was chosen as follows (Eq. 2.8);

$$\phi = \sum_{i=1}^{n} \left[R_{Ai} - R'_{Ai} \right]^2 \qquad 2.8$$

Where Φ is the objective function to be minimized (Φ_{min}) representing the sum of the squares of the difference between the observed and predicted rates, n is the number of experimental data, R_{Ai} and R'_{Ai} represent predicted and experimental rates, respectively. The values of rate parameters and Φ_{min}, are presented in Table 2.10.

Table 2.10: Values of kinetic parameters at different temperatures

Model	Rate Model	T (K)	k_1	k_2	ϕ_{min}
I	$r = \frac{k_1 ACD}{(1+k_2A)}$	363	5.98	55.1	4.19×10^{-11}
		373	12.6	67.7	1.63×10^{-10}
		383	25.7	63.8	8.11×10^{-10}
II	$r = \frac{k_1 ACD}{(1+k_2A)^3}$	363	1.40×10^{10}	1.42×10^{5}	1.97×10^{-8}
		373	3.49	1.10×10^{-5}	1.15×10^{-9}
		383	6.79	1.10×10^{-6}	5.80×10^{-9}
III	$r = \frac{k_1 A^{1.5}CD^{1.5}}{(1+k_2A)}$	363	2.08	1.52×10^{-5}	2.75×10^{-10}
		373	3.49	1.10×10^{-7}	1.15×10^{-9}
		383	1.65×10^{1}	7.87	1.25×10^{-9}
IV	$r = \frac{k_1 ACD}{(1+k_2A)^2}$	363	2.08	1.52×10^{-5}	2.75×10^{-10}
		373	3.49	1.10×10^{-7}	1.15×10^{-9}
		383	1.12×10^{1}	3.32×10^{2}	1.95×10^{-9}
V	$r = \frac{k_1 A^{0.5}CD}{(1+k_2A)^2}$	363	3.84×10^{-1}	1.52×10^{-5}	4.79×10^{-11}
		373	1.25×10^{8}	-9.29×10^{5}	6.40×10^{-8}
		383	9.76×10^{6}	1.58×10^{5}	3.08×10^{-7}

Where, A represents the concentrations of H_2 in MEK at the gas-liquid interface (kmol/m^3) respectively. C and D are the concentrations of the catalyst and camphene (kmol/m^3), respectively. The effect of CO partial pressure was very complex and hence was not considered for the kinetic modeling.

The discrimination of rate models was done based on the thermodynamic criteria, activation energy and the Φ_{min} values. The rate models II and III were rejected based on the thermodynamic criteria of inconsistency of equilibrium constant and high activation energy. Model V had rate parameters less than zero (–ve) and hence was rejected. In the remaining two models I and IV, the model IV was discriminated based on the higher Φ_{min} values than model I. Therefore, model I (Eq. 2.9) was considered the best model for representing the kinetics of hydroformylation of camphene in homogeneous medium using $Rh(CO)_2(acac)/P(OPh_3)_3$ catalyst.

$$r = \frac{k_1 ACD}{(1+ k_2 A)} \qquad 2.9$$

Where, *k* is the intrinsic rate constant (m^3/kmol), A represents the concentrations of H_2 in MEK at the gas-liquid interface (kmol/m^3). C and D are the concentrations of the catalyst and camphene (kmol/m^3), respectively the rate parameters for Eq. 2.5 for all the temperature are presented in Table 2.10 (entry 1). A comparison of the experimental rates with the rates predicted by Eq. 2.9 is shown in Figure 2.25, which shows a reasonably good fit of the data. The average deviation in the predicted and observed rates was found to be in the range of ± 5 %. The Arrhenius plot showing the effect of temperature on the rate parameters is shown in Fig. 2.26, from which the activation energy was evaluated as 84.7 kJ/mol. The dependence of the rate parameter k_2 on temperature shows opposite trend; however, it is important to note that this parameter may not be representative of a single equilibrium reaction step and is in fact a lumped parameter describing observed overall trends.

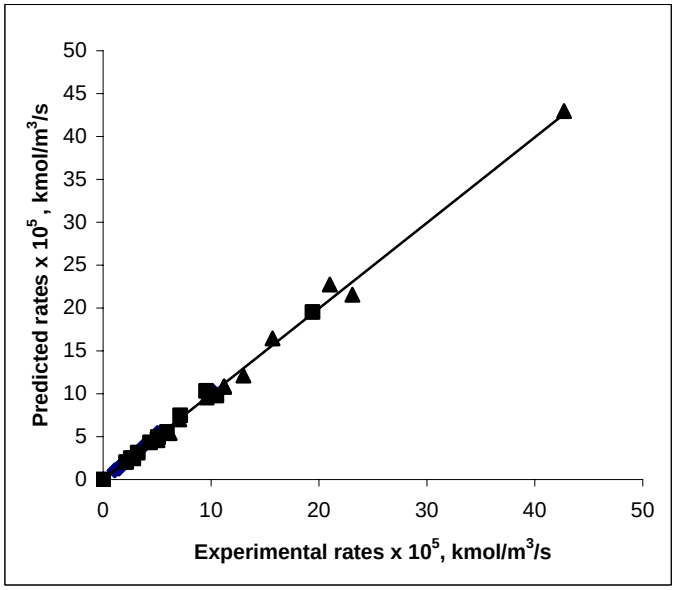

Figure 2.25: Comparison of experimental rates and rates predicted using model I

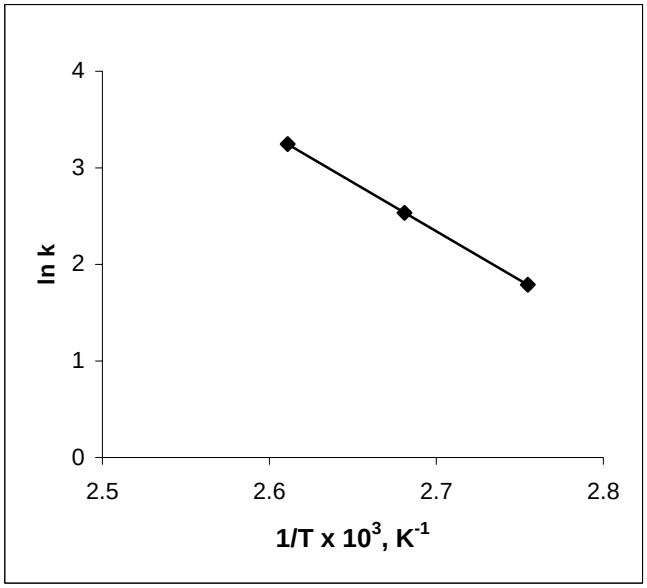

Figure 2.26: Temperature dependence of rate constant

The validity of the proposed model I was crosschecked by plotting the experimental and observed rates at different temperatures and concentrations of the variables as shown in Figure 2.27. The predicted and experimental trends are in good agreement indicating that the proposed model I (Eq. 2.5) is the best fit.

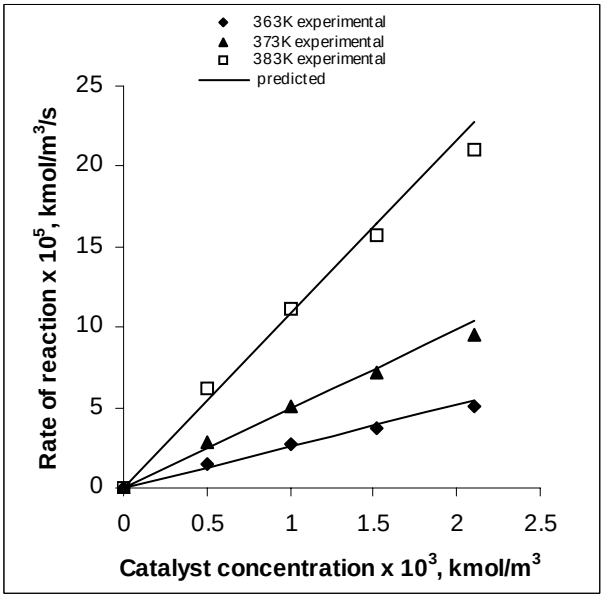

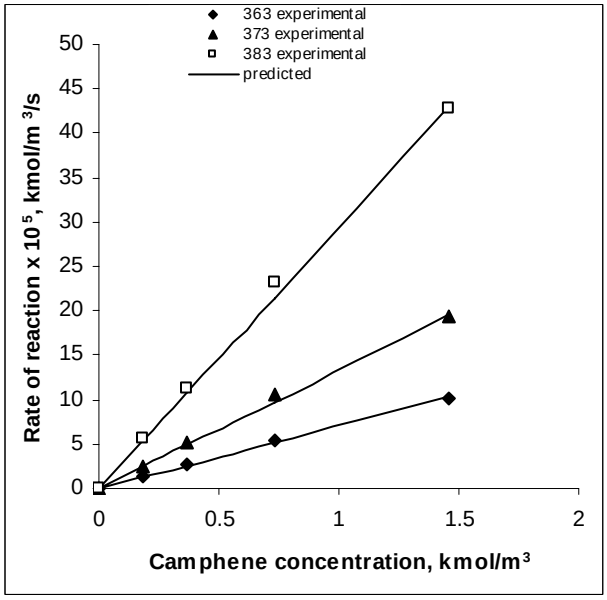

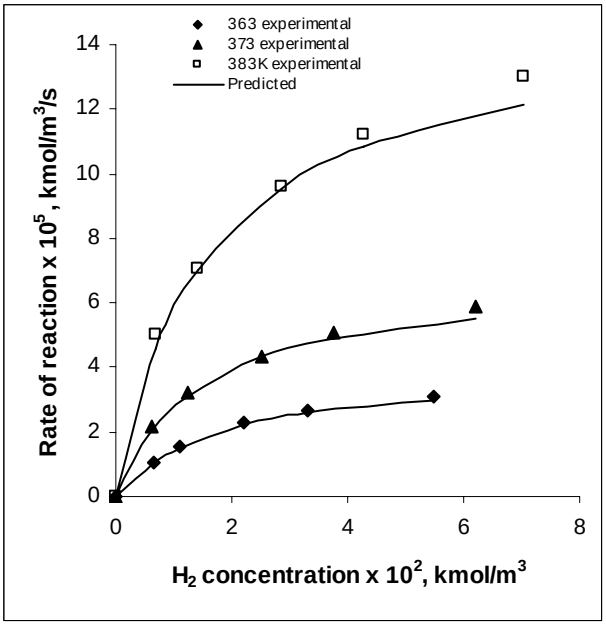

Figure 2.27: Validation of proposed rate model for various reaction parameters

2.4 Conclusions

The hydroformylation of various terpenes was performed using modified and unmodified Rh and Co complexes. In addition to this, Pt complex catalyst alongwith $SnCl_2$ was also tested. The hydroformylation products of terpenes were isolated and identified by GC-MS. It was observed that the Wilkinson's catalyst only hydroformylate terpenes having terminal double bonds and shows very poor activity. Hydroformylation of camphene in an aqueous biphasic medium using $HRhCO(TPPTS)_3$ catalyst also proceeds with a poor activity. The hydroformylation of terpenes and in particular camphene was efficiently catalyzed by the $Rh(CO)_2(acac)$ /$P(OPh)_3$ catalyst system. This catalyst was more efficient for hydroformylation of terpenes, as compared to Wilkinson complex. The $Rh(CO)_2(acac)/P(OPh)_3$ catalytic system was found to give the highest activity (TOF = 417 h^{-1}) and selectivity (100%) to aldehyde for hydroformylation of camphene. The product selectivity was slightly more towards the endo diasteriomers. (exo/endo = 45.5/54.5). It is also possible to hydroformylate neat camphene with high selectivity to aldehyde. The role of solvent, temperature, various phosphite ligands, P/Rh ratio and effect of temperature on the activity and selectivity of hydroformylation of camphene has been investigated. The $Rh(CO)_2(acac)/P(OPh)_3$ catalyst system is also an efficient catalyst for hydroformylation of limonene, carvone and β-pinene in addition to camphene.

The kinetics of hydroformylation of camphene using $Rh(CO)_2(acac)/P(OPh)_3$ in MEK has been investigated in a batch reactor in the temperature range of 363-383 K. The rate was found to be first order with respect to catalyst and substrate concentration. The rate was found to have a partial order dependence on P_{H2}. The plot of rate vs. ligand concentration passes through maxima and shows a typical case of inhibition at higher concentrations. In the lower concentration range the rate was found to be first order with respect to ligand.

The rate was found to have a very complex dependence on $P_{CO.}$ After an initial range of P_{CO} wherein a linear dependence was observed, the rate was almost independent of P_{CO} upto ~ 2 MPa. Thereafter the rate showed a positive order dependence followed by inhibition at high P_{CO} after attaining a maximum. The complex trend was stronger at higher temperature. This observation is different from the phosphine catalyzed reactions, where inhibition is observed at relatively lower CO pressure of 0.5 MPa. This observation may be due to the combination of the various steps in the mechanism. The data were fitted to numerous empirical rate equations and after rigorous discrimination of models, a rate equation of the type

$$r = \frac{k_1 ACD}{(1+ k_2 A)}$$

was proposed and kinetic parameters estimated. The model predictions were found to be in good agreement with the experimentally observed data with ±5 % error. The activation energy was calculated and found to be 84.7 kJ/mol.

Nomenclature

A	Concentration of hydrogen, kmol/m^3
B	Concentration of carbon monoxide, kmol/m^3
C	Concentration of catalyst, kmol/m^3
D	Concentration of camphene, kmol/m^3
H	Henry constant defined by equation 2.3
k_1	Intrinsic rate constants, m^3/kmol
k_2	Constant in Eq. 2.9 m^3/kmol
Pf	Final pressure MPa
Pi	Initial pressure MPa
R	Universal gas constant, kJ/kmol/K
r	Rate of hydroformylation, kmol/m^3/s.
R'_{Ai}	Experimental rates, kmol/m^3/s
R_{Ai}	Predicted rates, kmol/m^3/s
R_i	Reaction rate for the hydroformylation step (kmol/m_3/s)
t	Reaction time, h.
T	Temperature, K
V_g	Gas volume, m^3
V_L	Total liquid volume, m^3
X_a	Solubility of gas of the solute gas at pressure P_f , kmol/m^3/MPa
Φ	Parameter defined by Eq-2.8

References

1 (a) J. Hagen, K. Bruns, Henkel, *DE Patent 2849742*, **1980**. (b) S. Sirol, P. Kalck, *New J. Chem.,* **1997**, *21*, 1129. (c) J. C. LoCicero, R.T. Johnson, *J. Am. Chem. Soc.,* **1952**, *74* 2094. (d) E. Gusevskaya, J.A. Goncalves, *J. Mol. Catal. A :Chemical,* **1997**, *131*, 121. (e) C. M. Foca, E. N. Dos Santos, E. V. Gusevskaya, *J. Mol. Catal. A :Chemical,* **2002**, *185*, 17. (f) H. J. V.Barros, M. L. Ospina, E. Arguello, W. R. Rocha, E.V. Gusevskaya, E. N. dos Santos, *J. Organomet. Chem.,* **2003**, *671*, 150. (g) H. J. V. Barros, B. E. Hanson, E. V. Gusevskaya, E. N. dos Santos, *Applied catalysis*, **2004**, *278*, 57.

2 D. Evans, J. Osborn, G. Wilkinson, *J. Chem. Soc. A*, **1968**, 3133

3 Y. S. Varshavskii, T. G. Cherkasova, *Russ. J. Inorg. Chem.,* **1967**, *12*, 899

4 J. Chatt, L. M. Venanzi, *J. Chem. Soc. A*, **1957**, 4735

5 J. Chatt, L. M. Venanzi, *Olefin Coordination Compounds Part VI* **1957**.

6 R. Usan, *Inorganic Synthesis.* **1985**, *23*, 126.

7 M. Trzeciak, J. J. Ziolkowski, *Inorg. Chim. Acta Lett.,* **1982**, *64*, L267.

8 R. Tannenbaum, G. Bor, *J. Organomet. Chem.,* 1999, *585*, 18.

9 Boven M. V., Alemdaroglu N. H., Penninger J. M. L., *Ind. Eng., Prod. Res. Dev.* **1975**, *14 (4)*, 259.

10 G. Cavinato, L. Toniolo *Inorg.Chim. Acta*, **1981**, *52*, 39

11 (a) R. L. Pruett, J. A. Smith, *J. Org. Chem.* **1969,** *34*, 327. (b) R. L. Pruett, J. A. Smith, *S. African Pat. 6804937*, **1968** (to Union Carbide Coorporation); *Chem. Abstr.* **1969,** 71, 90819. (b) P. W. N. M. van Leeuwen, C. F. Roobeek, *J. Organomet. Chem.,* **1983,** *258,* 343. (c) P. W. N. M. van Leeuwen, C. F. Roobeek, *Brit. Pat. 2 068 377*, **1980** (to Shell); *Chem Abstr*-. **1984,** *101,* 191 142.

12 J. Falbe in *New Synthesis with Carbon monoxide* (Eds. B. Cornils and W.A. Hermann) Springler-verlag Berlien, Heidlberg, New york **1980** pp 84- 89.

13 M. Kranenburg, Y. E. M. vander Burgt, P. C. J. Kamer, P. W. N. M. van Leeuwen, K. Goubitz and J. Fraanje, *Organometallics*, **1995**, *14*, 3081

14 P. W. N. M. van Leeuwen, C. Claver *Rhodium Catalyzed Hydroformylation,* Kluwer Acadamic Publishers, Dordrecht, **2001** pp 35-62

15 O. R. Hughes, J. D. Unruh *J. Mol. Catal.,* **1981**, *12*, 71.

16 A. M. Trzeciak, J. J. Ziolkowski *J. Mol. Catal.* **1983**, 19, 41

17 (a) R. M. Deshpande, R.V. Chaudhari, *Ind. Eng. Chem. Res*. **1988**, *27*, 1996 (b) R. M. Deshpande, R. V.Chaudhari, *J. Catal.* **1989**, *115*, 326 (c) S. S. Divekar, R.M. Deshpande, R. V. Chaudhari, *Catal. Lett*.**1993**, *21*,191 (d) B. M. Bhanage, S. S. Divekar, R. M. Deshpande, R. V. Chaudhari, *J. Mol. Catalysis A: Chemical*, **1997**, *115*, 247 (e) R. M. Deshpande, S. S. Divekar, B. M. Bhanage, R. V. Chaudhari, *J. Mol. Catalysis A: Chemical,* **1992***, 77,* 13 (f) Y. Zhang1, Zai-Sha Mao, J. Chen, *Catalysis Today*, **2002**, *74*, 23 (g) G. Kiss, E. J. Mozeleski, K. C. Nadler, E. Van Driessche, C. DeRoover, *J. Mol. Catal. A: Chemical*, **1999**, *138*, 155

18 R. M. Deshpande, B. M. Bhanage, S. S. Divekar, S. Kanagasabapathy and R. V. Chaudhari, *Ind. Eng. Chem. Res*, **1998**, *37*, 2391

19 (a)H. Janecko, A. M. Trzeciak and J. J. Ziolkowski *J. Mol. Catal*., **1984**, *26*, 355. (b) A. M. Trzeciak, J. J. Ziolkowski *J. Mol. Catal.,* **1986**, *34*, 213. (c) A. M. Trzeciak, J. J. Ziolkowski, S. Aygen, R. Van Eldik *J. Mol. Catal.,* **1986**, *34*, 337. (d) A. M. Trzeciak, J. J. Ziolkowski *J. Mol. Catal.* **1988**, *43*, 335.

20 D. Evans, J. A. Osborn, G. Wilkinson, *J. Chem. Soc. A*, **1968**, 3133.

21 (a) A. Van Rooy, E. N. Orij, P. C. J. Kamer, P. W. N. M. van Leeuwen *Organometallics,* **1995**, *14*, 34. (b) T. Jongsma, G. Challa, P. W. N. M. van Leeuwen *J. Organomet. Chem.* **1991**, *421*, 121.

22 P. A. Ramachandran, R. V. Chaudhari, *Multiphase Catalytic Reactors* Gordon and Breach, London, **1983**

23 D. W. Marquardt, *J. Soc. Ind. Appl. Math*., **1963,** *11(2)*, 431.

CHAPTER 3
Hydroformylation of 1-Decene in Aqueous Biphasic Medium using Water-Soluble Rhodium- sulfoxantphos Catalyst

3.1 Introduction

Homogeneous catalysts offer a number of important advantages over their heterogeneous counterparts, like (i) high activity, as the catalyst is usually a dissolved metal complex and hence all catalytic sites are accessible, (ii) possibility to tune the chemoselectivity, regioselectivity, and/or enantioselectivity of the catalyst by proper arrangement and choice of ligand etc. However, inspite of the obvious advantages many homogeneous catalytic systems cannot be commercialized because of difficulties associated with catalyst-product separation and catalyst recovery/recycle, especially for expensive nobel metal catalysts. With particular reference to the hydroformylation reaction, the aldehyde products are non-volatile and thermally unstable in many cases and hence their separation from catalysts poses a serious challenge. To overcome these difficulties attempts were made to heterogenize the homogeneous catalysts. These catalysts could then combine the advantages of homogeneous catalyst i.e. high activity and selectivity with those of heterogeneous catalyst viz-long lifetime and ease of separation. Different methodologies for the heterogenization of the catalyst have been proposed. These could be either immobilization of catalyst on solid supports or heterogenization as a soluble catalyst in a different phase. The latter is generally termed as biphasic catalysis. Various biphasic systems are described in Chapter 1 (section 1.5.1.)

Biphasic catalysis using water-soluble metal complexes has been the most significant development in recent years[1]. The emergence of aqueous biphasic catalysis has extended the scope of homogeneous catalysis by simplifying the catalyst recovery from the product mixture and its subsequent recycle. The general principle of aqueous two-phase catalysis is the use of a water-soluble catalyst, which is insoluble in the organic phase containing reactants and products. The catalyst brings about particular transformation in the aqueous phase, and is removed from the desired product (organic phase) at the end of reaction by simple phase separation and decantation. It was after the work of Kuntz[2] on the synthesis of triphenylphosphine trisulfonate (TPPTS) ligand and its application in the hydroformylation of olefins that the research on water-soluble catalysis gained momentum. The concept has also been proven on a commercial scale for the hydroformylation of propene to butyraldehyde (300000 TPA) by Ruhrchemie-Rhône-

Poulenc using Rh/TPPTS catalyst[3], and other reactions as have been listed in Table 1.6 in Chapter 1.

The development of polar and water-soluble ligands and their incorporation into organometallic complexes is integral to aqueous phase catalysis. Water-soluble ligands containing phosphorous and nitrogen as a donor atoms are some of the most commonly utilized ligands. TPPTS is one of the most well known ligand for the aqueous-biphasic hydroformylation, owing to its high solubility in water (1.1kg/1L). Herrmann and Kohlpaintner[4] have reported that Rh complexes with other water-soluble ligands, such as BISBIS (sulfonated (2, 2'-bis (diphenylphosphinomethyl)-1, 1'-biphenyl), and bicyclic NORBOS (sulphonated phosphanorbonadiene), show improved selectivity and activity as compared to TPPTS in hydroformylation. Similarly, other chelating diphosphine ligands such as BINAS-Na[5] (sulphonated 2, 2'-bis (diphenylphosphinomethyl) - l, l'-binaphthalene), sulfonated Xantphos[6] (sulphonated 4,5 –bis(diphenylphosphino) 9,9 dimethylxanthene) also show high selectivity for linear aldehydes, which was ascribed to the large 'natural' bite angle of sulfoxantphos. Use of cationic[7], non-ionic[8] and surface-active phosphines[9],[10] as water-soluble ligands has also been proposed.

Although homogeneous hydroformylation has been applied to several long chain olefins, for the manufacture of a wide range of aldehydes/alcohols (oxo-alcohols), the biphasic catalytic process has so far been applied only to hydroformylation of propylene (Ruhrchemie-Rhône-Poulenc process) and butylenes[11], which have a reasonably high solubility in aqueous phase. The solubility of higher olefins like hexene, octene and the higher homologues in water is very poor and hence results in very poor rates in the aqueous biphasic hydroformylation. The use of co-solvents, surfactants and micelle forming reagents[12], super-critical CO_2-water biphasic system[13], supported aqueous-phase catalysis[14] and catalyst binding ligands (interfacial catalysis)[15] have been proposed to increase the poor rates observed in biphasic catalysis. The emphasis of these methods has been on enhancing the solubility of the substrates in water or by ensuring a better contact between the catalyst and substrates. The detailed account of literature for the rate enhancement in aqueous biphasic system has been presented in Chapter 1 section 1.5.1.4.

The use of cosolvents to enhance the solubility of the organic substrate in water has been reported earlier[16]. This results in a significant enhancement in the rate of reaction using Rh/TPPTS catalyst for hydroformylation of various olefins. Hydroformylation of propylene and hexene using Rh-sulfoxantphos catalyst in aqueous biphasic system was reported by van Leeween and coworkers[5] which gave very high n/b ratio. However, only one attempt was made on further improving the rates for the hydroformylation of higher olefins like 1-octene, and 1-decene using Rame α- or β- CD as an inverse phase transfer catalyst[17]. They observed around 60-70% olefin conversion in 24 hours (TOF=15 h^{-1}).

The kinetics of hydroformylation of olefins has been investigated in sufficient details for homogeneous systems, however, there are very few reports available on kinetic studies of hydroformylation in two-phase systems with water-soluble catalysts in the presence of a cosolvent [16c, 18]. Hydroformylation of olefins using water-soluble catalysis is an example of a gas-liquid-liquid catalytic reaction, in which reaction of two gaseous reactants (carbon monoxide and hydrogen) with the liquid phase olefin occurs in the presence of a water-soluble catalyst in a liquid-liquid dispersion. There are also no kinetic studies on the hydroformylation of higher olefins using Rh-sulfoxantphos catalyst. The high n/i ratio observed for this catalyst makes it a very important system to investigate from the point of view of understanding the kinetics and mechanism.

The main objective of this work was thus to develop a biphasic Rh-sulfoxantphos catalyst system for the hydroformylation of higher olefins such as hexene, octene, decene and dodecene. The effect of aqueous phase hold up, cosolvents and reaction parameters on the reaction rate and chemo and regioselectivity was investigated for 1-decene as a model substrate. The detailed investigation on the analysis of mass transfer effects followed by kinetic study on hydroformylation of 1-decene using water soluble $Rh(CO)_2(acac)$/sulfoxantphos catalyst in presence of NMP as a cosolvent, in a temperature range of 383-403 K has been presented in this chapter.

3.2 Experimental

3.2.1 Materials

Rhodium trichloride ($RhCl_3.3H_2O$) (Arora Matthey, India), triphenylphosphine (PPh_3), Xantphos (4,5–bis(diphenylphosphino) 9,9 dimethylxanthene), Triisooctylamine (Aldrich USA), were used as received without further purification. Sulphuric acid, dimethyl formamide (DMF), acetylacetone and sodium hydroxide (Loba Chemie, India) were used as received. Oleum of 25% (w/w of SO_3 in H_2SO_4) strength was prepared by dissolving the SO_3 gas (produced by the reaction of H_2SO_4 with P_2O_5) in concentrated H_2SO_4 (AR, 36N) in required proportion. Distilled degassed water was used in all operations. Solvents such as toluene, N methyl 2–pyrrolidone (NMP), ethanol, 1, 4-dioxane, methyl ethyl ketone (MEK), n-hexane and benzene were freshly distilled and degassed prior to use. Hydrogen and nitrogen supplied by Indian Oxygen Ltd. Mumbai, and carbon monoxide (> 99.8 % pure) from Matheson Gas Co., U.S.A. were used directly from cylinders. The syngas with 1:1 ratio of H_2:CO was prepared by mixing H_2 and CO in a reservoir in a 1:1 proportion.

3.2.2 Synthesis of sulfoxantphos (2, 7-bis(SO_3Na)-Xantphos)

The synthesis of sulfoxantphos was carried out by the procedure described by van Leeuwen and coworkers[5] (Scheme 3.1). For this purpose, a double jacketed 50 ml reactor was used. The reactor was designed so that operations under argon atmosphere were possible. The temperature was controlled by circulation of water using cryostat. In a typical experiment, Xantphos (**1)** (1 g, 1.73 mmol) was added slowly to oleum (2.9 ml 25% SO_3) over 4 h at 5ºC in a glass reactor. After the addition was complete, the resulting brown solution was warmed to room temperature and stirred for 16 h. After 16 h, 15 ml degassed ice water was added slowly to the solution, resulting in a white suspension. Another 20 ml of degassed water was added and the resulting yellowish solution was poured into a vigorously stirred solution of triisooctylamine (54 mmol, 2.3 ml) in 10 ml of toluene. The toluene layer was washed twice with water and a solution of NaOH (6.25 M) was slowly added until a pH of 12 was reached. The water layer was decanted and neutralized with a 3 M H_2SO_4 solution. Evaporation of the water layer gave a white solid. The solid was dissolved in methanol and refluxed for 30 minutes; a white suspension was obtained which was carefully filtered. The resulting clear solution of the filtrate was

evaporated to dryness resulting in a pale yellow solid product. Further purification was accomplished by refluxing the solid in ethanol, which after decantation and evaporation gave sulfoxantphos (**2)** as a white solid. Yield: 1.03 g (1.31 mmol; 76%). The purity of the ligand was checked by ^{31}P NMR (Figure 3.1) and elemental analysis which was consistent with that reported in the literature. ^{31}P $\{^{1}H\}$ NMR (CD_3OD; ppm): δ -14.69 (literature -14.7). Elemental analysis Found: C=58.9; H= 4.2; S= 8.1, Calculated C=59.8, H= 3.8; S= 8.2.

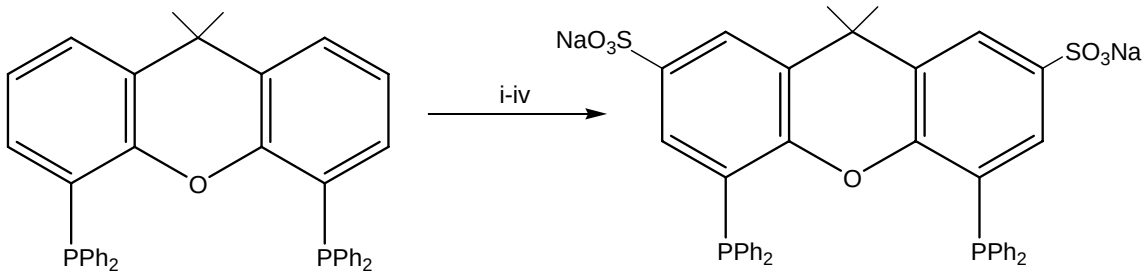

1 **2**

Scheme 3.1: Synthesis of sulfonated Xantphos (sulfoxantphos).

Reagents and conditions: (i) 25% SO_3/H_2SO_4, 5ºC to RT; (ii) triisooctylamine, toluene; (iii) NaOH; (iv) neutralization, MeOH-extraction, EtOH.

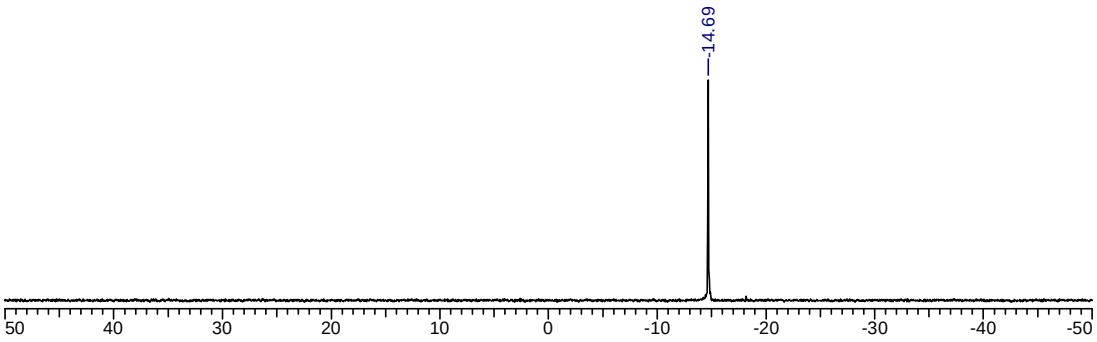

Figure 3.1: ^{31}P NMR spectrum of sulfoxantphos

3.2.3 Synthesis of $HRhCO(PPh_3)_3$

$HRhCO(PPh_3)_3$ was prepared by the procedure described earlier (Chapter 2 section 2.2.2(A)).

3.2.4 Preparation of $Rh(CO)_2(acac)$

$Rh(CO)_2(acac)$ was prepared by the procedure described earlier (Chapter 2 section 2.2.2(B)).

3.2.5 Preparation of (Xantphos)HRhCO(PPh_3)

The (Xantphos)HRhCO(PPh_3) catalyst was prepared by a procedure described by van Leeuwen and coworkers [19]. A solution of $HRh(CO)(PPh_3)_3$ (100 mg, 0.11 mmol) and Xantphos (63.6 mg, 0.11 mmol) in 10 mL of benzene was stirred for 4 h at 30ºC. The solvent was evaporated in vacuum. The resulting yellow solid was washed with 1 ml of methanol to remove PPh_3 and dried in vacuum. A quantitative yield was obtained. The IR spectra (KBr pellet) in Figure 3.2 show bands at 1992 cm^{-1} (νRh-H) and 1898 cm^{-1} (νCO). The elemental analysis of the complex was also done. [Found C=70.9; H= 4.8 Calculated for $C_{58}H_{48}O_2P_3Rh$: C=71.61; H= 4.98].

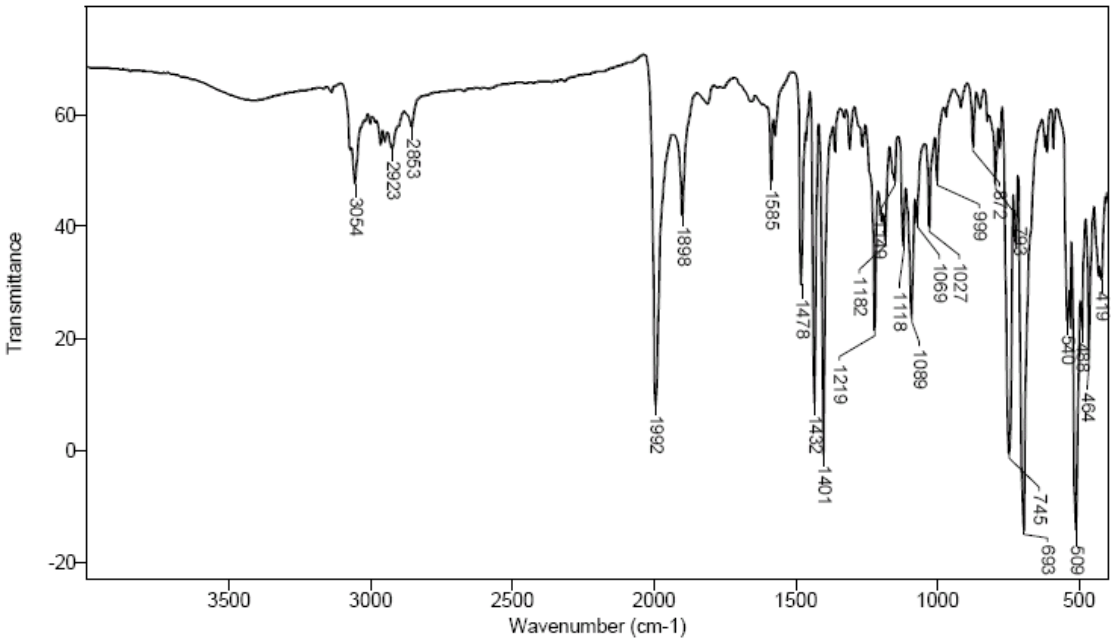

Figure 3.2: FTIR spectrum of (Xantphos)HRhCO(PPh_3)

3.2.6 Experimental setup

All the hydroformylation experiments were carried out in a 50 ml micro reactor, made of stainless steel, supplied by Amar Instruments Pvt. Ltd India. The reactor was provided with arrangements for sampling of liquid and gaseous contents, automatic temperature control and variable agitation speed. The reactor was designed for a working pressure of 20.4 MPa and temperature up to 523K. The experimental set up is similar to that shown in Figure 2.10 (Chapter-2).

3.2.7 Experimental procedure ($Rh(CO)_2(acac)$/ sulfoxantphos catalyst system)

In a typical experiment, sulfoxantphos and $Rh(CO)_2(acac)$ were mixed in the desired ratio, in 10 ml degassed water under argon atmosphere. The resulting yellowish solution was transferred into the autoclave. The autoclave was then flushed three times with nitrogen and syngas respectively, and pressurized to 200 psi with CO/H_2 and heated to 120ºC under stirring for 12 hours. Thereafter, the reactor was cooled to 25ºC and depressurized. A light yellow colored solution of the catalyst was formed. The reactor was then charged with the olefin and toluene (15 ml), which comprises the organic phase for the reaction. (N.B.: In the experiments when cosolvent was used, it was added before the addition of organic phase.) The contents were flushed with nitrogen and then with a mixture of CO and H_2 and heated to attain a desired temperature, and then a mixture of CO and H_2 (in a required ratio, 1:1) was introduced into the autoclave up to the desired pressure (4.14 MPa). A sample of the liquid mixture was withdrawn, and the reaction started by switching the stirrer on. The reaction was then continued at a constant pressure of $CO+H_2$ (1:1) by supply of syngas from the reservoir vessel through a constant pressure regulator. Since, in this study the major product formed was an aldehyde, supply of $CO+H_2$ at a ratio of 1:1 (as per stoichiometry) was adequate to maintain a constant composition of H_2 and CO in the reactor as introduced in the beginning. After the completion of reaction, the reactor was cooled and a final sample was taken for analysis. In each kinetic run, intermediate samples were withdrawn at specific time intervals and analyzed for reactants and products in order to check the progress of the reaction and material balance. It was generally observed that in this low conversion range (<15%) the rates of hydroformylation were constant. The reproducibility of the experiments was found to be in a range of 5-7%. Following this procedure, the effect of the catalyst and olefin concentrations, partial pressures of H_2 and CO, and temperature on the rate of hydroformylation was studied.

3.2.8 Analytical methods

^{31}P NMR spectrum was obtained on a Bruker AC-200 spectrometer in $CDCl_3$ at room temperature. The peak positions are reported with positive shifts in ppm, downfield of external H_3PO_4. FT-IR spectra were recorded on a Bio-Rad Spectrophotometer 175C. The reaction products were identified using GCMS, (Agilent GC 6890N with 5973 mass

selective detector instrument). Analysis of rhodium leaching to the organic phase was performed using Perkin-Elmer 1200 inductively coupled plasma with atomic emission spectra (ICP-AES), or GFAAS, [Graphite Furnace Atomic Absorption Spectrophotometer, (GBC Avanta Sigma Instruments, Australia, with photomultiplier tube (PMT) as the detector)].

The quantitative analysis of the olefins and hydroformylation products was carried out by an external standard method using a gas chromatographic technique. For this purpose, analysis was done over an HP-5 capillary column (30 M × 320 μm × 0.25 μm film thickness with a stationary phase of phenyl methyl siloxane) using HP 6890 gas chromatograph controlled by the HP Chemstation software and equipped with an auto sampler unit. Authentic standards were prepared in the range of concentrations of the reactants and products studied, and a calibration table was constructed for the quantification. The percentage conversion of olefin, selectivities to aldehyde, turn over number (TON) and turnover frequency (TOF h^{-1}) were calculated using the formulae given in Chapter 2 (section 2.2.5). The rate of the reaction was calculated by using Eq. 3.12. The standard GC conditions for the analysis of products are given in Table 3.1. Complete mass balance of the liquid phase components were thus obtained from the quantitative GC analysis. The observed syngas absorption was found to match with the products formed within ~ 5 % error. Thus, the complete mass balance of liquid and gases was established.

Table 3.1: Conditions for GC analysis

Injector (split) temperature	250ºC		
Flame ionization detector temperature	250ºC		
Inlet flow – total (He)	45.8 ml/min		
Split ratio for injector	50:1		
Column temperature	Rate (ºC /min)	T (ºC)	Hold time (min)
		70	1
	5	100	2
	10	180	2
	15	240	2
Column pressure	Rate (psi/min)	Pressure (Psi)	Hold time (min)
		5	23

A typical gas chromatograph showing the solvent toluene, decene, NMP cosolvent, and hydroformylation product undecanal and 2-methyl decanal under the conditions of GC analysis (Table 3.1) is shown in Figure 3.3.

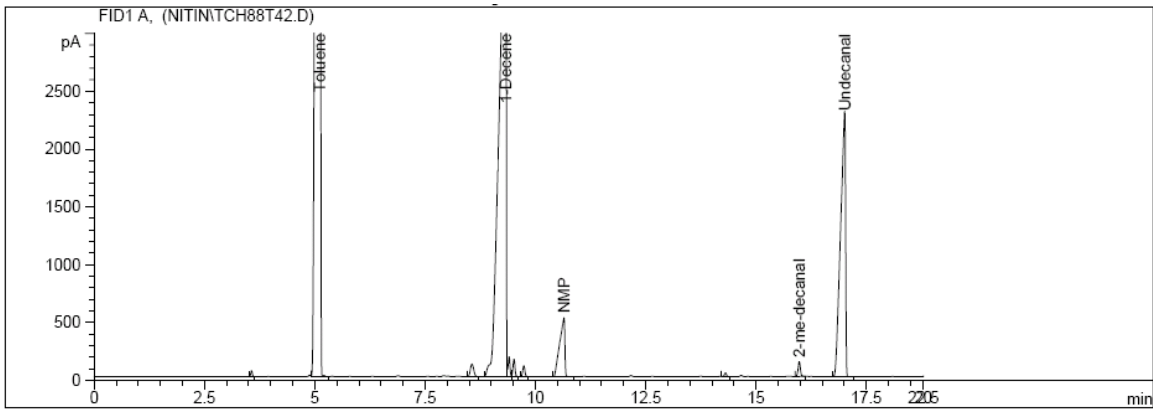

Figure 3.3: A GC chart of hydroformylation of 1-decene

3.3 Results and discussion

The objective of this work was to develop a biphasic catalytic system using the bidentate sulfoxantphos ligand for the hydroformylation of higher olefins. The activity of Rh-sulfoxantphos catalyst was screened for hydroformylation of various higher olefins in a water-toluene biphasic medium. Following this, the role of cosolvent in enhancing the rates of reaction was assessed for the hydroformylation of 1-decene. A detailed investigation on the effect of reaction parameters followed by kinetic study of hydroformylation of 1-decene was conducted using the water soluble $Rh(CO)_2(acac)$/ sulfoxantphos catalyst in presence of NMP as a cosolvent, in a water toluene biphasic medium in the temperature range of 383-403 K. The results are discussed in the following sections.

3.3.1Preliminary experiments

3.3.1.1 Hydroformylation of 1-decene using homogeneous (Xantphos)HRhCO(PPh_3)

The rhodium complexes of chelating diphosphine ligands such as Xantphos give exceptionally high regioselectivities to the linear aldehyde in the hydroformylation of olefins[19]. Preliminary experiments were conducted to standardize the reaction of

hydroformylation of 1-decene using Rh-Xantphos complexes in homogeneous toluene medium (Scheme 3.2). The main objective for studying the homogeneous reaction was for comparison of results with the biphasic reaction, (studied in the subsequent section).

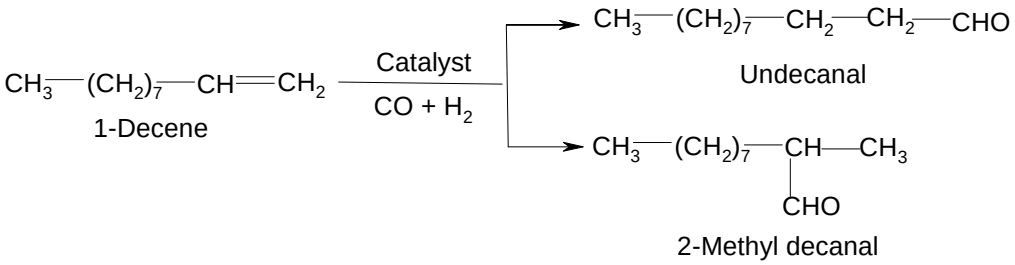

Scheme 3.2: Hydroformylation of 1-decene

The hydroformylation of 1-decene was carried out using both (i) the preformed (Xantphos)HRhCO(PPh_3) complex and (ii) the $Rh(CO)_2$(acac) precursor alongwith Xantphos ligand which also forms the similar active species insitu (Table 3.2).

Table 3.2: Hydroformylation of 1-decene in toluene medium

Run no	Catalyst	Conv-ersion (%)	Aldehyde selectivity (%)	Iso. olefin (%)	n/i ratio	TOF (h^{-1})	Time (h.)
1	(Xantphos)HRhCO (PPh_3)	97.3	95.5	4.5	39.7	33	10.8
2	$Rh(CO)_2$(acac)/ Xantphos	91.3	92.5	7.5	41.1	34	9.3

Reaction conditions (Run 1): *1-decene: 0.35 kmol/m^3, (Xantphos)HRhCO(PPh_3): 3.5 ×10^{-4} kmol/m^3, Xantphos:1.399 ×10^{-3} kmol/m^3 (Rh:L=1:4), T: 353K, P_{CO+H2}: 4.14MPa, agitation speed: 16.6 Hz, solvent: toluene.* ***(Run 2):*** *$Rh(CO)_2$(acac): 1.29 ×10^{-3} kmol/m^3, Xantphos: 6.394 ×10^{-3} kmol/m^3 (Rh:L=1:5) rest of the conditions are similar to that of run 1.*

The results in Table 3.2 show that both the Rh-Xantphos catalysts hydroformylate 1-decene with very high regioselectivity to the linear aldehyde (> 98%). The n/i ratio obtained was around 40 but the activity of the catalyst was poor (TOF = 34 h^{-1}) as compared to the $HRhCO(PPh_3)_3$ catalyst. The major product formed was the linear aldehyde, undecanal. A little amount of the 2-methyl decanal and isomerized olefin such as 2-decene and 3-decene (1-5%) was also observed. No other aldehyde products

formed by hydroformylation of isomerized decene were observed. The Rh-Xantphos catalyst suppresses isomerization of the terminal olefin to the internal olefin, which is a prominent side reaction in case of Rh-PPh_3 catalyst system and also gives high n/i ratio unlike the Rh-PPh_3 system which generally gives poor n/i ratio (0.5-0.7 for 1-decene).

3.3.1.2 Hydroformylation of higher olefins in aqueous biphasic system using Rh-sulfoxantphos catalyst

Hydroformylation of higher olefins using $Rh(CO)_2$(acac)/sulfoxantphos catalyst in a toluene-water biphasic system was studied at 393K. The complex $Rh(CO)_2$(acac) is highly insoluble in water, however, under syngas atmosphere and in presence of the chelating bidentate ligand sulfoxantphos, displacement of the acac ligand affords a new complex-(sulfoxantphos)$HRh(CO)_2$ which is highly soluble in water. Toluene was selected as the organic solvent mainly because of the ease of separation, low volatility, non-reacting, non-toxic nature and low solubility in water. The results on the hydroformylation of 1-hexene, 1-octene, 1-decene and 1-dodecene are shown in Table 3.3.

Table 3.3: Hydroformylation of higher olefins in aqueous biphasic system using Rh-sulfoxantphos catalyst

Sr. no	olefin	Conversion (%)	Aldehyde selectivity (%)	Iso. olefin (%)	n/i	TOF (h^{-1})
1	1-hexene	55.3	95.5	4.5	27.8	13.7
2	1-octene	13.4	98.1	1.9	28.3	2.8
3	1-decene	7.5	98.2	1.8	31.2	0.8
4	1-dodecene	2.9	98.4	1.6	34.8	0.2

Reaction conditions: *olefin: 1.07 kmol/$m^3_{(org.)}$, $Rh(CO)_2$(acac): 3.85 $\times 10^{-3}$ kmol/$m^3_{(aq.)}$, Sulfoxantphos:1.93 $\times 10^{-2}$ kmol/$m^3_{(aq.)}$ (Rh:L=1:5), T: 393K, P_{CO+H2}: 4.14 MPa, agitation speed: 20 Hz, solvent: toluene and water ε = 0.4, time: 24 h. total volume: 2.5 $\times 10^{-5}$ m^3*

The results show that the conversion of olefin and activity of the catalyst decreases sharply with increasing chain length of olefin. This observation is attributed to the poor solubility of the substrates in the aqueous catalyst phase, which reduces

drastically with increasing chain length of olefin. The major product formed was the linear aldehyde. A little, amount of the 2-methyl substituted aldehydes and isomerized olefins (1-5%) were also observed. Formation of other aldehyde products (by hydroformylation of isomerized internal olefins) was not observed. The rate of olefin isomerization also reduces with increasing chain length for this particular catalyst system. An interesting observation is the increase in the n/i ratio with increase in chain length of olefin, which is contradictory to the reaction in homogeneous medium using $HRhCO(PPh_3)_3$ catalyst. The comparison of the homogeneous reaction for 1-decene hydroformylation (see Table 3.2) with the biphasic reaction shows that the conversion and activity of biphasic reaction are very much low as compared to the reaction in homogeneous medium. Similarly, the linear to branched aldehyde ratio (n/i=31.2) for the hydroformylation of 1-decene in the aqueous biphasic medium is lower than that obtained for the reaction in homogeneous toluene medium (n/i= 41.1) in presence of Rh-Xantphos catalyst.

3.3.1.3 Origin of regioselectivity in hydroformylation using Rhodium-diphosphine complexes

The effect of diphosphines on selectivity in rhodium catalyzed hydroformylation has been studied by Hughes and Unruh[20]. They have observed that rhodium complexes formed from the reaction of $HRhCO(PPh_3)_3$ with various rigid chelating diphosphines such as dppe, dppp, dppb etc. led to increased linear to branched ratios when the ligand to rhodium ratio was 1.5 or higher. Initially, they proposed that the two monomeric rhodium species **3** and **4** (Figure 3.4) could be responsible for the increase in linear to branched ratio. In addition to monomeric species, a dimeric rhodium species **5**, (in which two ligands are chelating to one rhodium center) while one ligand is bridging between two rhodium centers is also suspected to enhance selectivity. These complexes were later actually observed by ^{31}P NMR[21]. The dimeric species **5** can produce the monomeric species **4** reversibly in presence of excess ligand. They have concluded that the high selectivity to the linear aldehyde could be due to the species having three phosphine ligands coordinated to Rh, at the step in the mechanism where Rh-H addition to coordinated olefin occurs i.e. (selectivity determining step).

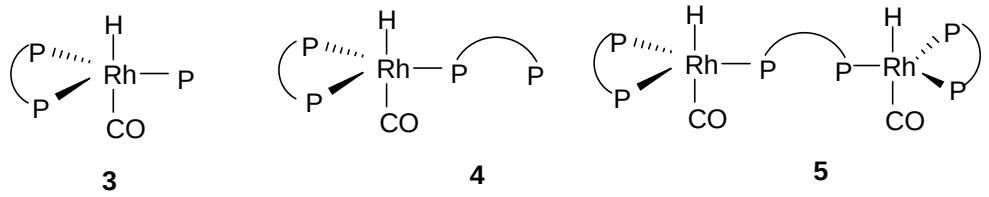

Figure 3.4: Rh-diphosphine complexes proposed by Hughes's[20]

An important study by Casey and co-workers[22] has indicated that the bite angle of bidentate diphosphines can have a dramatic influence on the regioselectivity of the rhodium-catalyzed hydroformylation of 1-alkenes. The ligands with smaller bite angles show a purely axial equatorial (ae) coordination which resulted in lower n/i ratio like those observed for monophosphines. For the bis-equatorially (ee) coordinated 2,2'-bis-((dipheny1phosphino)methyl)-1,l'-biphenyl (BISBI); a linear to branched aldehyde ratio as high as 66:l was reported, while the equatorially-axially coordinating (i.e. P-Rh-P = 90º) 1,2- is(diphenylphosphino)ethane (dppe) gave a linear to branched ratio of only 2.1. The observed selectivity is likely to be due to the bite angles of the ligands. When the bite angle of the diphosphine is changed with large increments from 78º(dppe) to 107º(trans-dppm-cyp), to 112 º (BISBI or Xantphos) higher n/i ratios were observed. The very high selectivity of Xantphos (calculated natural bite angle 111.7º) and BISBI (calculated natural bite angle 122.6º) indicates that the optimum bite angle in the range of 112- 120º is required, to achieve high n/i ratios. Selectivity in the hydroformylation reaction increases when the bite angle of the ligand becomes larger. The results obtained with these ligands revealed a regular increase of selectivity with an increasing bite angle, up to the point where the calculated bite angle has increased to such an extent that chelation is no longer possible.

The rigidity of the ligand backbone is also essential for obtaining high selectivity in the hydroformylation reaction, a fact explained by comparing the results obtained with BISBI ligand[19]. The rigidity of the ligands causes the chelated complexes to be stable, even at elevated temperatures. The more flexible BISBI ligand therefore shows lower aldehyde selectivity at elevated temperature (going from 40 to 80ºC selectivity drops substantially from 95.5 to 89.6% for hydroformylation of 1-octene). But for Xantphos ligand (due to the rigid structure), the selectivity was not lost even at higher temperatures

and the turnover frequency could be increased with temperature as the aldehyde selectivity is maintained (selectivity drops marginally from 98.3 to 97.7% when temperature is increased from 40 to 80ºC). This shows that the ligand rigidity becomes even more important at higher temperature. The Xantphos ligand has been shown to induce the highest selectivity reported so far for the formation of linear aldehydes with diphosphines in rhodium-catalyzed hydroformylation[19].

In order to investigate the coordination behavior of a series of Xantphos type ligands, the detailed spectroscopic study was reported by van Leeuwen and coworkers[6]. The ^{31}P NMR spectra led to the conclusion that the two phosphine moieties of the diphosphine in the complex were equivalent for all diphosphines. The coupling constants between the diphosphine phosphorous and PPh_3 show that these ligands are indeed coordinated bisequatorially. Bubbling of CO through a solution of (diphosphine)Rh(H)(CO)(PPh_3) (**7**) led to facile displacement of the PPh_3. The complex (diphosphine)Rh(H)$(CO)_2$ (**6**) formed by this exchange (presumably the catalytically active species in the hydroformylation reaction (Figure 3.5)) is stable under an atmosphere of CO. The ^{31}P NMR spectra of these compounds exhibit a clean doublet for the diphosphine, indicating that these ligands are also coordinated in a 'bis-equatorial fashion in these complexes (**6)**. The ^{1}H NMR spectra of the (Xantphos)Rh(H)(CO)(PPh_3) and (Xantphos)RhH$(CO)_2$ complexes show an inequivalence of the two methyl groups (on Xantphos), indicating a rigid conformation of the ligand (originating from the rigid xanthene backbone).

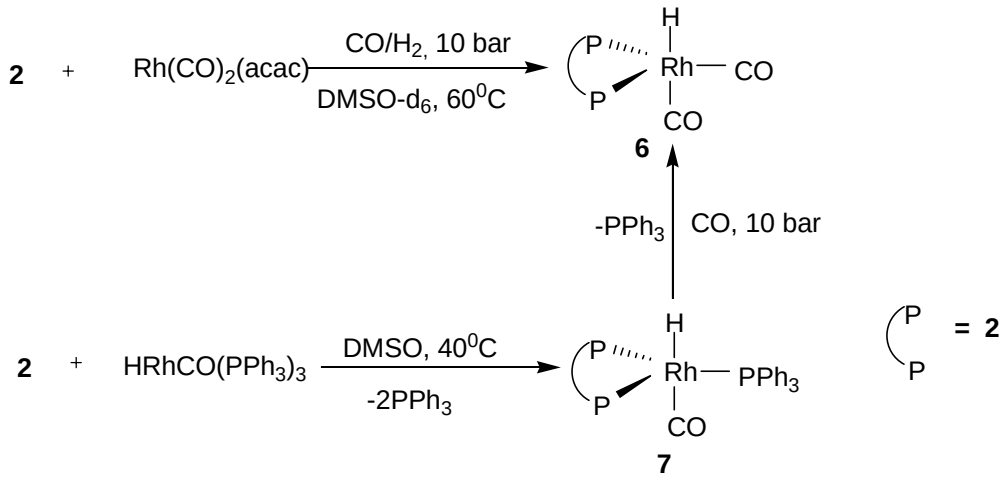

Figure 3.5: Active species in the hydroformylation reaction using sulfoxantphos ligand

3.3.1.4 Effect of cosolvent

One of the major limitations of aqueous phase catalysts is the poor rate of reaction obtained, especially for higher olefins. Several approaches have been proposed to enhance the reaction rates in biphasic medium as discussed earlier (Chapter 1, section 1.5.1.4). It has been reported that the addition of cosolvent to the biphasic system improves the solubility of higher olefins in the aqueous phase retaining the biphasic nature of the system[15]. Cosolvents like ethanol, methanol, acetonitrile, acetone, ethylene glycol and NMP have been found to enhance the rate several times in the hydroformylation of linear higher olefin using Rh-TPPTS catalyst[16]. Hence the effect of the cosolvent in enhancing the rates for our system was checked.

In the present work, hydroformylation of 1-decene was studied in the presence of several co-solvents such as ethanol, 1,4-dioxane, methyl ethyl ketone (MEK) and N-methylpyrrolidone-2 (NMP), and the results are shown in Figure 3.6.

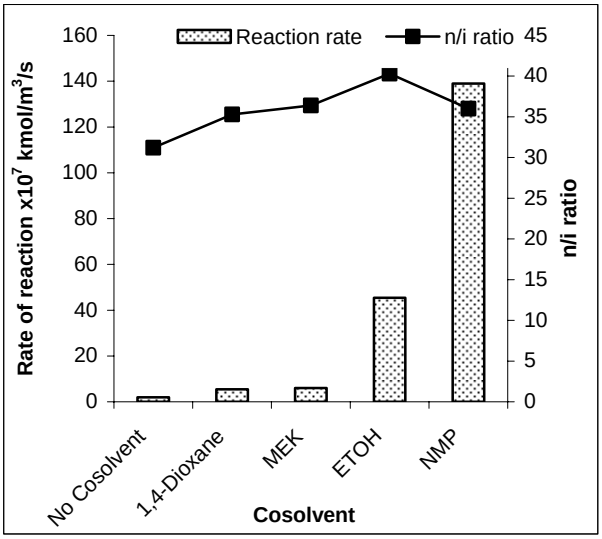

Figure-3.6: Effect of cosolvent on rate and n/i ratio in biphasic hydroformylation of 1-decene.

Reaction conditions: *1-decene: 1.07 kmol/m^3 $_{(org.)}$, $Rh(CO)_2(acac)$: 3.85 ×10^{-3} kmol/m^3 $_{(aq.)}$, sulfoxantphos: 1.93 ×10^{-2} kmol/$m^3_{(aq.)}$ (Rh:L=1:5), T: 393K, P_{CO+H2}: 4.14 MPa, agitation speed: 20 Hz, solvent: toluene-water-cosolvent, time: 8 h. total volume: 2.5 × 10^{-5} m^3*

Several fold rate enhancement was observed, depending on the cosolvent employed. The rates were improved marginally in 1, 4-dioxane, and MEK, whereas

drastic enhancement of rates were observed when ethanol and NMP were used as cosolvents. The highest activity was observed using NMP as cosolvent. No side products like isomerization or condensation product were observed.

One more interesting observation is that the regioselectivity to the undecanal was also improved in the presence of all the cosolvents studied, as compared to the reaction in biphasic medium (n/i increased from 31.2 to 40.3 using ethanol as a cosolvent). The presence of cosolvents in water enhances the solubility of substrate in aqueous catalyst phase and thereby increases the rates. In case of ethanol a 13 times rates enhancement was observed with n/i ratio of 40, however, acetal formation (by condensation of aldehyde and ethanol) was observed to a small extent (<5%). From the results in Figure 3.6, NMP was found to be the best cosolvent as it achieved very high rate enhancement and no side products were formed (rate enhancement 38 times over biphasic system). The only products formed were undecanal and 2-methyldecanal with a little isomerized decene (1.5%). The ICP analysis shows negligible leaching (0.05 ppm) of the rhodium to the organic phase. Further detailed study has been carried out using NMP as cosolvent.

3.3.1.5 Effect of NMP concentration

To achieve the optimum ratio of the water-cosolvent, the effect of percent NMP content (as a cosolvent) in the aqueous medium has been studied at 393 K for the hydroformylation of 1-decene using $Rh(CO)_2(acac)$/sulfoxantphos catalyst in the water-toluene biphasic medium. The reactions were carried out varying the NMP composition in the aqueous phase from 0-40% (v/v). The results are presented in Figure 3.7. The rate varies linearly with increasing NMP composition in the aqueous phase. The maximum rates were observed at water-NMP composition of 60:40 but simultaneously the n/i ratio reduces from 35.9 to 32.7. Therefore, the optimum ratio of water-NMP of 70:30 was chosen for further studies in order to maintain the advantage of high regioselectivity for the linear aldehyde, and high activity.

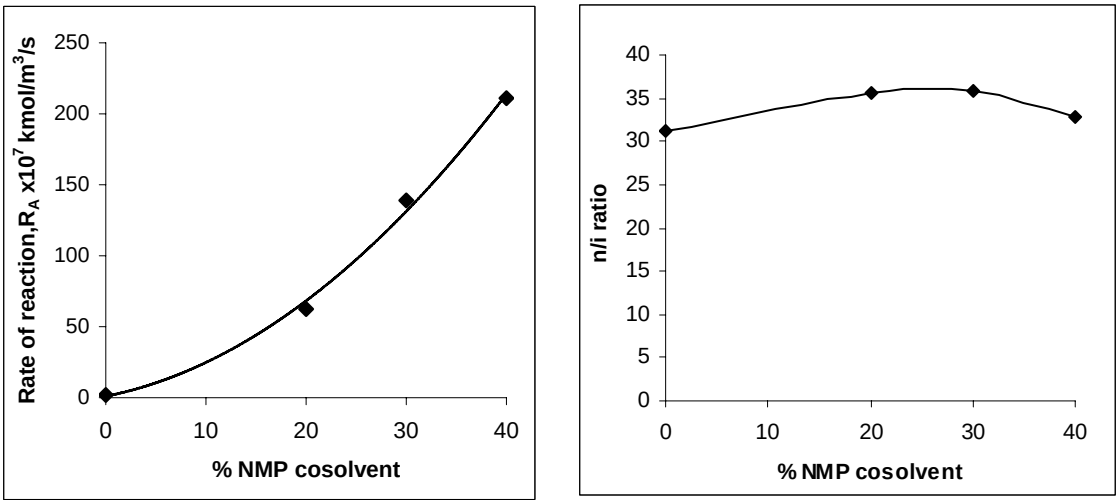

Figure-3.7: Effect of % NMP cosolvent on rate and n/i ratio in biphasic hydroformylation of 1-decene.

Reaction conditions : *1-decene:1.07 kmol/$m^3_{(org.)}$, $Rh(CO)_2(acac)$: 3.85 × 10^{-3} kmol/$m^3_{(aq.)}$, sulfoxantphos: 1.93 ×10^{-2} kmol/$m^3_{(aq.)}$ (Rh:L=1:5), T: 393K, P_{CO+H2}: 4.14 MPa, agitation speed: 20 Hz, solvent: toluene (1.2 ×10^{-5} m^3) water(0.7 ×10^{-5} m^3) and NMP(0.3 ×10^{-5} m^3), time: 8 h, total volume: 2.5 ×10^{-5} m^3*

3.3.1.6 Catalyst recycles study

The activity of the $Rh(CO)_2(acac)$/sulfoxantphos catalyst on recycle was also investigated in presence of NMP as cosolvent (30% v/v aqueous phase) at 393K. The recycle experiments were performed by separating the aqueous catalyst phase from the organic phase at the end of reaction, followed by addition of fresh organic phase alongwith 1-decene to the used aqueous catalyst phase. The results are presented in Figure 3.8. The aqueous catalytic phase was recycled for four times without a drop in activity and selectivity. An interesting observation was the improvement in the activity for the first recycle over the virgin reaction. This enhanced activity then remains constant for all the subsequent recycles. The enhancement of activity compared to the virgin reaction is due to the fact that the active catalyst species is available for reaction on recycle. The n/i ratio also remains more or less constant on recycle. The ICP analysis of the organic phase from each recycle shows negligible leaching (0.06, 0.03, 0.05, 0.08, 0.04 ppm respectively) of the rhodium to the organic phase. The recycle of the organic phase separated after the reaction with addition of fresh 1-decene, also does not show

hydroformylation activity, which indicates that the activity observed is solely due to the aqueous phase catalyst.

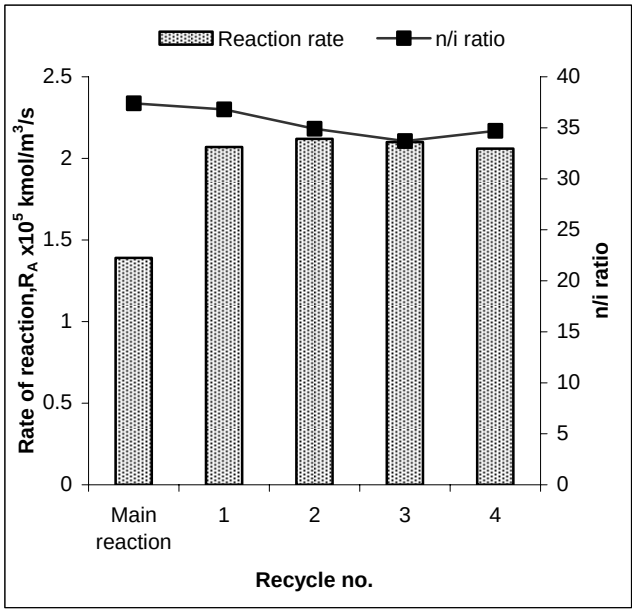

Figure-3.8: Effect of catalyst phase recycles study on reaction rate and n/i ratio.

Reaction conditions: *1-decene:1.07 kmol/$m^3_{(org.)}$, $Rh(CO)_2(acac)$: 3.85 ×10^{-3} kmol/$m^3_{(aq.)}$, sulfoxantphos:1.93 ×10^{-2} kmol/$m^3_{(aq.)}$ (Rh:L=1:5), T: 393K, P_{CO+H2}: 4.14 MPa, agitation speed: 20 Hz, solvent: toluene (1.2 ×10^{-5} m^3), water (0.7 ×10^{-5} m^3) and NMP (0.3 ×10^{-5} m^3) time: 8 h, total volume: 2.5 ×10^{-5} m^3.*

3.3.1.7 Effect of temperature

The effect of temperature on hydroformylation of 1-decene has been investigated in a temperature range of 383-403K at a $Rh(CO)_2(acac)$: 2.89 × 10^{-3} kmol/m^3, sulfoxantphos: 1.44 × 10^{-2} kmol/m^3, 1-decene: 1.07 kmol/m^3 and P_{CO+H2} =4.14 MPa. The results are shown in Figure 3.9. The rate varies linearly with temperature while the aldehyde selectivity is retained (> 97%). It was reported in literature[19] that in case of the chelating BISBI ligand the aldehyde selectivity decreases as the temperature increases due to the flexibility of BISBI backbone, which results in monodentate binding at elevated temperatures. But the rigidity of the Xantphos structure (originating from the rigid xanthene backbone) does not allow monodentate binding to the metal center in the reaction cycle and maintains its bidentate nature even at higher temperature and thus the selectivity to aldehyde is retained. The n/i ratio decreases from 37.5 to 31.3 with increase

in temperature due to the increase in the formation of 2-methyl decanal at higher temperature.

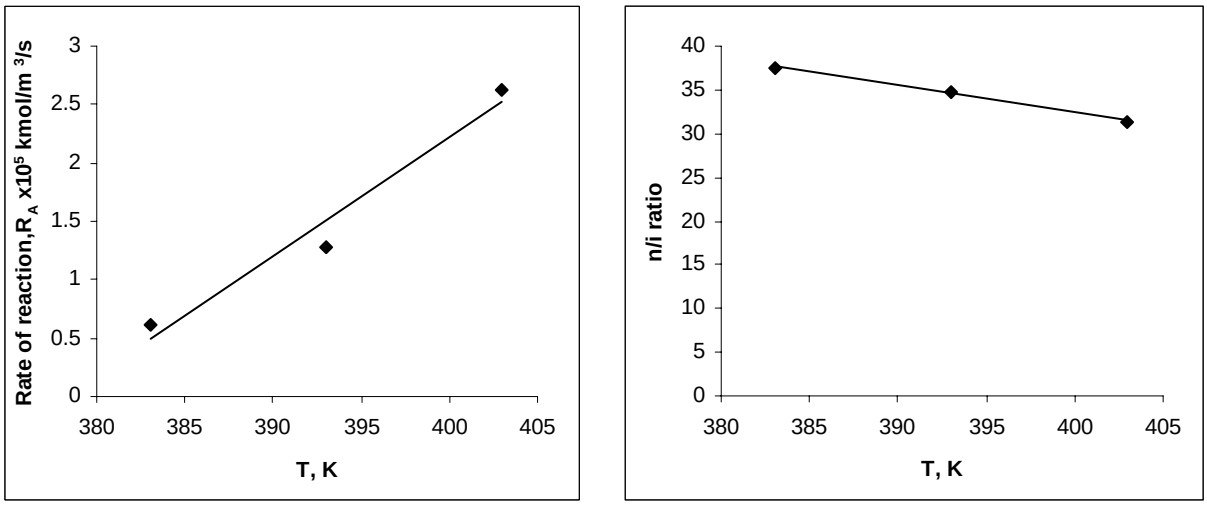

Figure-3.9: Effect of reaction temperature on rate and n/i ratio in the biphasic hydroformylation of 1-decene.

Reaction conditions: *1-decene: 1.07 kmol/m^3 $_{(org.)}$, $Rh(CO)_2(acac)$: 2.89 ×10^{-3} kmol/$m^3_{(aq.)}$, sulfoxantphos: 1.44 ×10^{-2} $_{(aq.)}$ kmol/m^3 (Rh:L=1:5), T: 383-403K, P_{CO+H2}: 4.14 MPa, total volume: 2.5 ×10^{-5} m^3, agitation speed: 20 Hz, solvent: toluene: water: NMP*

3.3.1.8 Screening of higher olefins hydroformylation in presence of NMP cosolvent

As discussed earlier, a dramatic rate enhancement was observed in aqueous biphasic hydroformylation of 1-decene in presence of NMP as cosolvent. The influence of the NMP cosolvent has also been studied on the hydroformylation of higher olefins using Rh-sulfoxantphos catalyst in aqueous biphasic medium. The results in Figure 3.10 show a several fold enhancement in rate for all higher olefins studied. The rate improvement for 1-hexene (4 fold), 1-octene (15 fold), 1-decene (38 fold) and 1-dodecene (96 fold) shows that the magnitude of rate enhancement is higher for the higher homologues like 1-decene and dodecene where the development of biphasic catalysis always remains a challenge. The presence of NMP enhances the solubility of the olefins in the aqueous phase leading to enhancement of rate. The n/i ratio also improved for 1-hexene (26 to 32.4), 1-octene (28.2 to 35.6), 1-decene (31.2 to 35.9) and 1-dodecene (32 to 36.8) compared to the reaction in aqueous biphasic medium, in absence of cosolvent.

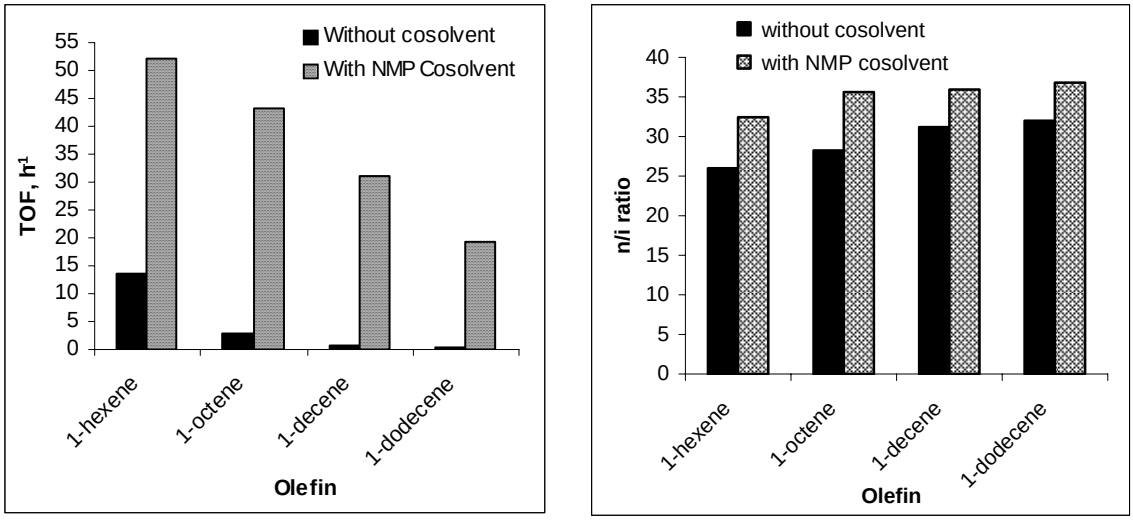

Figure 3.10: Comparison of rates and n/i ratio on hydroformylation of higher olefins in biphasic reaction with and without cosolvent.

Reaction conditions : *olefin :1.07 kmol/$m^3_{(org.)}$, $Rh(CO)_2(acac)$: 3.85 ×10^{-3} kmol/$m^3_{(aq.)}$, sulfoxantphos:1.93 ×10^{-2} kmol/$m^3_{(aq.)}$ (Rh:L=1:5), T: 393K, P_{CO+H2}: 4.14 MPa, agitation speed:20 Hz, solvent: toluene (1.2 ×10^{-5} m^3), water(0.7 ×10^{-5} m^3) and NMP (0.3 ×10^{-5} m^3), time: 8 h., total volume: 2.5 ×10^{-5} m^3*

3.4 Kinetics of hydroformylation of 1-decene using $Rh(CO)_2(acac)$/sulfoxantphos catalyst in water-toluene biphasic medium using NMP as cosolvent

$Rh(CO)_2(acac)$/sulfoxantphos catalyst was found to be active for the hydroformylation of higher olefins in presence of cosolvent in aqueous biphasic medium. This catalyst gives very high n/i ratios and hence investigation on the hydroformylation of 1-decene as a model substrate, using $Rh(CO)_2(acac)$/sulfoxantphos catalyst in a water toluene biphasic medium using NMP as cosolvent, were conducted. This catalyst/solvent system has the potential for further application in higher olefins hydroformylation and hence, such a study with 1-decene as a model substrate would be extremely important for reactor modeling purpose. Moreover no kinetic studies using the $Rh(CO)_2(acac)$/sulfoxantphos catalyst have been reported so far.

The effect of concentration of different parameters such as catalyst, 1-decene, sulfoxantphos, and hydrogen and carbon monoxide partial pressures on the initial rate of hydroformylation has been studied. The detailed investigation on mass transfer effects in aqueous-biphasic system is presented. A suitable rate equation has also been proposed

after rigorous model discrimination. The different kinetic parameters and the activation energy were also evaluated.

Prior to conducting the experiments to observe kinetic data, preliminary experiments were conducted to check the material balance and reproducibility of the experiments. For this purpose, a few experiments were carried out in which the amount of 1-decene consumed, products formed, and $CO+H_2$ consumed were compared for experiments at high conversion of 1-decene (>90%). A typical concentration time profile of the reaction is shown in Figure 3.11. It was observed that the product profile and selectivity is unchanged even at higher temperature. The rate of isomerisation of linear olefin to internal olefins is negligible. The major product formed is undecanal, alongwith 2-methyldecanal in minor quantity.

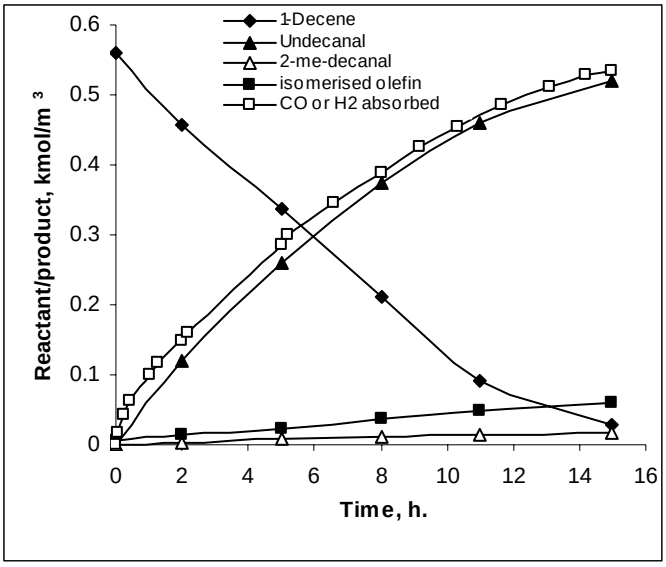

Figure 3.11: A typical Concentration-Time profile.

Reaction conditions: *1-decene: 1.07 kmol/$m^3_{(org.)}$, $Rh(CO)_2(acac)$: 3.85 ×10^{-3} kmol/$m^3_{(aq.)}$, sulfoxantphos: 1.93 ×10^{-2} kmol/$m^3_{(aq.)}$ (Rh:L=1:5), T: 393K, P_{CO+H2}: 4.14MPa, agitation speed: 20 Hz, solvent: toluene(1.2 ×10^{-5} m^3) water(0.7 ×10^{-5} m^3) and NMP (0.3 ×10^{-5} m^3), time: 15 h, total volume: 2.5 ×10^{-5} m^3.*

3.4.1. Solubility Data

For kinetic study, a knowledge of the solubility of H_2 and CO in organic and aqueous phases as well as in water-NMP mixture is required. The solubility of CO and H_2 in toluene, water and water-NMP (70:30 v/v) mixtures has been determined

experimentally in the temperature range of 383-403 K, by the procedure described by Chaudhari and coworkers[23]. The solubility of H_2 and CO was measured in a 5×10^{-5} m^3 capacity stirred autoclave designed for 13.5 MPa pressure. The experimental procedure used for the measurement of solubility and the formulae used for the calculation of Henrys constant were similar to that described in Chapter 2 (sections 2.3.5.2).

The plot of Henry's constant obtained for H_2 and CO in toluene, water and water-NMP mixtures (70:30 v/v) at various temperatures are presented in Figure 3.12, 3.13 and 3.14 respectively.

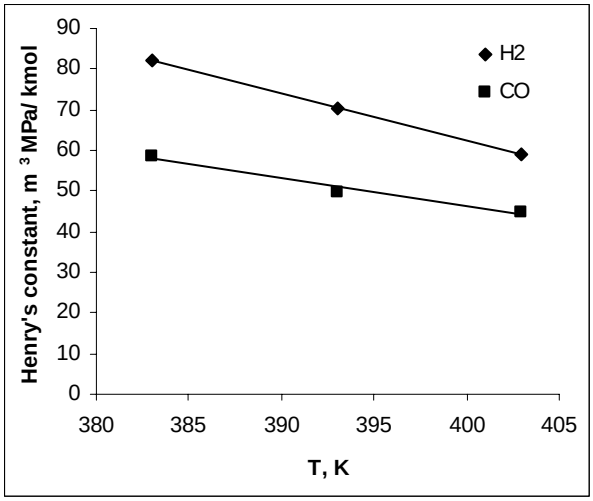

Figure 3.12: Henrys constant for H_2 (H_A) and CO (H_B) in toluene

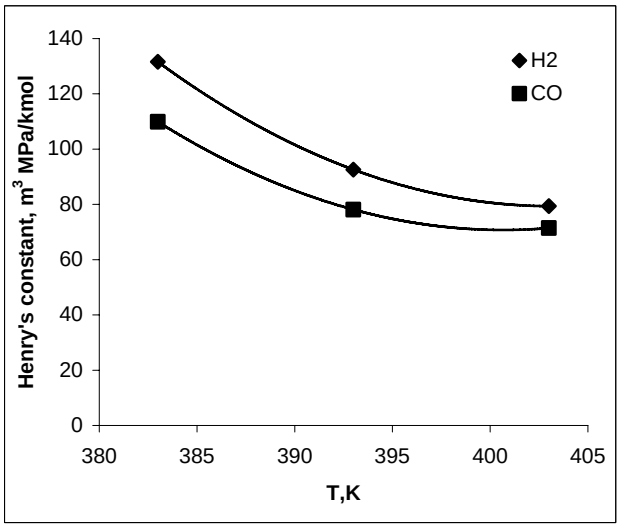

Figure 3.13: Henrys constant for H_2 (H_A) and CO (H_B) in water

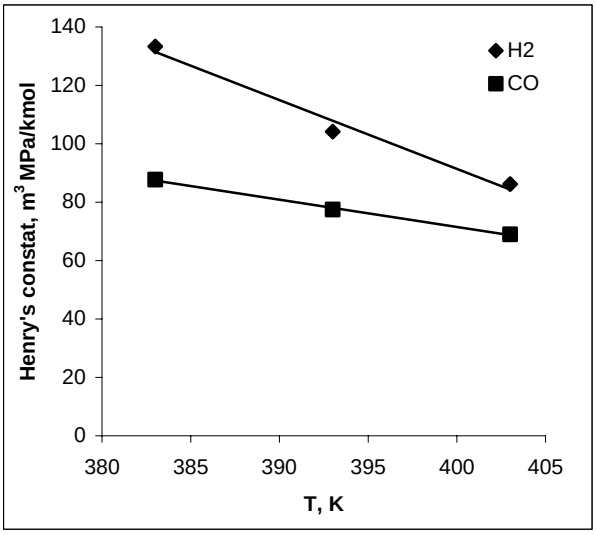

Figure 3.14: Henrys constant for H_2 (H_A) and CO (H_B) in water-NMP mixture (70:30 v/v)

The values of Henrys constant for H_2 and CO in toluene, water and water- NMP mixtures (70:30 v/v) are tabulated in Table 3.4.

Table 3.4: Henrys constant for H_2 (H_A) and CO (H_B) in Toluene, water and water-NMP mixture (70:30 v/v)

Solvent	383 K		393 K		403 K	
	H_A MPa m^3 /kmol	H_B MPa m^3 /kmol	H_A MPa m^3 /kmol	H_B MPa m^3 /kmol	H_A MPa m^3 /kmol	H_B MPa m^3 /kmol
Toluene	81.96	58.47	70.42	49.75	58.82	44.84
water	131.57	109.89	92.59	78.12	79.36	71.42
Water-NMP mixture (70:30 v/v)	133.33	87.71	104.16	77.52	86.20	68.96

The solubility of 1-decene in the aqueous phase was determined experimentally. The experimental data for liquid-liquid equilibrium for 1-decene in toluene- (water-NMP)

mixture at 393K is shown in Table 3.5. It was also observed that temperature had only a marginal effect on the solubility of 1-decene in the aqueous phase.

Table-3.5: Liquid-Liquid equilibrium data for 1-decene-(water-NMP)-toluene system

T, K	1-decene concentration (org) in organic phase, kmol/m^3	1-decene concentration (aq.) in aqueous phase (water-NMP) × 10^3, kmol/m^3
393	1.058	1.25
403	1.058	1.34

The Henry's constants for hydrogen (H_A) and carbon monoxide (H_B) (given in Table-3.4) and the partition coefficients for 1-decene (given in Table-3.5) were used to evaluate concentrations of H_2 and CO and 1-decene in the aqueous phase, required for rate analysis.

3.4.2 Evaluation of Kinetic regime

3.4.2.1 Physical description of the biphasic system

Hydroformylation of 1-decene in a biphasic medium is a multiphase reaction since, it involves three phases (gas-liquid-liquid) containing two gaseous reactants H_2 and CO with 1-decene as a liquid reactant in the organic medium and the Rh-sulfoxantphos catalyst in the aqueous medium. The overall reaction rate depends on transport of H_2 and CO to the liquid phase, followed by transport of dissolved H_2, CO and 1-decene from organic phase to aqueous phase and reaction in the aqueous catalyst phase. A schematic of biphasic hydroformylation reaction is shown in Figure 3.15.

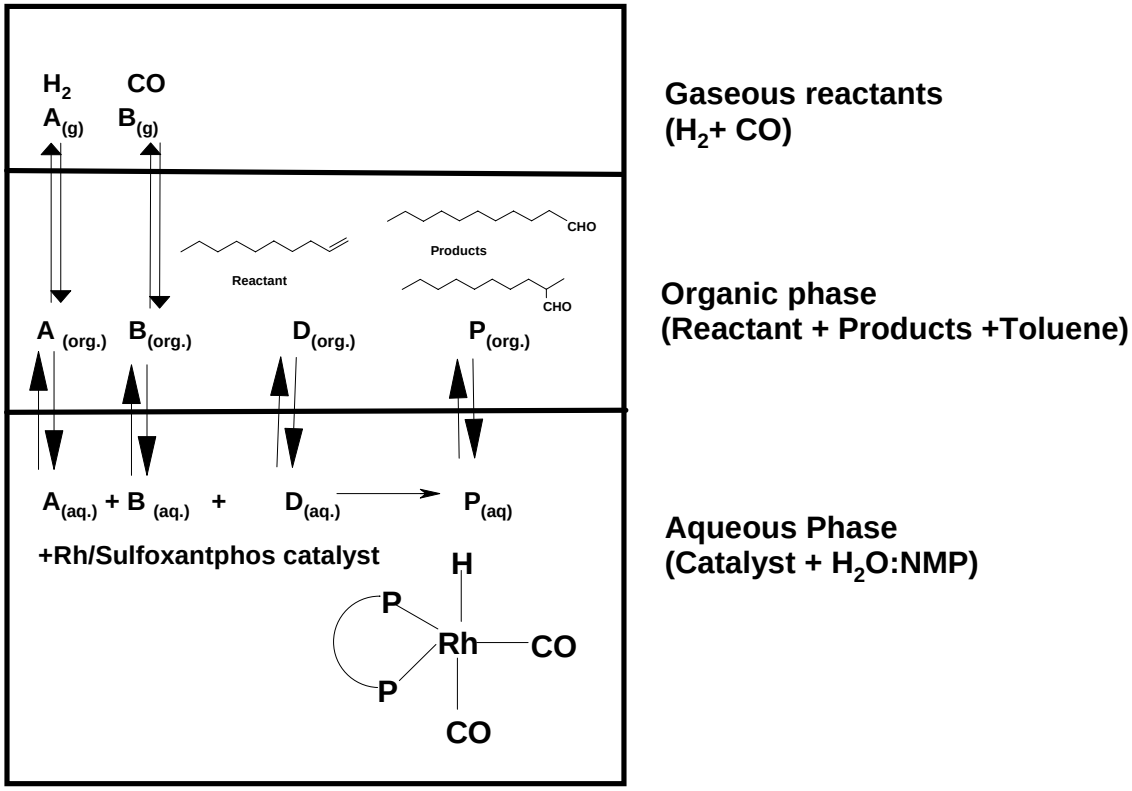

Figure 3.15: Schematic of biphasic hydroformylation of olefins

The factors affecting the rate behavior of gas-liquid-liquid catalytic reactions have been discussed by Chaudhari and coworkers[24]. The overall performance of such reactions would depend on a number of parameters such as reaction kinetics, gas-liquid and liquid-liquid mass transfer, solubility of gases in organic and aqueous phases, liquid-liquid equilibrium and the complex hydrodynamics of the dispersed liquid droplets. The various parameters/steps governing the rate of gas-liquid-liquid reactions are shown in Figure 3.16. In order to understand the rate behavior, detailed analysis of these phenomena with relevant experimental studies is necessary.

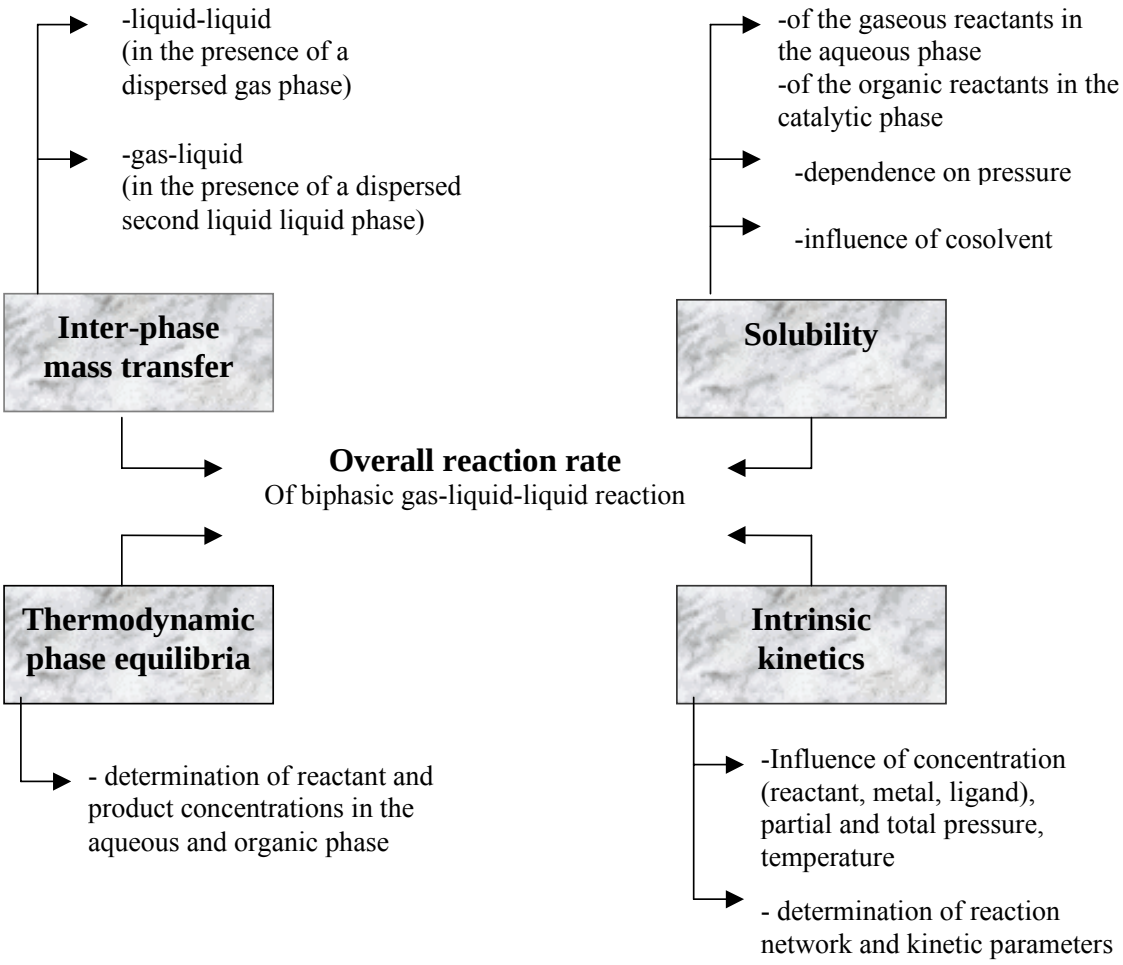

Figure 3.16: Parameters/steps in gas-liquid-liquid reactions[25]

3.4.2.2 Mass transfer effects in Gas-Liquid-Liquid (G-L-L) systems

For investigation of intrinsic kinetics of multiphase reactions, it is important to ensure that the rate data obtained are in the kinetic regime. A careful consideration must be given to the significance of mass transfer for kinetic analysis of a complex multiphase reaction involving gas-liquid-liquid system. For a gas-liquid-liquid reaction system, the overall rate would depend on the gas-liquid and liquid-liquid mass transfer and the intrinsic kinetics of the reaction in the aqueous phase.

3.4.2.3 Effect of agitation speed and aqueous phase hold up

A few experiments were carried out to investigate the effect of agitation speed and aqueous catalyst phase hold up on the rate of reaction. These experiments were important to understand the role of mass transfer and ensure that the reaction occurs in the kinetic regime. The following reaction conditions were used for carrying out experiments on the effect of the agitation speed: 1-decene: 1.071(org.) kmol/m^3, $Rh(CO)_2(acac)$: 5.13×10^{-3} kmol/m^3(aq.), sulfoxantphos(aq.): 2.56×10^{-2} kmol/m^3 , (Rh:L=1:5), T= 403K.

The effect of agitation speed on the rate of hydroformylation is shown in Figure 3.17. The rate was found to be independent of the agitation speed beyond 1000 rpm. This observation indicates that the mass transfer effects are not important above 1000 rpm. Therefore, all the reactions for kinetic study were carried out at an agitation speed of 1200 rpm to ensure that the reaction occurred in the kinetic regime.

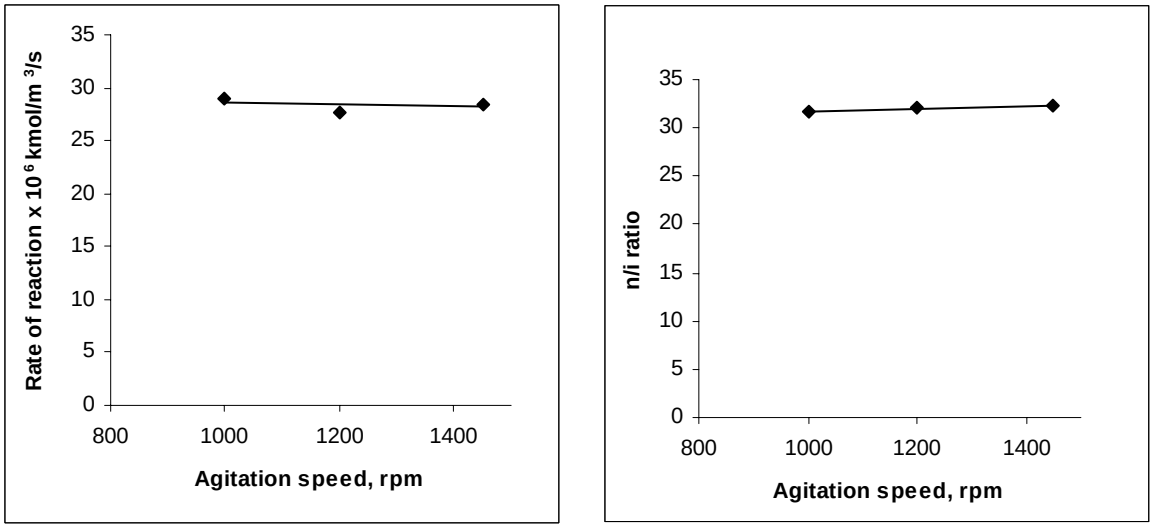

Figure-3.17: Effect of agitation speed on initial rate and n/i ratio in biphasic hydroformylation of 1-decene

Reaction conditions: *1-decene:1.07 kmol/$m^3_{(org.)}$, $Rh(CO)_2(acac)$: 5.13×10^{-3} kmol/$m^3_{(aq.)}$, sulfoxantphos: 2.56×10^{-2} kmol/$m^3_{(aq.)}$ (Rh:L=1:5), T: 403K, P_{CO+H2}: 4.14MPa, solvent: toluene (1.2×10^{-5} m^3) water (0.7×10^{-5} m^3) and NMP (0.3×10^{-5} m^3), time: 6 h, total volume: 2.5×10^{-5} m^3*

Figure 3.18 shows the effect of aqueous catalyst phase hold-up $(\varepsilon)_{aq.}$ on the rate of hydroformylation of 1-decene at 393K and agitation speed of 20 Hz. It was observed that the phase inversion takes place at aqueous phase hold up of about 0.5. For aqueous phase hold-up less than 0.5, the aqueous phase is the dispersed phase, as shown schematically in Figure 3.19 (a). In this case, the liquid-liquid interfacial area is determined by aqueous phase hold-up (ε). For aqueous phase hold-up greater than 0.5, the organic phase is the dispersed phase, as shown schematically in Figure 3.19 (b). In this case, the liquid-liquid interfacial area will be determined by the organic phase hold-up (1-ε).

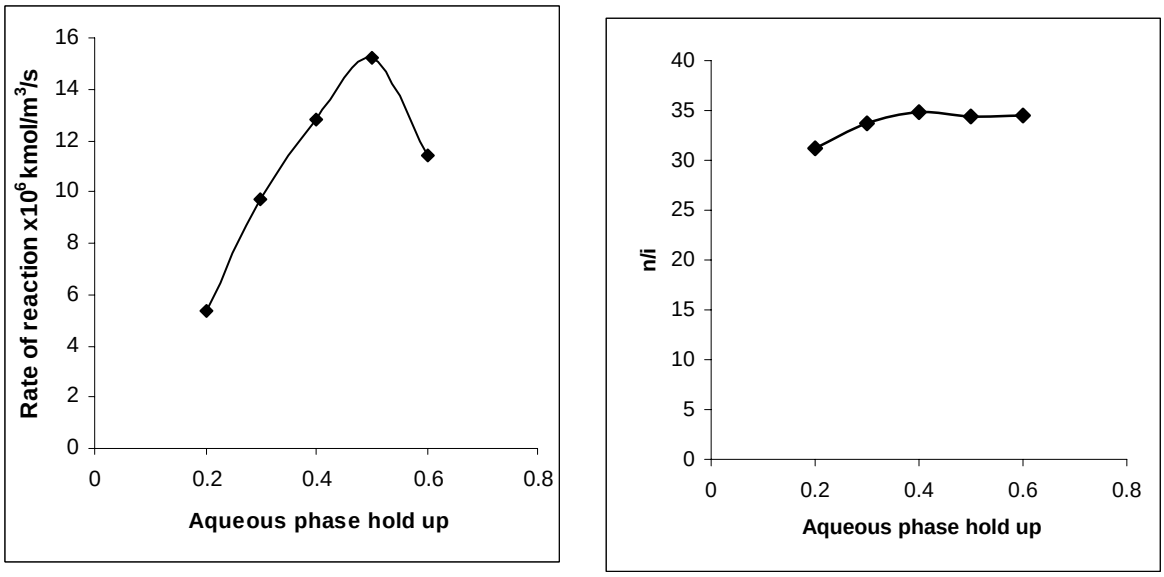

Figure-3.18: Effect of aqueous phase hold up on rate and n/i ratio in biphasic hydroformylation of 1-hexene.

Reaction conditions : *1-decene:1.07 kmol/$m^3_{(org.)}$, $Rh(CO)_2(acac)$: 3.85 ×10^{-3} kmol/$m^3_{(aq.)}$, sulfoxantphos:1.93 ×10^{-2} kmol/$m^3_{(aq.)}$ (Rh:L=1:5), T=393K, P_{CO+H2}: 4.14MPa, agitation speed: 20 Hz, solvent: toluene and water, time:9 h. total volume: 2.5 ×10^{-5} m^3*

At agitation speed of 1200 rpm (20 Hz), a plot of rate vs. aqueous (catalyst) phase hold-up (Figure 3.18) shows that the rate first increases with increase in aqueous phase hold up and then passes through a maximum. The regioselectivity to linear product is lesser at lower aqueous phase holdup and remains constant at $\varepsilon_{aq.}$=0.3-0.6. In kinetic

regime, the rate per unit volume of the aqueous phase is expected to remain constant with linear dependence on aqueous phase hold up. However, in the case where the reaction occurs essentially at liquid-liquid interface, it would depend on the liquid-liquid interfacial area, which is governed by both agitation speed and hold up of the dispersed phase. The results at aqueous phase hold up less than 0.5 indicate a kinetic regime. For higher aqueous phase hold up, the decreasing rate is a result of phase inversion with organic phase dispersed in continuous aqueous phase. In order to understand this effect a more detailed analysis of mass transfer in biphasic hydroformylation is necessary. For the purpose of kinetic studies the data below aqueous phase hold up of 0.5 were used, wherein kinetic regime prevails.

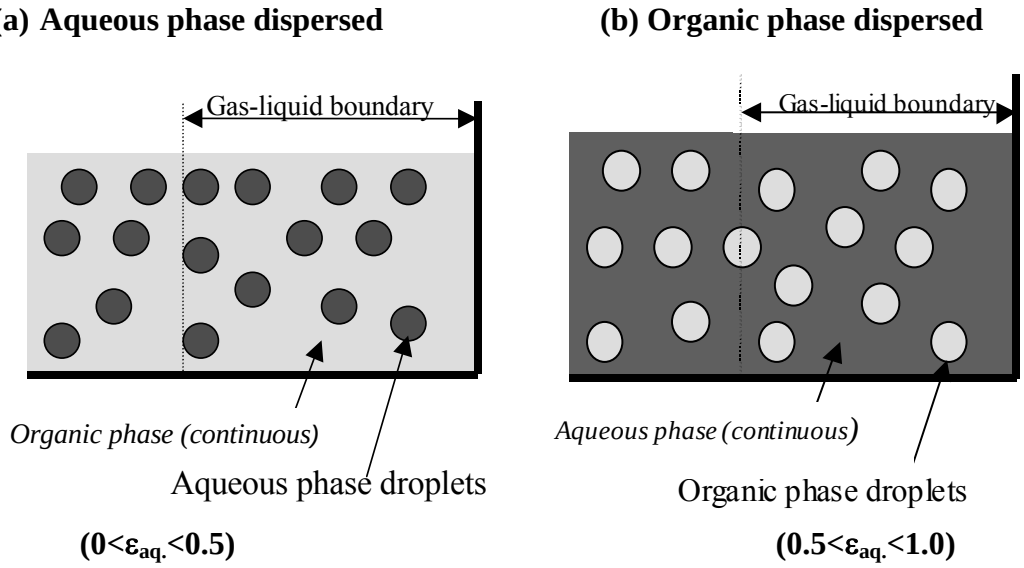

Figure-3.19: Schematic presentation of two different physical situations prevailing in the reactor depending upon the phase hold up

The gas-liquid-liquid reactions can be classified into two categories depending on which phase is dispersed and where the reaction occurs. For the present case, wherein aqueous catalyst phase is the reaction phase, we have:

- *Model A: aqueous phase is dispersed in organic phase ($\varepsilon_{aq.} < 0.5$) and*
- *Model B : organic phase is dispersed in aqueous phase ($\varepsilon_{aq.} > 0.5$)*

The important steps involved in a gas-liquid-liquid catalytic reaction are given in Table 3.6

Table 3.6: Important steps in an aqueous biphasic catalytic reaction

Case I: Aqueous droplets containing the dissolved catalyst dispersed in continuous organic liquid phase	**Case II:** Organic liquid phase dispersed in a continuous aqueous phase which contains the catalyst
Step	
(a) Transport of a gaseous reactants (A) and (B) from the bulk gas phase to gas/organic liquid interface	Transport of a gaseous reactants (A) and (B) from the bulk gas phase to gas/aqueous liquid interface.
(b) Transport of (A) and (B) through the gas/organic liquid interface into the bulk of the organic liquid	Transport of (A) and (B) through the gas/aqueous catalyst interface into the bulk of the aqueous catalyst phase.
(c) Transport of both dissolved (A) and (B) and liquid reactant (D) from organic phase to the organic/aqueous interface	Transport of liquid reactant (D) from the organic droplets to the organic/aqueous interface
(d) Transport of (A), (B) and (D) from the organic/aqueous interface to the aqueous phase catalyst	Transport of (D) from the organic/aqueous interface to the aqueous catalyst phase.
(e) Homogeneously catalyzed reaction of dissolved (A), (B) and D to product (P) in the bulk aqueous phase.	Homogeneously catalyzed reaction of dissolved (A), (B), and (D) to product (P) in the aqueous phase.
(f) Transport of water-immiscible product P from the aqueous to the organic phase.	Transport of water-immiscible product P from the aqueous to the organic liquid phase.

3.4.2.4 Gas-liquid mass transfer effect

The significance of gas-liquid mass transfer resistance was analyzed by comparing the initial rate of reaction and maximum possible rate of gas-liquid mass transfer. The gas-liquid mass transfer resistance is negligible if a factor α_1 defined as follows is less than 0.1 for the experimental conditions used.

$$\alpha_{1,A} = \frac{R_{\exp}}{k_L a_B C_{A,aq.}} \qquad 3.1$$

$$\alpha_{1,B} = \frac{R_{\exp}}{k_L a_B C_{B,aq.}} \qquad 3.2$$

Where, R_{exp} is the observed rate of hydroformylation (kmol/m^3), k_La_B the gas-liquid mass transfer coefficient and C_A *and* C_B represent the saturation solubility of reacting gases *i.e.* H_2 and CO in equilibrium with the gas phase concentration at the reaction temperature (kmol/m^3). The gas-liquid mass transfer coefficient (k_La_B) used in above equations was estimated by using a correlation (Eq. 3.3) proposed by Chaudhari and coworkers[26] for a reactor similar to that used in this work for agitation speed of 1200 rpm.

$$k_La_B = 1.48 \times 10^{-3} (N)^{2.18} \times (V_g / V_L)^{1.88} \times (d_I / d_T)^{2.1} \times (h_1 / h_2)^{1.16} \qquad 3.3$$

The terms involved in above equation are described in Table-3.7 along with the respective values obtained from the reactor and charge used in the present case.

Table-3.7: Parameters used for k_La_B calculations by Eq-3.3

Parameter	Description	Value
V_g	Gas volume (m^3)	4.5×10^{-5}
N	Agitation Speed (Hz)	20
V_L	Liquid volume (m^3)	2.5×10^{-5}
d_I	Impeller diameter (m)	1.6×10^{-2}
d_T	Tank diameter (m)	4.0×10^{-2}
h_1	Height of the impeller from the bottom (m)	1.1×10^{-2}
h_2	Liquid height (m)	2.1×10^{-2}

The k_La_B value for 1200 rpm (20 Hz) was evaluated as 0.22 s^{-1}.

The equilibrium solubilities for the gases given in Table 3.5 were used. The factor α_1 was calculated (taking R_{exp} as 9.7×10^{-5} and 2.39×10^{-6} kmol/m^3/s i.e. highest and lowest rates respectively) for both hydrogen and carbon monoxide and found to be in a range of 3.07×10^{-3} to 1.24×10^{-2} and 2.45×10^{-3} to 9.96×10^{-3}, respectively. Since the values of α_1 are very much less than 0.1 for both the gaseous reactants, gas-liquid mass transfer resistance can be assumed to be negligible.

3.4.2.5 Liquid-liquid mass transfer effect

The significance of liquid-liquid mass transfer resistance can be analyzed using a similar approach as used to analyze gas-liquid mass transfer, by comparing the initial rate of reaction with maximum rate of liquid-liquid mass transfer. Since the solubility of 1-decene in the aqueous phase is very low compared to that of hydrogen and carbon monoxide (Table 3.5), the liquid-liquid mass transfer is analyzed for transport of 1-decene across the liquid-liquid interface. The liquid-liquid mass transfer resistance is negligible if a factor α_2 defined as follows is less than 0.1.

$$\alpha_{2,\,D} = \frac{R_{exp}}{K_{ll}\, C_{D,aq}} \qquad 3.4$$

Where, K_{ll} is the liquid-liquid mass transfer coefficient and is given by Eq-3.5

$$K_{ll} = a_{ll} \times k_{l,aq} \qquad 3.5$$

Where, a_{ll} is the liquid-liquid interfacial area which is given by Eq-3.6.

$$a_{ll} = \frac{6\varepsilon}{d_P} \qquad 3.6$$

Where, d_P is the maximum drop diameter (m) and ε is the dispersed phase hold up. If we consider that the organic (dispersed) phase is present in the form of spherical droplets with a negligible slip velocity with respect to the continuous phase, $K_{l,aq}$ can be estimated (by using Sherwood number, Sh = 2.0) by Eq-3.7

$$k_{l,aq} = \frac{2\,D_{AB}}{d_P} \qquad 3.7$$

Therefore,

$$K_{ll} = \frac{12 D_{AB}\varepsilon}{{d_P}^2} \qquad 3.8$$

Where D_{AB} is the molecular diffusivity of 1-decene (m^2/s) in toluene calculated using Wilke and Chang correlation[27] given by Eq-3.11

For our experiments on hydroformylation, the system (toluene + water:NMP) was similar as used by Lagisetty and coworkers[28]. So the correlation given by Eq-3.9 was directly used for determining d_P and liquid-liquid interfacial area a_{ll} by Eq-3.6

$$\frac{d_P}{d_I} = 0.083\left(1 + C_T\ \varepsilon\right)^{1.2}\ We^{-0.6} \qquad 3.9$$

Where d_I is the impeller diameter (m), C_T constant (C_T=4)[22] dependent on the geometry of the vessel and agitator; and W_e is the Weber number calculated by Eq-3.10

$$W_e = \frac{N^2 {d_I}^3 \rho}{\sigma} \qquad 3.10$$

Here, ρ is the density of the continuous phase and σ is the interfacial tension

Diffusivity of 1-decene (D_{AB}) was calculated using Wilke-Chang Correlation[21] given in Eq-3.11

$$D_{AB} = \frac{7.4\times10^{-8} T (\phi M_B)^{1/2}}{\mu_B V_A^{\ 0.6}} \qquad 3.11$$

Where, Φ is the association parameter of the solvent; μ_B is the viscosity of organic solvent (P or kg/m.s), M_B is the molecular weight of the solvent; T is temperature (K), V_A is the solute molar volume. For agitation speed of 1200 rpm at which all experiments have been carried out, the values of α_2 were found to be in a range of 2.64×10^{-2} - 0.52×10^{-2}, which indicates a kinetic regime.

The initial rate data were analyzed to check the significance of gas-liquid and liquid-liquid mass transfer effect under the conditions used to study the kinetics. In these criteria $\alpha_1(\alpha_{gl})$, and $\alpha_2(\alpha_{ll})$which are defined as the ratios of the observed rates to the maximum rates of gas-liquid and liquid-liquid rates, respectively, were calculated for both the gas phase reactants. It was found that the rate data obtained with Rh-sulfoxantphos catalyst were in the kinetic regime, under the given set of conditions and can be reliably used to evaluate the intrinsic kinetic parameters. The results are also consistent with the negligible effect of agitation shown in the Figure 3.17 in section 3.4.2.3 of this chapter.

3.4.3 Initial rate data

In order to study the kinetics of the hydroformylation of 1-decene several experiments were carried out in the range of conditions as shown in Table 3.8. The initial rates of hydroformylation were calculated from the plots of product formation as a function of time. Under the conditions chosen for kinetic study, no side reactions were found to occur and hence, these data would be representative of the overall

hydroformylation of 1-decene to the corresponding aldehydes. The initial rates of hydroformylation were calculated from the aldehyde product formation as a function of time. The rate of hydroformylation was calculated as follows (Eq. 3.12):

$$R = \frac{\text{Slope of product formation vs. time plot}}{\text{Total Volume of liquid (Aqueous + Organic)}} \qquad 3.12$$

Table 3.8: Range of conditions used for kinetic studies:

Concentration of $Rh(CO)_2(acac)$ $(kmol/m^3)_{(aq.)}$	1.93×10^{-3} –5.79×10^{-3}
Concentration of 1-decene $(kmol/m^3)_{(org.)}$	0.53-1.59
Concentration of sulfoxantphos ligand $(kmol/m^3)_{(aq.)}$	5.78×10^{-3} –2.6×10^{-2}
Partial pressure of hydrogen (MPa)	0.34-3.1
Partial pressure of carbon monoxide (MPa)	0.17-3.1
Temperature (K)	383 – 403
Solvent	Toluene: Water: NMP
Agitation speed (Hz)	16.6-18.3
Reaction volume (m^3)	2.5×10^{-5}

3.4.3.1 Effect of catalyst concentration

The effect of catalyst concentration on the rate of hydroformylation of 1-decene was studied in the temperature range of 383-403 K, 1-decene concentration of 1.07 $kmol/m^3$ and a total pressure of $CO+H_2$ = 4.14 MPa (CO/H_2 = 1) and keeping Rh:L ratio of 1:5. The results are shown in Figure 3.20. The rate was found to be linearly dependent on the catalyst concentration, indicating first order kinetics. A first order dependence is expected from the mechanism described by van Leeuwen and coworkers[29] (Figure 3.20). Increase in catalyst concentration will increase concentration of active catalyst species in the reaction, which leads to rate enhancement. This observation of linear dependence on the catalyst concentration excludes any involvement of dimeric species in the reaction cycle in the concentration range investigated, as the formation of inactive dimeric species is known to retard the rate of reaction[8]. The n/i ratio slightly increases at higher catalyst concentration.

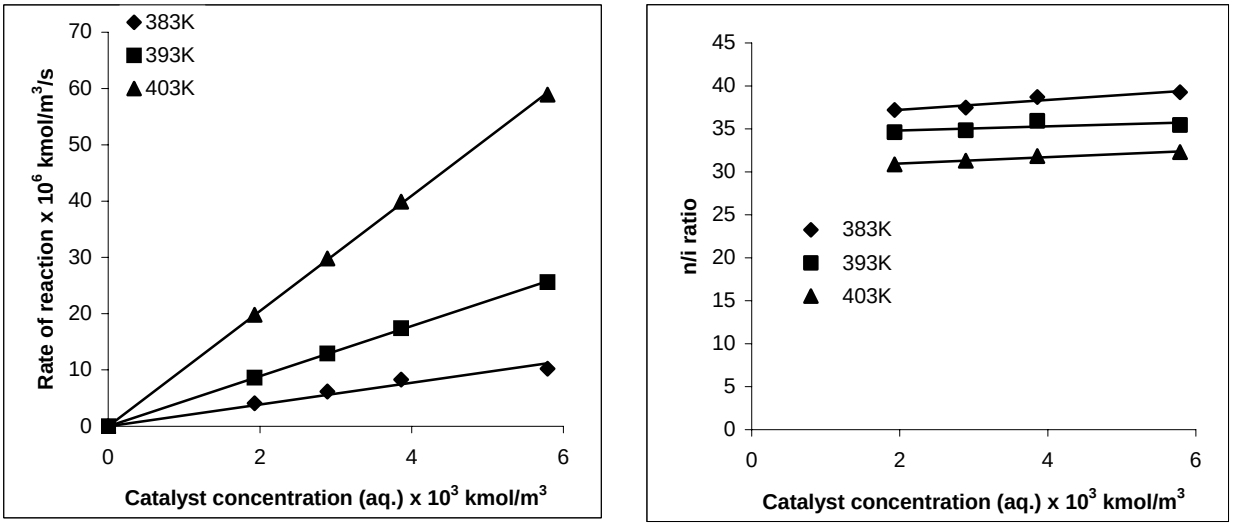

Figure 3.20: Effect of catalyst concentration on the rate and n/i ratio in biphasic hydroformylation of 1-decene.

Reaction conditions: *1-decene: 1.07 kmol/$m^3_{(org.)}$, sulfoxantphos: 9.6 ×10^{-3}- 2.89 × 10^{-2} kmol/$m^3_{(aq.)}$ (Rh: L=1:5), T: 383-403K, P_{CO+H2}: 4.14 MPa, total volume: 2.5 ×10^{-5} m^3, agitation speed: 20Hz, solvent: toluene: water: NMP*

3.4.3.2 Hydroformylation mechanism using diphosphine ligand

The mechanism of the hydroformylation of olefins using diphosphine ligands in homogeneous medium is not clearly understood. The addition of Xantphos ligand to the $Rh(CO)_2$(acac) in presence of syngas generates a species $HRh(CO)_2$(Xantphos). High Pressure IR (HPIR) study have shown that the catalyst exists as a trigonal bipyramid $HRh(CO)_2$(Xantphos) complex, which is present in two isomers, labeled according to the position of the phosphine ligands as equatorial-equatorial (**6ee**) and equatorial-axial (**6ae**)(Figure 3.21). Both isomers are in rapid equilibrium, the 6**ee** isomer being predominant over the **6ae** one. Bidentate ligand having wide bite angles such as BISBI or Xantphos will lead to formation of bisequatorial (**6ee**) species, on the other hand in case of diphosphine having small bite angle (e.g. dppe, dppp) the **6ae** conformation is prefered[29]. The rate of interconversion between these two species is much higher than CO dissociation and hydride migration rates. The alkene complex is obtained from $HRh(CO)_2$(diphosphine) by dissociating one carbonyl molecule. Carbonyl dissociation rates for (formyl)$Rh(CO)_2$(diphosphine) clearly indicate that the equatorial CO dissociates orders of magnitude faster than the apical carbonyl. These results suggest that

the **ee** isomer might be more active than the **ae** one and that alkene could coordinate to the **ee** resulting tetracoordinated rhodium complex directly without relaxing to the more stable square-planar complex. All above arguments point to the fact that the key intermediate might be the **ee** HRh(CO)(alkene)(Xantphos) complex, for which still two isomers can be distinguished depending on the relative hydride and carbonyl positions along the trigonal axis[30].

It is assumed that alkene insertion is irreversible and rapid preequilibria exist for CO and alkene association and dissociation. The rate-determining step can be either CO dissociation or alkene coordination or alkene insertion, all involve intermediates in equilibrium. However, it is still neither clear if the rate-determining and the selectivity determining steps coincide nor if the selectivity is determined by the HRh(CO)(alkene)(diphosphine)(**7**) intermediate which is never observed experimentally. Rest of the steps in mechanism are similar that observed by Wilkinson and coworkers[31].

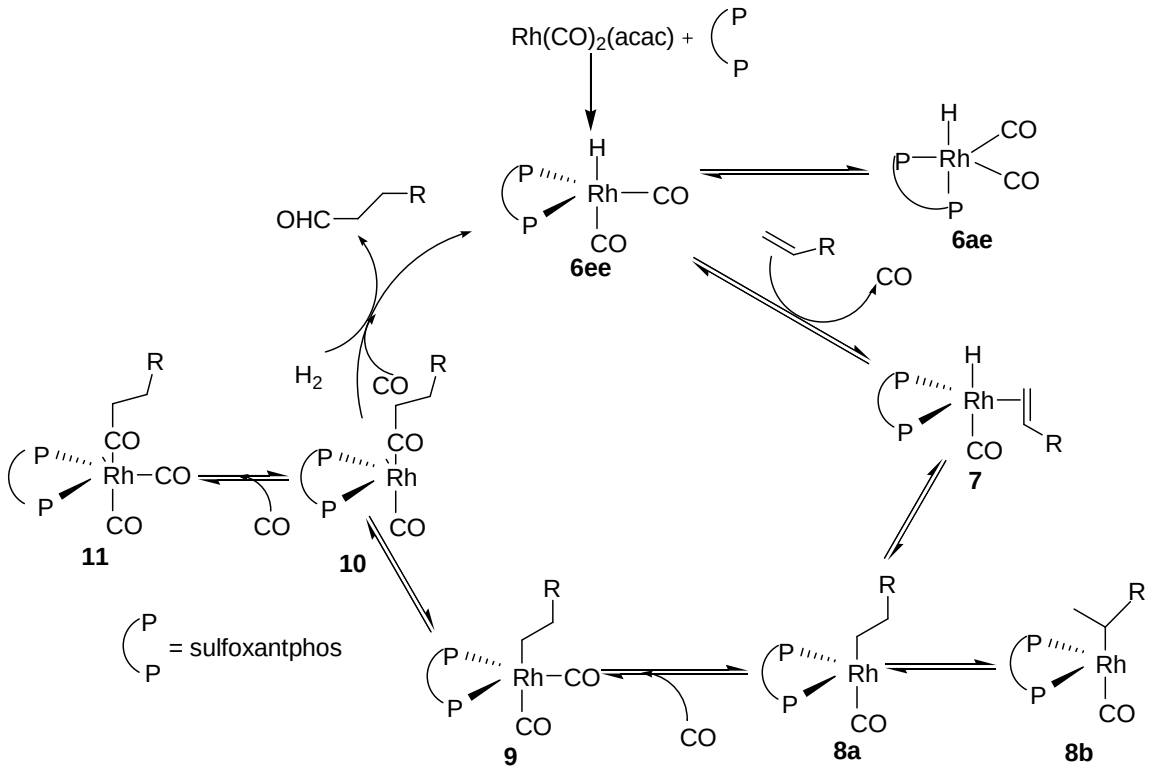

Figure 3.21: Mechanism of hydroformylation of olefins using diphosphine ligand having wide bite angles

3.4.3.3 Effect of 1-decene concentration

Figure 3.22 shows the effect of 1-decene concentration on the rate of hydroformylation at a total pressure of 4.14 MPa (CO/H_2 = l), and a catalyst concentration of 2.89 × 10^{-3}, kmol/m^3, sulfoxantphos concentration of 1.44 ×10^{-2} kmol/m^3 (Rh:L=1:5) in a temperature range of 383-403K. The rate was found to have a linear dependence on 1-decene concentration. The n/i ratio remains unaffected even at higher 1-decene concentration. It is reported that the rate determining step in the hydroformylation of 1-octene with Xantphos ligand is an early stage in the catalytic cycle and one of the rate limiting reaction is coordination of alkene and insertion of olefin into Rh-H bond [32]. A first order dependence with respect to 1-decene is thus expected.

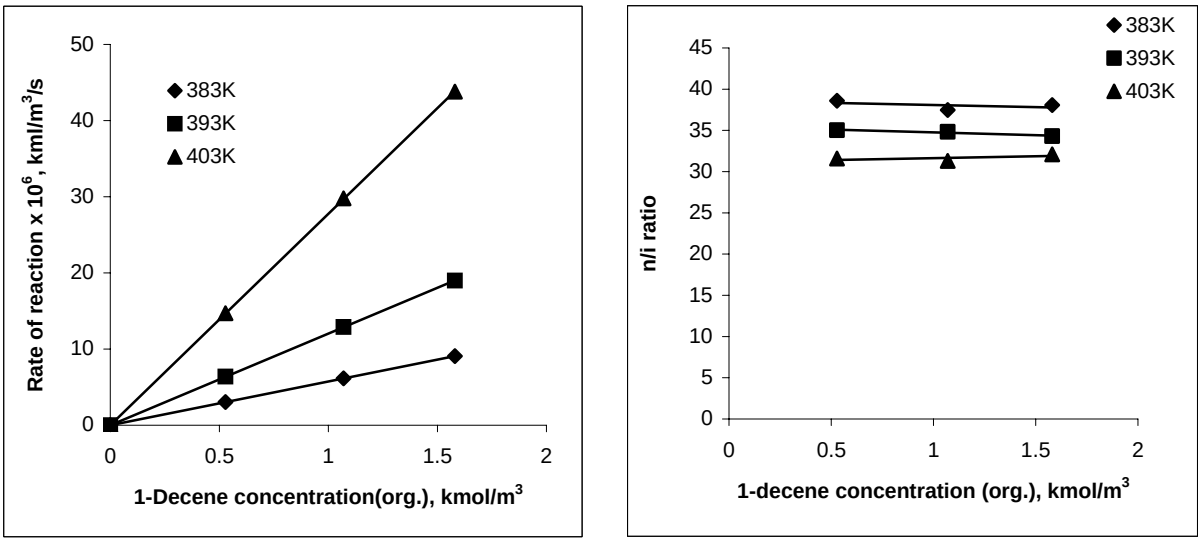

Figure-3.22: Effect of 1-decene concentration on rate and n/i ratio in the biphasic hydroformylation of 1-decene.

***Reaction conditions**: Rh(CO)$_2$(acac): 2.89 ×10^{-3} kmol/$m^3_{(aq.)}$, sulfoxantphos: 1.44 ×10^{-2} kmol/$m^3_{(aq.)}$ (Rh:L=1:5),, T: 383-403K, P_{CO+H2}: 4.14MPa, total volume: 2.5 ×10^{-5} m^3, agitation speed: 20Hz, solvent: toluene: water: NMP*

3.4.3.4 Effect of ligand concentration

Figure 3.23 shows the effect of sulfoxantphos concentration on the rate of hydroformylation at constant Rh(CO)$_2$(acac) concentration of 2.89 ×10^{-3} kmol/m^3 in a temperature range of 383-403 K. The ligand concentration was varied from Rh:L= 1:1 to 1:9. The plot of rate vs. ligand concentration passes through maximum. In the initial

range (Rh:L< 1:2) the rate shows first order dependence while at higher concentrations typical inhibition kinetics was observed[33]. The higher rates observed at lower ligand concentration is the result of the faster CO dissociation, which enhances olefin coordination to the rhodium center (see Figure 3.21). Inhibition at higher ligand concentration is due to the crowding of ligand around the metal center, which prevents the olefin coordination. At still higher concentration of ligand, the rate of hydroformylation of 1-decene becomes independent of the ligand concentration. At low Rh:L ratio the isomerization of terminal olefin to internal olefin was predominant which results in very low n/i ratio. The n/i ratio drops from 34 (Rh:L=1:9) to 7 (Rh:L = 1:2) and 4 (Rh:L = 1:1). This is probably due to the formation of rhodium carbonyl species at lower ligand concentration, which favors the simultaneous isomerization of terminal olefin to internal olefin followed by their hydroformylation. At higher ligand concentration the n/i ratio remains constant as seen in Figure 3.23.

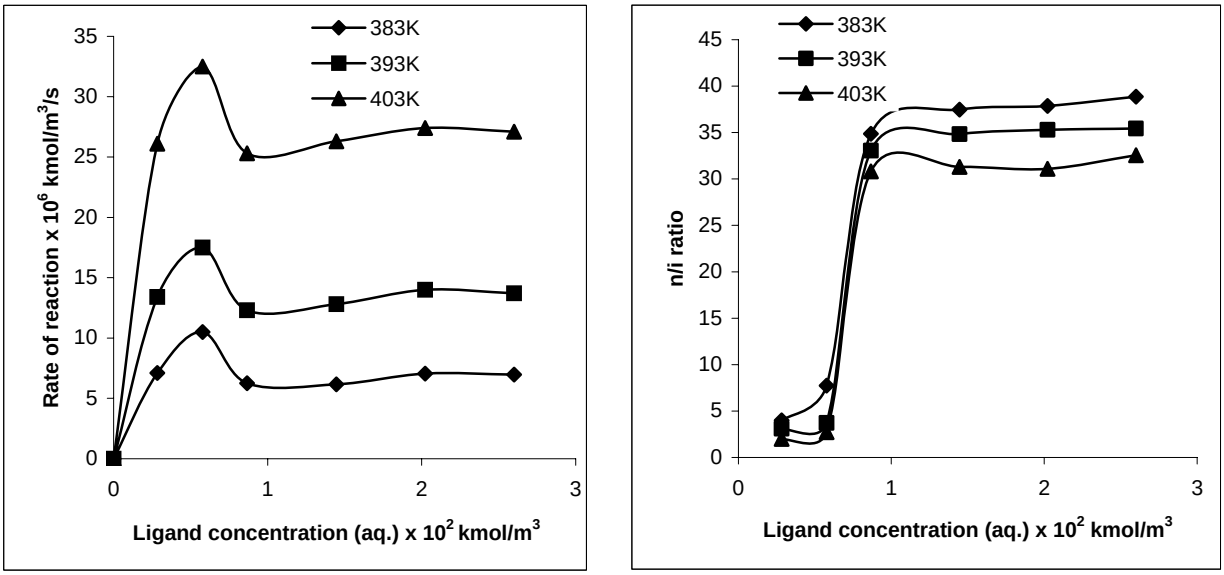

Figure 3.23: Effect of ligand concentration on rate and n/i ratio in the biphasic hydroformylation of 1-decene.

Reaction conditions: *1-decene: 1.07 kmol/$m^3_{(org.)}$, $Rh(CO)_2(acac)$: 2.89 ×10^{-3} kmol/$m^3_{(aq.)}$, (Rh:L=1:1-1:9), T: 383-403K, P_{CO+H2}: 4.14MPa, total volume: 2.5 ×10^{-5} m^3, agitation speed: 20Hz, solvent: toluene: water: NMP*

3.4.3.5 Effect of partial pressure of H_2

The effect of partial pressure of hydrogen on the rate of hydroformylation of 1-decene was investigated at a constant CO partial pressure of 2.07 MPa, 1-decene concentration of 1.071 kmol/m^3, $Rh(CO)_2(acac)$ concentration of 2.89 $\times 10^{-3}$ kmol/m^3 and sulfoxantphos concentration of 1.44 $\times 10^{-2}$ kmol/m^3 (Rh:L=1:5). The results are shown in Figure 3.24. The rate of reaction was found to have fractional order dependence on P_{H2}. This positive effect is observed as hydrogen is required for the regeneration of the active catalytic species in the reaction cycle (See Figure 3.21)**.** Similar positive dependence on P_{H2} is also reported for hydroformylation of styrene using homogeneous Rh-BDPP ((2S, 4S)-bis (diphenylphosphinopentane) catalyst systems[29]. The n/i ratio increases marginally with P_{H2} and decreases at higher H_2 pressure and higher temperature.

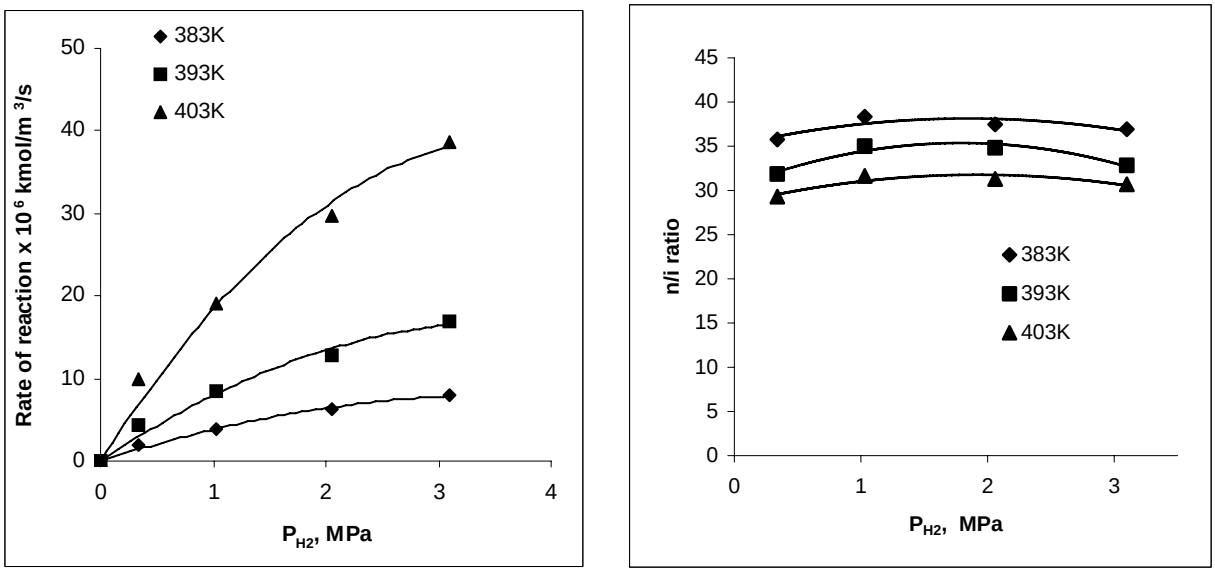

Figure 3.24: Effect of partial pressure of hydrogen on rate and n/i ratio in the biphasic hydroformylation of 1-decene.

Reaction conditions: *1-decene: 1.07 kmol/m$^3_{(org.)}$, $Rh(CO)_2(acac)$: 2.89 $\times 10^{-3}$ kmol/m$^3_{(aq.)}$, sulfoxantphos:1.44 $\times 10^{-2}$ kmol/m$^3_{(aq.)}$ (Rh:L=1:5), T: 383-403K, P_{CO} : 2.07MPa, total volume: 2.5 $\times 10^{-5}$ m^3, agitation speed: 20Hz, solvent: toluene: water: NMP*

3.4.3.6 Effect of partial pressure of CO

The effect of P_{CO} on the rate of hydroformylation of 1-decene was studied at a constant H_2 partial pressure of 2.07 MPa, 1-decene concentration of 1.07 kmol/m^3 and a

catalyst concentration of 2.89 × 10^{-3} kmol/m^3 and sulfoxantphos(aq.):1.44 ×10^{-2} kmol/m^3 (Rh:L=1:5). The results are shown in Figure 3.25. The rate was found to be inversely dependent on the CO partial pressure. As per the mechanism (Figure 3.20) of hydroformylation of olefins using diphosphine ligand, the inhibition in the rate of hydroformylation is due to the side reactions leading to the formation of the inactive species (RCO)Rh$(CO)_2$(diphosphine) (**11**). The equilibrium leading to the formation of **11** will be more pronounced at higher pressures of CO causing a sharp decrease in the rate of reaction as observed in this work. The formation of such species reduces the effective concentration of the active catalytic species and hence, the rate of reaction is reduced. It has been observed that at lower CO pressure the isomerization of olefin increases due to the predominance of competitive β-hydride elimination step. The aldehyde obtained by the hydroformylation of this isomerized olefin reduces the n/i ratio drastically. The n/i ratio of 37.5 at 2.07 MPa of CO diminishes to 15 at 0.068 MPa of CO partial pressures at 383K.

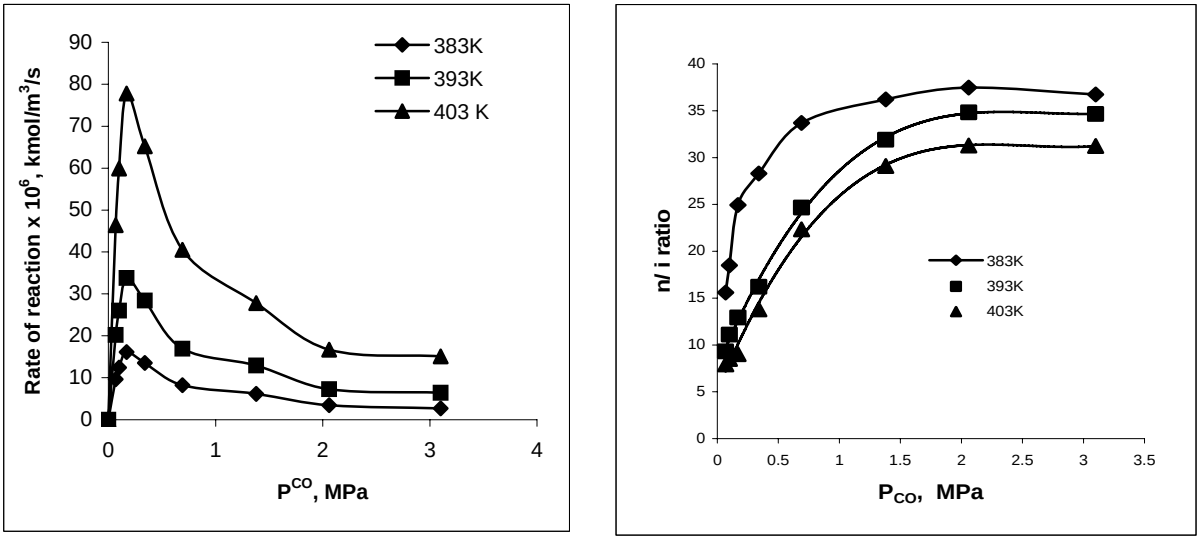

Figure 3.25: Effect of partial pressure of carbon monoxide on rate and n/i ratio in the biphasic hydroformylation of 1-decene.

Reaction conditions: *1-decene: 1.07 kmol/$m^3_{(org.)}$, $Rh(CO)_2(acac)$: 2.89 ×10^{-3} kmol/$m^3_{(aq.)}$, sulfoxantphos:1.44 ×10^{-2} kmol/$m^3_{(aq.)}$ (Rh:L=1:5), T: 383-403K, P_{H2} :2.07MPa, total volume: 2.5 ×10^{-5} m^3, agitation speed: 20Hz, solvent: toluene: water: NMP*

3.4.3.7 Kinetic modeling: For the purpose of development of rate models, an empirical approach was followed. Prior to discrimination of rate equations, the rate data were analyzed for the importance of mass transfer resistances. In the current case, this was more important since the reaction is a typical gas–liquid–liquid (G-L-L) reaction. The rates in G-L-L system were depends on the liquid-liquid interfacial area, which is governed by both agitation speed and hold up of the dispersed phase. The effect of agitation speed and aqueous phase hold up on the rate was investigated. The rate was found to be independent of the agitation speed (Figure 3.17, section 3.4.2.3), while the results of aqueous phase hold up of 0.5 indicates the data were representative of the true kinetics of the reaction (Figure 3.18, section 3.4.2.3). Also the analysis of the initial rate data according to the criteria laid down by Ramachandran and Chaudhari[34] confirmed that the gas–liquid ($\alpha_{gl)}$ and liquid–liquid (α_{1l}) mass transfer resistances were negligible, as discussed in section 3.4.2.4. The initial rate data were hence used to evaluate the intrinsic kinetic parameters.

In order to fit the observed rate data, several rate equations were examined using a nonlinear regression analysis. The results on the kinetic parameters estimated for the different models are presented in Table 3.5. For this purpose, an optimization program based on Marquardt's method[35] was used. The objective function was chosen as follows (Eq. 3.13);

$$\phi = \sum_{i=1}^{n} \left[R_{Ai} - R'_{Ai} \right]^2 \qquad 3.13$$

Where Φ is the objective function to be minimized (Φ_{min}) representing the sum of the squares of the difference between the observed and predicted rates, n is the number of experimental data, R_{Ai} and R'_{Ai} represent predicted and experimental rates, respectively. The values of rate parameters and Φ_{min}, are presented in Table 3.5.

Table 3.5: Values of kinetic parameters at different temperatures

Model	Rate Model	T (K)	k_1	k_2	k_3	ϕ_{min}
I	$r = \frac{k_1 ABCD}{(1+k_2A)(1+k_3B)^2}$	383	6.20×10^{2}	3.56	3.23×10^{2}	1.25×10^{-11}
		393	1.05×10^{3}	4.37	3.76×10^{2}	3.44×10^{-11}
		403	1.69×10^{3}	5.23	5.45×10^{2}	1.79×10^{-10}
II	$r = \frac{k_1 ABCD}{(1+k_2A)(1+k_3B^2)}$	383	8.38	3.91×10^{1}	3.24×10^{-1}	6.25×10^{-10}
		393	4.16×10^{2}	3.32×10^{1}	4.50×10^{4}	6.91×10^{-11}
		403	6.98×10^{2}	2.69×10^{1}	3.55×10^{4}	3.66×10^{-10}
III	$r = \frac{k_1 ABCD}{(1+k_2A)(1+k_3B)^3}$	383	2.66×10^{2}	1.68×10^{-1}	1.17×10^{2}	1.15×10^{-11}
		393	7.75	7.62×10^{-3}	1.21×10^{-2}	2.76×10^{-9}
		403	6.39×10^{2}	1.37×10^{-2}	8.91×10^{1}	2.28×10^{-10}
IV	$r = \frac{k_1 ABCD}{(1+k_2A)(1+k_3B)}$	383	4.10×10^{5}	6.18×10^{1}	1.39×10^{6}	1.94×10^{-10}
		393	4.36×10^{5}	4.98×10^{1}	8.64×10^{5}	7.97×10^{-10}
		403	-1.97×10^{6}	4.14×10^{1}	-2.04×10^{6}	4.20×10^{-9}
V	$r = \frac{k_1 A^{1.5}B^{1.5}CD}{(1+k_2A)(1+k_3B)}$	383	4.10×10^{5}	6.18×10^{1}	1.39×10^{6}	1.94×10^{-10}
		393	6.25×10^{2}	3.42×10^{1}	9.89×10^{1}	3.19×10^{-11}
		403	-1.97×10^{6}	4.14×10^{1}	-2.04×10^{6}	4.20×10^{-9}

Where, A and B represent the concentrations of H_2 and CO in toluene at the gas-liquid interface (kmol/m^3) respectively. C and D are the concentrations of the catalyst per unit aqueous phase and 1-decene per unit organic phase (kmol/m^3), respectively and r is the rate of hydroformylation per unit total phase per second. The ligand concentration effect was not considered for the purpose of modeling.

The discrimination of rate models was done based on the thermodynamic criteria, activation energy and the Φ_{min} values. The rate models II and III were rejected based on the thermodynamic criteria of inconsistency of equilibrium constant and activation energy. Models IV and V have rate parameters less than zero (or –ve) and higher Φ_{min} values than model I hence were rejected. Therefore, model I (Eq. 3.14) was considered

the best model for representing the kinetics of hydroformylation of 1-decene in aqueous biphasic system in presence of cosolvent using Rh/sulfoxantphos catalyst.

$$r = \frac{k_1 ABCD}{(1+ k_2A)(1+ k_3B)^2} \qquad 3.14$$

Where, *k* is the intrinsic rate constant ($m^9/kmol^3/s$), A and B represent the concentrations of H_2 and CO in toluene at the gas-liquid interface ($kmol/m^3$) respectively. C and D are the concentrations of the catalyst and 1-decene ($kmol/m^3$), respectively. The rate parameters for Eq. 3.14 for all the temperature are presented in Table 3.5 (entry 1). A comparison of the experimental rates with the rates predicted by Eq. 3.14 is shown in Figure 3.26, which shows a reasonably good fit of the data. The average deviation in the predicted and observed rates was found to be in the range of ± 5 %. The Arrhenius plot showing the effect of temperature on the rate parameters is shown in Fig. 3.27, from which the activation energy was evaluated as 64.76 kJ/mol. The dependence of the rate parameters k_2 and k_3 on temperature show opposite trends; however, it is important to note that these parameters may not be representative of a single equilibrium reaction step and are in fact lumped parameters describing observed overall trends.

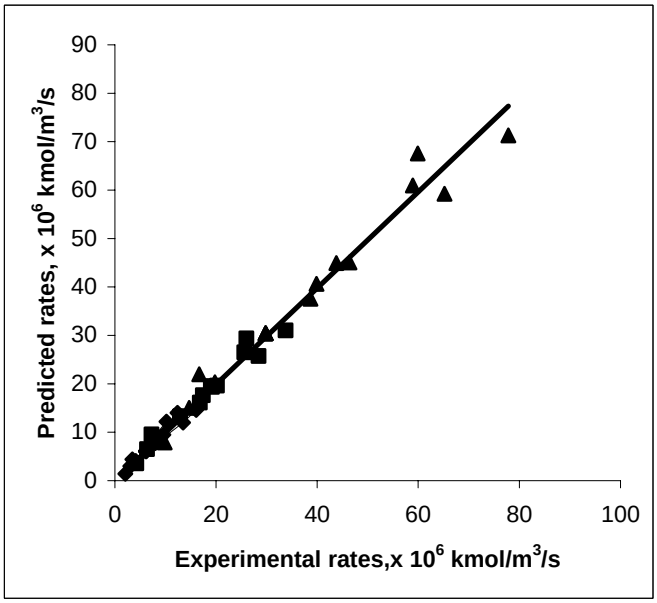

Figure 3.26: Comparison of experimental rates and rates predicted using model I

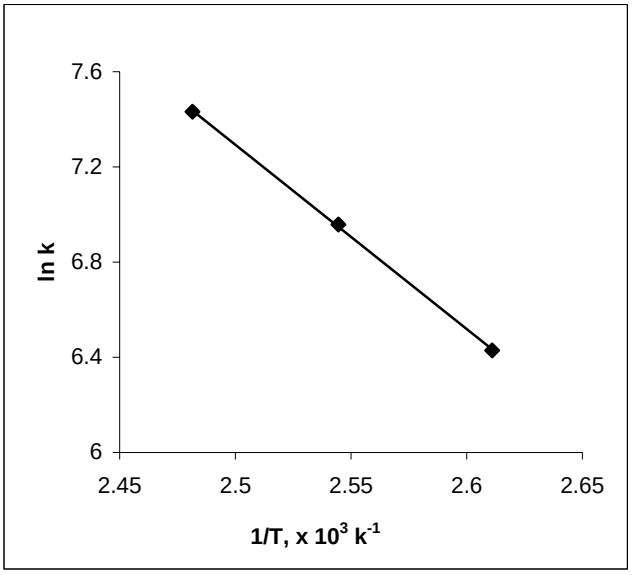

Figure 3.27: Temperature dependence of rate constant

The validity of the proposed model I was crosschecked by plotting the experimental and observed rates at varying concentrations of the variables for all temperature (Figure 3.28). The model was found to predict the trends in good agreement with experimental observations.

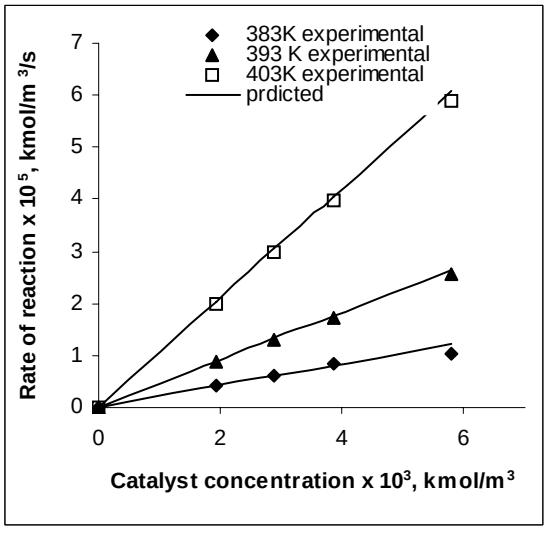

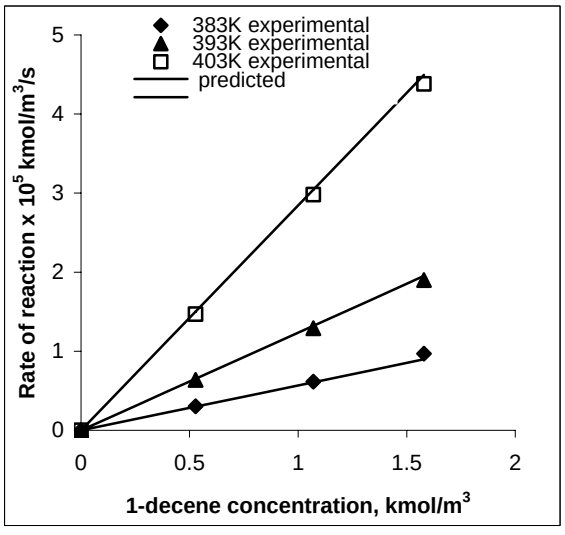

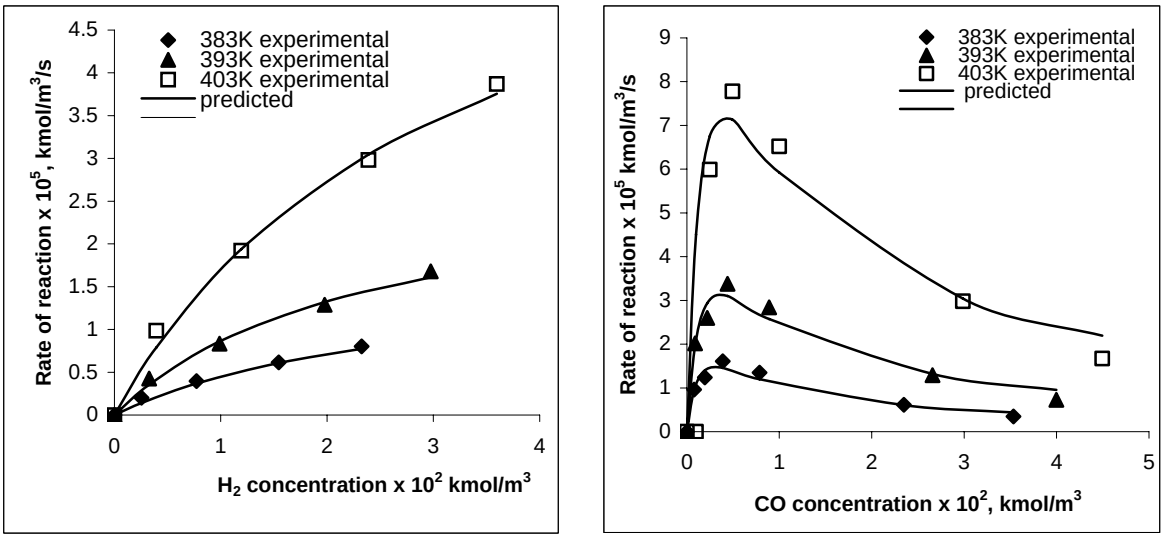

Figure 3.28: Verification of proposed rate model for various reaction parameters

3.5 Conclusions

The water-soluble Rh/sulfoxantphos catalyst shows poor activity for hydroformylation of higher olefins in aqueous biphasic medium as compared to the reaction in homogeneous medium. The rate and n/i ratio decreases with increase in chain length of olefin. The addition of cosolvents to the aqueous catalyst phase enhances the reaction rate and chemo, and regioselectivity dramatically. N-methyl pyrrolidone (NMP) was found to be the best cosolvent, which enhances the rate by several folds, as well as increases n/i ratios for all the higher olefins studied, compared to the reaction in aqueous biphasic medium. The rate enhancement is more predominant for 1-decene and 1-dodecene hydroformylation. The water: NMP ratio of of 7:3 was found to be the optimum ratio to ensure high activity and negligible leaching of the rhodium to the organic phase. The aqueous catalyst phase was recycled for several times. An improvement in the activity for the first recycle over the virgin reaction was observed. This activity then remains constant for subsequent recycles.

The kinetics of hydroformylation of 1-decene has been studied in the presence of NMP as a cosolvent, using water-soluble Rh/sulfoxantphos as a catalyst. The detailed investigation on mass transfer effects shows that the reaction operates in kinetic regime. This fact is also supported by the studies on the influence of agitation speed and aqueous phase hold up on rate. The rate was found to be first order with respect to catalyst and olefin concentrations and partial order with hydrogen partial pressure. The rate versus ligand and CO concentration passes through a maximum, indicating negative order dependence at higher pressures. At lower ligand and CO partial pressures the n/i is ratio drastically affected. The following rate equation has been proposed based on the observed rate data, which is in good agreement with the experimental rates obtained.

$$r = \frac{k_1\, ABCD}{(1+ k_2A)\,(1+ k_3B)^2}$$

The activation energy was calculated to be 64.76 kJ/mol.

Nomenclature

A	Concentration of hydrogen, kmol/m^3
a_{ll}	Liquid-Liquid interfacial area, m^2/m^3
B	Concentration of carbon monoxide, kmol/m^3
C_T	Constant dependent on the geometry of the vessel and agitator
C_A	The saturation solubility of H_2, kmol/m^3
C_B	The saturation solubility of CO, kmol/m^3
C	Concentration of catalyst, kmol/m^3
D_{AB}	Molecular diffusivity of 1-decene, m^2/s
D	Concentration of 1-decene, kmol/m^3
d_I	Impeller diameter, m
d_P	Maximum drop diameter, m
d_T	Tank diameter, m
h_1	Height of the impeller from the bottom, m
h_2	Liquid height, m
k_1	Reaction rate constant, $m^9/kmol^3/s$
k_2, k_3	constant in Eq. 3.14, m^3/kmol
k_La_B	Gas-liquid mass transfer coefficient, s^{-1}
K_{ll}	Liquid-liquid mass transfer coefficient
M_B	Molecular weight of the solvent B
N	Agitation Speed, Hz
R	Universal gas constant (kJ/kmol/K)
R'_{Ai}	Experimental rates
R_{Ai}	Predicted rates
Sh	Sherwood number
T	Temperature (K)
V_A	Solute molar volume at its normal boiling point, m^3/kg mol (*For further calculations refer Transport Processes and unit operations by Christie J. Geankoplis, third edition, 1997*)
V_g	Gas volume, m^3

V_L Liquid volume, m^3

We Weber number defined by Eq-3.10

Greek Symbols

φ Association parameter of the solvent

ε Dispersed phase hold up

ρ Density of the continuous phase, kg/m^3

σ Interfacial tension, dynes/cm

Φ Parameter defined by Eq-3.13

$\alpha_{2\,D}$ Parameter defined by Eq-3.4

μ_B Viscosity B in kg/m.s

$\alpha_{l,A}$ Parameter defined by Eq-3.1

$\alpha_{l,B}$ Parameter defined by Eq-3.2

References

1 B. Cornils, W.A. Hermann (Eds) *Aqueous-Phase Organometallic Catalysis: Concepts and Application,* Wiley VCH Verlag GmbH, Weinheim, **1998**.

2 (a) E. Kuntz, *FR 2,314,910*, **1975**, *US 4,248,802* (1981); (b) E. Kuntz, *CHEMTECH*, **1970**, 570

3 (a) B. Cornils, J. Falbe, *Proc. 4th Int. Symp. on Homogeneous Catalysis,* Leningrad, Sept. **1984**, p. 487; (b) H. Bach, W Gick, E. Wiebus, B. Cornils, Abstr. *1st IUPAC Symp. Org. Chemistry,* Jerusalem **1986**, p. 295; (c) E. Wiebus, B. Cornils, *Chem. Ing. Tech.,* **1994**, *66*, 916; (d) B, Cornils, E. Wiebus, *CHEMTECH*, **1995**, *25*, 33

4 (a)W. A. Herrmann, C. W. Kohlpaintner, *Angew Chem. Int. Ed. Engl.* **1993**, *32*, 1524 (b) H. Ding, J. Kang, B.E. Hanson, C.W. Kohlpaintner, *J. Mol. Catal. A: Chemical,* **1997,** *124*, 21.

5 W.A. Herrmann, C.W. Kohlpaintner, R.B. Manetsberger, H. Bahrmann, Kottmann, *J. Mol. Catal. A: Chemical,* **1995**, *97*, 65

6 M. S. Goedheijt, P. C. J. Kamer, P. W. N. M. van Leeuwen *J. Mol. Catal. A: Chemical,* **1998**, *134*, 243.

7 A. Hebler, S. Kucken, O. Stelzer, J. Blotevogel-Baltronat, W. S. Sheldrick, *J. Organomet. Chem.,* **1995**, *501*, 293.

8 D. J. Darensbourg, N. W. Stafford, F. Joo, J. H. Reibenspies, *J. Organomet. Chem.,* **1995,** *488*, 99.

9 H. Ding, B. E. Hanson, T. Bartik, B. Bartik, *Organometallics,* **1994,** *13,* 3761

10 R. M. Deshpande, Purwanto, H. Delmas, R. V. Chaudhari, *I & EC Res.,* **1996**, *35*, 3927.

11 (a) B. Cornils, E.G. Kuntz, *J Organomet. Chem*., **1995,** *502*, 177 (b) B. Cornils, W.A. Herrmann, R.W Eckl, *J. Mol. Catal. A*, **1997**, *116*, 27.

12 H. Chen, Y. Li, J. Chen, P. Cheng, Y. He, X. Li, *J. Mol. Catal. A: Chemical,* **1999**, *149,* 1.

13 B. M. Bhanage, Y. Ikushima, M. Shirai, M. Arai, *Chem. Commun.*, **1999**, 1277.

14 J. P. Arhancet, M. E. Davies, J. S. Meroal, B. E. Hanson, *Nature,* **1988**, *339*, 454.

15 R. V. Chaudhari, B. M. Bhanage, R. M. Deshpande, H. Delmas, *Nature,* **1995**, *373*, 501.

16 (a)F. Monteil, R.V. Kastrup, A.A. Ostwald *Catal. Lett.,* 1985, *2*, 85.(b) Purwanto, H. Delmas *Catal. Today*, 1995, *24*, 134. (c) R. M. Deshpande, Purwanto, H. Delmas, R. V. Chaudhari, *Ind. Eng. & Chem. Res*., 1996, *35*, 3927. (d) H. Zang *Catal. Today,* 2002, *74*, 23. (e) R. M. Deshpande, Purwanto, H. Delmas, R.V. Chaudhari, *J. Mol. Catal. A: Chemical*, **1997,** *126***, 133**. (f) F. Monteil, R.Dueau, P. Kalck *J. Organomet. Chem.,* **1994**, *480*, 177. g) I. Hablot, J. Jenck, G. Casamatta, H. Delmas, *Chem. Eng. Sci.,* 1992, *47*, 1267.(h) P. Kalck, P. Escaffre, F. Serein-Spriau, A. Thorez, B. Besson, Y. Colleuille, R. Perron, *New J. Chem.* 1988, *12*, 687.

17 L. Leclercq, F. Hapiot, S. Tilloy, K. Ramkisoensing, J. N. H. Reek, P. W. N. M. van Leeuwen, E. Monflier, *Organometallics*, **2005,** *24*, 2070.

18 Ph. D. Thesis of Vinod Nair University of Pune , India **1999**.

19 M. Kranenburg, Y. E. M. Van der Burget, P. C. J. Kamer, P. W. N. M. van Leeuwen *Organometallics,* **1995**, *14*, 3081

20 O. R. Hughes, J. D. Unruh, *J. Mol. Catal.,* **1981**, *12*, 71

21 O. R . Hughes, D. A. Young, *J. Am. Chem. Soc.* **1981**, *103*, 6636.

22 (a) T. J. Devon, G. W. Philips,; T. A, Puckette, J. L Stavinoha, J. J. Vanderbilt, *U.S. Patent 4,694,109* (to Eastman Kodak), **1989**. (b) C. P. Casey, G. T. Whiteker, M. G. Melville, L. M. Petrovich, J. Gamey, D. R. Powell, *J. Am. Chem. Soc.,* **1992**, *114*, 5535.

23 R. M. Deshpande, B. M. Bhanage, S. S. Divekar, S. Kanagasabapathy and R. V. Chaudhari, *Ind. Eng. Chem. Res*, **1998**, *37*, 2391.

24 R. V. Chaudhari, A. Bhattacharya, B. M. Bhanage *Catal. Today* **1995**, *24*, 123.

25 P. Claus, M. Baerns in *Aqueous-Phase Organometallic Catalysis: Concept and applications,* (Eds. B. Cornils, W. A. Hermann.) Wiley- VCH, New York **1998**.

26 R. V. Chaudhari, R. V. Gholap, G. Emig, H. Hofmann, *Can. J. Chem.,* **1987,** *65* 744

27 C. R. Wilke, P. Chang, *AICheE. J.*, **1955**, *1*, 264

28 J. S. Lagisetty, P. K. Das, R. Kumar, K. S. Gandhi, *Chemical Eng. Science*, **1986**, *41*, 65

29 I. d. Rio, O. Pamies, P. W. N. M. van Leeuwen, C. Claver *J. Organomet. Chem.,* **2000**, *608*, 115.

30 J. J. Carbo, F. Maseras, C. Bo, P. W. N. M. van Leeuwen *J. Am. Chem.Soc.* **2001**, *123,* 7630.

31 D. Evans, J. A. Osborn, G. Wilkinson, *J. Chem. Soc. A*, **1968**, 3133.

32 **(**a) L. A. van der Veen, M. D. K. Boele, F. R. Bregman, P. C. J. Kamer, P. W. N. M. van Leeuwen, K. Goubitz, J. Fraanje, H. Schenk, C. Bo *J. Am. Chem. Soc.,* **1998**, *120*, 11616. (b) L. A. van der Veen, P. H. Keeven, G. C. Schoemaker, J. N. H. Reek, P. C. J. Kamer, P. W. N. M. van Leeuwen, M. Lutz, and A. L. Spek *Organometallics,* **2000,** *19,* 872.

33 P. W. N. M. van Leeuwen, C. Claver (Eds.) *Rhodium Catalyzed Hydroformylation,* Kluwer Academic Publishers **2000,** pp. 76.

34 P. A. Ramachandran, R. V. Chaudhari, *Multiphase Catalytic Reactors,* Gordon and Breach, London, **1983**

35 D. W. Marquardt, *J. Soc. Ind. Appl. Math.*, **1963,** *11(2)*, 431.

CHAPTER 4
Synthesis, Characterization and Catalytic Activity of Novel Heterogenized Catalyst for Hydroformylation of Olefins

4.1 Introduction

Homogeneous catalysis, using soluble metal complexes, provides selective synthetic routes under mild operating conditions for valuable chemicals ranging from basic organic precursors to bulk chemicals. However, their practical applications have been limited by difficulties in catalyst product separation at industrial scales. In most of the homogeneously catalyzed processes, the catalyst product separation is carried out by simple distillation. In the cases where the products are not volatile suitable co-solvents may be added to make the system biphasic and to solublize either catalyst or product exclusively. The catalyst can be isolated by separating the two phases. Alternately, the catalyst may also be separated by precipitation, by addition of a suitable additive and removed as a sludge. In these processes some catalyst losses invariably take place, and hence such processes are not viable when costly metals such as rhodium, palladium or platinum are used. To overcome these issues attempts were made to heterogenize the homogeneous catalyst[1]. These catalysts could then combine the advantages of homogeneous catalysts i.e. high activity and selectivity, with those characteristic of heterogeneous catalysts viz-long lifetime and ease of separation, and stability.

As discussed in Chapter-1 section 1.5, different approaches were proposed, to heterogenize the homogeneous catalysts, with the goal of retaining the advantage of high activity at milder operating conditions and selectivity similar to homogeneous catalysts. The heterogenization of homogeneous complexes are broadly classified as 'biphasic catalysis', where the catalytic complex is heterogenized on liquid support[2] and 'solid supported catalyst' where, the catalysts are immobilized on organic or inorganic supports[3]. For the solid supported catalysts the stability of the complex is of prime importance to ensure that it does not leach from the support to the liquid phase in the course of the reaction. At the same time the high activity, selectivity, and original configuration of the catalytic complex has also to be retained. Inspite of several publications in this direction, only in a few cases[4] have efficient heterogeneous catalysts been developed for reactions like hydroformylation.

It is also important to note that all the commercialized hydroformylation processes employ homogeneous rhodium or cobalt complex catalysts[5]. In Chapter-3, a detailed investigation on the hydroformylation of higher olefins in aqueous biphasic medium has

been presented. Effective catalyst product separation for hydroformylation of 1-decene in biphasic medium (water-toluene) using $Rh(CO)_2(acac)$/sulfoxantphos catalyst system has been studied in detail. It has been observed that the rate of reaction for hydroformylation of 1-decene is lower under biphasic conditions as compared to the homogeneous catalytic systems. This could be attributed to the relatively lower solubility of higher olefins in water compared to the organic medium (toluene). Addition of a cosolvent can enhance the solubility of the reacting olefin in the aqueous phase, thereby enhancing the activity and also retain the biphasic nature of the system for effective catalyst-product separation. This catalyst can be recycled without any loss in the activity. It may be noted that the ideal cosolvent should satisfy the requirements described in chapter 1 section 1.5.1.4.

Another approach to overcome the poor solubility of the reacting olefin (and hence poor rates) is by conducting the reaction in an organic phase but using heterogenized homogeneous catalysts, immobilized on solid supports.

Various methods of heterogenization of homogeneous complexes by immobilizing them onto solid supports have been discussed in Chapter 1 section 1.5.2. Different heterogenization techniques using a variety of supports (with varying properties, like acidity, redox behavior, pore size/distribution, channel sizes, surface areas, chemical stabilities etc.) have been used widely for reactions like hydrogenation, oxidation, isomerization, and hydroformylation etc[4]. With the exception of biphasic catalysis no other approach has been found to be commercially attractive because these catalysts suffer either from lower selectivity and activity (TON), or low recyclability, and catalyst leaching[6]. This clearly indicates a need for the development of a true heterogeneous catalyst for hydroformylation reactions.

A novel approach has been demonstrated by Hu et. al.[7] for the development of heterogenized hydrogenation catalyst. Here, the simplistic approach of precipitating the homogeneous catalyst as its insoluble salt has been applied. The precipitation of ruthenium and rhodium complexes of phosphonated BINAPs as the zirconate species has resulted in providing a heterogenized catalyst for chiral hydrogenation of aromatic ketones and β-keto esters. This catalyst is very stable and recyclable.

In this chapter, a similar yet novel concept for heterogenization of homogeneous complexes is proposed, which is termed as ‘ossification’. For ossification the

immobilization of water soluble $HRhCO(TPPTS)_3$ is achieved by precipitating it as an insoluble salt of Gr. 2 metals such as Ca, Sr or Ba. It is also possible to precipitate the complex onto a porous support, and such catalysts are termed as 'supported ossified catalysts'. A detailed investigation on this heterogenized rhodium complex catalyst for hydroformylation of various classes of olefins (in particular higher olefins) has been presented in this chapter to demonstrate the activity, selectivity and stability of these catalysts. A detailed characterization of the catalysts has also been discussed. The kinetics of hydroformylation of 1-decene using carbon supported ossified catalyst is also investigated.

4.2 Experimental

4.2.1 Materials

Rhodium trichloride ($RhCl_3.\ 3H_2O$), obtained from Arora-Matthey was used as received. 1-hexene, 1-octene, 1-decene, 1-dodecene, styrene, vinyl acetate (VAM), camphene, cyclohexene (> 99% pure), ZrO_2 and La_2O_3 were obtained from Sigma-Aldrich, USA. $Ba(NO_3)_2$, $Ca(NO_3)_2$, $Sr(NO_3)_2$, PPh_3, SiO_2, TiO_2, Al_2O_3 and MgO were procured from Loba Chemie, India. The solvents, ethanol, methanol, methyl ethyl ketone (MEK), octanol, toluene, cyclohexane and n-hexane etc. were freshly distilled, dried and degassed prior to use. Oleum of 65% (w/w of SO_3 in H_2SO_4) strength was prepared by dissolving the SO_3 gas (produced from the reaction of H_2SO_4 with P_2O_5) in concentrated H_2SO_4 in required proportion. Distilled degassed water was used in all operations. Propylene and hydrogen gas supplied by Indian Oxygen, Mumbai, India and carbon monoxide (> 99.8% pure, Matheson Gas, USA) were used directly from the cylinders. The syngas mixture (H_2+CO) in 1:1 ratio was prepared by mixing H_2 and CO in a reservoir vessel, in that ratio.

4.2.2 Synthesis of TPPTS

Sulfonation reactor set up

For synthesis of triphenyl phosphine trisulfonate (TPPTS)**,** a double-jacketed 1 L glass reactor equipped with a high-speed half-moon stirrer was used. This reactor was designed so that operation under argon atmosphere was possible. The temperature was controlled by circulation of water using a cryostat. A similar reactor of larger volume was

used for neutralization of the crude reaction mixture. The procedure used was similar to that reported in the literature[8].

Reaction charge for the synthesis of TPPTS

- SO_3/TPP =12 (molar ratio)
- $SO_3/(SO_3 + H_2SO_4 + TPP) = 34\%$ (w/w)
- $H_2SO_4/ (SO_3 + H_2SO_4 + TPP) = 56\%$(w/w)

Procedure

200 g of 98% pure sulfuric acid was introduced into the sulfonation reactor. The acid was cooled under constant stirring to 12-15ºC by means of a cryostat. 50 g of triphenyl phosphine (TPP) (190.75 mmol) was introduced slowly at 15ºC over a period of 30-45 min. This gave a homogeneous yellow coloured solution of TPP in sulfuric acid. 280 g (141.48 ml, d=1.98 at 35ºC) of 65% oleum (SO_3 content: 2.275 mol) was transferred into the addition funnel from the oleum receiver. This oleum was then introduced in the sulfonation reactor containing TPP solution in sulfuric acid, over a period of 40-45 minutes maintaining a maximum temperature of 15ºC with rapid stirring. The temperature of the reaction mixture was then raised to 22ºC and was maintained for 76 hours using a cryostat. This step of keeping the reaction mixture at 22ºC is critical for optimum yield of TPPTS. Thereafter, the temperature of the reactor was lowered to ~ 10ºC and 50 g of distilled water was introduced while maintaining the temperature at 10ºC. This addition is necessary to quench the excess SO_3 present after the sulfonation reaction is complete. The addition of water is highly exothermic, and hence temperature was maintained at < 10ºC while adding water. This gave a solution of sulfonated triphenyl phosphine in sulphuric acid. This reaction mixture was further diluted to approximately 800 ml under cooling (10ºC). This diluted solution was then transferred into a neutralization reactor under argon atmosphere. The reactor was similar to the reaction vessel but of a larger capacity (approx. 3 litres). The solution was neutralized using 50% (w/w) degassed sodium hydroxide solution maintaining 10ºC temperature. The reaction mixture obtained was in a slurry form. The neutralized mixture was then filtered and the filtrate was evaporated under reduced pressure at 50-60ºC till the volume reduced to about 250 ml from the initial two liters. 1.5 liters of methanol was added to the above solution and the mixture was refluxed under argon atmosphere for 2 hours. TPPTS

dissolved in methanol completely, which was filtered hot, with the solid residue comprising only sodium sulphate. The filtrate was evaporated under reduced pressure. The solid TPPTS obtained was recrystallized from ethanol, weighed and stored under argon atmosphere. The yield was found to be 80-85%. ^{31}P NMR analysis (Figure 4.1) shows singlet at δ= -5.15 (TPPTS) and δ= 35.22 (OTPPTS) which is consistent with that reported in the literature[9], showing approximately 95% TPPTS and 5% OTPPTS formation as shown in Figure 4.1. No further purification of TPPTS was undertaken for use as a ligand for the preparation of water-soluble catalyst precursors.

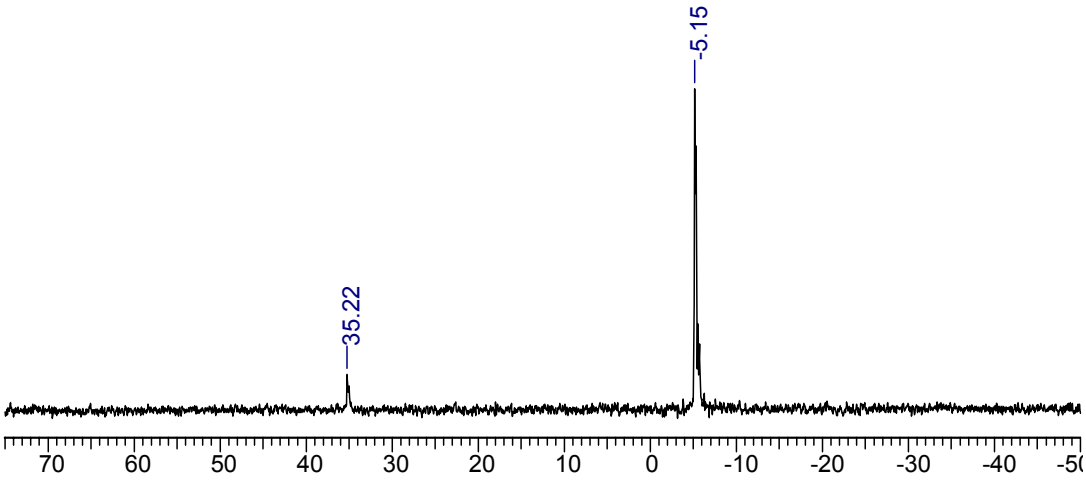

Figure 4.1: ^{31}P NMR spectrum of TPPTS

4.2.3 Synthesis of $Rh(CO)_2(acac)$

The complex was prepared as per the procedure described in Chapter 2 section 2.2.2(B).

4.2.4 Synthesis of $HRh(CO)(TPPTS_3)_3$ (catalyst C-I)

The complex was prepared by the procedure described by Hanson and coworkers[10]. A TPPTS solution (400 mg (0.704 mmol) in 1 ml water) was added to 50 mg $Rh(CO)_2(acac)$ (0.193 mmol) in a small two neck round bottom flask containing argon. H_2:CO (1:1) mixture was introduced into the flask at room temperature and atmospheric pressure. The color of the solution changes from maroon to yellow in 5 minutes. The solution was stirred under syngas atmosphere. After 6 hr of stirring the solution was filtered under a positive flow of argon to remove small amounts of Rh metal. 8 ml of absolute alcohol saturated with H_2/CO was added to yield a yellow precipitate. The solid was collected and washed with absolute alcohol and vacuum dried.

380 mg of $HRhCO(TPPTS)_3$ was obtained. The FTIR spectra of the complex shows stretching frequencies at 2007.8 cm^{-1} (υ Rh-H), 1926 cm^{-1} (υ C=O). The liquid ^{31}P NMR spectrum in D_2O shows 44.2 δ (d) (J Rh-P 150Hz), 34.2 δ (s) OTPPTS which is consistent with the literature[4]. The characterization is presented in section 4.3.1

4.2.5 Synthesis of unsupported ossified catalyst (Barium salt of $HRhCO(TPPTS)_3$ (catalyst C-II)

To a warm saturated solution of $Ba(NO_3)_2$ an aqueous solution of $HRhCO(TPPTS)_3$ (100 mg (0.05mmol) in 5 ml water) was added dropwise with constant stirring under argon atmosphere. Immediately a yellow precipitate of $HRhCO(TPPTS\text{-}Ba_{3/2})$ was obtained. The precipitate was filtered and washed with cold and hot water respectively. Quantitative yield of barium salt of $HRhCO(TPPTS)_3$ was obtained. The precipitate was soxhleted with water and toluene respectively for about 12 hours to remove the unreacted catalyst. Using similar procedures calcium and strontium salts of $HRhCO(TPPTS)_3$ were obtained, but in these cases very low yields were obtained, as the calcium and strontium salts are more soluble in water as compared to barium salts. This compares well with the solubility of Gr. 2 sulfates, (very similar in properties with sulfites) where solubility in water decreases down the group as shown in Table 4.1.

Table 4.1: Solubility of Gr. 2 metal sulfates in water[11]

Sr. no	Compound	Solubility g/100 g of water
1	$MgSO_4.7H_2O$	25.5
2	$CaSO_4$	2.1×10^{-2}
3	$SrSO_4$	1.3×10^{-2}
4	$BaSO_4$	2.4×10^{-4}

4.2.6 Synthesis of supported ossified catalyst (catalyst C-III)

The dispersed heterogenized catalyst was synthesized from the water-soluble metal complex $HRhCO(TPPTS)_3$ precipitating it as its barium salt on a porous support.

In a typical case, an aqueous solution of 20% $Ba(NO_3)_2$ (2 g, 8.51 mmol) was added to 10 grams of support. The mixture was refluxed for 4-5 hours with stirring and evaporated to dryness to get barium nitrate impregnated support. The solid supported

barium salt of $HRhCO(TPPTS)_3$ was prepared by taking 1.5 gram of above prepared $Ba(NO_3)_2$ impregnated support in a small two-neck round bottom flask. An aqueous solution of $HRhCO(TPPTS)_3$ (131.5 mg, (7×10^{-2} mmol) in 5 ml water) was added dropwise under constant stirring in a positive flow of argon under warm condition, followed by 5 ml of an aqueous solution of 240.5 mg TPPTS, (0.42 mmol, Rh:P=1:6). The stirring was continued for 4-5 hours. The mixture was filtered and the precipitate was washed 2-3 times with cold and hot water respectively. The solid catalyst obtained was soxhleted using water and toluene for 12 hours each to remove the unreacted catalyst and TPPTS. The precipitate was dried under vacuum (yield= 1.73 g.). Using a similar procedure ossified $HRhCO(TPPTS)_3$/Ba catalyst dispersed on supports like carbon, SiO_2, TiO_2, Al_2O_3, ZrO_2, La_2O_3, and MgO were prepared. For kinetic studies the catalyst was prepared in a big batch, to ensure that the same catalyst was used throughout.

4.2.7 Synthesis of TPPTS-$Ba_{3/2}$ and carbon supported TPPTS-$Ba_{3/2}$

To a saturated aqueous solution of $Ba(NO_3)_2$ (15-20 ml), a solution of TPPTS (600 mg, (1.05mmol) in 5 ml distilled degassed water) was added drop wise with constant stirring in a two-neck flask under argon atmosphere. Immediately, a white precipitate of TPPTS-$Ba_{3/2}$ was obtained. The precipitate was filtered and washed with cold and hot water. Quantitative yield was obtained.

To prepare a carbon supported TPPTS-$Ba_{3/2}$, an aqueous solution of TPPTS (200 mg, (0.349 mmol) in 5 ml water) was added slowly to a $Ba(NO)_3$ impregnated carbon (0.5 g) with constant stirring under warm condition and argon atmosphere. The solution was filtered and washed with cold and hot water. The yield of carbon supported TPPTS-$Ba_{3/2}$ was 0.49 g.

4.2.8 Experimental set up and procedure

The experimental setup and procedure for performing hydroformylation reactions was the same as described in Chapter-2, except that heterogeneous catalysts were used in place of the homogeneous catalysts.

4.2.9 Analytical methods

FT-IR of the catalysts was recorded on a Bio-Rad Spectrophotometer 175C. Liquid ^{31}P NMR spectra were obtained on a Bruker AC-200 or MSL-300 spectrometer in D_2O at room temperature. ^{31}P solid state NMR (CP-MAS) spectra of all the heterogeneous materials were obtained on a UXNMR, Bruker Analytische Messtechnik GmbH FT-NMR spectrometer at 5 or 8 kHz. The chemical shifts were referred to H_3PO_4 at 0 ppm and the spectra were collected with a flip angle of 45° and 6000 real data points. X-ray photoelectron spectroscopy (XPS) measurements were recorded using a VG Microtech ESCA 3000 instrument at 10^{-10} torr Pressure, a pass energy of 50 eV, and using unmonochromatized Mg-K_α (photon energy –1253.6 eV) as the radiation. Powder X-ray diffraction (XRD) spectra were obtained at room temperature on a Rigaku D MAX III VC diffractometer using Ni-filtered Cu-K_α radiation, λ = 1.5404 Å, where 2θ ranges were from 2° to 80° at a scan rate of 8°/min. For scanning electron microscopy (SEM), the crystalline supports were suspended in isopropanol, cast on gold plated discs, followed by drying under vacuum and were imaged on a Philips XL 30 Instrument. Energy dispersive X-ray analysis (EDX) was recorded on Philips XL 30 Instrument, while transmission emission spectroscopy (TEM) was recorded on Perkin Elmer Instrument. Specific surface areas of the samples were determined by the BET method using N_2 adsorption measured with an Omnisorb CX-100 Coulter Instrument. Inductively coupled plasma with atomic emission spectra (ICP-AES) analysis (Perkin-Elmer 1200 instrument) or GFAAS analysis (GBC Avanta Sigma Instruments Australia, with photo multiplier tube (PMT) as detector) was performed for quantifying rhodium leaching. The quantitative analysis of reactants and products was carried out by a gas chromatographic method on a HP-5 (5% phenylmethyl siloxane as a stationary phase) capillary column. For this purpose, HP 6890 gas chromatograph was used. The standard GC conditions for the analysis of reactant and hydroformylation products of different olefins are as described in Chapter 3 section 3.2.8. All the olefin hydroformylation products were identified by GC-MS (Agilent GC 6890N with 5973 mass selective detector instrument).

4.3 Results and discussion

The main objective of this work was to synthesize heterogeneous catalysts by immobilization of the homogeneous water soluble complex catalyst, their characterization using various spectroscopic techniques and the evaluation of their performance in hydroformylation of olefins. Here, we describe a simple method for the synthesis of novel heterogenized catalysts which are highly stable and active for the hydroformylation of olefins. The methodology is termed as 'ossification.' The ossification is the biological terminology for the process of bone formation, in which connective tissues, such as cartilage are turned to bone or bone-like tissue. Bone tissue matrix consist of abundant inorganic components alongwith organic components. They are mineral salts, mainly hydroxyapatite (a crystallized form of tricalcium phosphate), some calcium carbonate, and small amounts of magnesium hydroxide, fluoride and sulphate. They give the bone its unique characteristic among all the other tissues: an exceptional hardness which allows it to resist compression.

The major component of bone is calcium phosphate where the trivalent phosphate anion is bonded to the divalent calcium which gives unique hardness to the bone. In a similar way it is possible that the trivalent sulphite (group) anion of water soluble TPPTS ligand on interaction with the Gr. 2 metal can produce a material which is resistant to the harsh condition of temperature and pressure.

Our approach of ossification of catalysts involves heterogenization of homogeneous water soluble metal complex catalysts, $HRh(CO)(TPPTS)_3$ by its precipitation as sulphites of Gr.2 elements such as Ca, Sr or Ba. The resulting heterogenized catalyst is not only insoluble in water but also in a majority of organic solvents. In a typical case, the catalyst is formed by interaction of barium nitrate with an aqueous solution of $HRh(CO)(TPPTS)_3$ [catalyst C-I] to form a precipitated Ba^{+2} salt of $HRh(CO)(TPPTS)_3$ [catalyst C-II]. It is also possible to obtain such catalyst on solid supports termed as 'supported ossified catalyst'. This catalyst is formed by interaction of $Ba(NO_3)_2$ impregnated support with an aqueous solution of $HRh(CO)(TPPTS)_3$ and NaTPPTS [1:6], to form a precipitated Ba^{+2} salt of $HRh(CO)(TPPTS)_3$ and free $TPPTS\text{-}Ba_{3/2}$ where Ba^{+2} is adsorbed on the support surface by physical adsorption [catalyst C-III]. This method of immobilization is generic in nature and can be applied to a variety of

catalysts supports, and catalytic reactions. Moreover, precipitation onto a support using a pre-adsorbed Ba^{+2} species provides a highly dispersed, active and stable form of catalyst C-II with a much larger surface area. These catalysts give a significantly enhanced activity for the hydroformylation of higher olefins. A schematic representation of the catalyst is shown in Figure 4.2(a) and the proposed structure of the catalyst species could exist in the polymeric form as shown in Figure 4.2(b) or as a dimer.

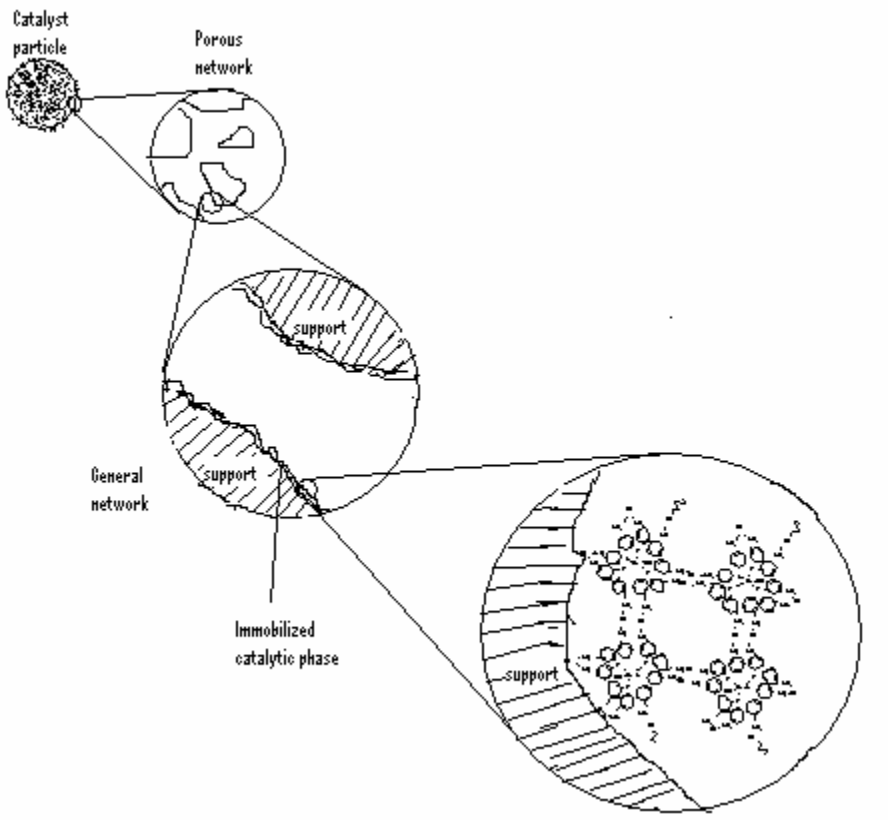

Figure 4.2(a): Schematic presentation of the ossified catalyst.

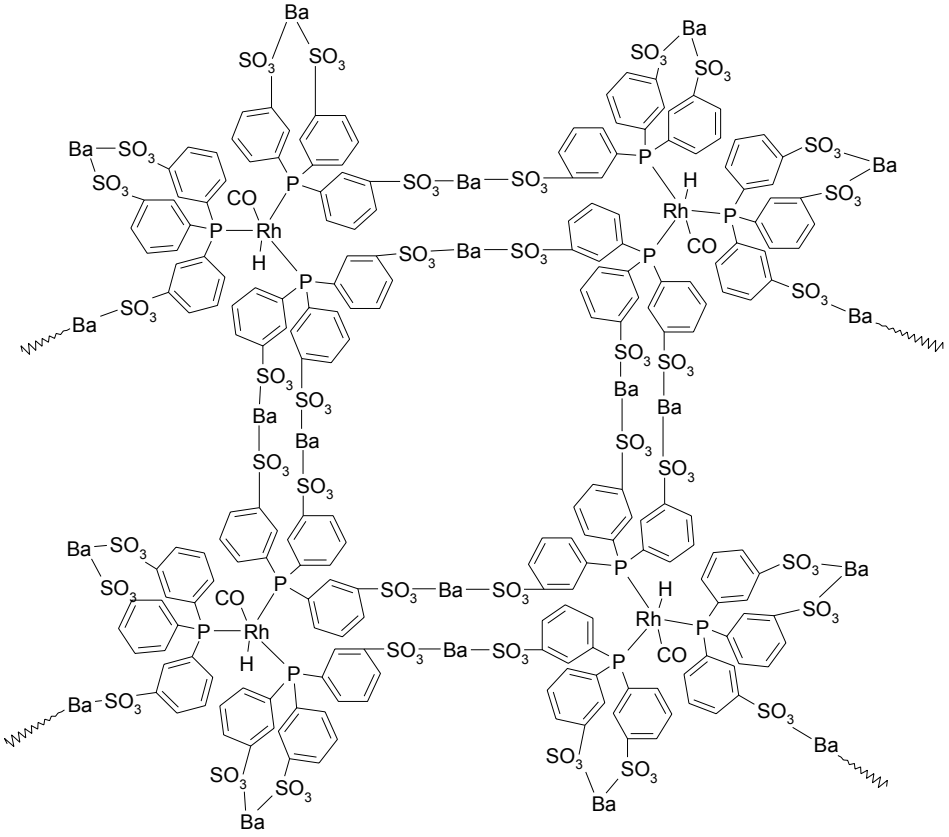

Figure 4.2(b): Proposed structure of the ossified catalyst.

The catalyst C-I, catalyst C-II and catalyst C-III were characterized by FTIR, solid state ^{31}P NMR, powder XRD, SEM, TEM, EDX and XPS. The BET surface area, pore size and pore volume was also measured. The detailed characterization is discussed below.

4.3.1 Characterization of unsupported and supported ossified catalyst

4.3.1.1 FT-IR spectra

An infrared spectrum gives valuable information for all the functional groups of the catalyst system. IR spectra of $HRh(CO)(TPPTS)_3$ [catalyst C-I], unsupported ossified catalyst [catalyst C-II] and supported ossified catalyst [catalyst C-III] are shown in Figure 4.3, 4.4 and 4.5 respectively. Most of the investigation using supported ossified catalyst is mainly on carbon support. However, since carbon supported ossified catalyst showed total absorbance in the IR region, a similar catalyst was prepared on silica support [catalyst C-IV] and was characterized using DRIFT-IR. Weak bands at 1866 (νCO) cm^{-1}

and 1998 (νRh-H) cm^{-1} were observed corresponding to carbonyl and and Rh-H stretching frequencies respectively. whereas the corresponding values for the catalysts C-I and catalyst C-II were 1926 and 2008 cm^{-1} and 1977 and 2063 cm^{-1} respectively. The shift to lower frequencies as compared to the water-soluble complex could be due to support-catalyst interaction. The weak bands observed are probably due to the lower loading of the complex on support.

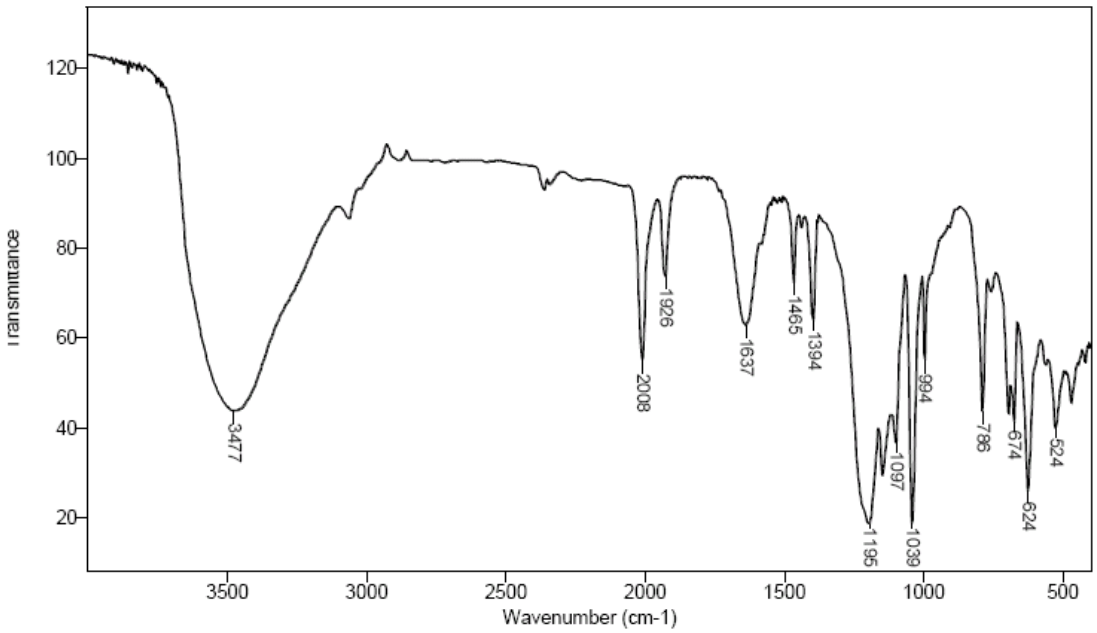

Figure 4.3: FT-IR spectra of catalyst C-I

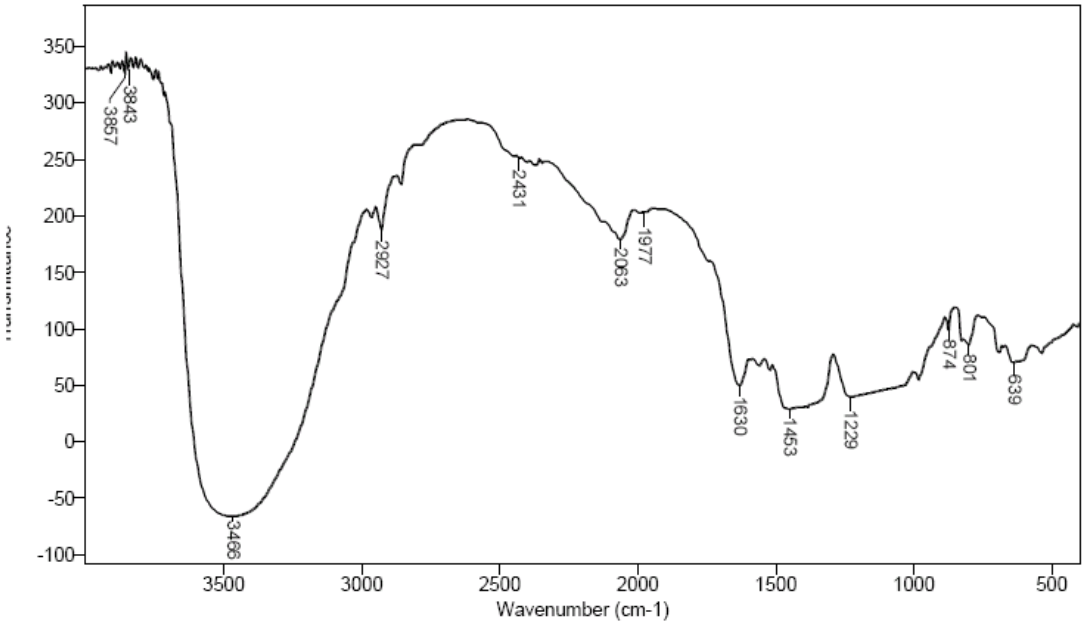

Figure 4.4: FT-IR spectra of catalyst C-II

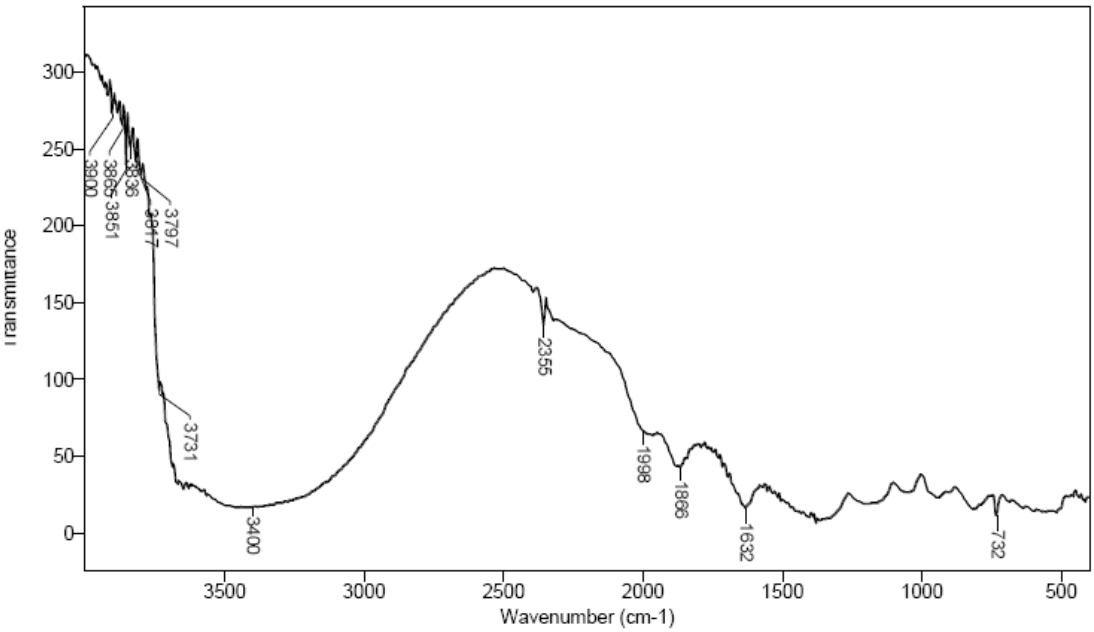

Figure 4.5: FT-IR spectra of catalyst C-IV

4.3.1.2: ^{31}P solid state NMR

In literature, the supported catalysts have been characterized by a variety of methods, but multinuclear solid state NMR has turned out to be a particularly useful method. In order to know the interactions of the different components of the heterogeneous catalyst system, (metal complex to support) and seek conclusive evidence of the heterogeneous nature of complexes, ^{31}P solid state NMR of the catalyst C-I, (Figure 4.6), catalyst C-II (Figure 4.7) and catalyst C-III (Figure 4.8) were recorded. The solid state ^{31}P NMR of catalyst C-I shows a singlet at 44.25 δ and 28.23 δ. The signal at 44.25 δ was attributed to the coordinated phosphine and the signal at 28.23 δ was attributed to the OTPPTS. The other signals are referred as the side bands in solid state NMR at 8 KHz. The solid-state ^{31}P NMR of unsupported ossified catalyst (catalyst C-II) showed a singlet at 30.13 δ. When the same complex was precipitated on support i.e carbon supported ossified catalyst (catalyst C-III) it shows a signal at 2.51 δ and a multiplet at 23.89 δ. The signal at 2.51 δ is due to the free TPPTS-$Ba_{3/2}$ as an excess of TPPTS is used in the preparation of the supported complex. The multiplet at 23.89 δ may arise from the mixing of the signals from the coordinated phosphine and phosphine oxide. The shift in the signals as compared to catalyst C-II could be a result of interaction of the catalyst with support. The solid state ^{31}P NMR of the catalyst C-III after reaction (Figure 4.9) is identical (signal at 2.42 δ and a multiplet at 24.37 δ) showing no change in catalyst even after reaction. To confirm the chemical shifts for the uncoordinated TPPTS-$Ba_{3/2}$, the TPPTS-$Ba_{3/2}$ and C-TPPTS-$Ba_{3/2}$ were synthesized separately and characterized. The solid state ^{31}P NMR of TPPTS-$Ba_{3/2}$ (Figure 4.10) shows a singlet at -2.85 δ due to the P^{III} (deshielded compared to TPPTSNa (-5.15 δ (s)) and a singlet at 32.60 δ due to the P^{V} i.e OTPPTS$Ba_{3/2}$ (lesser deshielding compared to the bound OTPPTSNa 35.28 δ (s)). On the other hand the ^{31}P NMR of C-TPPTS-$Ba_{3/2}$ (Figure 4.11) shows a singlet at 3.41 δ and 24.30 δ (s) due to the P^{III} and P^{V} respectively. As with TPPTS-$Ba_{3/2}$, here also P^{III} is more deshielded than TPPTS-$Ba_{3/2}$ (-2.85 δ) while P^{V} is more shielded than OTPPTS$Ba_{3/2}$ (32.60 δ). These shifts are solely due to the catalyst-support interaction. The ^{31}P solid state NMR signal values are tabulated in Table 4.2.

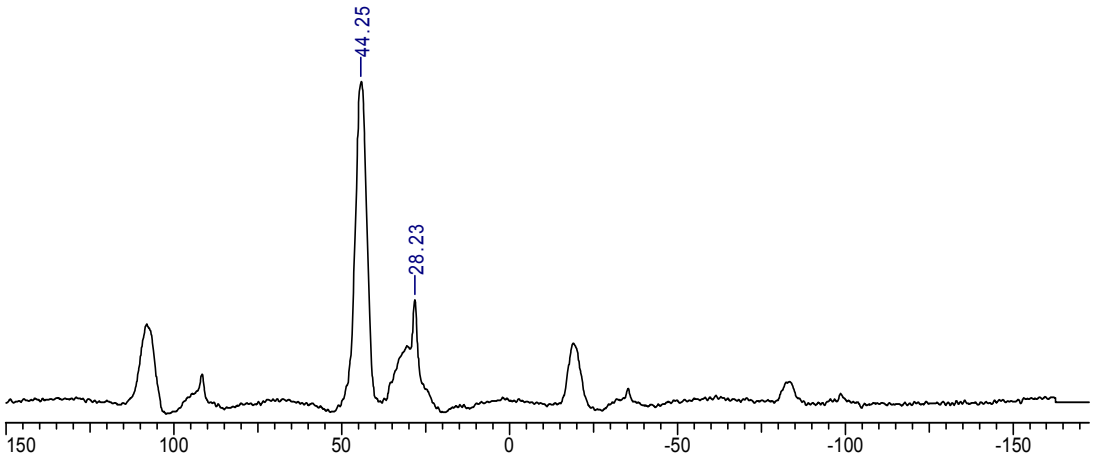

Figure 4.6: Solid state ^{31}P NMR spectrum of catalyst C-I

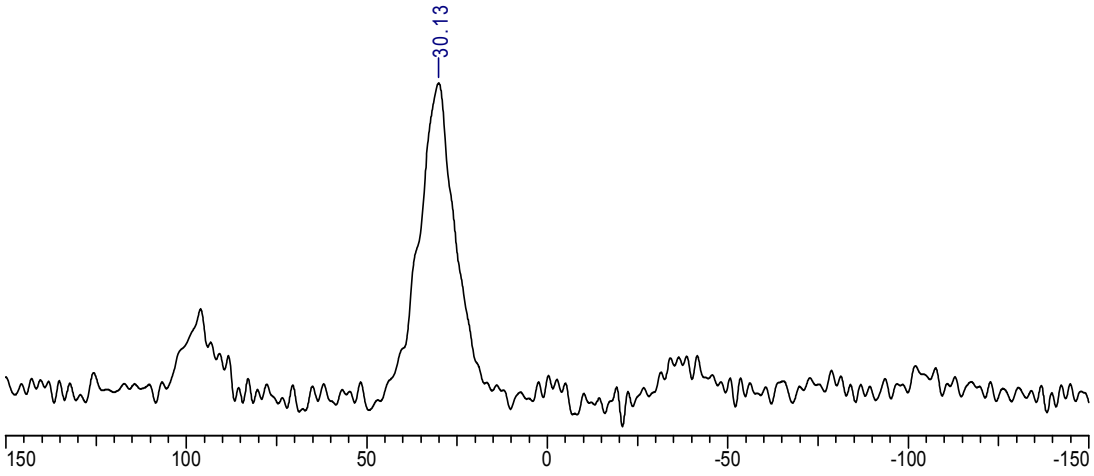

Figure 4.7: Solid state ^{31}P NMR spectrum of catalyst C-II

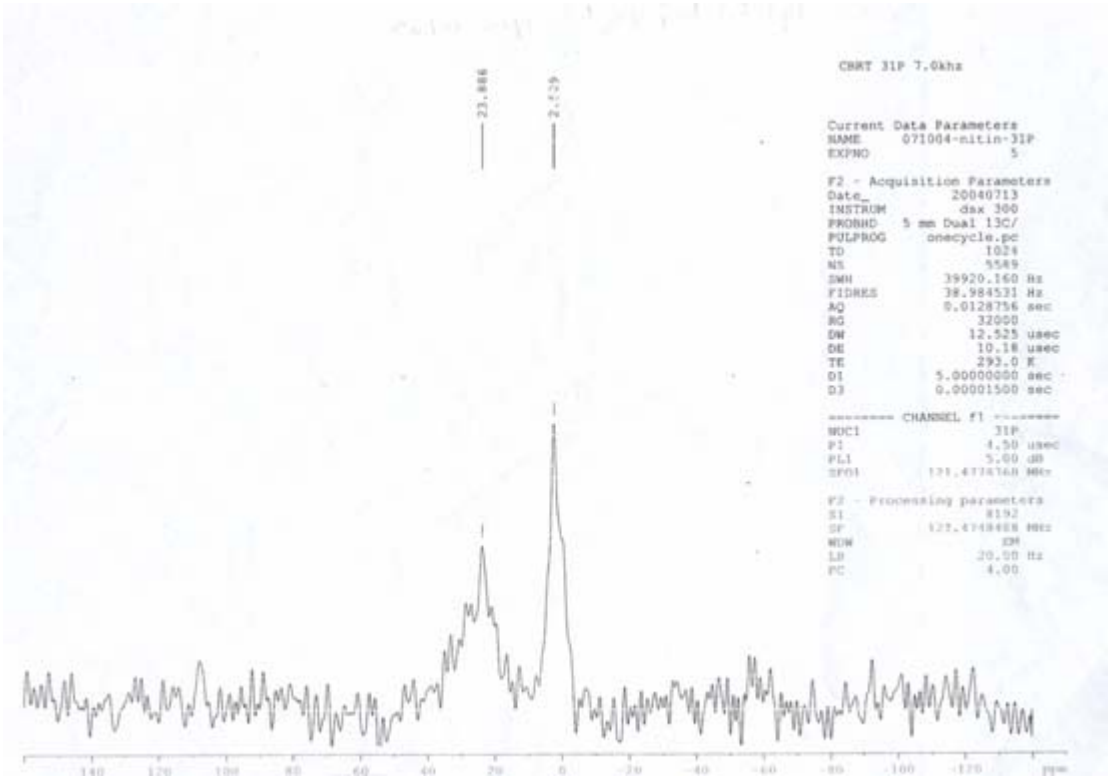

Figure 4.8: Solid state ^{31}P NMR spectrum of catalyst C-III before reaction

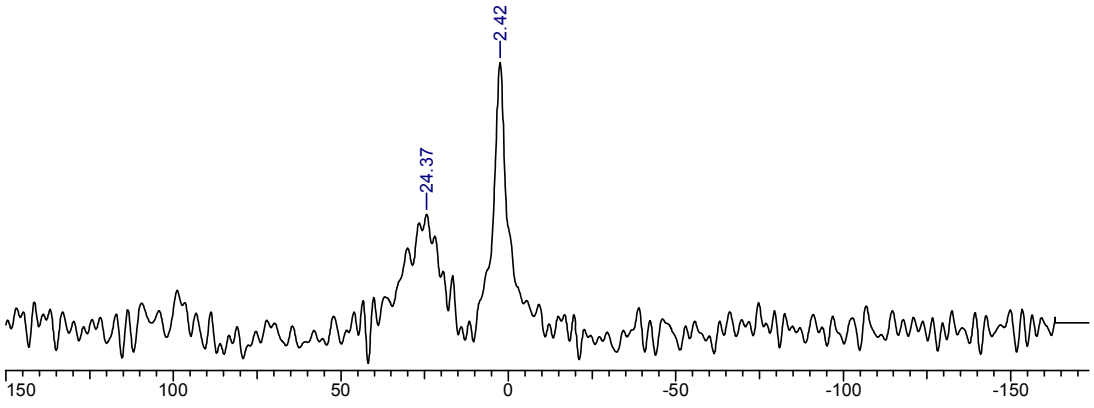

Figure 4.9: Solid state ^{31}P NMR spectrum of catalyst C-III after reaction

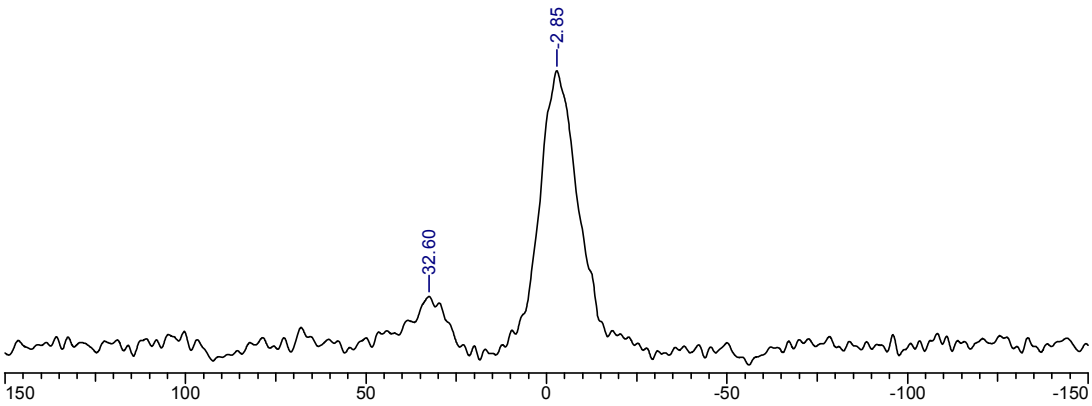

Figure 4.10: Solid state ^{31}P NMR spectrum of TPPTS Ba $_{3/2}$

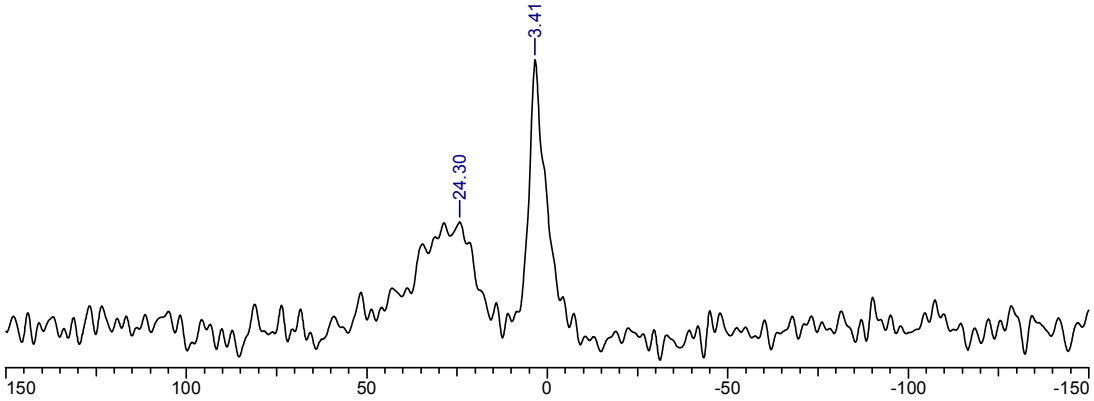

Figure 4.11: Solid state ^{31}P NMR spectrum of C-TPPTS Ba $_{3/2}$

Table 4.2: Solid state NMR values of ossified catalysts

Sample	P^{III} (bound to Rh)	P^{V} (Phosphine Oxide unbound)	P^{III} Excess TPPTSBa (unbound)	Description
Catalyst C-I	44.25δ(s)	28.23 δ(s)		
Catalyst C-II	30.13δ (s).	-		
Catalyst C-III	23.89 δ (m)		2.51 δ(s)	Multiplet could be due to mixing of P^{III} and P^{V} Peaks
Catalyst C-III after reaction	24.37δ(m)		2.42 δ(s)	Multiplate could be due to mixing of P^{III} and P^{V} Peaks
(Catalyst C-IV)	27.51 δ (m)			Multiplate could be due to mixing of P^{III} and P^{V} Peaks
TPPTS-$Ba_{3/2}$		32.60 δ (s)	-2.85 δ(s),	
C-TPPTS-$Ba_{3/2}$		24.30 δ (s)	3.41 δ(s),	

4.3.1.3 Powder-XRD analysis

Figure 4.12 shows the superimposed powder X -ray diffraction pattern of the ossified catalysts. The XRD pattern of the catalyst C-II, C-III and C-IV were identical although, a significant peak at 43.1º, observed for the catalyst C-II, which could be attributed to Rh (111) plane, indicates very high concentration of rhodium in catalyst C-II (Unsupported ossified catalyst). The poor signal at similar 2θ values for C-III and C-IV indicate lower concentration of rhodium. In addition, a crystallite size of ca. 9 nm has been calculated by using Scherrer's equation[12] for Rh (111) in catalyst C-II.

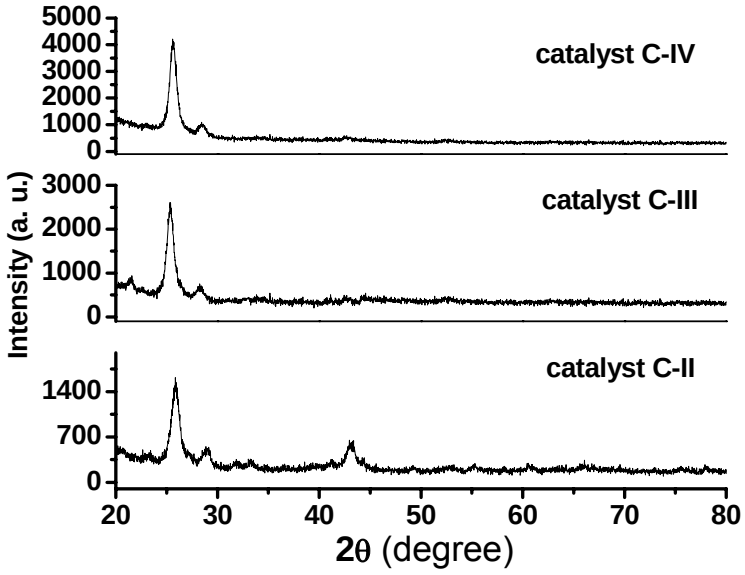

Figure 4.12: Superimposed XRD (powder pattern) spectra of catalyst C-II, C-III and C-IV

4.3.1.4 X-ray photoelectron spectroscopy (XPS) analysis

Surface analysis by XPS spectra was carried out in terms of the binding energy values of various elements present (rhodium, phosphorus, carbon, oxygen and barium) in the catalyst, and the supports after the necessary $C_{(1s)}$ correction (Figure 4.13). XPS of these catalysts were also performed after hydroformylation reactions in order to record any changes in the oxidation states or binding energy values[13]. These were in compliance with the literature values (Table 4.3, 4.4 and 4.5). The binding energy values before and after the reaction were almost similar, which proves that the oxidation state of the

elements remain unaltered even after the reaction. It also suggests that all rhodium is present in +1 oxidation state without undergoing any irreversible change from its original oxidation state in $HRh(CO)(TPPTS)_3$. Two peaks corresponding to S $2p_{3/2}$ are observed at 166.8 and 168.8 eV indicates the presence of different environment like $BaSO_4$ (168.8eV) and trace amount of precursor (166.8 eV), where the π-cloud of phenyl rings could shift the binding energy to the lower value.

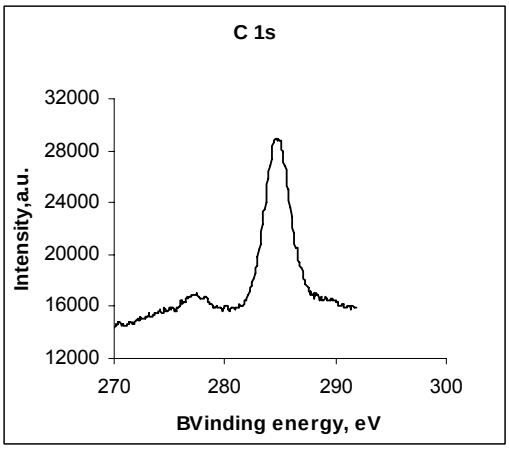

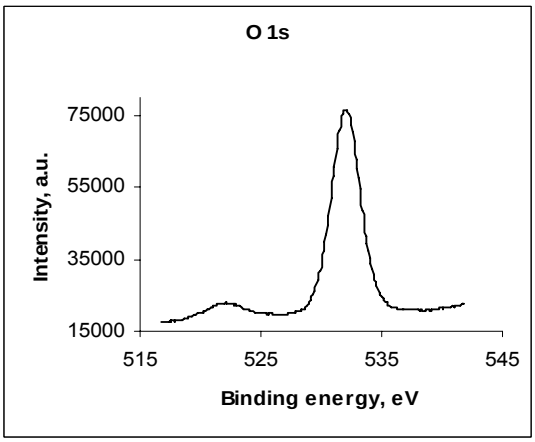

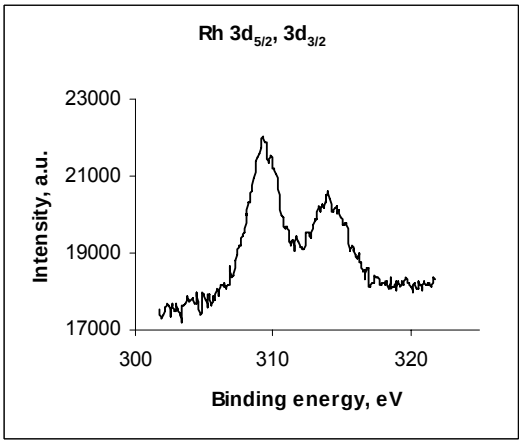

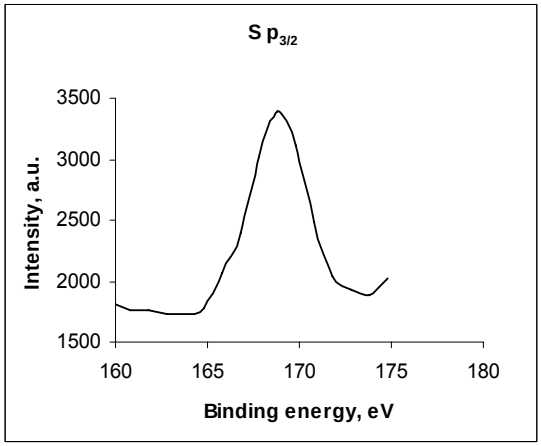

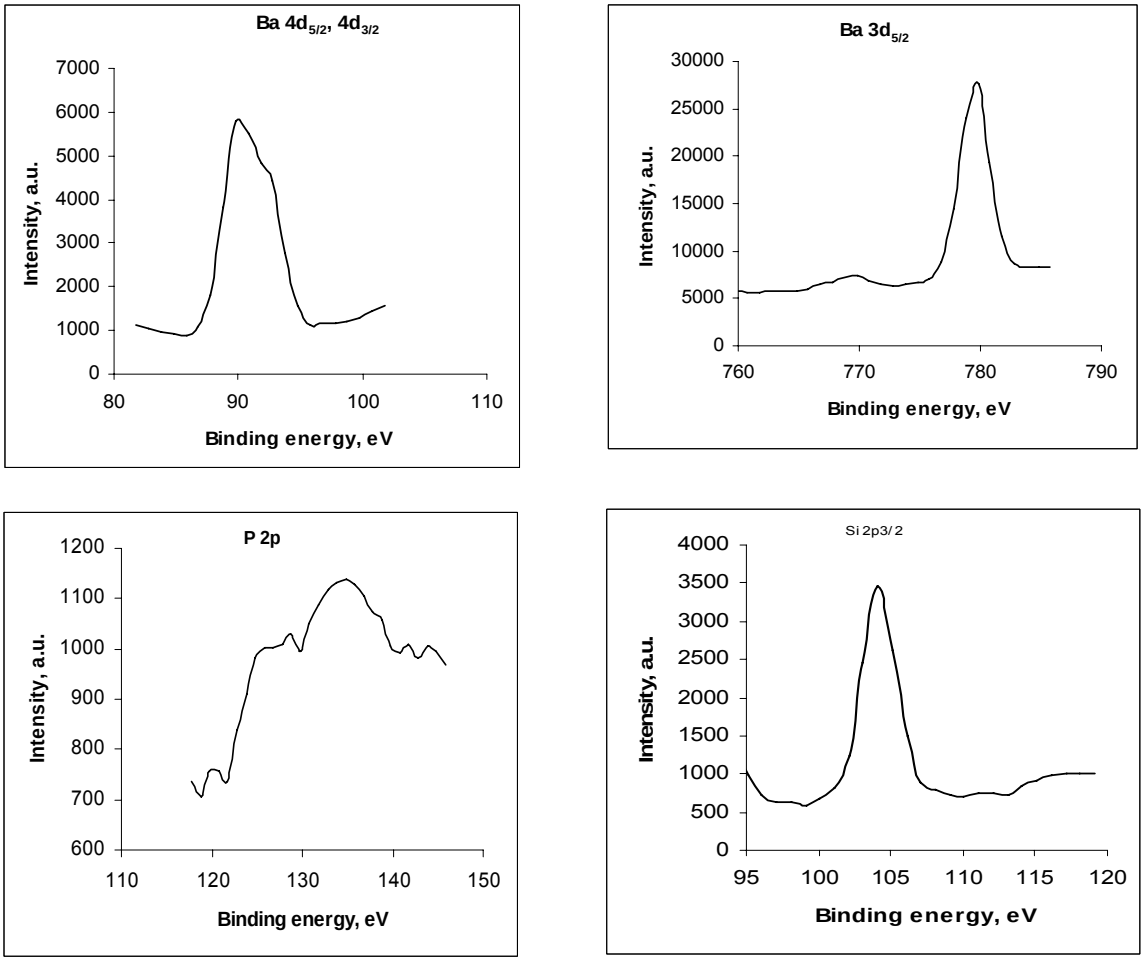

Figure 4.13: Representative X-ray photoelectron spectra (XPS) of catalyst C-II, (similar XPS were obtained for the Catalyst CIII and CIV (refer Table 4.3, 4.5 and 4.6). The spectra for Si $2p_{3/2}$ was observed only for Catalyst C-IV)

Table 4.3: XPS analysis of Catalyst C-II

Values (eV)	C	Ba			P	S	O	Rh	
	1s	$3d_{5/2}$	$4d_{3/2}$	$4d_{5/2}$	2p	$2p_{3/2}$	1s	$3d_{5/2}$	$3d_{3/2}$
Observed	293.2	789	101.0	98.2	141	177	540	317.6	322.2
Corrected*	285	780.8	92.8	89.8	132.8	168.8	531.8	309.4	314.0
Literature	285	780.6	92.8	90.5	131.2	168.3	531	309.1	313.9

Table 4.4: XPS analysis of Catalyst C-III

Values (eV)	C	Ba			P	S	O	Rh	
	1s	$3d_{5/2}$	$4d_{3/2}$	$4d_{5/2}$	2p	$2p_{3/2}$	1s	$3d_{5/2}$	$3d_{3/2}$
Observed	284.4	783	93.0	90.8	133.6	171.0	534	309.9	314.7
Corrected*	285	783.6	93.6	91.4	134.0	171.6	534.6	309.3	314.1
Literature	285	780.6	92.8	90.5	131.2	168.3	531	309.1	313.9

Table 4.5: XPS analysis of Catalyst C-IV

Values (eV)	C	Ba			P	S	Si	O	Rh	
	1s	$3d_{5/2}$	$4d_{3/2}$	$4d_{5/2}$	2p	$2p_{3/2}$	$2p_{3/2}$	1s	$3d_{5/2}$	$3d_{3/2}$
Observed	291.9	787	99	97.0	135.9	176	110	540	316.9	321
Corrected*	285	781.1	93.1	91.9	130.0	170.1	104.1	534.1	310.0	314.1
Literature	285	780.6	92.8	90.5	131.2	168.3	102.5	531	309.1	313.9

*All the values were corrected to $C_{(1s)}$ with binding energy of 285 eV using adventitious carbon.

4.3.1.5 Scanning Electron Microscopy (SEM) and Energy Dispersive X-ray Analysis (EDAX or EDX)

Topography and morphology of the catalyst samples were investigated using scanning electron microscopy (SEM). Topography gives the surface features of an object or "how it looks", its texture; and morphology gives the shape, size and arrangement of the particles making up the object that are lying on the surface of the sample or have been exposed by grinding or chemical etching. The micrographs of the catalyst C-II and C-III and C-IV are shown in Figure 4.14, 4.15 and 4.16 respectively. The micrograph of unsupported ossified catalyst shows that the catalyst is present in free form as well as in cluster form. On the other hand for the supported ossified catalyst, catalyst particles are unevenly distributed on the support. The SEM image of the catalyst shows catalyst particle as a white spots on the support (carbon or silica particles).

EDX or EDAX is a technique used for identifying the elemental composition of the specimen, or in an area of interest (areas ~ 1 micrometer in diameter). EDX analysis was carried out on the SEM instrument. Figure 4.17 and 4.18 shows the EDX of catalyst C-II and C-III. EDX performed in selected region of the SEM micrograph produced strong signals for Rh, Ba, S and O. The elemental ratios are slightly different from those obtained from chemical elemental analysis of the bulk sample. EDX gives elemental ratios for any selected surface, and a non-uniform distribution of metal on support can be a plausible reason for this observation.

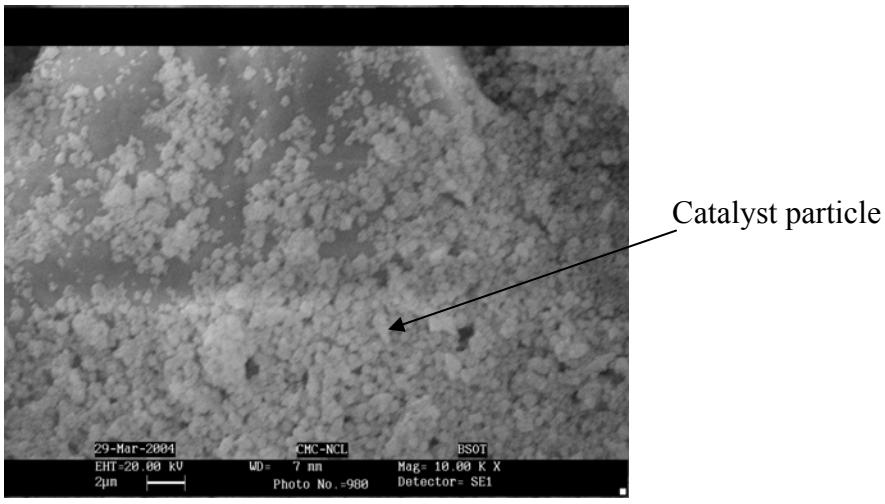

Figure 4.14: SEM image of catalyst C-II

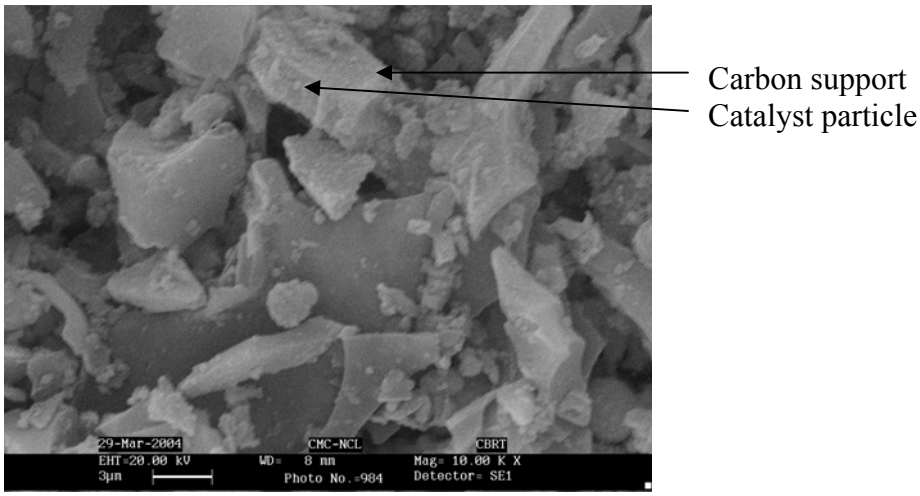

Figure 4.15: SEM image of catalyst C-III

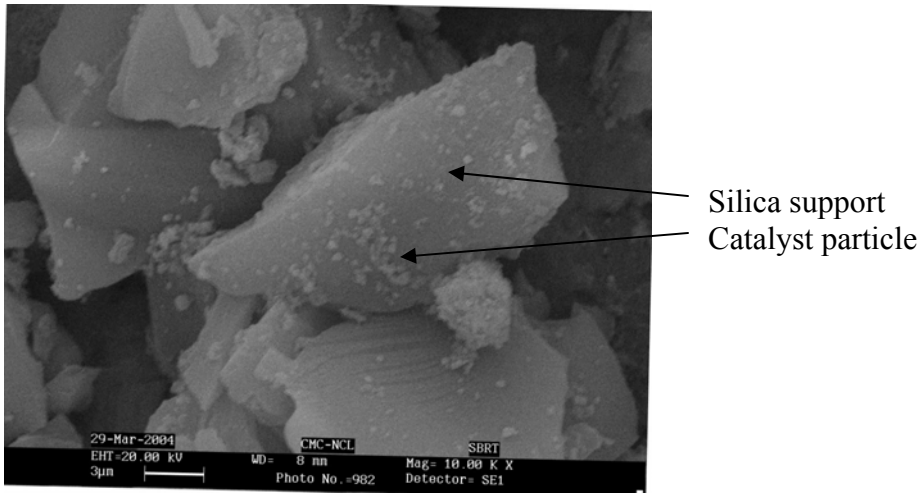

Figure 4.16: SEM image of catalyst C-IV

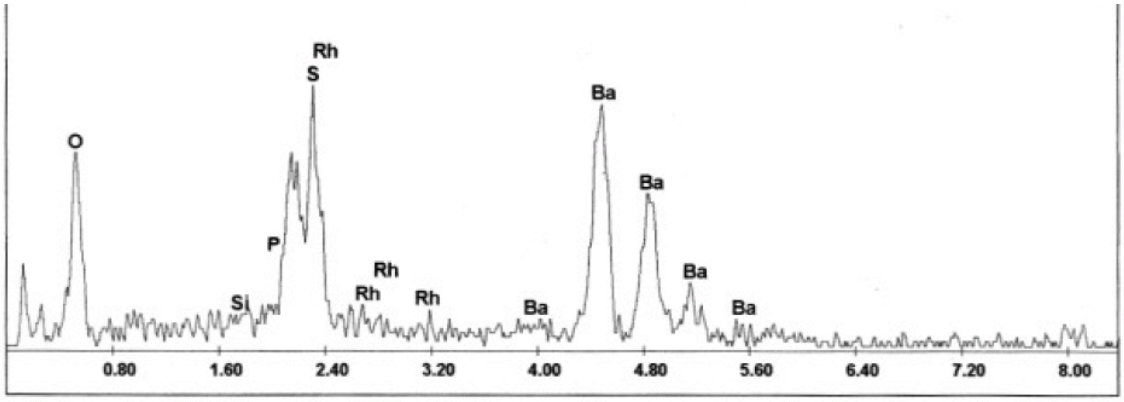

Figure 4.17: EDX spectrum of catalyst C-II

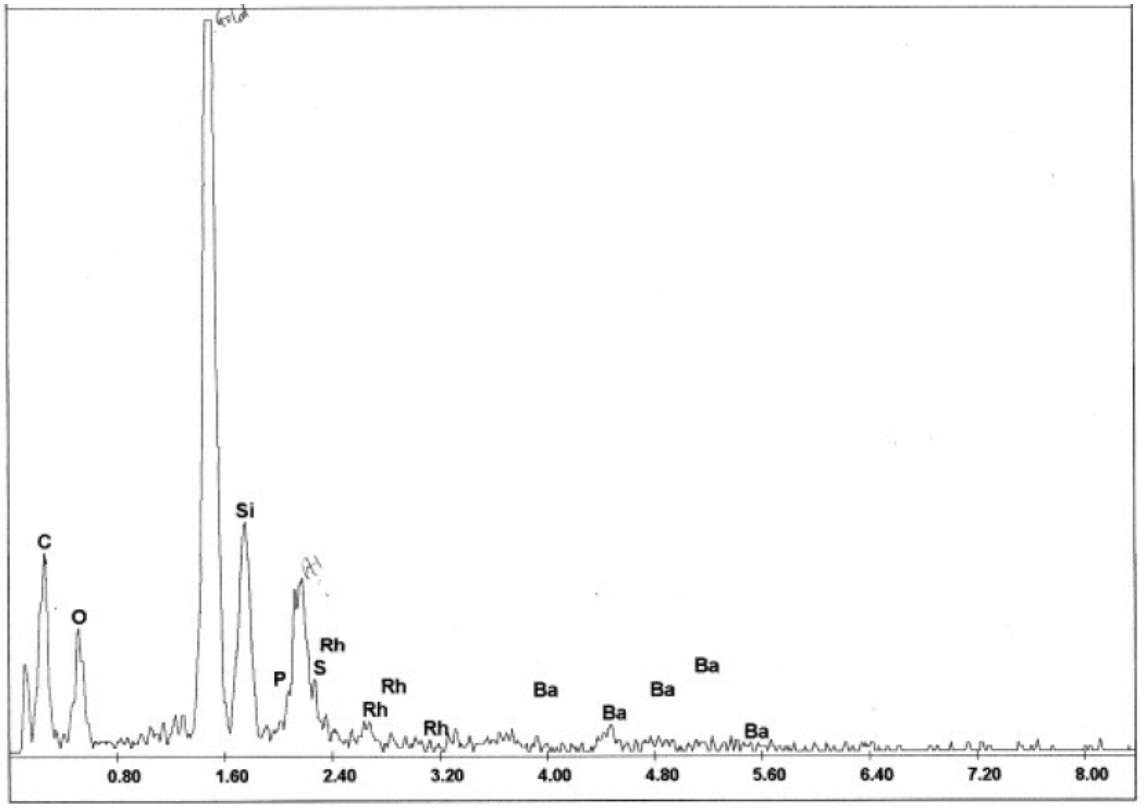

Figure 4.18: EDX spectrum of catalyst C-III

4.3.1.6 Transmission Emission Microscopy (TEM)

The TEM analysis gives the size, shape and arrangement of the particles which make up the specimen as well as their relationship to each other on the scale of atomic diameters. TEM analysis was done by dispersing the catalyst samples in isopropanol and placing them on holey copper grids. The instrument was operated at an accelerating voltage of 100KV for imaging the samples. The TEM images of the catalyst C-II, carbon support and catalyst C-III are shown in Figure 4.19, 4.20 and 4.21 respectively. The TEM image of C-III shows a $HRh(CO)(TPPTS\text{-}Ba_{3/2})_3$ average particle size of 150-200 nm as against ~300 nm for catalyst C-II.

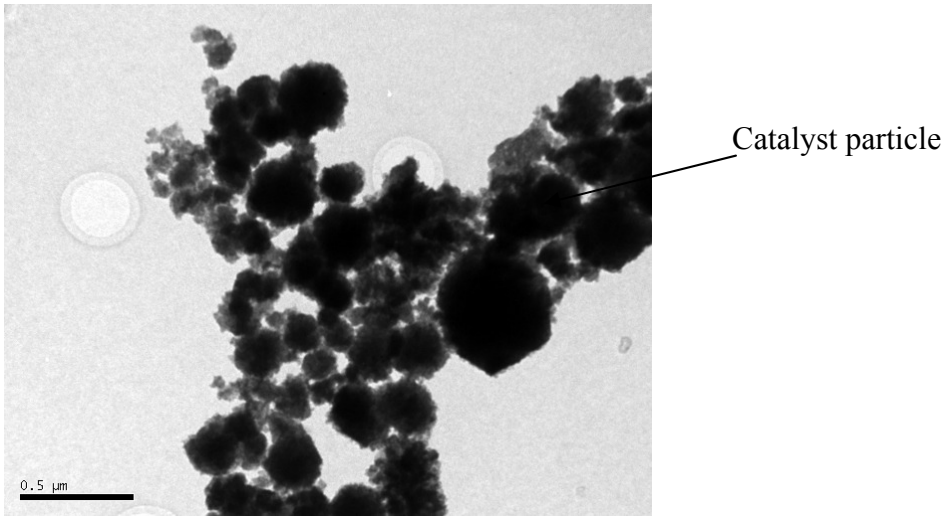

Figure 4.19: TEM image of catalyst C-II

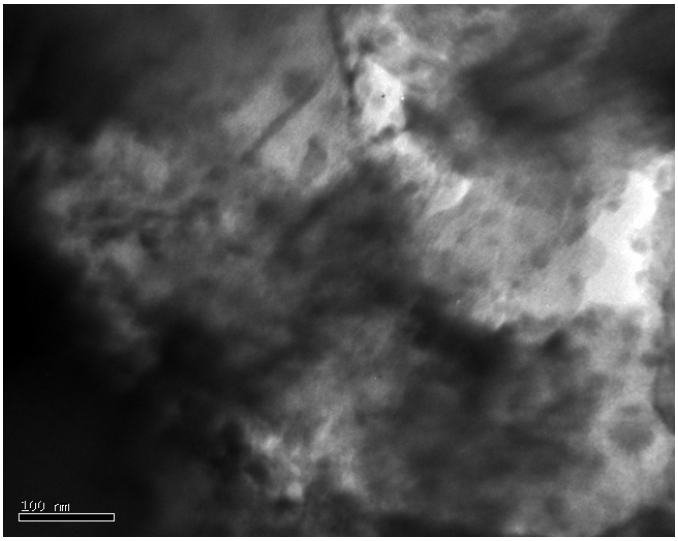

Figure 4.20: TEM image of carbon support

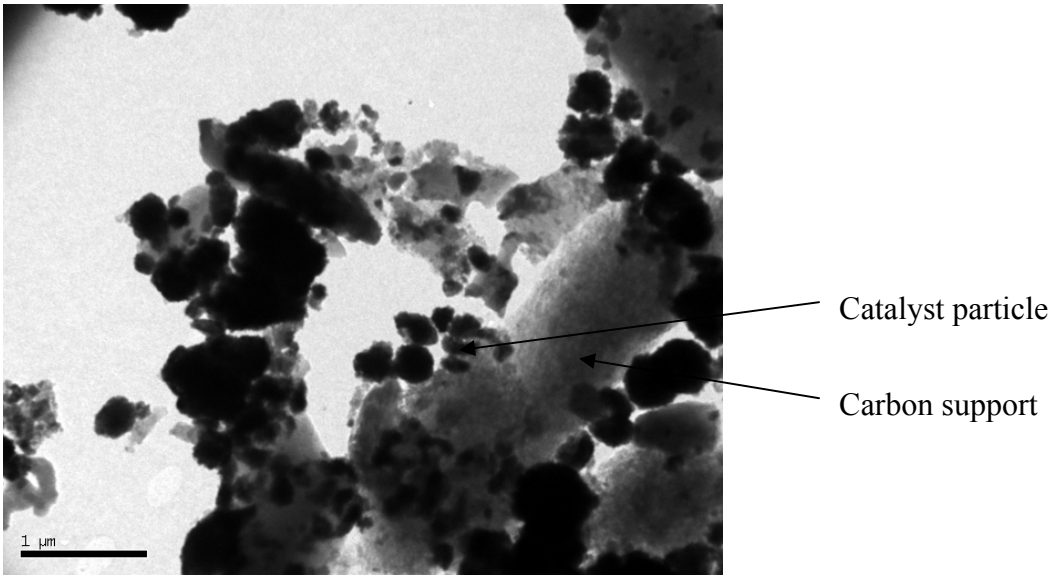

Figure 4.21: TEM image of catalyst C-III

4.3.1.7 BET surface area, pore size and pore volume analysis

The gas adsorption technique may be used to measure the specific surface area and pore size distribution of powdered or solid materials. Nitrogen is used in our study to measure BET surface because of its lower saturation vapor pressures at liquid nitrogen temperature. The surface area of catalyst C-III showed a reduction as compared to the virgin support carbon, (36.43 and 158.3 m^2/g respectively). As expected the pore volume also dropped to 0.066 cm^3/g for C-III as compared to 0.133cc/g for the support. The catalyst was found to block smaller pores with diameters below 35 A^o and the pores with size of 35 A^o were in maximum number. For the support, the average pore diameter was 33 A^o. The physical characteristics of support and ossified catalysts are shown in Table 4.6.

Table 4.6: Physical characteristics of support and ossified catalyst.

Sr. no	Material	S_{BET} m^2/g	Total pore volume cm^3/g	Micropore area m^2/g
1	Activated carbon	158.3	0.133	70.67
2	Catalyst C-III	36.43	0.066	25.41
3	High surface area microporous carbon	1142	0.54	1008
4	Microporous carbon supported ossified catalyst	1124	0.51	994
5	Mesoporous carbon	1027	1.0	125
6	Mesoporous carbon supported ossified catalyst	390	0.80	33

The data interpretation using the above instrumental techniques reveals the physical interaction between precipitated complex and the support. The catalyst is also in a true heterogenized form, unevenly distributed onto the support.

4.3.2 Feasibility of hydroformylation of olefins using ossified (unsupported) catalyst C-II

Initially hydroformylation of 1-hexene and 1-decene was carried out at 343 K in toluene using catalyst C-II. Very little hydroformylation activity was observed. When the reaction temperature was increased upto 373K, reaction occurs after an induction period of 20 minutes. More than 99 % 1-hexene conversion was obtained with good aldehyde selectivity with a TOF of 157 h^{-1} (Table 4.7, entry 1). The aldehyde products constitutes of heptanal, 2-methyl-hexanal, 2-ethyl-pentanal and 2-propyl-butanal. The n/i ratio was also improved compared to that in homogeneous organic phase reaction in toluene. The final reaction solution shows slightly yellowish colour. To confirm whether the reaction was occurring due to leaching of metal to the organic phase, recycle of the solid catalyst was carried out. The result shows that catalyst activity drops on recycle for hydroformylation of 1-hexene. The ICP analysis shows a rhodium leaching of > 2 % showing the predominant rhodium leaching in the organic phase. Hydroformylation of 1-decene was also carried out under similar reaction conditions with almost 100% conversion and 94 % aldehyde selectivity (Table 4.7 entry 2). The aldehyde products

constitutes of undecanal, 2-methyl decanal, 2- ethyl-nonanal, 2- propyl-octanal, and 2-butyl-heptanal. In this case also rhodium leaching (2.4%) was observed in the reaction crude. The low hydroformylation activity observed for the catalyst C-II is probably due to the fact that only the surface rhodium complex is available for the reaction and that a majority of the catalyst is inside the solid catalyst particles/clusters. As regards the leaching of the rhodium into the organic phase, one of the possible reasons is the absence of any free TPPTS ligand. (The catalyst was prepared using the complex without any excess ligand) The free $TPPTSBa_{3/2}$ if available may bind to any free rhodium and can thus reduce or prevent leaching.

Table 4.7: Hydroformylation of 1-hexene and 1-decene using unsupported ossified catalyst (Catalyst C-II):

Sr. no	Substrate	Conversion (%)	Aldehyde selectivity (%)	Isomerized olefin (%)	n/i	TOF h^{-1}	Rh Leaching (%)
1	1-hexene[a]	100	99.3	0.7	0.8	157	2.8
Recycle of 1	1-hexene[a]	97.6	95.1	4.9	0.9	95	2.6
2	1-decene[b]	99.9	94.1	5.9	0.6	85	2.4

Reaction conditions: *olefin: 0.394 kmol/m^3, catalyst: 3.7 kg/m^3 (1.68 ×10^{-3} kmol/m^3), T: 373K, agitation speed: 16.6 Hz, P_{CO+H2} (1:1): 4.48 MPa, solvent: toluene, total charge: 2.7 ×10^{-5} m^3, reaction time: a=1.7 h, b= 2.3 h.*

4.3.3 Feasibility of hydroformylation of olefins using supported ossified catalyst

The activity of the ossified catalyst C-II (Table 4.7) is rather low as compared to that of other reported heterogenized catalysts[14]. One of the methods to increase the activity of the catalyst is to see whether a highly dispersed form of the ossified catalysts could be prepared over different supports, for application to hydroformylation. The envisaged advantages are:

1. The unsupported ossified catalyst is in the form of lumps having low surface area while the supported ossified catalyst is well dispersed with a relatively high surface area.
2. In the unsupported ossified catalyst only the catalyst on the surface is available for reaction while high dispersion in supported catalyst provides easy accessibility of the catalyst.
3. A lower loading of metal is possible for the supported catalyst to achieve high TOFs
4. The properties of support can also been used for tuning the activity and selectivity of the catalyst.

Initially, silica and carbon supported ossified catalysts (catalyst C-III and C-IV) were prepared in presence of excess TPPTS. Both these supported ossified catalysts were tested for the hydroformylation of olefins. The silica supported ossified catalyst (Catalyst C-IV) showed good activity for hydroformylation 1-decene, but the activity decreases on recycle (Table 4.8).

Table 4.8: Hydroformylation of 1-decene using catalyst C-IV

Sr. no.	Reaction	Conversion (%)	Aldehyde selectivity (%)	Isomerized olefin (%)	n/i	TOF h^{-1}	Rh Leaching (%)
1	Fresh catalyst[a]	100	93.4	6.6	0.5	642	1.8
2	First Recycle[b]	100	95.4	4.6	0.6	573	1.4
3	Second recycle[c]	99.5	97.5	2.5	0.9	394	1.3

Reaction conditions: *1-decene: 0.493 kmol/m^3, catalyst: 11.5 kg/m^3 (0.44 wt/wt % Rh), T: 353 K, P_{CO+H2} (1:1): 4.8 MPa, agitation speed: 16.6 Hz, solvent: toluene, total charge: 2.7× $10^{-5}m^3$, reaction time:a= 3.0 h, b=3.7h, c=5.3 h.*

The carbon supported ossified catalyst (catalyst C-III) was tested for its activity for the hydroformylation of 1-hexene and 1-decene. The results in Table 4.9 show that the

carbon supported ossified catalyst is active (TOF=589 h^{-1}) for hydroformylation of 1-hexene with good selectivity (>98%) to aldehyde. The activity and selectivity of the catalyst is maintained even after two recycles (entry 1, 2 and 3, Table 4.9). Similarly, catalyst C-III shows good activity and selectivity for the hydroformylation of 1-decene (entry 4, Table 4.9). Although the carbon supported ossified catalyst is less active as compared to silica supported catalyst, the catalyst is highly stable and recyclable. In addition, the catalyst shows negligible rhodium leaching to the organic phase. Both the supported ossified catalysts [catalyst C-III and C-IV], showed better performance over the ossified catalyst C-II.

Table 4.9: Hydroformylation of 1-hexene and 1-decene using carbon supported ossified catalyst

Sr. No.	Reaction	Substrate	Conv-ersion (%)	Aldehyde selectivity (%)	Isomerized olefin (%)	n/i	TOF h^{-1}	Rh leaching (%)
1	Fresh catalyst	1-hexene[a]	100	98.4	1.6	1.4	589	0.08
2	First recycle	1-hexene[a]	100	96.3	3.7	1.3	570	0.04
3	Second recycle	1-hexene[a]	99.6	96.1	3.9	1.2	562	0.05
4	Fresh catalyst	1-decene[b]	98.5	98.7	1.3	0.7	465	0.07

Reaction conditions: *substrate: 0.99 kmol/m^3, catalyst: 6.25 kg/m^3 (0.37wt/wt % Rh) kmol/m^3), T: 353 K, agitation speed: 16.6 Hz, P_{CO+H2}(1:1): 4.14 MPa, solvent: toluene, total charge : 8.0 ×10^{-5}, reaction time a= 5.3 h, b=6.1 h.*

A comparison of the performance of the catalysts C-III and C-IV with the conventional homogeneous and biphasic systems using $HRh(CO)(PPh_3)_3$ and $HRh(CO)(TPPTS)_3$ respectively under identical reaction conditions (T=353K) is shown in Table 4.10.

Table 4.10: Results comparison for hydroformylation of 1-decene using homogeneous, biphasic, and catalyst C-III and C-IV.

Catalyst	Conversion (%)	Aldehyde selectivity (%)	Final isomerized olefin (%)	n/i	TOF (h^{-1})	Time (h.)
Homogeneous[a]	99	100	-	0.4	1490	1.5
Biphasic[b]	88.8	71	29	0.7	38	12.0
Catalyst C-IV[c]	100	93.4	6.6	0.5	642	3.0
Catalyst C-III[d]	98.5	98.7	1.3	0.7	465	6.1

a=Reaction conditions for homogeneous reaction $HRhCO(PPh_3)_3$: 2.18 $\times 10^{-4}$ kmol/m^3, $Rh:PPh_3$ = 1:6 (excess), 1-decene : 0.423 kmol/m^3, T: 353K, P_{CO+H2}(1:1): 4.8 MPa, agitation speed : 16.6 Hz, solvent : toluene, total charge: 2.5 $\times 10^{-5}$ m^3,
b= Reaction conditions for biphasic reaction $HRh(CO)(TPPTS)_3$: 5.24 $\times 10^{-3}$ kmol/$m^3_{(aq.)}$, $Rh:TPPTS_{(aq.)}$=1:6 (excess), 1-decene: 0.704 kmol/$m^3_{(org.)}$, T: 353K, agitation speed : 16.6 Hz, P_{CO+H2} (1:1) : 4.8 MPa, solvent : toluene + Water (aqueous phase hold up=0.4), total charge : 2.5 $\times 10^{-5}$ m^3.
c and d reaction conditions as mentioned for the Table 4.8 and 4.9 respectively.

From the Table 4.10 it is clear that the activity of the silica and carbon supported ossified catalyst is lower than that of homogeneous catalyst but more than biphasic catalysis by 12–16 times!

The above results reveal that the novel supported ossified catalysts are active for the hydroformylation of higher olefins and that the carbon supported ossified catalyst is more stable and can be reused. Hence further detailed studies were carried out using carbon supported ossified catalyst (catalyst C-III) and 1-decene as a model substrate for higher olefins hydroformylation.

4.3.4 Hydroformylation of olefins using catalyst C-III

4.3.4.1 Solvent effect on catalyst activity and selectivity in hydroformylation of 1-decene

Solvents are known to play a major role in deciding the activity as well as selectivity in hydroformylation reactions[14]. To assess the role of solvents for hydroformylation of 1-decene, reactions were undertaken in a number of solvents using

carbon supported ossified catalyst (catalyst C-III) and the results are presented in Table 4.11.

High isomerization activity was observed in highly polar solvents like methanol and ethanol. The activity for hydroformylation was surprisingly very low in alcohol solvents. This trend is contradictory to the homogeneously catalyzed reactions, wherein high activity is observed in solvents like methanol and ethanol. For solvents like octanol, p-xylene, and toluene a good hydroformylation activity was observed, but the n/i ratio was poor. Surprisingly, the highest activity was observed in solvents like toluene, n-hexane and xylene which are relatively nonpolar[15].

Table 4.11: Solvent screening studies for hydroformylation of 1-decene

Sr. no	Solvent	Conversion (%)	Aldehyde selectivity (%)	Isomerized olefin (%)	n/i	TOF (h^{-1})	Time (h.)
1	Methanol	80.1	44.6	55.4	3.9	29	10.3
2	Ethanol	92.6	61.2	38.8	1.8	68	24.4
3	MEK	97.9	49.5	50.5	3.1	147	9.8
4	Octanol	96.9	100	-	0.9	168	17.9
5	p-Xylene	98.4	100	-	0.9	309	10.0
6	Toluene	98.5	98.7	1.3	0.7	460	6.1
7	Cyclohexane	98.8	97	3.0	0.9	227	10.3
8	n-Hexane	96.8	100	-	0.9	305	9.9

Reaction conditions: *catalyst: 5.88 kg/m^3 (0.37 wt/wt % Rh), 1-decene: 0.62 kmol/m^3, T: 353K, agitation speed: 16.6Hz, P_{CO+H2}(1:1): 4.14 MPa, total charge: 8.5 ×10^{-5} m^3.*

4.3.4.2 Recycle study and leaching analysis

To check the stability, the catalyst C-III was recycled at a higher temperature of 373K (Figure 4.22). For these studies, a known amount of 1-decene was added to the reactor at the end of each reaction and the reaction continued further.

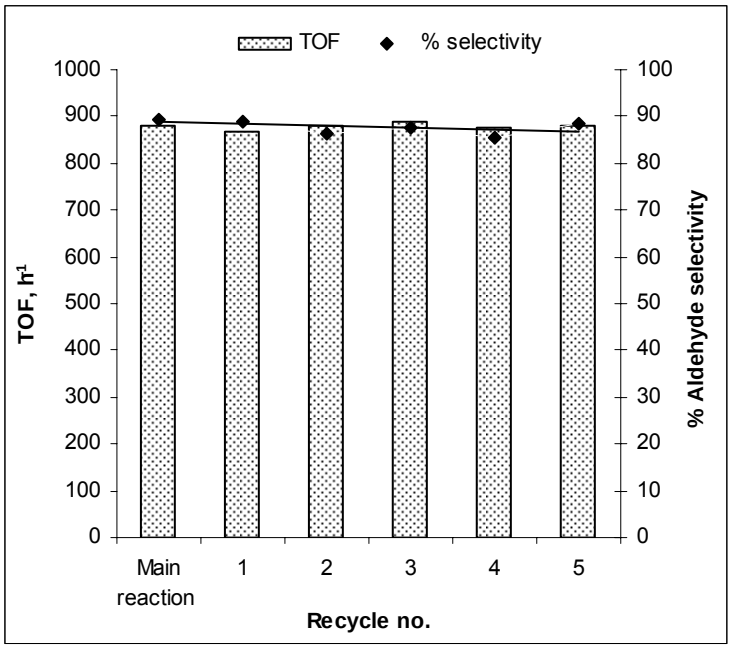

Figure 4.22: Recycle studies for hydroformylation of decene using catalyst C-III.

***Reaction conditions**: catalyst C-III: 3.7 kg/m^3 (0.37 wt/wt % Rh), 1-decene: 0.39 kmol/m^3, T: 373K, agitation speed: 20Hz rpm, P_{CO+H2} (1:1): 4.14 MPa, total charge: 2.7 ×10^{-5} m^3 , solvent : toluene, time: 2.8 h.*

The results in Figure 4.22 show that the catalyst is stable and the activity and selectivity of the catalyst was maintained during several recycles. The ICP analysis shows overall negligible leaching (~0.6 % of rhodium metal taken) to the organic phase, at the end of fifth recycle. No activity was observed when the organic phase was recycled without any catalyst. This shows that the activity is solely due to the carbon supported catalyst. The spectroscopic study of the catalyst before and after the reaction showed that the catalyst was intact (refer Figure.4.8 and 4.9).

4.3.4.3 Hydroformylation of various classes of olefins using carbon supported ossified catalyst

The catalyst C-III (Rh = 0.37 % wt/wt), was tested for the hydroformylation of various classes of olefins at 373K and a syngas pressure of 4.14 MPa, in toluene solvent. The catalyst C-III was found to be very effective for the hydroformylation of linear, cyclic and functionalized olefins and terpenes as shown in Table 4.12.

The important feature of this catalyst was the high activity observed for higher olefins like 1-decene and 1-dodecene where the availability of true heterogeneous catalysts has been a challenge. For hydroformylation of 1-decene a 95.1% conversion was obtained with 89.5% aldehyde selectivity. The final n/i ratio was 0.51. This low n/i is observed because isomerization of olefins also occurs and hydroformylation of the internal olefins yields only branched products. The initial n/i ratio wherein the major reaction is hydroformylation of 1-decene is 2.8 (Figure 4.23a). The TOF was 880 h^{-1}. When the same reaction is conducted at 353K, the isomerization activity is strongly reduced (Figure 4.23b) leading to improved n/i ratios (n/i = 0.75) even at higher conversions. The catalyst C-IV, a silica supported barium salt of $HRhCO(TPPTS)_3$ also gave high TOF for hydroformylation of 1-decene, but appreciable amount of leaching (~3-4% Rh) was observed at 373K.

Table 4.12: Hydroformylation of olefins using catalyst C-III

Sr. no	Substrate	Conversion (%)	Aldehyde selectivity (%)	Final isomerized olefin (%)	n/i	TOF (h^{-1})	Time (h)
1	1-Hexene	99.4	95.8	4.2	0.64	1261	2.22
2	1-Octene	97.3	92.4	7.6	0.56	1089	2.42
3	1-Decene	95.1	89.5	10.5	0.51	880	2.83
4	1-Dodecene	99.3	88.0	12.0	0.49	748	3.42
5	Styrene	99.1	97.6	2.4	1.14	1578	1.80
6	Camphene	66.1	98.3	1.7	1.18*	298	6.42
7	VAM	33.8	96.6	3.4	1.00	240	3.92
8	Cyclohexene	76.7	100	-	-	752	3.00
9	#Propylene	98.7	100	-	0.9	3503	4.0

Reaction conditions: *catalyst C-III: 3.7 kg/m^3 (0.37 wt/wt % Rh), substrate: 0.39 kmol/m^3 , T: 373K, agitation speed: 20Hz, P_{CO+H2} (1:1): 4.14 MPa, total charge: 2.7 ×10^{-5} m^3, solvent: toluene; * endo / exo. # : 1.466 kmol/m^3*

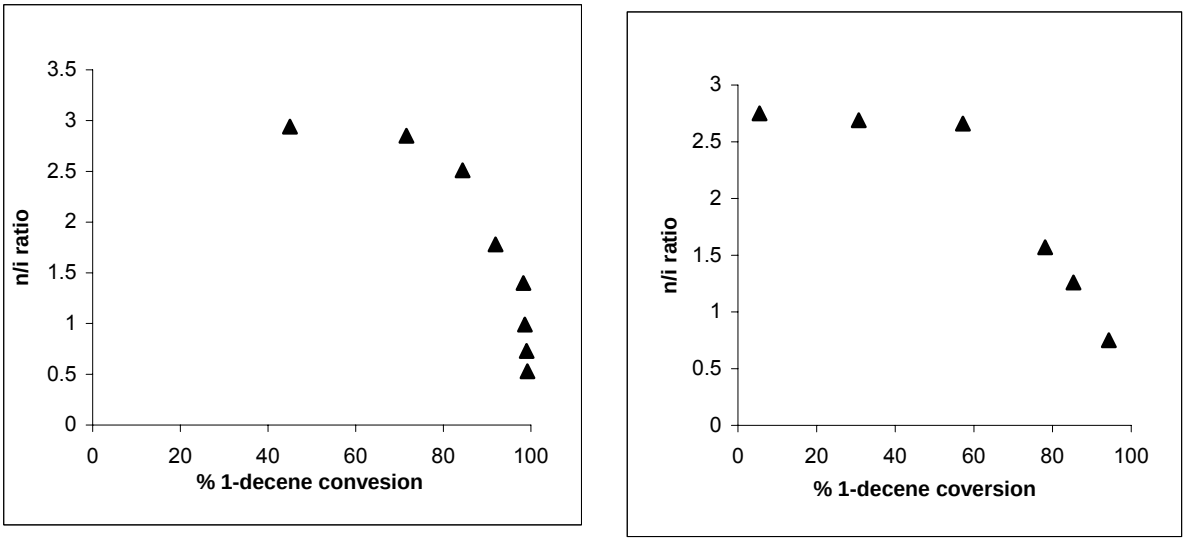

(**a**) (**b**)

Figure 4.23: 1-decene conversion vs. n/i ratio at **(a)** 373 K and (**b**) 353K.

Reaction conditions: *catalyst: 3.7 kg/m^3 (0.37 wt/wt $^{\%}$ Rh), 1-decene: 0.39 kmol/m^3, agitation speed: 20Hz, P_{CO+H2}(1:1): 4.14 MPa, total charge: 2.7 ×10^{-5} m^3, solvent: toluene reaction time (a)=2.8 h, (b)= 6.2 h.*

4.3.4.4 Comparison of unsupported, supported ossified catalysts with other reported heterogenized catalysts for hydroformylation of 1-decene

The hydroformylation results obtained using catalyst C-III, carbon supported barium salt of $HRhCO(TPPTS)_3$ (Rh= 0.37 % wt/wt), for the hydroformylation of 1-decene at 373K was compared with the other reported heterogenized catalysts and the results are presented in Figure 4.24. The carbon supported ossified catalyst gives 95.1% conversion of 1-decene with 89.5% aldehyde selectivity and TOF of 880 h^{-1} (Bar A in Figure 4.24). When the ossified catalyst C-II, (unsupported ossified) was used, a TOF of 85 h^{-1} was obtained (Bar B in Figure 4.24). This shows that although, the precipitation of the barium salt of $HRh(CO)(TPPTS)_3$ provides a heterogeneous catalyst for hydroformylation, only the complex on the surface of the particle is available for the reaction, which explains the lower TOF observed. In comparison with other heterogenized catalysts, the carbon-supported catalyst was more active than the anchored[16] (Bar C, Figure 4.24), encapsulated[12a] (Bar D, Figure 4.24) or tethered $HRh(CO)(PPh_3)_3$ catalysts[12b] (Bar E, Figure 4.24) for hydroformylation of 1-decene. The

catalyst C-III clearly shows around 2-3 fold rate enhancement over the best heterogenized catalyst reported as shown in Figure 4.24. Considerable leaching was also observed in case of the anchored and encapsulated catalyst. The catalyst C-III was thus found to be superior to the earlier reported heterogenized catalysts with respect to its activity, selectivity and stability.

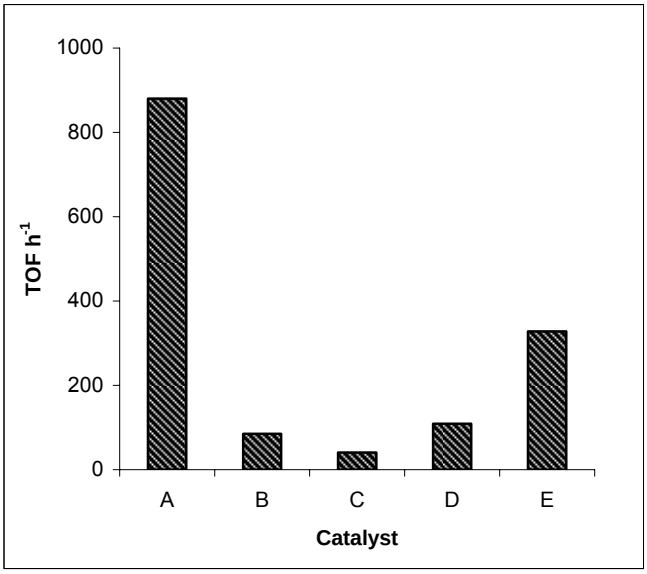

Figure 4.24: Comparison of activity for hydroformylation of 1-decene using different heterogenized catalysts.

Reaction conditions: ***A****: Catalyst C-III: 3.7 kg/m^3 (0.37 wt/wt % Rh), 1-decene: 0.391 kmol/m^3, T: 373K, P_{CO+H2}(1:1): 4.14 MPa, agitation speed: 20Hz, total charge: 2.7 × 10^{-5} m^3, solvent: toluene, time: 2.8 h.;* ***B****: Catalyst C-II: 3.7 kg/m^3 (1.68 ×10^{-3} kmol/m^3), 1-decene: 0.39 kmol/m^3, T: 373K, agitation speed: 16.6Hz, P_{CO+H2} (1:1): 4.14 MPa, total charge: 2.7 ×10^{-5} m^3, solvent : toluene, time: 2.3 h.;* ***C****: Anchored catalyst[14], Rh_2-MCM-41;* ***D****:Encapsulated catalyst[12a], wk-MCM48;* ***E****: Tethered catalyst[12b], wk-PTA-Y*

The performance of the dispersed catalyst C-III, although lower by a third compared to the activity of the homogeneous catalyst (TOF= 2750 h^{-1}), was better than the aqueous biphasic catalyst (TOF= 156 h^{-1}) by almost five folds[17].

4.3.4.5 Role of Support

In heterogeneous catalytic systems, the support is known to play a major role in dictating activity and selectivity of the catalyst. The ossified catalyst has a different type of heterogenized system and hence it was of interest to observe the role of supports on the activity and selectivity of the catalyst for hydroformylation reaction using the supported

ossified HRhCO(TPPTS-$Ba_{3/2}$) catalysts. In that context barium salt of $HRhCO(TPPTS)_3$ supported on various inorganic supports like SiO_2, TiO_2, Al_2O_3, ZrO_2, La_2O_3 and MgO was prepared and their activity was assessed for the hydroformylation of 1-decene.

The supported ossified catalysts prepared on different supports were tested for the hydroformylation of 1-decene and the results are presented in Table 4.13. All the catalysts showed good hydroformylation activity.

Table 4.13: Support screening for hydroformylation of 1-decene at 353K

Sr. no	Support	Rh content (% w/w)	Conv-ersion (%)	Aldehyde selectivity (%)	Final isomerized olefin (%)	n/i	TOF (h^{-1})	Time, (h.)	Leaching (%)
1	SiO_2	0.44	100	93.4	6.6	0.4	642	3.0	1.80
2	Activated Carbon	0.37	98.5	98.7	1.3	0.73	465	6.2	0.07
3	Al_2O_3	0.436	98.5	92.1	7.9	0.72	887	3.7	9.30
4	ZrO_2	0.675	99.1	85.8	14.2	0.86	767	3.7	2.36
5	TiO_2	0.655	92.7	97.4	2.6	0.77	838	3.7	4.06
6	La_2O_3	0.688	99.5	55.3	44.7	2.31	435	3.7	2.58
7	MgO	0.59	55.3	68.1	31.9	2.63	206	3.7	2.77

Reaction conditions: *catalyst: 3.7 kg/m^3, substrate: 0.39 kmol/m^3, T: 353 K, agitation speed: 20Hz, P_{CO+H2} (1:1) 4.14 MPa, total charge: 2.7 ×10^{-5} m^3, solvent: toluene, time 6.2 h.*

SiO_2, Al_2O_3, ZrO_2, TiO_2 supported catalysts show higher activity than activated carbon, La_2O_3 and MgO supported catalysts. A very high leaching of the rhodium metal to the organic phase was observed in case of the catalyst supported on SiO_2, Al_2O_3, ZrO_2, and TiO_2. Higher rates of isomerization were observed using supports like La_2O_3 and MgO. The catalyst supported on carbon is sufficiently active and stable and shows negligible leaching.

Table 4.14 shows the comparison of results of supported ossified catalyst on various carbons for hydroformylation of 1-decene at 353K. The ossified catalyst

supported on high surface area microporous carbon (1141 m^2/g) gave a slightly higher activity compared to the catalyst C-III (surface are of the activated carbon = 158.3 m^2/g). When the same catalyst was supported on mesoporous carbon having a surface area of 1027 m^2/g, a 20% rate improvement (TOF= 541 h^{-1}) was observed. This rate enhancement could be due to the large pore diameter (39 Å) of the mesoporous carbon which is sufficient to accommodate the bulky metal complex. The sorption study of the catalysts shows a decrease in the surface area of the support after immobilization of the metal complex (see Table 4.6). Hence interaction of the olefins and diffusion of the product is easier in the case of the catalyst supported on mesoporous carbon compared to catalyst supported on microporous high surface area carbon and catalyst C-III.

Table 4.14: Comparison of results of supported ossified catalyst on various carbons for hydroformylation of 1-decene at 353K

Sr. no	Catalyst support (surface area m^2/g)	Conv-ersion (%)	Aldehyde Selectivity (%)	Final isomerised olefin (%)	n/i	TOF (h^{-1})	Time, (h.)	Leaching (%)
1	Activated carbon (158.3)	98.5	98.7	1.3	0.73	465	6.1	0.07
2	Microporous carbon (1141)	97.2	99.2	0.8	0.74	473	6.0	0.09
3	Mesoporous carbon (1027)	99.4	96.9	3.1	0.65	541	5.4	0.06

Reaction conditions: *catalyst: 3.7 kg/m^3 (0.37% w/w), 1-decene: 0.39 kmol/m^3, T: 353 K, agitation speed: 20 Hz, P_{CO+H2} (1:1) 4.14 MPa, total charge 2.7 ×10^{-5} m^3, solvent: toluene.*

4.3.5 Kinetics of hydroformylation of 1-decene using carbon supported ossified catalyst

Structurally, since the supported ossified catalyst is analogous to the water soluble $HRhCO(TPPTS)_3$, it was of interest to investigate the kinetics and mechanism of the reaction using the supported ossified catalyst and compare with the trends reported using

the homogeneous and water soluble catalysts. Detailed investigations on the intrinsic kinetics of hydroformylation of 1-decene using carbon supported ossified catalyst were undertaken. Preliminary reactions were conducted to asses the material balance and reproducibility of the experiments. For this purpose, a few experiments were carried out in which the amount of 1-decene consumed, aldehyde products formed, and $CO+H_2$ consumed were compared, particularly for experiments at high conversion of 1-decene (>90% conversion). A typical concentration time profile is shown in Figure 4.25. In general, it was observed that the consumption of ($CO+H_2$) and 1-decene was consistent with the amount of total aldehyde products formed. Also, in the range of conditions covered in this work, the products formed were primarily undecanal and 2- methyl-decanal alongwith other isomeric aldehydes in small quantities, which was confirmed by GCMS or by comparison with authentic standard samples on GC. Thus, the overall hydroformylation kinetics could be followed by observing the consumption of syngas, and formation of aldehyde products (via sampling) as a function of time.

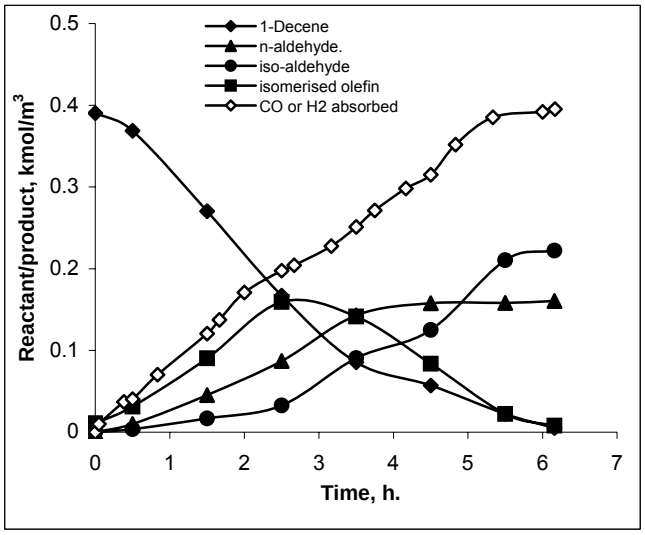

Figure 4.25: Concentration-Time profile for hydroformylation of 1-decene.

Reaction conditions: *catalyst: 3.7 kg/m^3 (0.37 w/w % Rh), 1-decene: 0.39 kmol/m^3 , T: 353 K, agitation speed: 20 Hz, P_{CO+H2}(1:1): 4.14 MPa, total charge: 2.7 ×10^{-5} m^3, solvent: toluene, time: 6.2 hr.*

4.3.5.1 Solubility data

For the purpose of kinetic study, knowledge of the solubility of the gaseous reactants in the reaction medium is often essential. For the CO toluene and H_2-toluene

systems, the solubility data were obtained experimentally by a procedure described by Purwanto et al[18]. The solubility data obtained is consistent with the values obtained by the extrapolation of the reported solubility data[19] (Figure 4.26). The data presented in Table 4.15 were used in the calculation of the concentrations of dissolved CO and H_2 in the liquid medium.

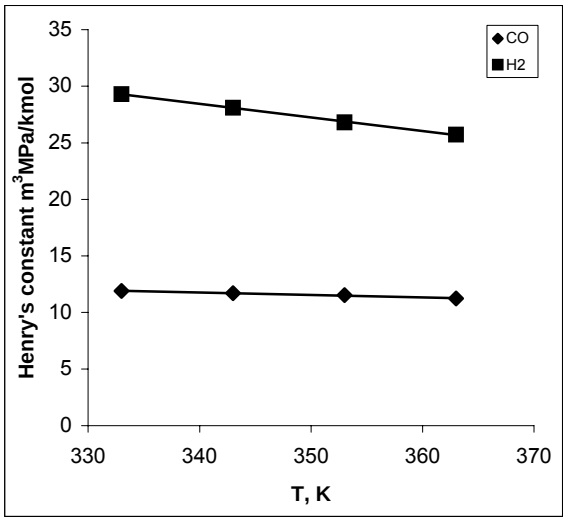

Figure 4.26-: Solubility of H_2 and CO in toluene: Extrapolation of the literature data[17]

Table-4.15: Henry's constants for CO and H_2 in toluene

Sr. no	T(K)	CO (m^3 MPa/kmol)	H_2 (m^3 MPa/kmol)
1	343	11.70	28.10
2	353	11.53	26.80
3	363	11.24	25.73

4.3.5.2 Evaluation of Kinetic regime

4.3.5.2.1 Effect of agitation speed

For the kinetic study it is essential that reaction should operate in the kinetic regime and not under the condition where mass transfer is controlling. For that purpose the effect of agitation speed on the rate of reaction was studied and the results are presented in Figure 4.27. The rate was found to be independent of the agitation speed

beyond 1000 (16.6 Hz) rpm, which clearly indicates that the reaction is in kinetic regime. Therefore, all the reactions for kinetic studies were carried out at an agitation speed of 1200 (20 Hz) rpm to ensure that the reaction occurred in the kinetic regime.

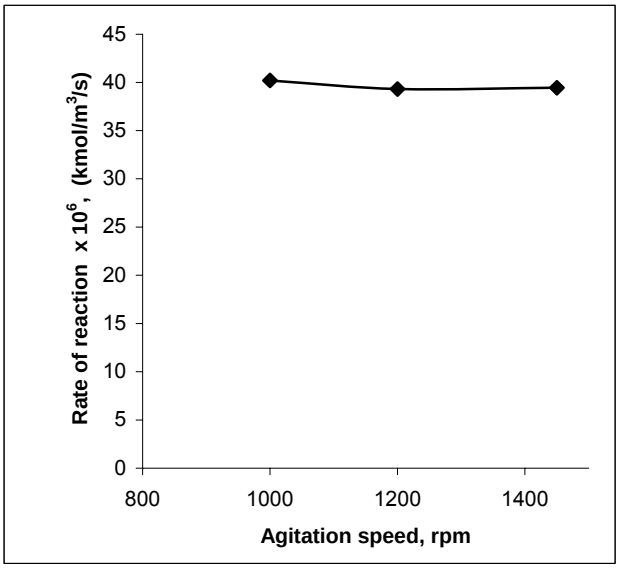

Figure 4.27: A plot of rate of hydroformylation of 1-decene vs. agitation speed

Reaction conditions: *catalyst: 3.7 kg/m^3 (0.37 w/w $^{\%}$ Rh), 1-decene: 0.39 kmol/m^{3,} T: 363 K, P_{CO+H2} (1:1): 4.14 MPa, total charge: 2.7 × 10^{-5}m^3, solvent: toluene, time: 1 h.*

4.3.5.2.2 Mass transfer effects

The analysis of overall rate of reaction for three phase (gas-liquid-solid, G-L-S) catalytic reactions is given by Ramachandran et al[20]. The important steps involved in a gas-liquid-solid catalytic reaction for hydroformylation of olefins are:

1. Transport of gas phase reactants A (H_2) and B (CO) from the gas phase to the bulk liquid.
2. Transport of A and B and liquid reactant 1-decene (D) from the bulk liquid phase to the catalyst (C) surface.
3. Intraparticle diffusion of A and B and liquid reactant 1-decene in the pores of the catalyst.
4. Adsorption of A and B on the catalyst surface followed by a chemical reaction with 1-decene to yield the products.

The following criteria described by Ramachandran and Chaudhari[18] were used to check the significance of various mass-transfer effects.

1. Gas-Liquid mass transfer

The significance of gas-liquid mass transfer resistance was analyzed by comparing the rate of reaction, R_i (kmol/m^3/s) and the maximum possible rate of gas-liquid mass transfer. The gas-liquid mass transfer resistance is negligible if a factor α_{gl} as defined in Eq-4.1 is less than 0.1.

$$\alpha_{gl} = \left[\frac{R_i}{k_L a_B C_i^*} \right] < 0.1 \qquad 4.1$$

Where, $k_L a_B$ is the gas-liquid mass transfer coefficient and Ci^* is the saturation solubility of reacting gases (i.e. CO or H_2) in equilibrium with the gas phase concentration at the reaction temperature (kmol/m^3). The gas-liquid mass transfer coefficient ($k_L a_B$) used in above equation was calculated using a correlation proposed by Chaudhari and coworkers[21] (Eq-4.2) for a reactor similar to that used in this work.

$$k_L a_B = 1.48 \times 10^{-3} (N)^{2.18} \times \left(\frac{V_g}{V_L} \right)^{1.88} \times \left(\frac{d_I}{d_T} \right)^{2.1} \times \left(\frac{h_1}{h_2} \right)^{1.16} \qquad 4.2$$

The terms involved in above equation are described in Table 4.16 along with the respective values obtained from the reactor and charge used in the present case.

Table 4.16: Parameters used for $k_L a_B$ calculations by Eq-4.2

Parameter	Description	Value
V_g	Gas volume (m^3)	45×10^{-6}
N	Agitation speed (Hz)	20
V_L	Liquid volume (m^3)	27×10^{-6}
d_I	Impeller diameter (m)	1.6×10^{-2}
d_T	Tank diameter (m)	4.0×10^{-2}
h_1	Height of the impeller from the bottom (m)	1.1×10^{-2}
H_2	Liquid height (m)	2.2×10^{-2}

$k_L a_B$ at 1200rpm (20 Hz) was calculated as 0.17 s^{-1}.

The factor α_{gl} was calculated (for taking R_A as 7.14×10^{-5} kmol/m^3/s which is the highest rate observed) for both hydrogen and carbon monoxide and was in the range 6.85

$\times 10^{-4}$ to 1.96×10^{-3}. Since the values of α_{gl} are very much less than 0.1 for both the gaseous reactants, gas-liquid mass transfer resistance can be assumed to be negligible.

2. Liquid-Solid mass transfer

The liquid-solid mass transfer resistance can be considered unimportant if a factor α_{ls} (the enhancement factor) defined in Eq. 4.3 is less than 0.1.

$$\alpha_{ls} = \left[\frac{R_i}{k_S a_P C_i *} \right] < 0.1 \qquad 4.3$$

Where, k_s is the liquid to solid mass transfer coefficient (s^{-1}), and a_p is the interfacial area of the particles per unit volume of the liquid phase (m^2/m^3) defined by Eq. 4.4

$$a_p = \frac{6w}{\rho_p d_p} \qquad 4.4$$

Where, w is the catalyst mass per unit volume of the reactor (kg/m^3), ρ_p is the density of the catalyst particle (kg/m^3) and d_p is the particle diameter (m). Substituting for all the required values (w = 3.7 kg/m^3), average density of the particle = 4.72×10^2 kg/m^3 and average particle diameter for carbon supported ossified catalyst = 50 μ we get the value of a_p as 942 m^2/m^3.

k_s, the liquid to solid mass transfer coefficient, can be calculated based on the Equation proposed by Sano and coworkers[22] (Eq 4.5)

$$\frac{k_S d_P}{DF_c} = 2 + 0.4 \left[\frac{e(d_p)^4 (\rho_l)^3}{(\mu_l)^3} \right]^{0.25} \left[\frac{\mu}{\rho_l D} \right]^{0.33} \qquad 4.5$$

Where, d_p is particle diameter (m). D is the molecular diffusivity (m^2/s), F_c is the shape factor assumed to be unity for spherical particles, ρ_l is the density of the liquid (kg/m^3), μ_l is the viscosity of the liquid (P or kg/m.s) and e is the energy supplied to the liquid per unit mass (m^2/s). Prasher and Wills[23] give the following equation for calculation of e (Eq. 4.6)

$$e = \frac{P}{\rho_L V_L} = \frac{8 N^3 d_1^{\,5} \psi}{d_T L} \qquad 4.6$$

Where, P is Power consumption for agitation ($kg/m^2/s^3$), ρ_L is density of liquid phase (kg/m^3), V_L is the total volume (m^3), N is the speed of agitation (s^{-1}), d is diameter of

impeller (m), Ψ is the correction factor (this correction factor is reported to be non-significant for low catalyst loadings and for catalysts with low densities), L is the total height of the liquid (m)

Based on the Eq-4.5, the value of k_s was calculated as 1.24×10^{-3} ms^{-1} at 1200 rpm (20Hz). The value of overall mass transfer coefficient, $k_s a_p$ (required in Eq-4.5) was calculated as 1.168 s^{-1}. The factor α_{ls} were calculated for both hydrogen and carbon monoxide (taking R_A as 7.14×10^{-5} $kmol/m^3/s$) and found to be in the range of 2.85×10^{-4} to 9.97×10^{-5} respectively. Since the values of α_{1s} are less than 0.1 for both the gaseous reactants, liquid-solid mass transfer resistance can be assumed to be negligible.

3. Intraparticle diffusion

Pore diffusion is considered to be negligible if a factor φ defined as follows (Eq. 4.7) is less than 0.2

$$\varphi_{\exp} = \frac{d_P}{6}\left[\frac{\rho_P R_A}{w D_e C_i^*}\right]^{0.5} < 0.2 \qquad 4.7$$

Where, C_i^* is the concentration of the dissolved gas at the catalyst surface ($kmol/m^3$), D_e is the effective diffusivity (m^2/s). Since, g-l and l-s mass transfer resistance were found to be negligible, in evaluation of above criteria the surface concentration of A and B were assumed to be the same as that at the g-l interface.

In the absence of complex phenomenon such as surface diffusion and restricted diffusion, the problem of predicting effective diffusivity D_e can be reduced to predicting the tortuosity factor, defined by Eq. 4.8

$$D_e = \frac{D_M \varepsilon_P}{\tau} \qquad 4.8$$

Where, ε_p is the porosity of the catalyst, D_M is the molecular diffusivity of the solute in the liquid medium (m^2/s) and D_M was calculated using a correlation proposed by Wilke and Chang[24] (Eq. 4.9).

$$D_{AB} = \frac{7.4 \times 10^{-8} T (\phi M_B)^{1/2}}{\mu_B V_A^{0.6}} \qquad 4.9$$

Where, Φ is the association parameter of the solvent; μ_B is the viscosity of solvent (P or kg/m.s), M_B is the molecular weight of the solvent ; T is temperature (K), V_A is the solute molar volume. Based on the equation given by Eq-4.7, the value of φ_{exp} was calculated to be in the range of 8.2×10^{-3} - 1.62×10^{-3} for both the gases, which is less than 0.2 and hence, intraparticle diffusion can also be considered unimportant under these conditions.

The initial rate data were thus analyzed to check the significance of gas-liquid, liquid-solid and intraparticle mass transfer effects under the conditions used to study the kinetics. In these criteria α_{gl}, α_{1s} and φ_{exp}, which are defined as the ratios of the observed rates to the maximum rates of gas-liquid, liquid-solid and intraparticle mass transfer rates, respectively, were calculated for both the gas phase reactants. It was found that the rate data obtained with carbon supported ossified catalyst were in the kinetic regime, under the given set of conditions and can be reliably used to evaluate the intrinsic kinetic parameters. The results are also consistent with the negligible effect of agitation shown in the Figure 4.27 in section 4.3.5.2.1 of this chapter.

4.3.5.2.3 Initial rate data

The kinetics of the hydroformylation of 1-decene using carbon supported ossified catalyst was investigated in the range of conditions shown in Table 4.17 in toluene as per the procedure described earlier (section 4.2.8).

Table 4.17: Range of conditions used for the kinetic studies

Catalyst loading (Kg/m^3) 0.37 wt/wt % Rh	1.85 – 7.4
Concentration of 1-decene ($kmol/m^3$)	0.098-0.78
Partial pressure of hydrogen (MPa)	0.68-5.41
Partial pressure of carbon monoxide (MPa)	0.34-9.65
Temperature (K)	343 - 363
Solvent	Toluene
Agitation speed (Hz)	16.6-20.0
Reaction volume (m^3)	2.7×10^{-5}

The initial rates of hydroformylation were calculated from the plot of aldehyde formation as a function of time. A typical plot showing rate of aldehyde formation is

shown in Fig. 4.28. Under the conditions chosen for the kinetic study, no side reactions were found to occur and hence, these data would be representative of the overall hydroformylation of 1-decene to the corresponding aldehydes. An induction period of 10, 20 and 30 minutes was observed at the temperatures of 363 K, 353 K, and 343K respectively. Hence for the calculation of the rate, the data was corrected for the induction period. The rate of hydroformylation was calculated as follows (Eq. 4.10):

$$R = \frac{\text{Slope of product formation vs. time plot}}{\text{Volume of liquid}} \qquad 4.10$$

These were essentially initial rates of reaction, observed under differential conditions. The results showing the dependence of the rates on different parameters and a kinetic model based on these data are discussed in the following sections.

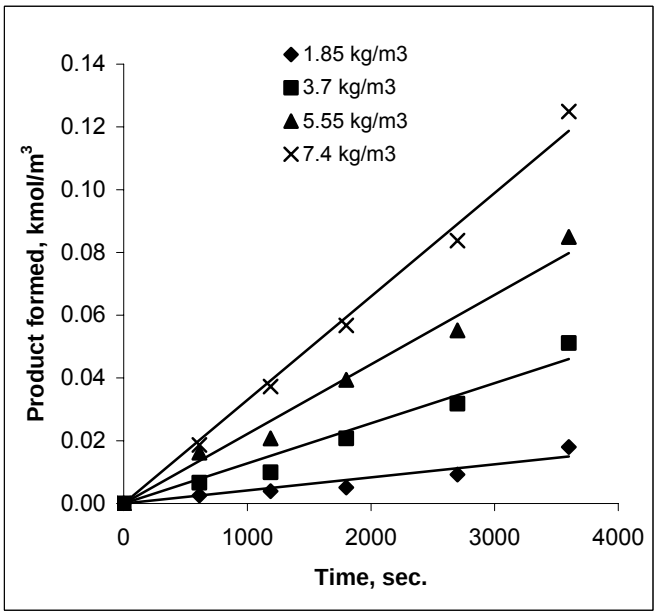

Figure 4.28: A plot of product formation vs. time for different catalyst concentrations

Reaction conditions: *1-decene: 0.39 kmol/m^3, T: 353 K, agitation speed: 20 Hz, P_{CO+H2} (1:1): 4.14 MPa, total charge: 2.7 × 10^{-5}m^3, solvent: toluene, time: 1h.*

4.3.5.2.3.1 Effect of catalyst loading

The effect of catalyst loading on the rate of hydroformylation of 1-decene was studied in the temperature range of 343-363 K, 1-decene concentration of 0.39 kmol/m^3 and a total pressure of $CO+H_2$ = 4.14 MPa (CO/H_2 = 1). The results are shown in Figure 4.29. The rate was found to be linearly dependent on the catalyst concentration, indicating a first order kinetics. An increase in concentration of catalyst will cause an increase in effective active catalyst concentration as seen from the mechanism in Figure 4.30 thereby increasing the rate of reaction, and hence a first order dependence is observed.

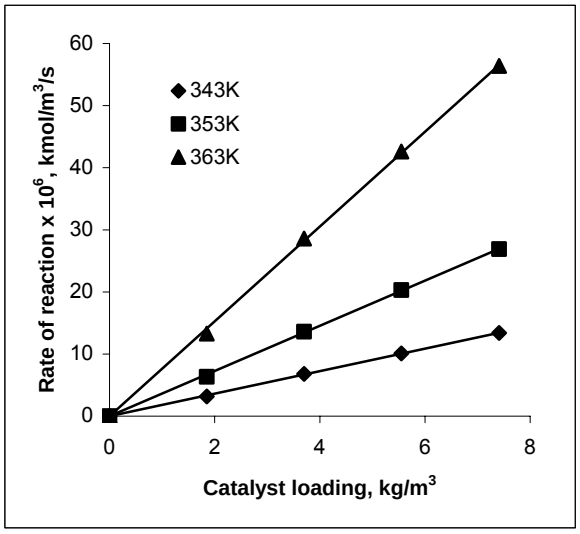

Figure 4.29: A plot of rate vs. catalyst loading in hydroformylation of 1-decene

Reaction conditions: *1-decene: 0.39 kmol/m^3, T: 343-363 K, agitation speed: 20Hz, P_{CO+H2} (1:1): 4.14 MPa, total charge: 2.7 ×10^{-5} m^3, solvent: toluene*

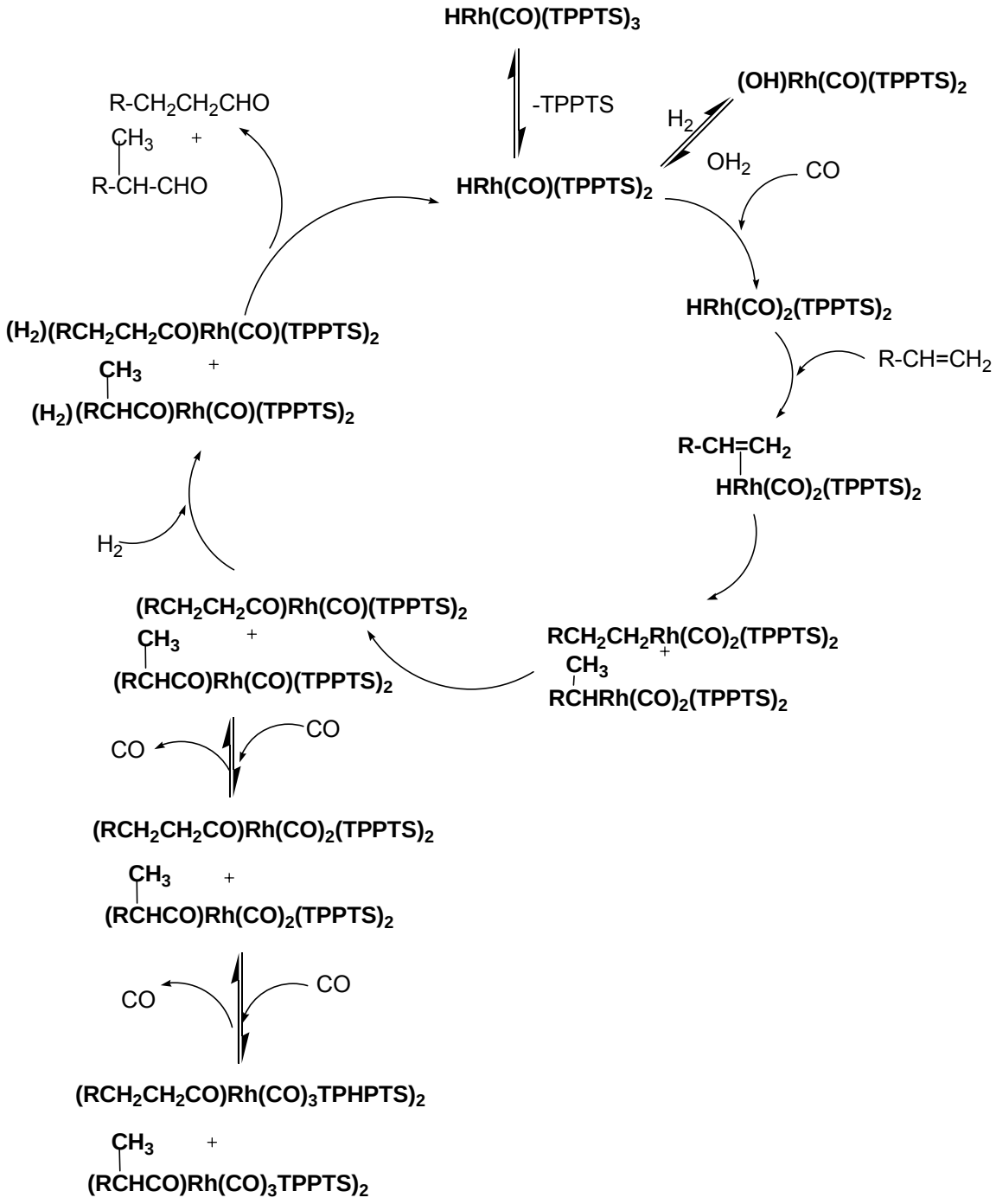

Figure 4.30: Mechanism of hydroformylation of olefins using $HRhCO(TPPTS)_3$ catalyst

4.3.5.2.3.2 Effect of 1-decene concentration

Figure 4.31 shows the effect of 1-decene concentration on the rate of hydroformylation in the temperature range of 343-363K. The plot of rate vs. 1-decene concentration passes through maximum. The rate was found to have a linear dependence on

1-decene in the initial concentration range. At higher substrate concentration, typical substrate inhibited kinetics was observed. This could be due to the formation of diolefinic species. Such observation has been reported in kinetics of hydroformylation of olefins using heterogeneous catalysts[25] as well as homogeneous[26] and biphasic[27] catalysts.

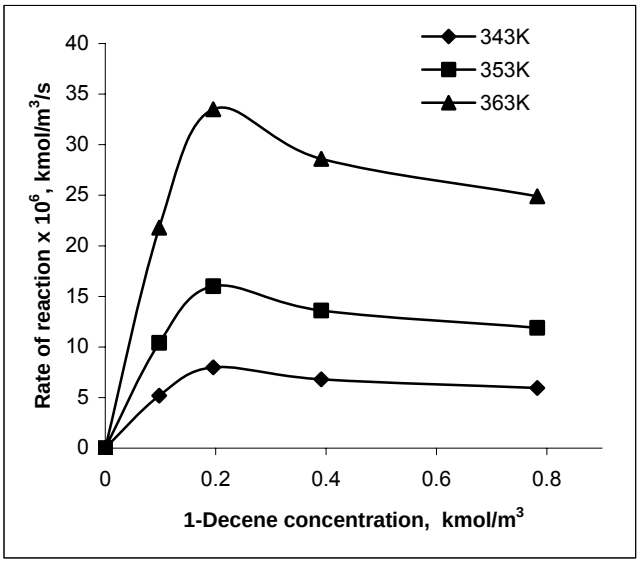

Figure 4.31: A plot of rate vs. 1-decene concentration effect in the hydroformylation of 1-decene

Reaction conditions: *catalyst: 3.7 kg/m^3 (0.37 w/w $^{\%}$ Rh), T: 343-363 K, agitation speed: 20Hz, P_{CO+H2} (1:1): 4.14 MPa, total charge: 2.7 ×10^{-5} m^3, solvent: toluene*

4.3.5.2.3.3 Effect of partial pressure of hydrogen

The effect of partial pressure of H_2 on the rate of hydroformylation of 1-decene was investigated at a constant CO partial pressure of 2.07 MPa and the results are shown in Figure 4.32**.** The rate of reaction was found have a first order dependent on P_{H2}**.** As per the hydroformylation mechanism (Figure 4.30) the oxidative addition of H_2 is the rate determining step. Hence with increasing pressure of hydrogen the rate enhancement is observed.

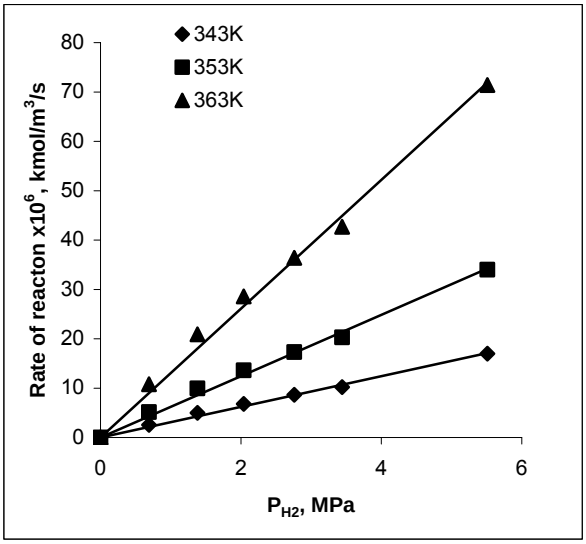

Figure 4.32: A plot of rate vs. P_{H2} for the hydroformylation of 1-decene.

Reaction conditions: *catalyst: 3.7 kg/m^3 (0.37 w/w $^{\%}$ Rh), 1-decene: 0.39 kmol/m^3, T: 343-363 K, agitation speed: 1200 rpm, P_{CO}: 2.07 MPa total charge: 2.7 ×10^{-5} m^3, solvent: toluene*

4.3.5.2.3.4 Effect of partial pressure of carbon monoxide

The effect of P_{CO} on the rate of hydroformylation of 1-decene was studied keeping a constant H_2 partial pressure of 2.07 MPa; the results are shown in Figure 4.33. A plot of rate vs. CO partial pressure passes through maximum. In the initial pressure range the rate was found to be the first order with P_{CO} and inversely dependent P_{CO} at higher CO pressures. As per the mechanism of rhodium-catalyzed hydroformylation, using triphenyl phosphine trisulfonate ligand, where inhibition with CO occurs at a much lower pressure range 0.3- 0.5 MPa[25, 28]. In some cases inhibition is also reported at CO partial pressure higher than 3.5 MPa[29], while in a few cases a positive order[17, 30] dependence has also been observed. In the case of the supported ossified catalysts, the inhibition is observed at relatively higher P_{CO}, which could be due to the presence of excess $TPPTSBa_{3/2}$ ligand on the support. This makes the phosphine easily available to the metal center and prevents the formation of inactive dicarbonyl and tricarbonyl species at lower CO pressures. The role of carbon support on adsorption of H_2 and CO gases is also suspected for the observed trend. It was observed experimentally that the solubility of both the gases are slightly higher in presence of carbon supported ossified catalyst (may be due to adsorption of gases on carbon) as compared to the solubility in solvent

alone. The inhibition is more pronounced at 363 K whereas it is barely observed at the lower temperature of 343K. This is in contrast to the trends observed in homogeneous rhodium-catalyzed hydroformylation, using triphenyl phosphine ligand, where inhibition with CO occurs at a much lower pressure range[22, 31].

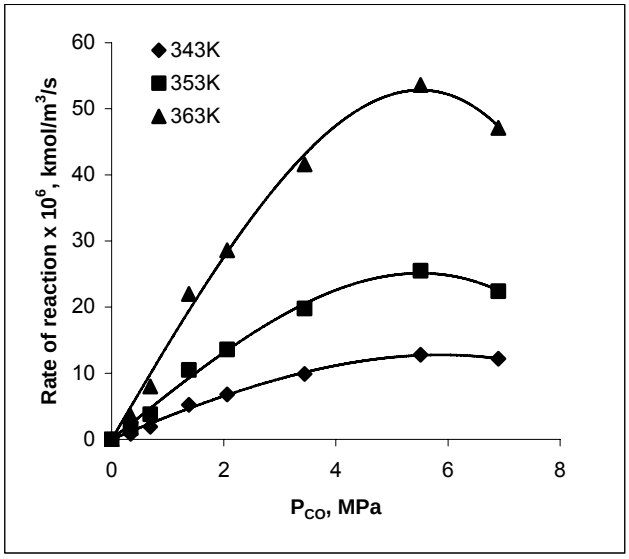

Figure 4.33: A plot of rate vs. P_{CO} for the hydroformylation of 1-decene.

Reaction conditions: *catalyst: 3.7 kg/m^3 (0.37 w/w $^{\%}$ Rh), 1-decene: 0.39 kmol/m^{3,} T: 343-363 K, agitation speed: 20Hz, P_{H2}: 2.07 MPa, total charge: 2.7 ×10^{-5} m^3, solvent: toluene*

4.3.5.2.3.5 Kinetic models

For the purpose of development of rate models, an empirical approach was followed. Prior to discrimination of rate equations, the rate data were analyzed for the importance of mass transfer resistances. In the current case, this was more important since the reaction is a typical gas–liquid–solid (G-L-S) reaction. The effect of agitation speed on the rate was investigated at the highest catalyst concentration and at highest temperature. The rate was found to be independent of the agitation speed, and hence the data were representative of the true kinetics of the reaction (Figure 4.27, section 4.3.5.2.1). Also the analysis of the initial rate data according to the criteria laid down by Ramachandran and Chaudhari[20] confirmed that the gas–liquid ($\alpha_{gl)}$, liquid–solid (α_{1s}) and intra-particle mass transfer resistances (φ_{exp}) were negligible, as discussed in section 4.3.5.2.2. The initial rate data were hence used to evaluate the intrinsic kinetic parameters.

In order to fit the observed rate data, several rate equations were examined using a nonlinear regression analysis. The results on the kinetic parameters estimated for the different models are presented in Table 4.18. For this purpose, an optimization program based on Marquardt's method[32] was used. The objective function was chosen as follows;

$$\phi = \sum_{i=1}^{n} \left[R_{Ai} - R'_{Ai} \right]^2 \qquad 4.10$$

Where Φ is the objective function to be minimized (Φ_{min}) representing the sum of the squares of the difference between the observed and predicted rates, n is the number of experimental data, R_{Ai} and R'_{Ai} represent predicted and experimental rates, respectively. The values of rate parameters and Φ_{min}, are presented in Table 4.18.

Table 4.18: Values of kinetic parameters at different temperatures

Model	Rate Model	T (K)	k_1	k_2	k_3	ϕ_{min}
I	$r = \frac{k_1 ABCD}{(1+k_2D)^2 (1+k_3B)^2}$	343	3.14×10^{-3}	3.95	9.58×10^{-1}	8.76×10^{-12}
		353	5.92×10^{-3}	4.97	9.46×10^{-1}	3.60×10^{-11}
		363	1.16×10^{-2}	5.90	9.24×10^{-1}	1.54×10^{-10}
II	$r = \frac{k_1 ABCD}{(1+k_2D^2) (1+k_3B^2)}$	343	1.43×10^{-3}	1.76×10^{1}	2.95	8.12×10^{-12}
		353	3.27×10^{4}	4.90×10^{8}	9.17×10^{-4}	1.20×10^{-9}
		363	4.49	3.40×10^{4}	1.82×10^{-2}	5.24×10^{-9}
III	$r = \frac{k_1 ABCD}{(1+k_2D) (1+k_3B)}$	343	1.51×10^{-2}	7.23×10^{1}	2.64	1.13×10^{-11}
		353	2.88×10^{-2}	7.35×10^{1}	2.61	4.60×10^{-11}
		363	5.17×10^{-1}	6.95×10^{2}	2.52	2.06×10^{-10}
IV	$r = \frac{k_1 ABCD}{(1+k_2D)^2 (1+k_3B)}$	343	3.42×10^{-3}	3.98	2.72	9.78×10^{-12}
		353	6.29×10^{-3}	3.93	2.64	4.00×10^{-11}
		363	5.67×10^{2}	3.91	3.65×10^{5}	2.31×10^{-9}
V	$r = \frac{k_1 ABCD}{(1+k_2D)^3 (1+k_3B)^3}$	343	2.52×10^{-3}	1.90	5.84×10^{-1}	9.57×10^{-12}
		353	1.26×10^{3}	3.82×10^{3}	-1.47×10^{-1}	6.08×10^{-9}
		363	9.42×10^{-3}	1.91	5.62×10^{-1}	1.68×10^{-10}

Where, A and B represent the concentrations of H_2 and CO in toluene at the gas-liquid interface (kmol/m^3) respectively. C and D are the concentrations of the catalyst and 1-decene (kmol/m^3), respectively.

The discrimination of rate models was done based on the thermodynamic criteria, activation energy and the Φ_{min} values. The rate models II and III were rejected based on the thermodynamic criteria of inconsistency of equilibrium constant and high activation energy. Models V have rate parameters less than zero (–ve) and hence were rejected. In the remaining two models I and IV, the model IV was discriminated based on the higher Φ_{min} values than model I. Therefore, model I (Eq. 4.11) was considered the best model for representing the kinetics of hydroformylation of 1-decene using carbon supported ossified catalyst.

$$r = \frac{k_1 \, ABCD}{(1+ k_2 D)^2 \, (1+ k_3 B)^2} \qquad 4.11$$

Where, *k* is the intrinsic rate constant (m^9/$kmol^3$/s), A and B represent the concentrations of H_2 and CO in toluene at the gas-liquid interface (kmol/m^3) respectively. C and D are the concentrations of the catalyst and 1-decene (kmol/m^3), respectively the rate parameters for Eq. 4.11 for all the temperature are presented in Table 4.18 (entry 1). A comparison of the experimental rates with the rates predicted by Eq. 4.11 is shown in Figure 4.34, which shows a reasonably good fit of the data. The average deviation in the predicted and observed rates was found to be in the range of ± 5 %. The Arrhenius plot showing the effect of temperature on the rate parameters is shown in Fig. 4.35, from which the activation energy was evaluated as 67.94 kJ/mol. The dependence of the rate parameters K_2 and K_3 on temperature show opposite trends; however, it is important to note that these parameters may not be representative of a single equilibrium reaction step and are in fact lumped parameters describing observed overall trends.

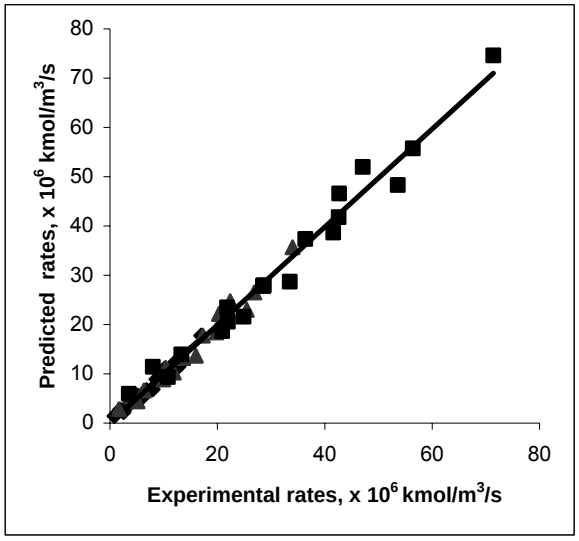

Figure 4.34: Comparison of experimental rates and rates predicted using model I

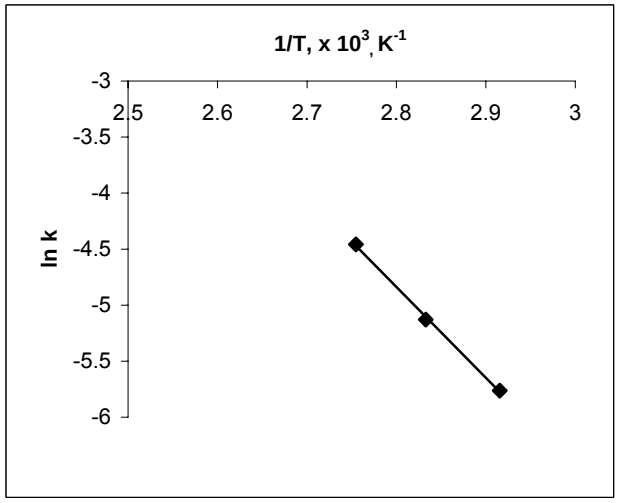

Figure 4.35: Temperature dependence of rate constant

The validity of the proposed model I was crosschecked by plotting the experimental and observed rates at varying concentrations of the variables for all temperature (Figure 4.36). The model was found to predict the trends in good agreement with experimental observations.

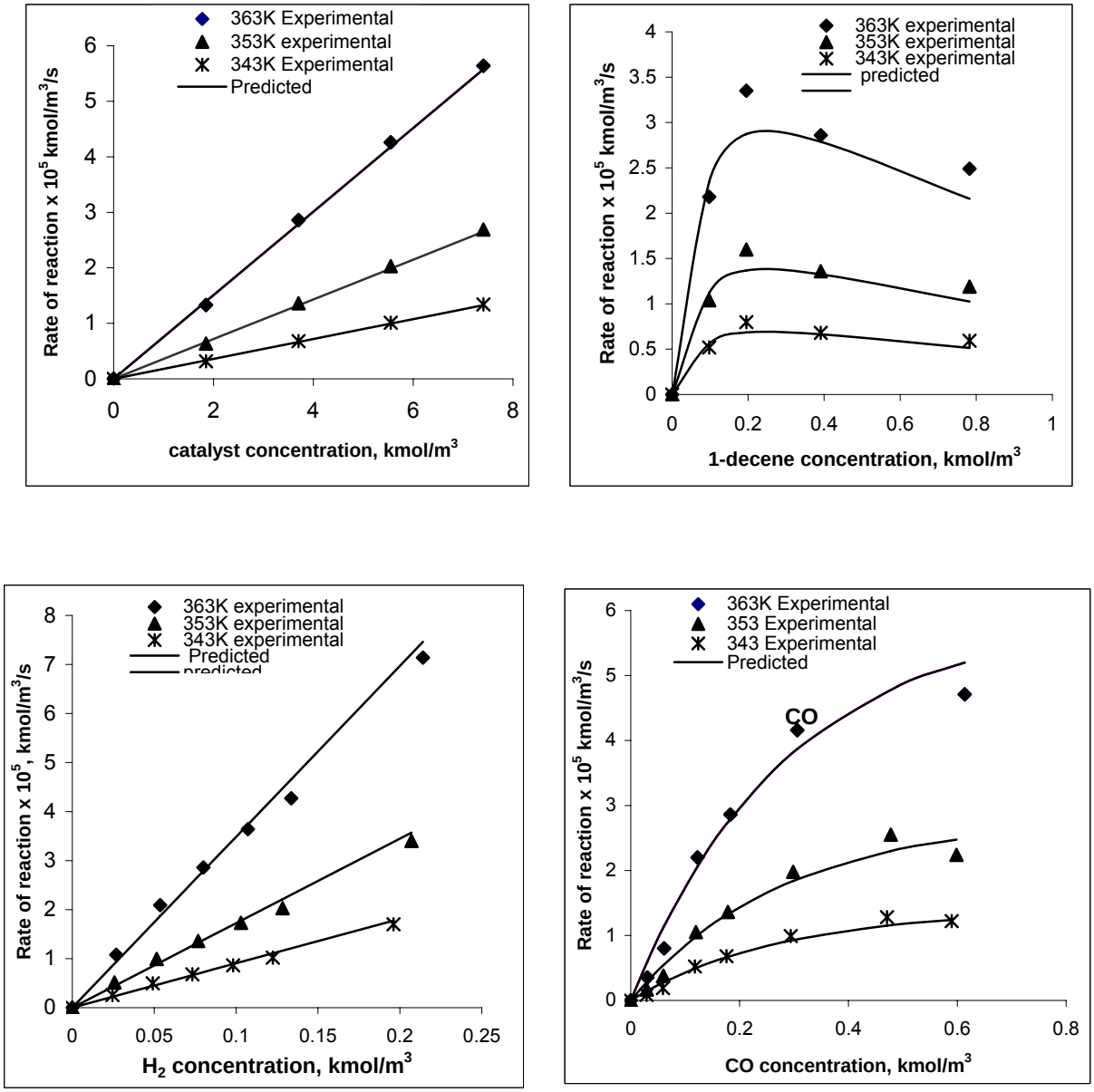

Figure 4.36: Validation of proposed rate model for various reaction parameters

4.4 Conclusions

A methodology for immobilization of Rh complex catalysts which gives molecularly dispersed heterogeneous catalysts has been applied for hydroformylation of olefins. The method (ossification) involves conversion of a water-soluble Rh complex catalyst (containing sulfonate groups) to its heterogeneous form as a barium salt on solid support.

The unsupported as well as supported ossified catalysts were synthesized. The catalysts were characterized by the various techniques such as FTIR, solid state ^{31}P NMR, powder XRD, SEM, TEM, EDX and XPS. The BET surface area, pore size and pore volume was also measured. The detailed characterization shows the catalyst is truly heterogenized form of his homogeneous analogous $HRhCO(TPPTS)_3$.

These catalysts were tested for hydroformylation of various classes of olefins and showed significant improvement of catalytic activity as compared to other reported heterogenized catalysts. The effect of solvent, nature and type of support and reaction parameters was also investigated. The catalyst is stable and can be recycled without any loss in activity. The carbon supported ossified catalyst was found to have a higher activity and the stability compared to the same catalyst on other supports.

The detailed analysis of the various mass transfer effects in G-L-S system was evaluated. The kinetics of 1-decene hydroformylation using carbon supported ossified catalyst in toluene has been investigated in a temperature range of 343-363 K. The rate was found to be first order with respect to catalyst and partial pressure of hydrogen. The plots of rate vs. 1-decene concentration as well as P_{CO} passed through maxima and show a typical case of inhibition at higher concentrations. In the lower concentration range the rate was found to be first order with respect to 1-decene and P_{CO}.

This kinetics using the carbon supported ossified catalyst is different from kinetics observed in homogeneous and biphasic catalysis with respect to the substrate concentration effect which shows substrate inhibition effect at higher substrate concentration. An unusual observation for this catalyst is the positive order with respect to P_{CO} up to a pressure of 5-6 MPa. Other parametric effects were found to be similar to that observed in homogeneous and biphasic media. A rate equation has been proposed based on the observed data, which is in full agreement with the experimental rates obtained. The activation energy was calculated to be 67.94 kJ/mol.

Although the isomerization activity is high for this catalyst (similar to the analogous $HRhCO(TPPTS)_3$ catalyst) the concept can be applied to other catalysts which yield a high n/i ratio. This approach is generic in nature and can easily be extended to other catalytic systems. It is also possible to heterogenize numerous organometallic complex catalysts by this technique, on to a variety of supports inclusive of carbon.

Impact of ossification methodology:

1. This technique yields a highly dispersed catalyst having a significantly higher activity (TOF) for hydroformylation of olefins compared to other known heterogenized catalysts.
2. This method of immobilization is generic in nature and can be applied to a variety of supports, catalysts and catalytic reactions[33].
3. The proper combination of suitable cations and anions can also yield similar types of catalysts.

Nomenclature

A	Concentration of reacting gases H_2
a_p	Interfacial area of the particle (m^2/m^3)
B	Concentration of reacting gases CO
C	Concentration of catalyst
C_i*	Saturation solubility of reacting gases (i.e. CO and H_2) in equilibrium with the gas phase concentration at the reaction temperature (kmol/m)
C_i*	Concentration of the gas at the surface ($kmol/m^3$)
D	molecular diffusivity (m/s)
D	Concentration of 1-decene
D_e	Effective diffusivity (m^2/s)
d_I	Impeller diameter (m)
D_M	Molecular diffusivity of the solute in the liquid medium (m^3/s)
d_p	Particle diameter (m),
d_T	Tank diameter (m)
e	Energy supplied to the liquid
F_c	Shape factor assumed to be unity for spherical particles
h_1	Height of the impeller from the bottom (m)
h_2	Liquid height (m)
H	Henry's Law Constant (MPa m^3/kmol)
k_1	Reaction rate constants ($m^9/kmol^3/s$)
k_2, k_3	Constant in Eq. 4.11 (m^3/kmol)
k_La_B	Gas-liquid mass transfer coefficient
k_s	Liquid to solid mass transfer coefficient (s)
M_B	Molecular weight of the solvent
N	Agitation Speed (Hz)
R	Universal gas constant (kJ/kmol/K)
R'_{Ai}	Experimental rates
R_{Ai}	Predicted rates
R_A	Overall rate of the reaction ($kmol/m^3/s$)
R_i	Reaction rate for the hydroformylation step ($kmol/m^3/s$)

T	Temperature (K)
V_A	Solute molar mass
V_g	Gas volume (m)
V_L	Total liquid volume (m)
w	Catalyst mass per unit volume of the reactor (kg/m)
α_{gl}	Enhancement factor defined by Eq-4.1
α_{ls}	Enhancement factor defined by Eq-4.3
ε_p	Porosity of the catalyst
M_B	Viscosity of the solvent
μ_l	Viscosity of the liquid (P or kg/m.s).
ρ_l	Density of the liquid (kg/m)
ρ_p	Density of the catalyst particle (kg/m)
Φ	Parameter defined by Eq-4.10
φ_{exp}	Parameter defined by Eq-4.7

References

1 B. Cornils, W.A. Hermann (Eds.) *Applied Homogeneous Catalysis with Organometallic Complexes,* VCH, Weinheim, **2002**,*Vol 2* pp 602-663.

2 B. Cornils, W. A. Herrmann (Eds.), *Aqueous Phase Organometallic Catalysis,* VCH, Weinheim, **1998**.

3 F.R. Hartley, *Supported Metal Complexes*, Reidel, Dordrechiet, **1985**.

4 (a) E. Schwab, S. Mecking, *Organometallics*, **2001**, *20*, 5504. (b) D. J. Cole-Hamilton, *Science*, **2003**, *299*, 1702 (c) D. de Groot, *Chem. Commun.,* **2001**, *20*, 5504 (d) S. C. Bourque, H. Alper, L. E. Manzer, P. Arya, *J. Am. Chem. Soc*, **2000**, *122*, 956 (e) I F. J. Vankelecom, P.A. Jacobs, in *Chiral Catalyst Immobilization and Recycling*,(Eds. D.E. De Vos, I.F.J. Vankelecom, P.A. Jacobs) Wiley/VCH, New York, **2000**, pp. 19–80 and 211–234 (f) A. J. Sandee, J. N. H. Reek, P. C. J. Kamer, P. W. N. M. Van Leeuwen, *J. Am. Chem. Soc.,* **2001**, *123*, 8468. (g) A. J. Sandee, J. N. H. Reek, P. C. J. Kamer, P. van Leeuwen, *Angew. Chem. Int. Ed.* **1999**, *38*, 3231. (h) N. J. Meehan, A. J. Sandee, J. N. H. reek, P. C. J. Kamer, P. W. N. M. van Leeuwen, M. Poliakoff, *Chem. Commun.*, **2000**, 1497 (i) L. Huang, W. S. Kawi, *J. Mol. Catal. A: Chemical*, **2003**, *206*, 371 (j) M. Nowotny, T. Maschmeyer, B. F. G. Johnson, P. Lahuerta, J. M. Thomas, J. E. Davies, *Angew Chem. Int. Ed.*, **2001**, *40*, 955 (k) K. Mukhopadhyay, A. B. Mandale, and R. V. Chaudhari, *Chem. Mater.,* **2003**, *15,* 1776 (l) R. L. Augustine, S. K. Tanielyan, *Chem. Commun.,* 1999, 1257. (m) K. Mukhopadhyay, R. V. Chaudhari, *J. Catal.*, **2003**, *213*, 73.

5 H. Bahrmann, H. Bach, *Ullmann's Encycl. Chem. 5th Edition*, **1991**, *Vol. A18*, 321.

6 W. Davies, L. Matty, D.L. Hughes, P.J. Reider, *J. Am. Chem. Soc.*, **2001**, *123*, 10139.

7 (a) A. Hu, H. L. Ngo, W. Lin *J. Am. Chem. Soc.* **2003**, *125*, 11490. (b) A. Hu, H.L. Ngo, W. Lin *Angew. Chem. Int. Ed. Engl.* **2003**, *42*, 6000.

8 B.M. Bhanage, S.S.Divekar, R.M.Deshpande, and R.V. Chaudhari *Organic Process Research and Development* **2000**, *4*, 342.

9 T. Bartik, B. Bartik, B. E. Hanson, T. Glass, W. Bebout, *Inorg. Chem.* **1992**, *31*, 2667.

10 J. P. Arhancet, M. E. Davis, J. S. Merola, B. E. Hanson *J. Catal.* **1990**, *121*, 327.

11 http://www.ausetute.com.au/solrules.html

12 P. Scherrer, *Gött. Nachr*. **1918**, *2*, 98,

13 *Handbook of X-Ray Photoelectron Spectroscopy,* Physical Electronics, Perkin Elmer, **1979**.

14 (a) K. Mukhopadhyay, A.B. Mandale, R.V. Chaudhari *Chem. Mater.* **2003**, *15*, 1766. (b) K. Mukhopadhyay, R.V. Chaudhari *J. Catal* **2003**, *213*, 73.

15 J. Falbe (Eds.) *New Synthesis with Carbon Monoxide* Springler-Verlag Berlien, Heidelberg, New york **1980,** pp 84-89.

16 M. Nowotny, T. Maschmeyer, Brian F.G. Johnson, P. Lahuerta, J.M. Thomas, J. E. Davies, *Angew. Chem. Int. Ed. Engl.* **2001**, *5*, 40.

17 Reaction conditions for homogeneous reaction $HRhCO(PPh_3)_3$: 2.18 $\times 10^{-3}$ kmol/m^3, $Rh:PPh_3$ = 1:6 (excess), 1-decene : 0.43 kmol/m^3, T: 373K , P_{CO+H2}(1:1): 4.14 MPa, agitation speed : 16.6Hz, solvent : toluene, total charge: 2.5 $\times 10^{-5}$ m^3, time : 0.9 h. (b) Reaction conditions for biphasic reaction $[Rh(COD)Cl]_2$: 1.48 $\times$ 10^{-3} kmol/m^3 (aq.), Rh:TPPTS=1:6 (excess) 1-decene: 0.7 kmol/m^3 (org.), T: 373K, agitation speed : 16.6 Hz, P_{CO+H2} (1:1) : 4.14 MPa, solvent : toluene + water (aqueous phase hold up=0.4), total charge : 2.5 $\times$ 10^{-5} m^3, time : 6.6 h.)

18 Purwanto, R. M. Deshpande, R. V. Chaudhari, H. Delmas, *J. Chem. Eng. Data,* **1996**, *41*, 1414

19 Vinod Nair, *Hydroformylation of olefins using homogeneous and biphasic catalysts*, Ph. D. thesis, University of Pune, **1999**.

20 P. A. Ramachandran, R. V. Chaudhari, *Multiphase Catalytic Reactors* Gordon and Breach, London, **1983**.

21 R. V. Chaudhari, R. V. Gholap, G. Emig, H. Hoffmann *Can. J. Chem. Eng.,* **1987**, 65, 744.

22 Y. Sano, N. Yamaguchi, T. Adachi, *J. Chem. Engg. Jpn.* **1974**, *7*, 255.

23 B. D. Prasher, G. B. Wills, *Ind. Eng. Chem. Proc. Des. Dev.* **1973**, *12*, 351.

24 C. R. Wilke, P. Chang, *AIChE. J.*, **1955**, *1*, 264.

25 (a) U. J. Jauregui-Haza, E. P. Fontdevila, P. Kalck, A. M. Wilhelm,H. Delmas *Catal. Today,* **2003**, *79–80*, 409. (b) U. J. Jauregui-Haza, O. Dıaz-Abın, A. M. Wilhelm, H. Delmas *Ind. Eng. Chem. Res.* **2005**, *44*, 9636.

26 (a) R. M.Deshpande, R. V.Chaudhari, *Ind. Eng. Chem. Res.* **1988,** *27*, 1996. (b) R. M. Deshpande, R. V.Chaudhari, *J. Catal.,* **1989**, *115*, 326.

27 A. H. G. Cents, D. W. F. Brilman, and G. F. Versteeg *Ind. Eng. Chem. Res.* **2004,** *43,* 7465.

28 (a) P. Purwanto, H. Delmas *Catal. Today* **1995**, *24*, 135 (b) R. M. Deshpande, Purwanto, H. Delmas, R. V. Chaudhari, *Ind. Eng. Chem. Res.* **1996**, *35,* 3927. (c) R.M. Deshpande, B. M. Bhanage,S. S. Divekar, S. Kanagasabapathy, R. V. Chaudhari *Ind. Eng. Chem. Res.* **1998**, *37,* 2391.

29 R. Chansarkar, *Hydroformylation of substituted olefins using homogeneous and heterogeneous catalysts*, Ph.D. Thesis, University of Pune, **2005**.

30 B.M. Bhanage, *Studies in hydroformylation of olefins using transition metal complex catalysts*, Ph.D. Thesis, University of Pune, **1995**.

31 (a) S. S. Divekar, R. M. Deshpande, R. V. Chaudhari, *Catal. Lett.*, **1993**, *21*, 191.(b) B.M. Bhanage, S. S. Divekar, R.M. Deshpande, R.V. Chaudhari, *J. Mol. Catal. A: Chemical*, **1997**, *115*, 247. (b) V. S. Nair, S. P. Mathew, R.V. Chaudhari, *J. Mol. Catal A: Chemical*. **1999**, *143*, 99. (d) R. Chansarkar, K. Mukhopadhyay, A. A. Kelkar, R. V. Chaudhari *Catal. Today* **2003**, *79–80*, 51.

32 D. W. Marquardt, *J. Soc. Ind. Appl. Math*., **1963,** *11(2)*, 431.

33 (a) R.V. Chaudhari, A. N. Mahajan *US 7026266*, **2003**. (b) B. R. Sarkar, R. V. Chaudhari, *J. Catal.* **2006**, *242*, 231.

APPENDIX I

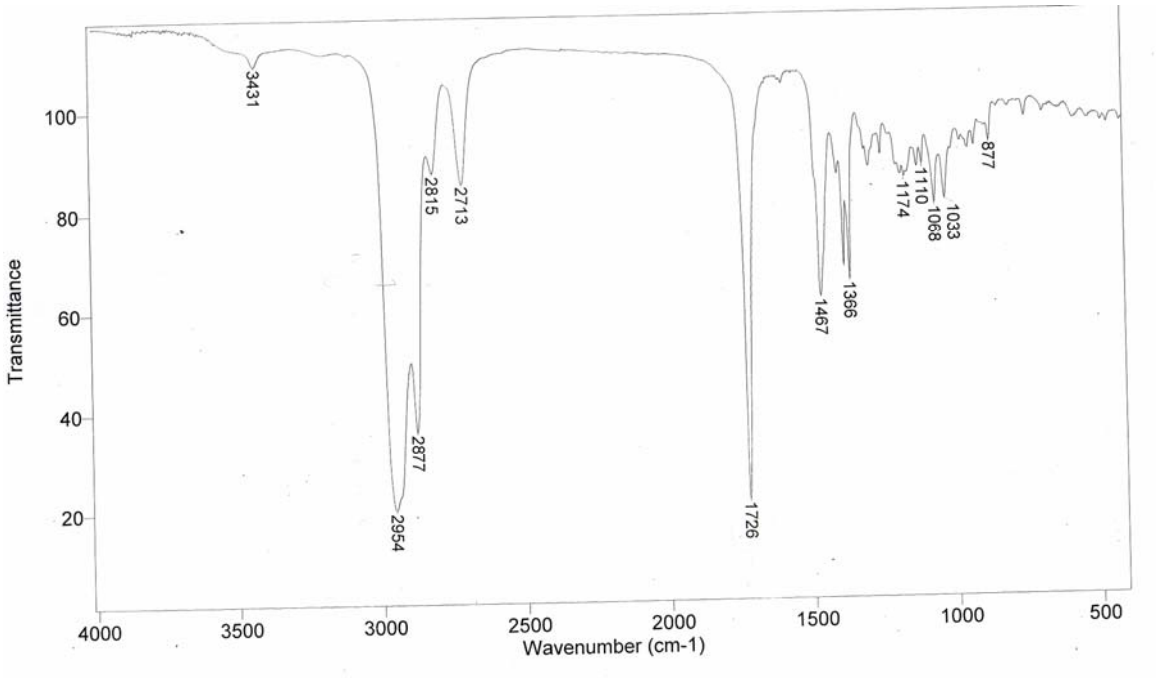

Figure 1: FTIR spectra of 3,3- Dimethyl-2-norbornaneacetaldehyde **7a** and **7b**

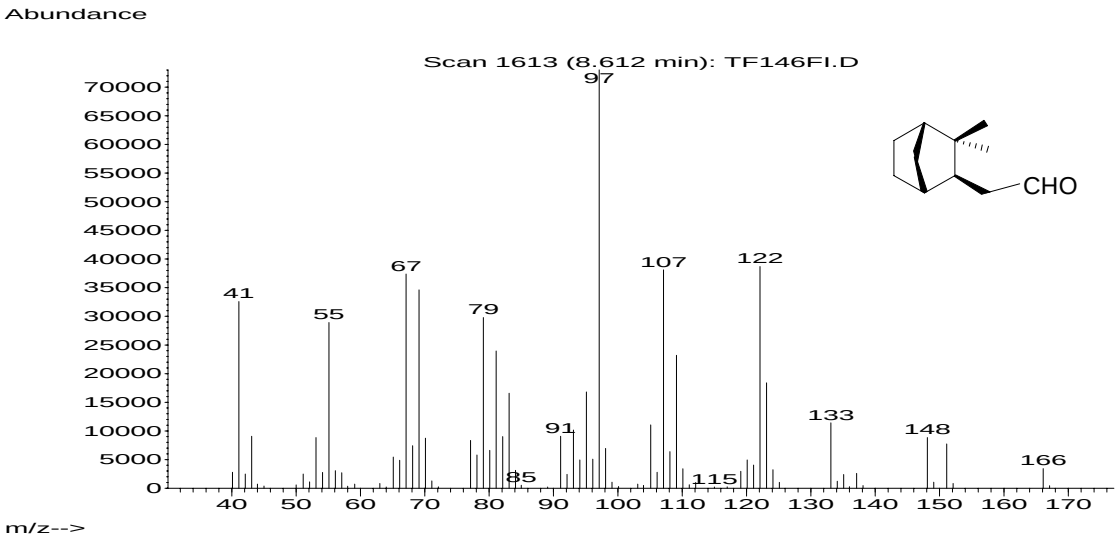

Figure 2: Mass spectra of 3,3- Dimethyl-2-norbornaneacetaldehyde (exo **7a**, shorter GC retension time)

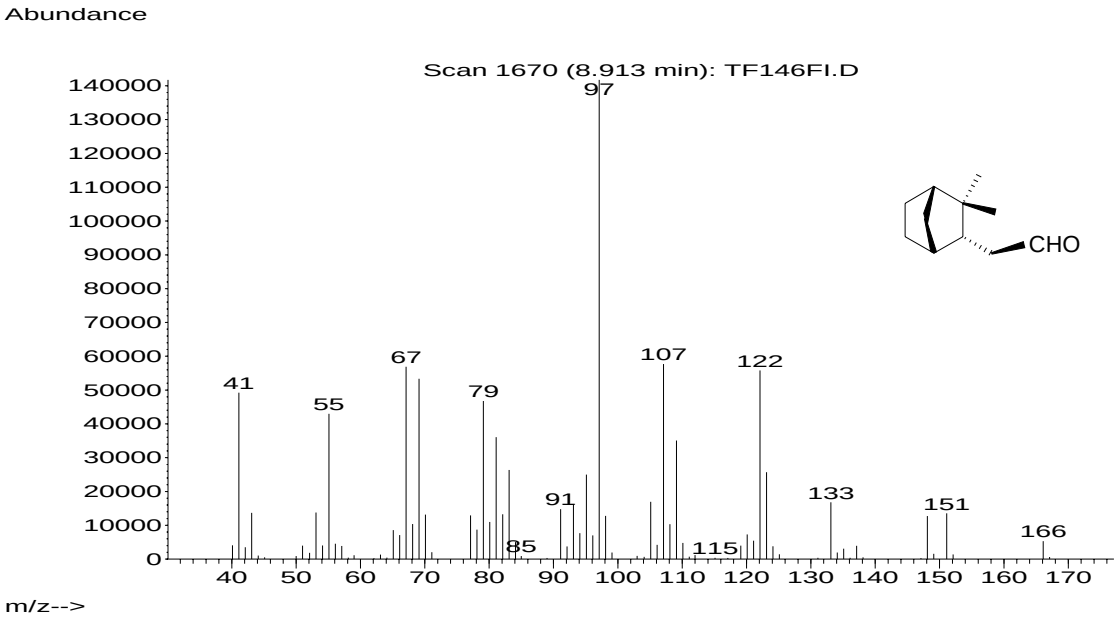

Figure 3: Mass spectra of 3,3-Dimethyl-2-norbornaneacetaldehyde (endo **7b**, longer GC retention time)

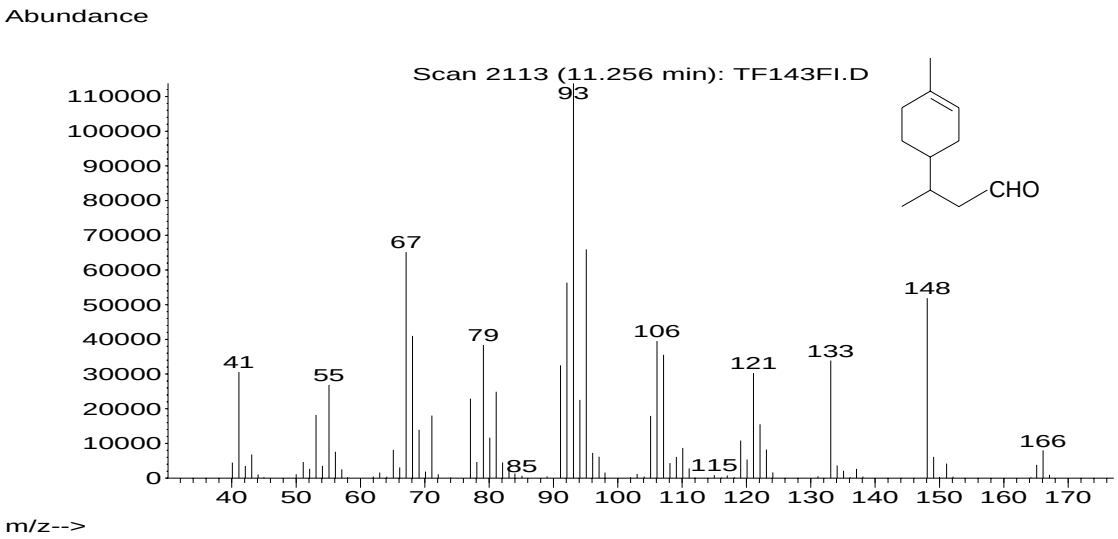

Figure 4: Mass spectra of 3-(4Methylcyclohex-3-enyl) butanal **11**

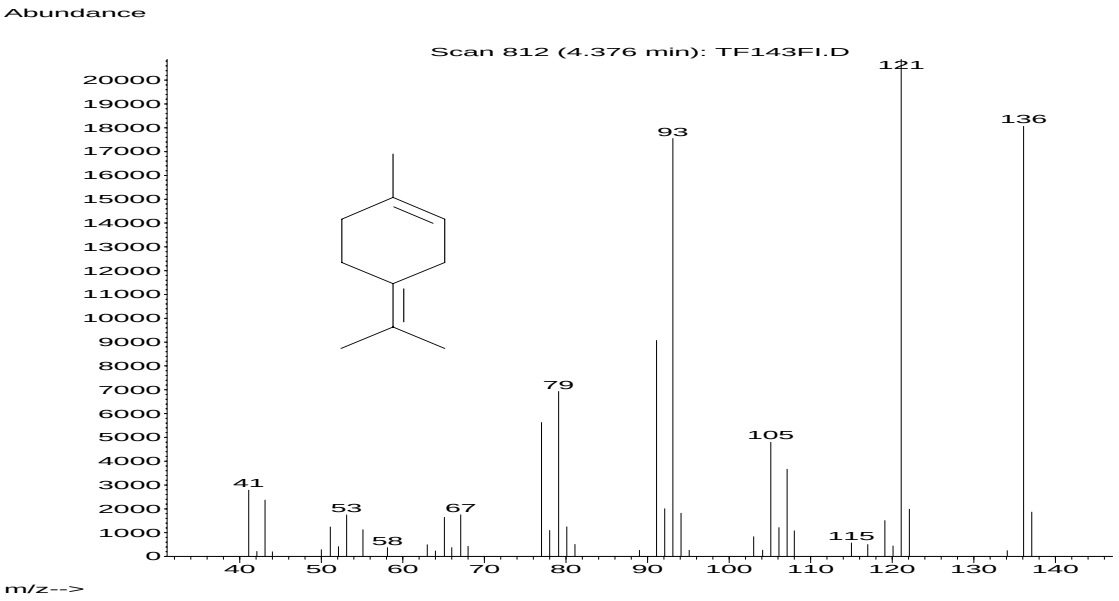

Figure 5: Mass spectra of 1-methyl-4-(propan-2-ylidene) cyclohex-1-ene **12** (Isomerized limonene)

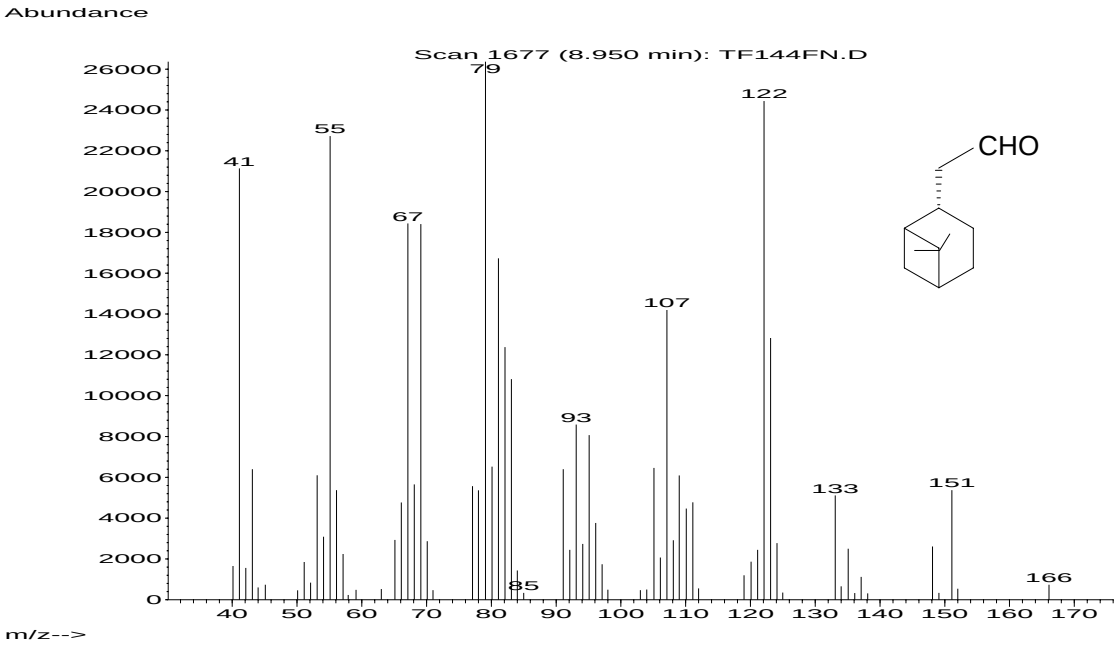

Figure 6: Mass spectra of 10-Formylpinane (trans **13b**, shorter GC retention time)

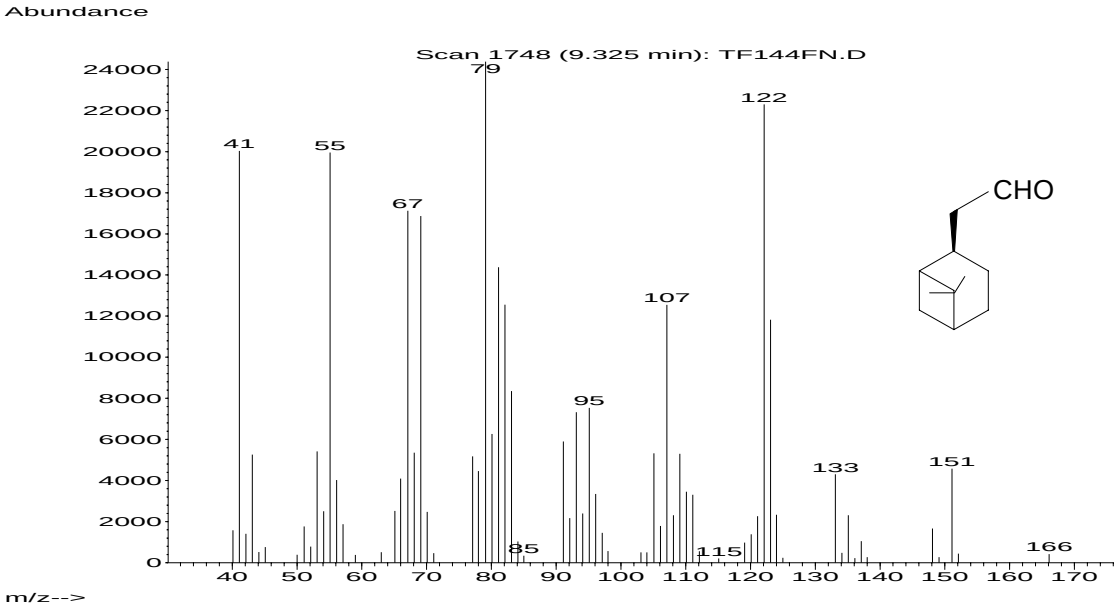

Figure 7: Mass spectra of 10-Formylpinane i.e. (cis **13a**, longer GC retention time)

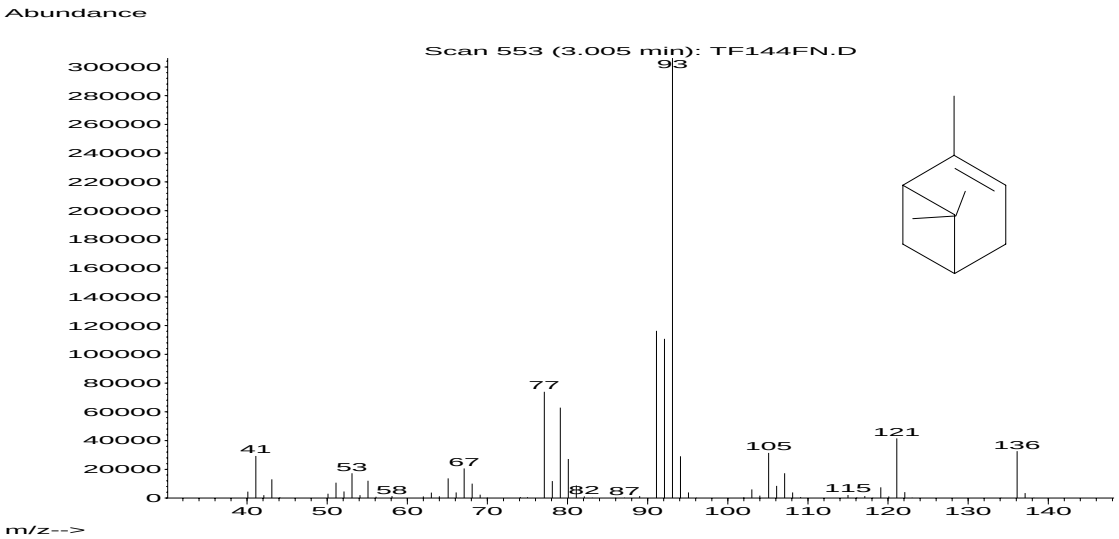

Figure 8: Mass spectra of α-pinene **14** (Isomerised product of β-pinene)

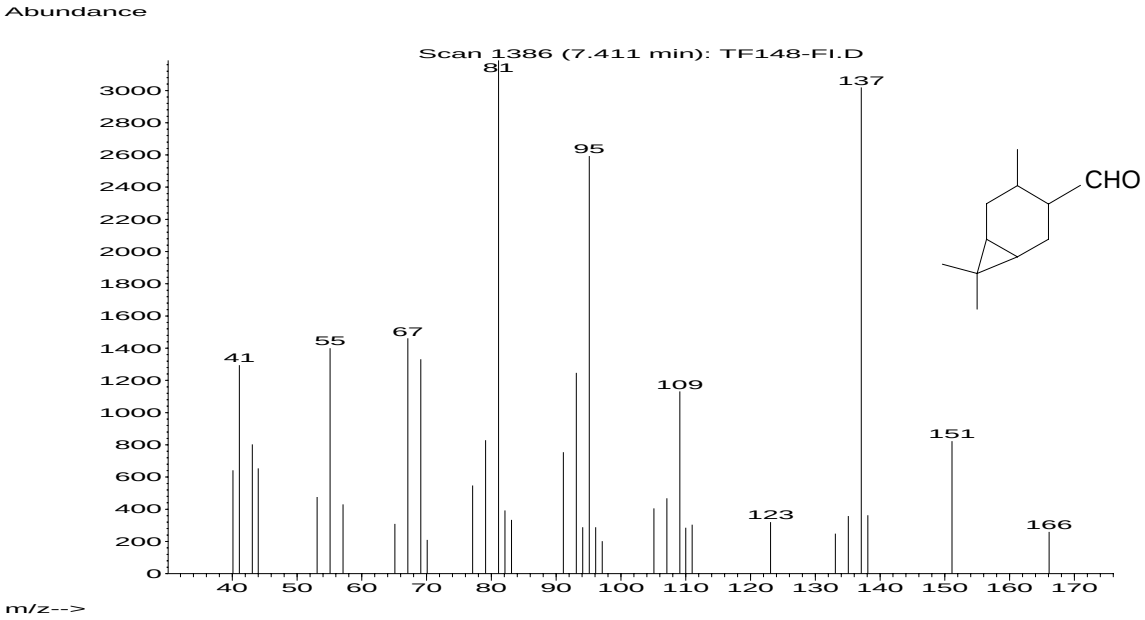

Figure 9: Mass spectra of 2-caranecarbaldehyde **15** or (3,7,7-trimethylbicyclo [4.1.0]heptane-2-carbaldehyde)

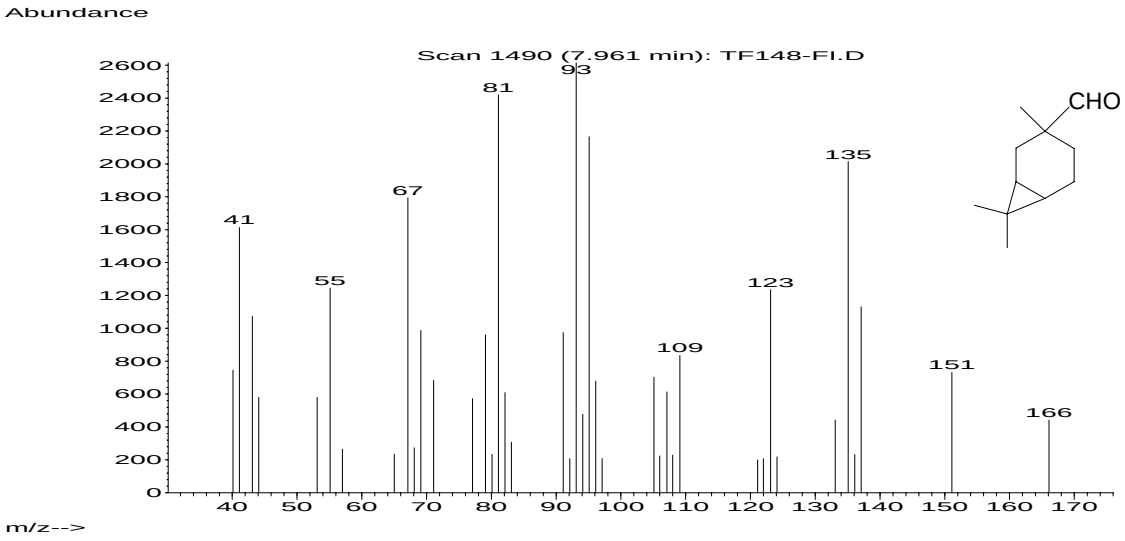

Figure 10: Mass spectra of 3-caranecarbaldehyde **16** or (3,7,7-trimethylbicyclo [4.1.0] heptane-3-carbaldehyde)

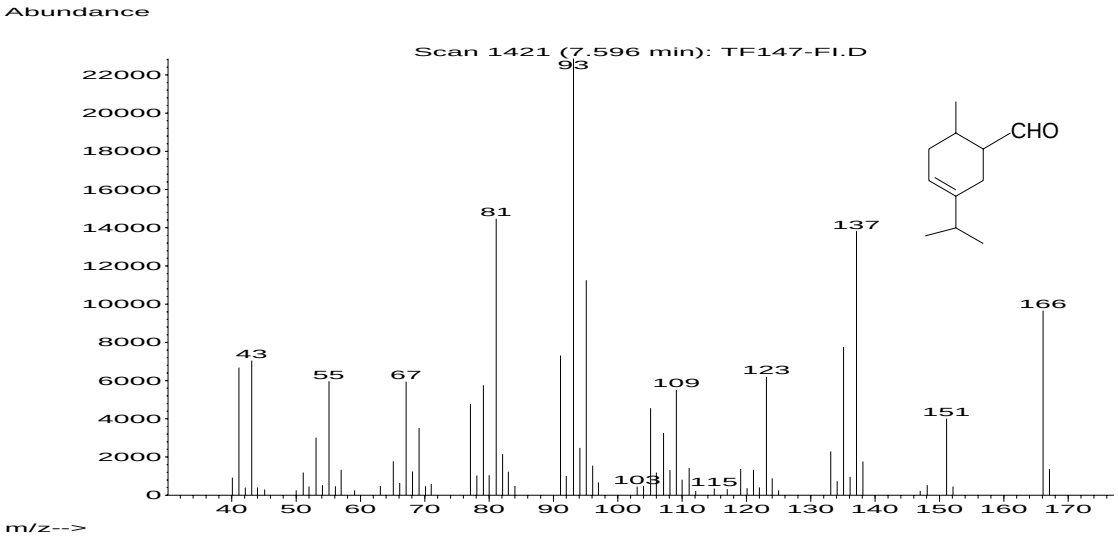

Figure 11: Mass spectra of 3-isopropyl-6-methylcyclohex-3-enecarbaldehyde **17** (major)

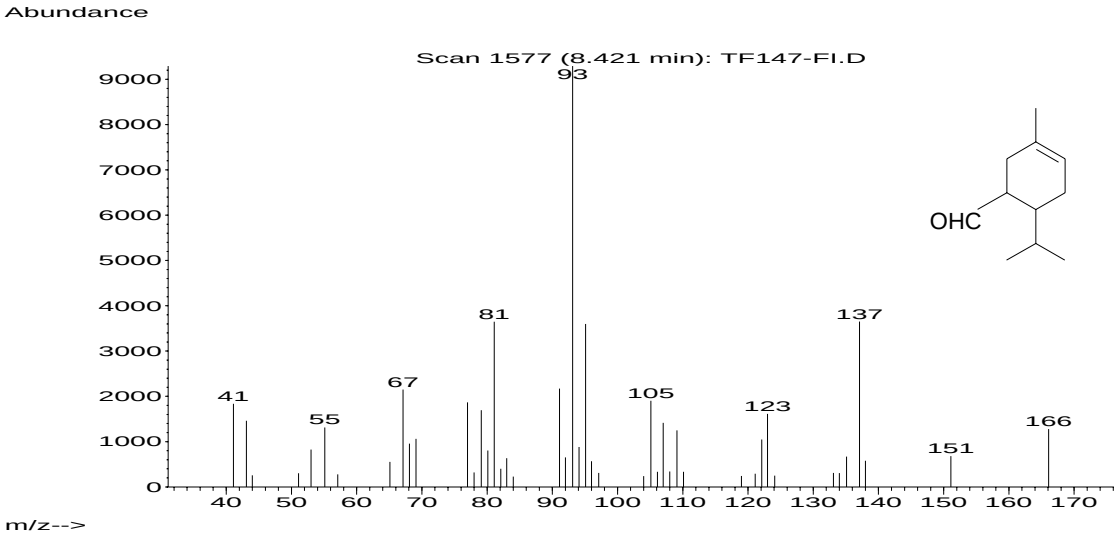

Figure 12: Mass spectra of 6-isopropyl-3-methylcyclohex-3-enecarbaldehyde **18** (minor)

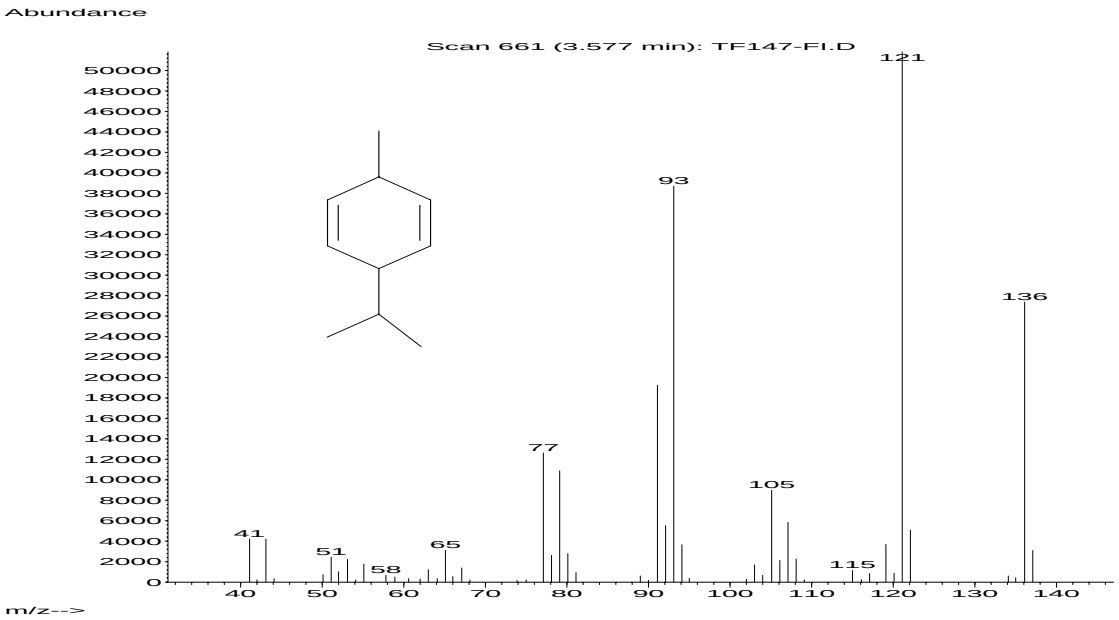

Figure 13: Mass spectra of 3-isopropyl-6-methylcyclohexa-1,4-diene **21** (Isomerized product)

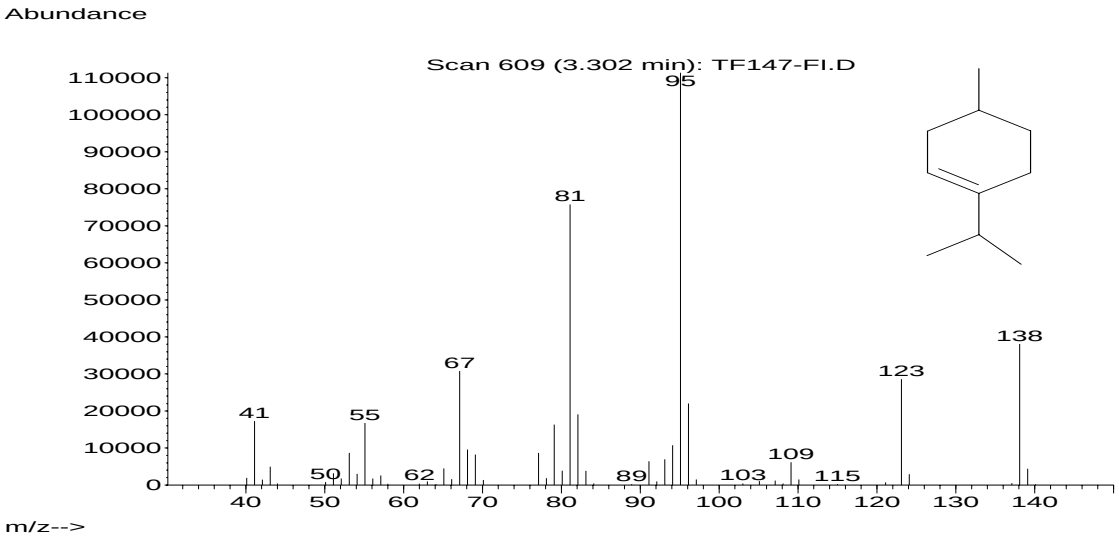

Figure 14: Mass spectra of 1-isopropyl-4-methylcyclohex-1-ene **19**

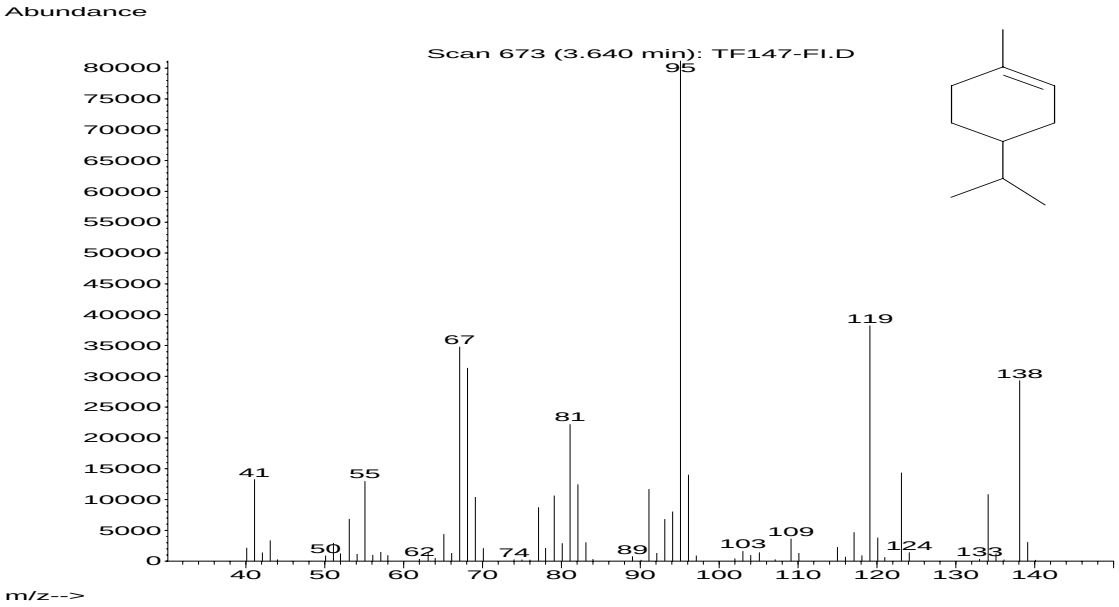

Figure 15: Mass spectra of 4-isopropyl-1-methylcyclohex-1-ene **20**

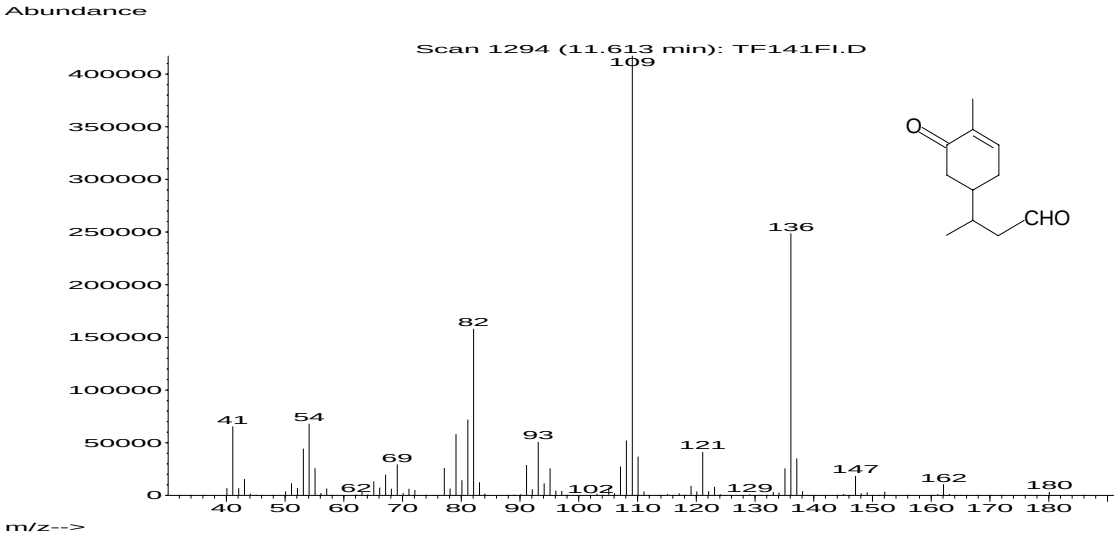

Figure 16: Mass spectra of 3-(4-Methylcyclohex-4-en-3-onyl) butanal **22**(Major)

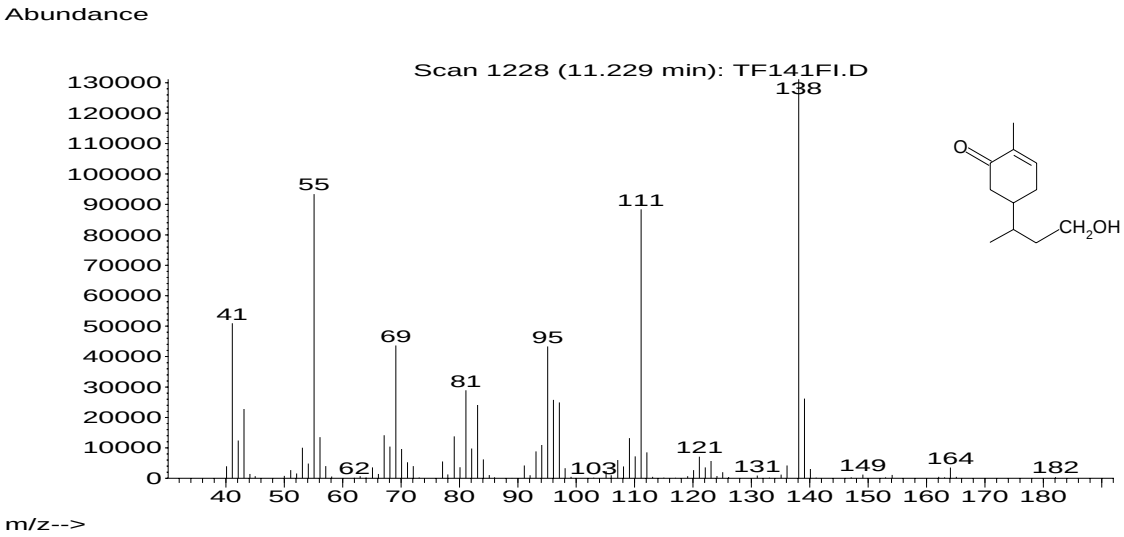

Figure 17: Mass spectra of 3-(4-methyl-3-oxocyclohexyl)butanal **24**

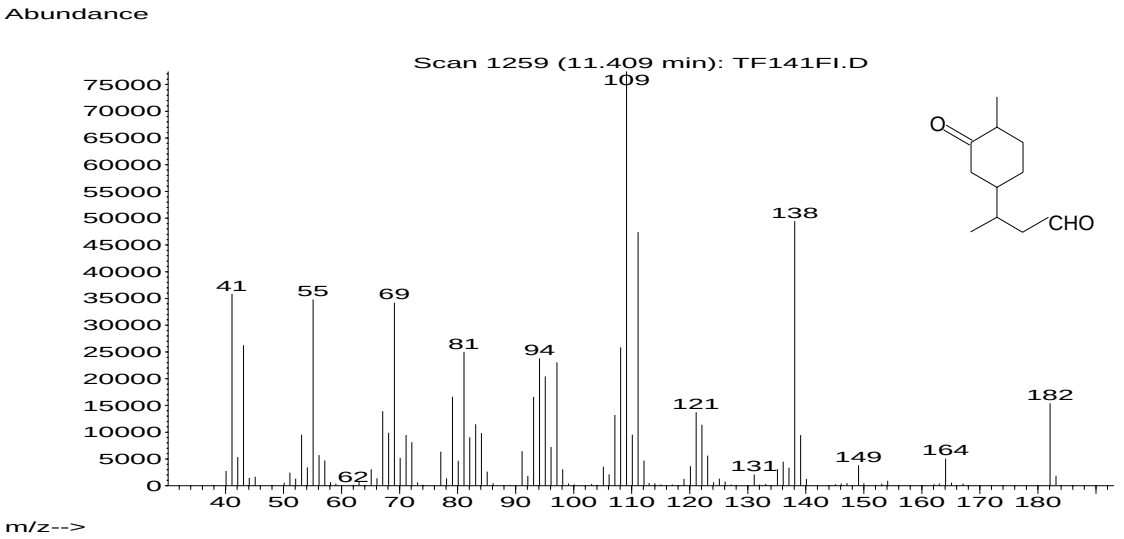

Figure 18: Mass spectra of 5-(4-hydroxybutan-2-yl)-2-methylcyclohex-2-enone **23** (alcohols)

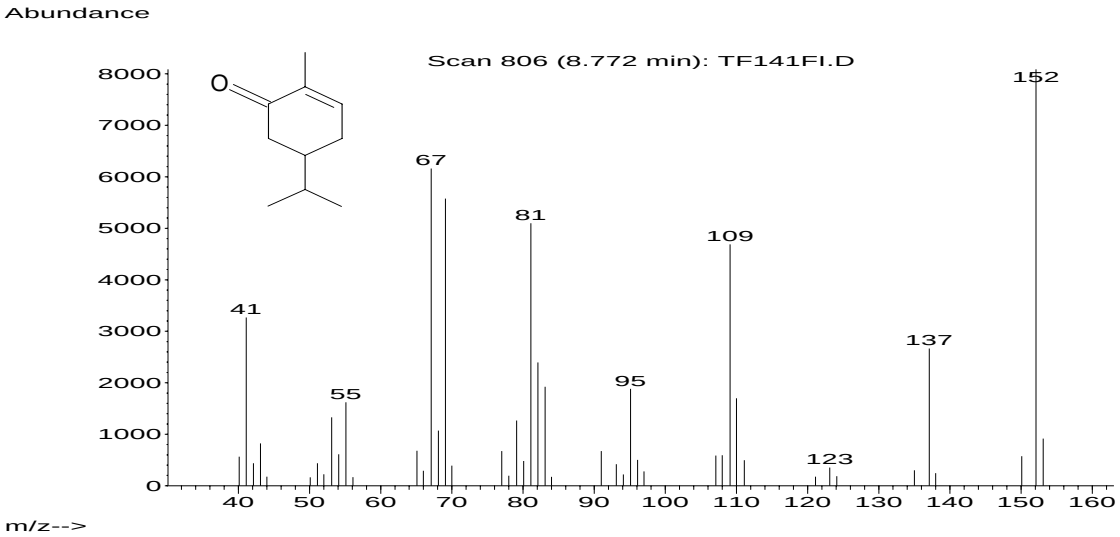

Figure 19: Mass spectra of 5-isopropyl-2-methylcyclohex-2-enone **25**

Publications/Symposia

- Hydroformylation of olefins using dispersed molecular catalysts on solid supports
  N.S.Pagar, R.M.Deshpande and R.V.Chaudhari
  Catalysis Letters 2006, 110 (1–2), 129-133.
- Kinetics of hydroformylation of camphene using homogenous rhodium complex catalyst
  N.S.Pagar, R.M.Deshpande and R.V.Chaudhari
  Proceedings of International Conference on Molecules to Material, 2006 pp 289-294.
- Synthesis, characterization and catalytic study of mesoporous carbon materials prepared via mesoporous silica using non-surfactant templating agents
  A.J. Chandwadkar, P. Karandikar, M. S. Agashe, N. E. Jacob, R. K . Jha, R. Kumar, **N. S. Pagar,** R. M. Deshpande and R. V. Chaudhari
  Communicated to **Central European Journal of Chemistry**
- Hydroformylation of terpenes using rhodium phosphite complex catalyst: Activity, Selectivity and Kinetic study
  N. S. Pagar, K.B. Rajurkar**,** R. M. Deshpande and R. V. Chaudhari
  To be communicated **Journal of Molecular Catalysis:Chemical**
- Hydroformylation of 1-decene in aqueous biphasic medium using Rh-Sulfoxantphos catalyst: Activity Selectivity and Kinetic study
  N. S. Pagar, K.B. Rajurkar**,** R. M. Deshpande and R. V. Chaudhari
  To be communicated **Applied Catalysis: General.**
- Kinetics of hydroformylation of 1-decene using carbon supported ossified $HRhCO(TPPTS)_3$ rhodium catalyst.
  N. S. Pagar, K.B. Rajurkar**,** R. M. Deshpande and R. V. Chaudhari
  To be communicated **Industrial Engineering and Chemical Research**

- Kinetics of hydroformylation of camphene using homogenous rhodium complex catalyst.

  N. S. Pagar, R. M. Deshpande and R. V. Chaudhari

  Oral Presentation in International Conference on Molecules to Material (ICMM)-2006, at Longowal Punjab, India March 3-4, 2006.

- Hydroformylation of terpenes using homogenous rhodium complex catalyst.

  N. S. Pagar, R. M. Deshpande and R. V. Chaudhari

  Poster Presentation, Science Day, National Chemical Laboratory, Pune 411008 India, February 2004.

- Kinetics of hydroformylation of 1-decene using carbon supported ossified rhodium catalyst.

  N. S. Pagar, R. M. Deshpande and R. V. Chaudhari

  Oral Presentation in CAMURE-6 and ISMR-5, National Chemical Laboratory Pune-411008, India January 14-17, 2007.

- Hydroformylation of 1-decene in aqueous biphasic medium using Rh-sulfoxantphos catalyst: Activity Selectivity and Kinetic study

  N. S. Pagar, R. M. Deshpande and R. V. Chaudhari

  Oral presentation 18th National Symposium & Indo-US Seminar on Catalysis, Indian Institute of Petroleum Dehradun, India April 16-18, 2007